PMFSEL Report No. 87-8
DECEMBER 1987

RECENT STUDIES ON REINFORCED CONCRETE BEAM-COLUMN JOINTS IN JAPAN

by

Yukinobu Kurose

Partially Supported by
National Science Foundation
Grant No. ECE-8320398

PHIL M. FERGUSON STRUCTURAL ENGINEERING LABORATORY
Department of Civil Engineering / Bureau of Engineering Research
The University of Texas at Austin

Any opinions, findings, conclusions, or recommendations expressed in this publication are those of the author and do not necessarily reflect the views of the National Science Foundation.

ABSTRACT

An outline of recent studies in Japan on reinforced concrete beam-column joints is presented. The background to the studies is introduced and Japanese design approaches for the joints are described. A number of Japanese studies were conducted under the U.S.-New Zealand-Japan-China Cooperative Project on Design of Reinforced Concrete Beam-Column Joints and are described in detail. Other research which has been reported in the Japanese literature is presented. The report contains a design example for an interior joint. A description of concrete and reinforcement commonly used in Japan is provided.

ACKNOWLEDGEMENTS

The dissemination of the material in this report was supported by the National Science Foundation under Grant ECE-8320398. The author compiled the report while a research scholar at The University of Texas on assignment from Shimizu Construction Co. of Japan. The support of NSF and Shimizu Construction Co. is gratefully acknowledged.

CONTENTS

LIST OF TABLES

LIST OF FIGURES

Figure

1. INTRODUCTION

The seismic behavior of RC (reinforced concrete) beam-column joints is not yet fully understood although the behavior of structural members framing into the joints (beams and columns) is well understood from analytical and experimental studies. Joints are rarely of concern in structural design of RC buildings because past strong earthquakes have caused very little damage to joints in Japan. Although many RC buildings were severely damaged in the 1968 Tokachioki Earthquake (M 7.9), only a few buildings suffered damage in the joints. For example, concrete crushing was observed in exterior joints in the penthouse of Hachinohe City Hall (Fig. 1.1).[1] A Hakodate University building which collapsed due to column failure (Fig. 1.2) was the special case where eccentric joints appeared to cause overstress in the columns and led to failure (Fig. 1.3).[2]

At present in Japan the Building Standard Law has no requirements for the safety of the joints as related to seismic forces. Accordingly, the *AIJ* (Architectural Institute of Japan) *Standard for RC Buildings*[3] contains no provisions for design of joints. This is probably due to the following reasons.

1. Joints suffered little damage in past earthquakes in Japan.
2. Joints are three-dimensionally confined by members so that they are expected to carry large shear forces.
3. Generally, in Japan beam and column sections have such large dimensions that the joints are big enough to keep shear stresses low.
4. Generally beam and column sections are so underreinforced that shear forces acting on the joints are expected to be small even when plastic hinges form at the joint face.

However, the situation has changed so that joints are not always safer than beams and columns because a recent trend in construction is toward using higher strength concrete and larger size reinforcing bars to minimize structural member dimensions. Occasionally heavy reinforcement is placed in small beam and column sections so that large shear forces are expected to act on joints which have a small volume. The joints are likely to be the most critical element in the building because the strength is dependant on the sectional properties of members framing into them and because the joints are difficult to reinforce. This is particularly true in RC high-rise buildings.

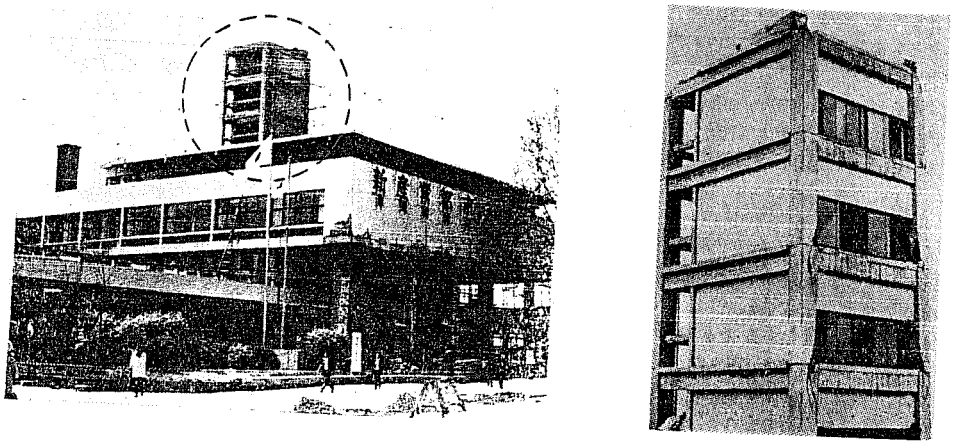

Fig. 1.1 Penthouse of Hachinohe City Hall (1968 Tokachioki Earthquake)

Fig. 1.2 Hakodate University (1968 Tokachioki Earthquake)

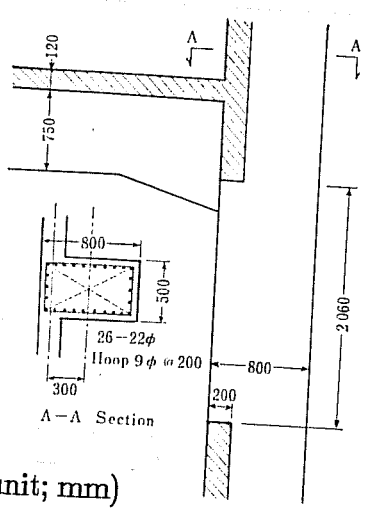

Fig. 1.3 Beam-column joint in Hakodate University

2. JAPANESE DESIGN OF REINFORCED CONCRETE BEAM-COLUMN JOINTS

2.1 Code Provisions

The *AIJ Standard for Reinforced Concrete Structures*[3] contains no provisions for design of beam-column joints except the requirements for development length of reinforcing bars anchored in the joints. However, the *AIJ Standard for SRC* (Steel Reinforced Concrete) *Structures*[4] contains an article to cover beam-column joints. According to the article, the joint is defined as the region having the effective width $b_j = (b_b + b_c)/2$ and the effective depths j_b and j_c as shown in Figs. 2.1 and 2.2. The following equation should be used to design SRC joints subjected to shear forces under seismic loading conditions as shown in Figs. 2.3 and 2.4.

$$eV_c \cdot \tau_{RC} + V_S \cdot \tau_S > \min\left(\frac{uM_{b1} + uM_{b2}}{1+\xi}, \frac{uM_{c1} + uM_{c2}}{1+\eta}\right) \tag{1}$$

where

eV_c = effective volume of joint concrete (cm^3)
$eV_c = b_j \times rj_b \times rj_c$, $b_j = (b_b + b_c)/2$
V_S = volume of steel panel (cm^3)
($V_S = pt_w \times sj_b \times sj_c$, pt_w = panel thickness)
τ_{RC} = shear stress carried by reinforced concrete (kgf/cm^2)
τ_S = shear stress carried by steel panel (kgf/cm^2)
uM_b = beam moment capacity ($kgf \cdot cm$)
uM_c = column moment capacity ($kgf \cdot cm$)
ξ = Db/n'
η = Dc/ℓ'

The shear stress carried by reinforced concrete τ_{RC} is the sum of the concrete contribution τ_c and the steel contribution τ_S.

$$\left.\begin{aligned} \tau_{RC} &= \tau_c + \tau_S \\ \tau_c &= 2\psi f_S \\ \tau_S &= p_w f_{wy} \end{aligned}\right\} (kgf/cm^2) \tag{2}$$

where

f_S = allowable shear stress of concrete (kgf/cm^2)
$f_S = \min[F_c/20, 1.5 \times (F_c/100 + 5)]$
ψ = confinement coefficient of the joint
$\psi = 3$ for interior joint (+–shaped joint)
$\psi = 2$ for exterior joint (⊢–shaped joint)
$\psi = 1$ for corner joint (L–shaped joint)

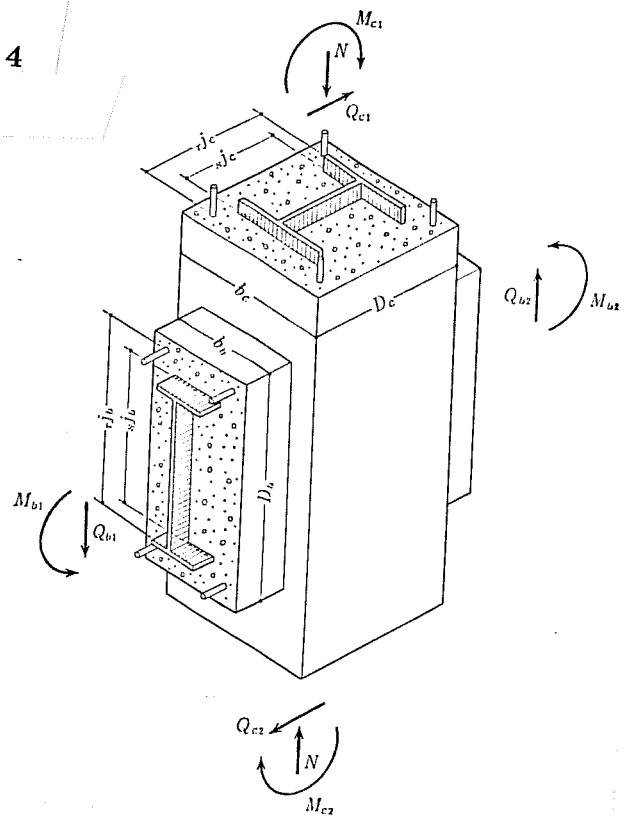

Fig. 2.1 SRC beam-column joint

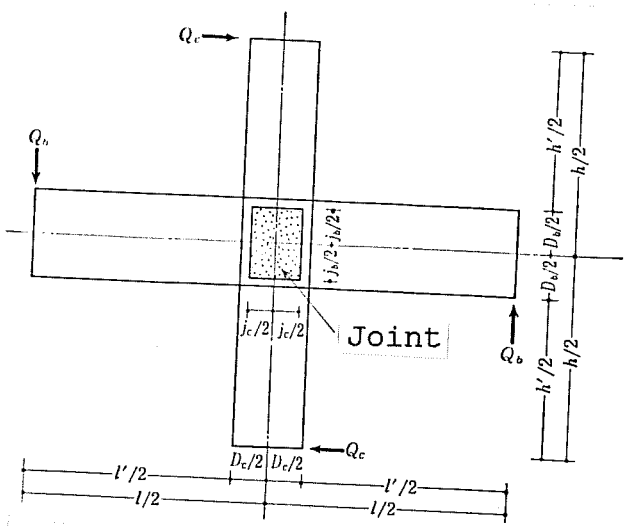

Fig. 2.2 Subassembly dimensions

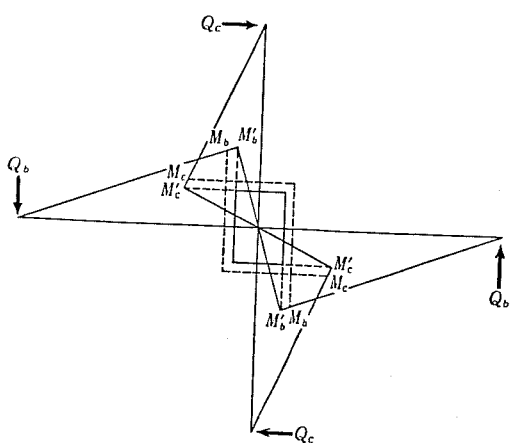

Fig. 2.3 Moment distribution

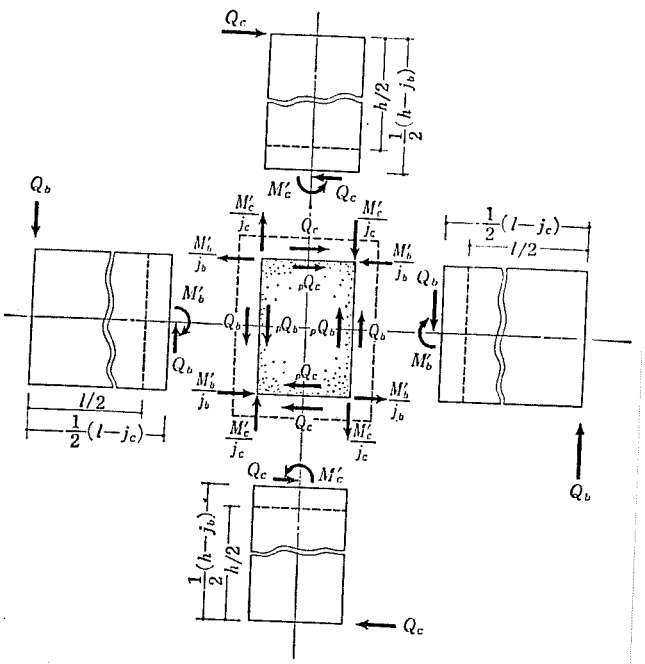

Fig. 2.4 Forces acting on joint

F_c = concrete strength (kgf/cm^2)
p_w = joint reinforcement ratio
$p_w = A_w/(bc \times s)$
A_w = sectional area of a set of joint stirrups (cm^2)
s = spacing of joint stirrups (cm)
f_{wy} = yield strength of joint stirrups (kgf/cm^2)

The above equations are sometimes applied to reinforced concrete structures. It should be noted that the concrete contribution in interior joints is six times higher than the allowable shear stress used to design beams and columns.

2.2 Design Recommendations

Several equations for joint shear strength were derived from various beam-column joint tests.[7,9] The equation recommended in the AIJ publication[5] was proposed by Kamimura from test results of 23 interior joints which failed in shear (Fig. 2.6). Although some of those specimens were subjected to a constant axial force through the column, the axial force was found to influence the joint shear strength very little.[7] The equation is as follows:

$$\left.\begin{aligned} \tau_p &= (0.78 - 0.0016F_c)F_c + \frac{1}{2}\,p_w\,f_{wy} \quad \text{for} \quad F_c \le 244 \text{ kgf/cm}^2 \\ \tau_p &= 95.1 + \frac{1}{2}\,p_w\,f_{wy} \quad \text{for} \quad F_c > 244 \text{ kgf/cm}^2 \end{aligned}\right\} \tag{3}$$

where

τ_p = shear strength for RC interior joints (kgf/cm^2)
F_c = concrete strength (kgf/cm^2)
p_w = joint reinforcement ratio
f_{wy} = yield strength of joint stirrups (kgf/cm^2)

In this equation, the joint shear strength is defined as the sum of the concrete and steel contributions. However, the steel contribution is half that in the AIJ equation for SRC joints (Eq. 2). Using half the steel contribution was found to give better correlation with the test results than when all the steel was used.[7]

Reference 5 gives an indication of the joint shear stress carried by concrete from test data. The following equation was used to calculate the joint shear stress carried by concrete.

$$\tau_c = \min\left\{\frac{\Sigma uM_b}{(1+\xi)eV_c}\ ,\ \frac{\Sigma uM_c}{(1+\eta)eV_c}\right\} - \frac{1}{2}p_w\,f_{wy} \tag{4}$$

where τ_c = shear stress carried by concrete (kgf/cm). (See the notation in Eqs. 1 and 2.)

- Joint shear failure in test
- ○ Beam flexural failure in test
- ■ Hakodate University (damaged in Tokachioki Earthquake)
- □ No joint damage in Tokachioki and Miyagioki (68, 78) Earthquakes
  (Assume $P_w = 0$ for joints in actual buildings)

$$\text{Volume ratio} = \frac{\text{joint effective volume } eV_c}{\text{beam volume} + \text{column volume}} * 100$$

$$\text{beam volume} = \text{width} \bullet \text{depth} \bullet \text{span length}$$
$$\text{column volume} = \text{width} \bullet \text{depth} \bullet \text{story height}$$

τ_c : shear stress carried by concrete

F_c : compressive strength of concrete

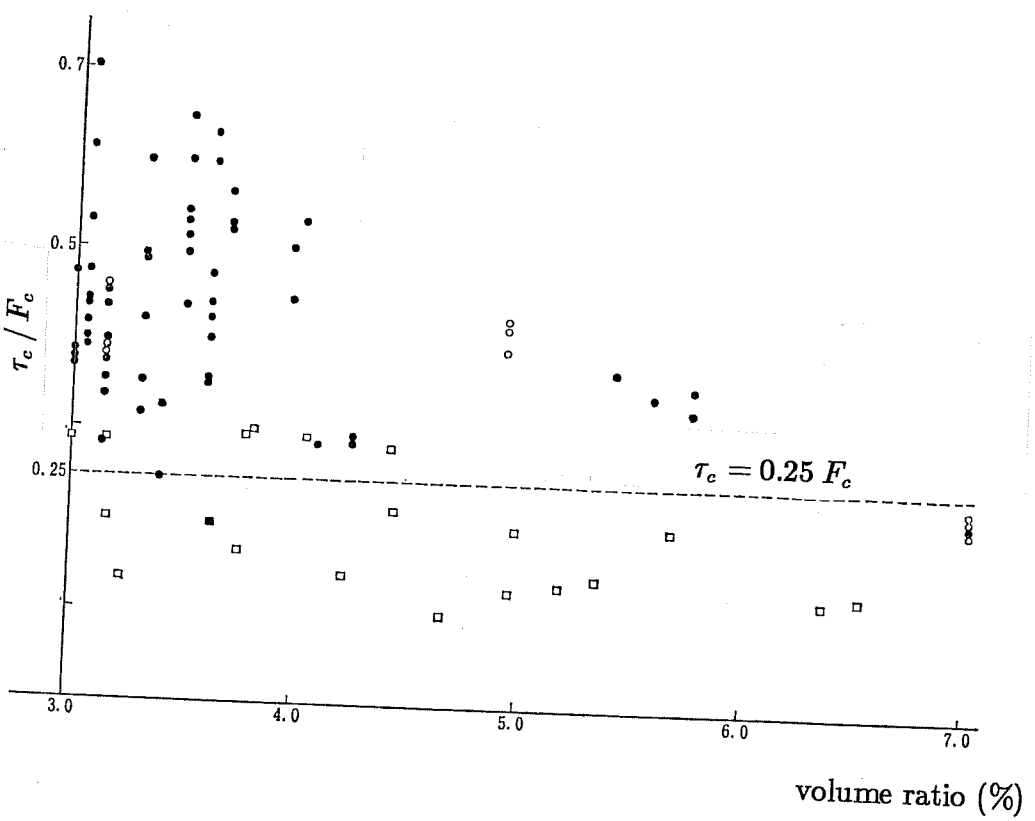

Fig. 2.5 Joint shear stress carried by concrete

Figure 2.5 shows the results for interior (cruciform-shaped) joints. It can be seen in this figure that most of the interior joints failed in joint shear when the concrete stress was

higher than $0.25\,F_c$. Generally, it is believed that exterior and corner joints have lower strength than interior joints. Thus, referring to the confinement coefficient ψ in the AIJ equation for SRC joints (Eq. 2), the following equation was proposed as the allowable joint shear stress carried by concrete.[5]

$$\tau_c \leq 0.25\,\beta F_c \tag{5}$$

where

$$\begin{aligned} \beta &= 1 \quad \text{for interior joints (+ shape)} \\ &= \tfrac{2}{3} \quad \text{for exterior joints (⊢ or T shape)} \\ &= \tfrac{1}{3} \quad \text{for corner joints (L shape)} \end{aligned}$$

The draft code for design of RC buildings with D51 reinforcing bars[6] contains provisions to ensure the safety of beam-column joints against shear and bond failure.

According to the commentary of the draft code, the joints should be designed for shear using Kamimura's equation (Eq. 3) shown in Fig. 2.6.[6] Test results with D51 bars are also plotted with solid circles.[10] D16 or larger bars are recommended as lateral reinforcement.

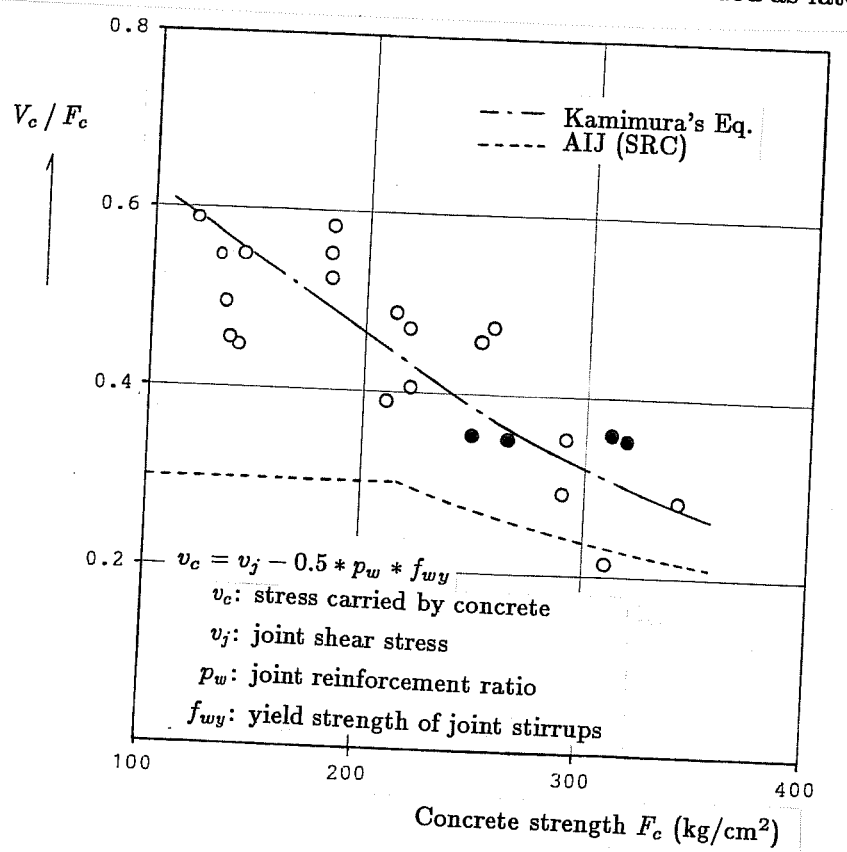

Fig. 2.6 Joint shear stress carried by concrete

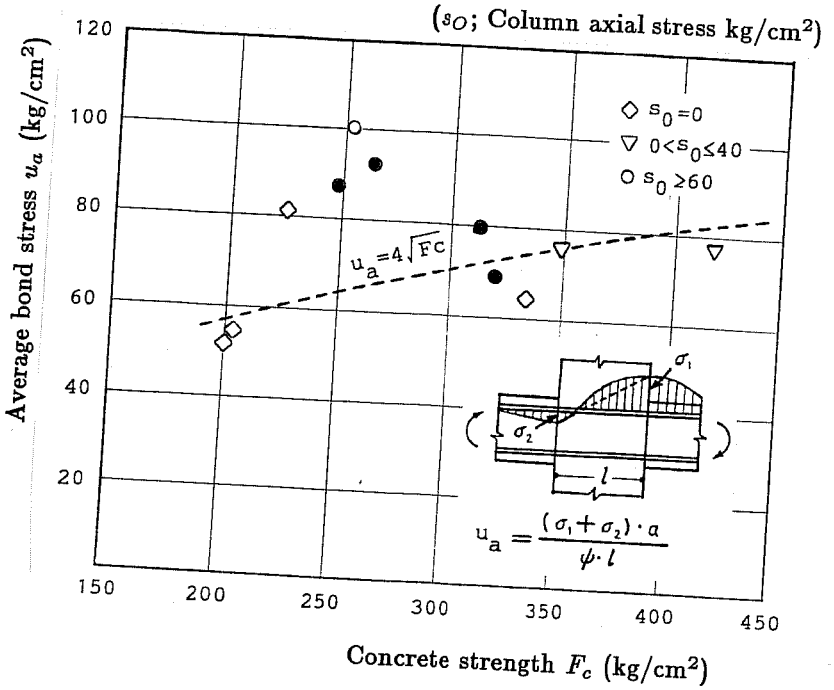

Fig. 2.7 Beam bar bond stress within joint depth

The draft code describes a method to design the joints for bond stress along beam longitudinal D51 bars. The following equation may be used to evaluate the ultimate bond stress and examine the joint depth required for beam bar development.[6]

$$u_a = 4\sqrt{F_c} \tag{6}$$

where

u_a = ultimate bond stress (kgf/cm²)
F_c = concrete strength (kgf/cm²)

This equation was derived from test results of interior joint specimens which failed in beam flexure as shown in Fig. 2.7. The average bond stresses calculated from bar stresses measured at the maximum load stage are shown. Solid circles show the results of tests with D51 bars.[10] Using u_a from Eq. 6, the minimum joint depth (column depth in general) is given by the following equation.[6]

$$h_{min} = f_y \cdot d_b/(4 \cdot u_a) \tag{7}$$

where

h_{min} = minimum joint depth (cm)
f_y = yield strength of longitudinal bar (kgf/cm²)
d_b = bar diameter (cm)

In this equation, longitudinal bars are assumed to be at tensile yielding at one end of the joint and at zero stress at the other end. Therefore, the minimum joint depth gives the minimum development length for longitudinal bars such that tensile stresses will not be present throughout the joint.

The minimum development length for D51 bar anchorage is also provided in the draft code as shown in Table 2.1.[6] The values in the *AIJ Standard for RC Structures*[3] for D6 to D41 bars are shown in parentheses for comparison.

2.3 Design Practice

In Japan, RC buildings are designed for loads (mainly seismic loads) specified by the *Building Standard Law and Enforcement Order*. The requirements in the *Buildings Standard Law and the Enforcement Order* are outlined elsewhere.[11] Details of the design generally meet provisions in the *AIJ Standard for RC Structures*.[3] However, the design of beam column joints is left to the designers' judgment, because the AIJ Standard does not cover the joints. Particularly in the case of low-to-medium-rise buildings, the joints are seldom designed. Usually a nominal amount of lateral reinforcement such as D10 hoops spaced at 15 cm is arranged in the joints of those buildings conforming to conventional construction specification. On the contrary, the joints are carefully designed in the case of high-rise buildings where high strength concrete and large size reinforcing bars are used to reduce structural member dimensions and thus jeopardize the joints.

Generally the joints are designed for forces generated by a beam hinge mechanism. Therefore, the design of the joints is usually carried out after proportioning the beam and column sections. The AIJ equations for SRC joints (Eqs. 1 and 2) or Kamimura's equation (Eq. 3) are commonly used to design the joints for shear.

It should be noted that those equations are based on the test results of interior (+ shaped) joints without transverse beams. The beneficial effect of the transverse beams on the joint shear strength is usually disregarded in the design. As shown in Fig. 2.8, the joints have three variations with the number of transverse beams (0, 1 and 2). However, in the usual design, these differences are not considered. Generally the joints are designed independently in two principal directions so that no biaxial effect is considered. If three beams frame into a joint, the joint is classified as an interior joint in the two-beam direction and as an exterior joint in the one-beam direction. According to the AIJ equation (Eq. 2), the joint has different shear strength in the two directions.

As part of the joint design, the column depth is examined using Eqs. 6 and 7. Sometimes the column depth is specified by the straight bar development length of 20 times bar diameter. The value of 20 is commonly used as the minimum ratio of column depth-to-beam-bar diameter in the design of high-rise buildings.

Table 2.1 Minimum Development Length of D51 Bar Terminating in Joint

Steel Grade	Nominal Yield Strength (kgf/cm^2)	$F_c \leq 250$ kgf/cm²		$F_c > 250$ kgf/cm²	
		Type 1	Type 2	Type 1	Type 2
SD30	3000	27d (30d)	18d (20d)	24d (25d)	16d (15d)
SD35	3500	36d	24d	32d	21d
SD40	4000	(35d)	(25d)	(30d)	(20d)

F_c: Concrete strength, d: Bar diameter
( ): Requirements in *AIJ Standard for RC Structures*

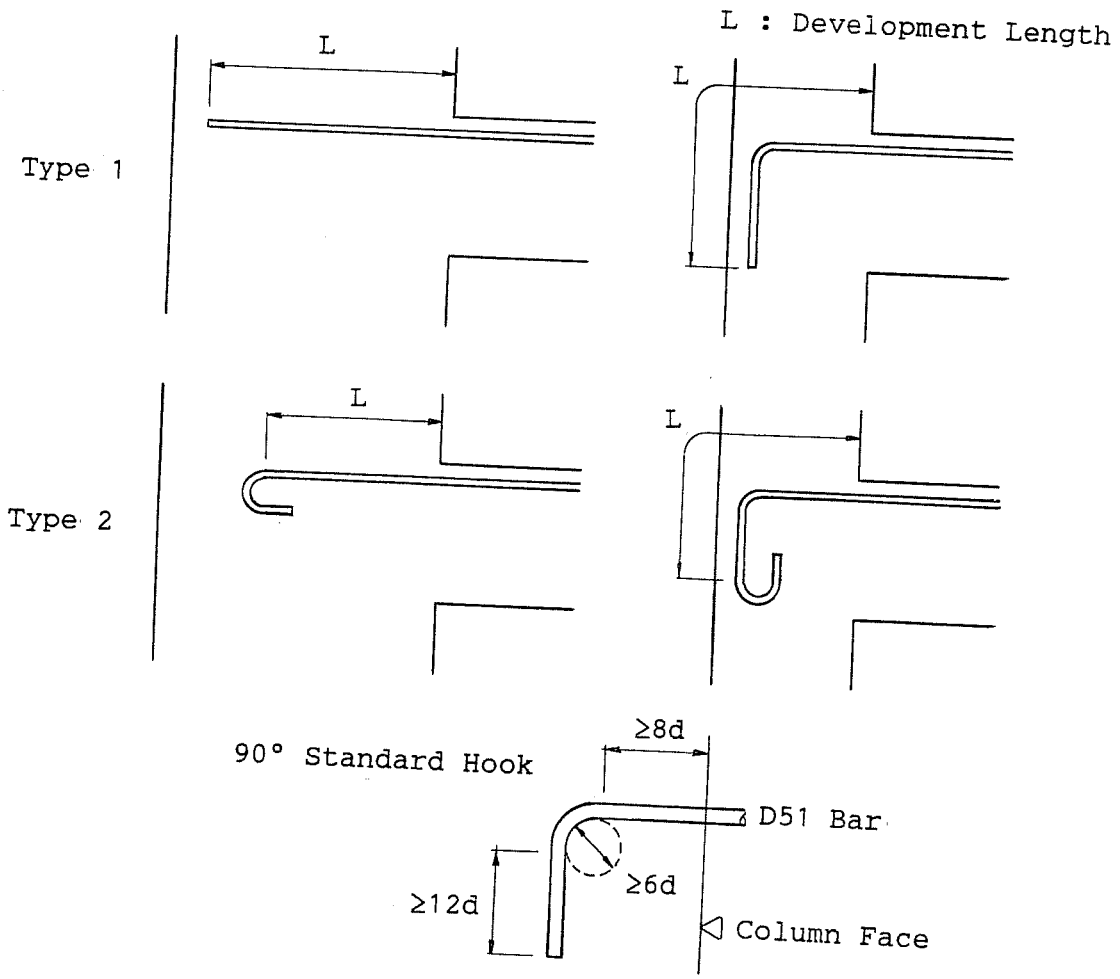

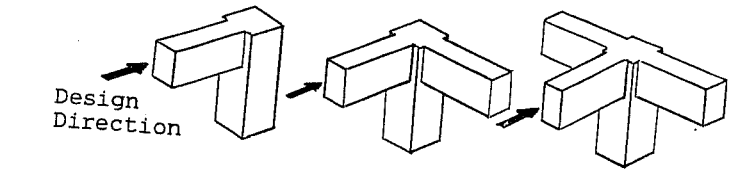

(a) Corner joints

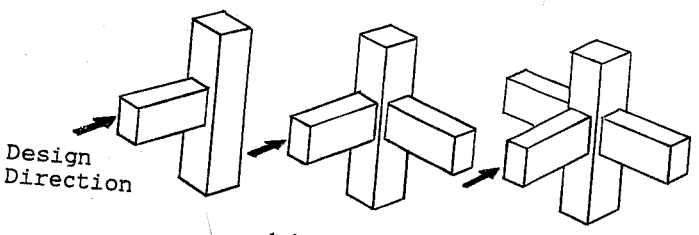

(b) Exterior joints

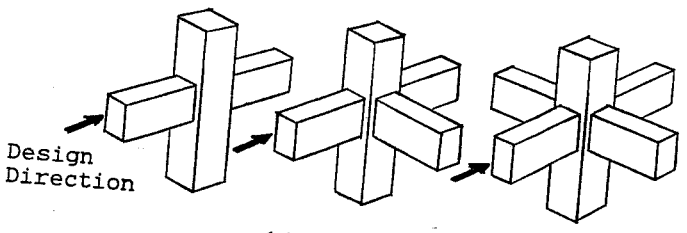

(c) Interior joints

Fig. 2.8 Joint variations with transverse beams

After proportioning of beams, columns and joints a dynamic response analysis is carried out to check the design of high-rise buildings.

The inelastic frame model as well as the mass-spring-dashpot model is used in the analysis.[12,13] The joints are generally idealized as rigid zones so that no shear distortion is considered. Inelastic deformations are concentrated at member end plastic hinges in the frame model.[14] Takeda's hysteretic model[15] is commonly used to simulate the hysteretic behavior of the plastic hinges. The dynamic analysis reported in Ref. 16 accounted for the joint shear distortion by incorporating joint shear panels into the frame model. The shear stress-distortion relations for the joint panels were simulated by the degrading trilinear hysteretic model.

An example of a joint design is given in Appendix A. Other examples are given in Ref. 17. The general design procedure for RC medium-rise buildings is outlined in Ref. 23. Appendix B describes concrete and reinforcing bars in common use in Japan.

3. U.S.-N.Z.-JAPAN-CHINA COOPERATIVE PROJECT ON DESIGN OF REINFORCED CONCRETE BEAM-COLUMN JOINTS– JAPANESE CONTRIBUTIONS

3.1 Summary of Meetings

Under the U.S.-N.Z.-Japan Project on Design of Reinforced Concrete Beam-Column Joints, a trilateral cooperative research project among the United States, New Zealand, and Japan has been underway since 1984. The People's Republic of China (P.R.C.) recently began participating in the project.

The first meeting was held in Monterey, California, July 30 to August 1, 1984. The purpose of the first meeting was as follows:

1. To discuss design approaches in New Zealand, U.S., and Japan for beam-column joints in frames designed to resist seismic lateral forces.
2. To initiate a collaborative research effort aimed at investigating the differences between the design approaches and explaining those differences to practicing engineers.

An overview of design codes in U.S., N.Z., and Japan clarified the differences in design approaches for joints in those countries. Reports on studies of joints were presented and discussed. Six research reports were prepared for the meeting by Japanese participants.[17–22]

The second meeting was held in Tokyo, Japan, May 29 to 30, 1985. After a brief review of the Monterey meeting, current studies on joints were presented and discussed. The presentations included seven research reports from Japanese participants.[23–29] The design of test specimens for the cooperative program was reported by the participating research groups. Testing methods were discussed and agreed on as follows.

1. Column failure should be prevented. Simultaneous bidirectional loading is desired after the mechanical properties are defined under uniaxial loading.
2. The yield deflection should be determined to be 1.33 times the deflection observed at three-quarters of the calculated ultimate load. The ultimate load should be calculated as follows; (a) use measured material properties (no strain hardening), (b) use the effective width of slab to be 600 mm on each side of a beam (the total width of $600 \times 2 + 400 = 1{,}600$mm), (c) consider the ultimate moments at the critical sections of both beams, (d) use a capacity reduction factor of unity.
3. The test should be controlled by displacement following the loading history shown in Fig. 3.1. At completion of cycles in a given direction, deflection will be held at neutral (zero) position while cycling in orthogonal direction.

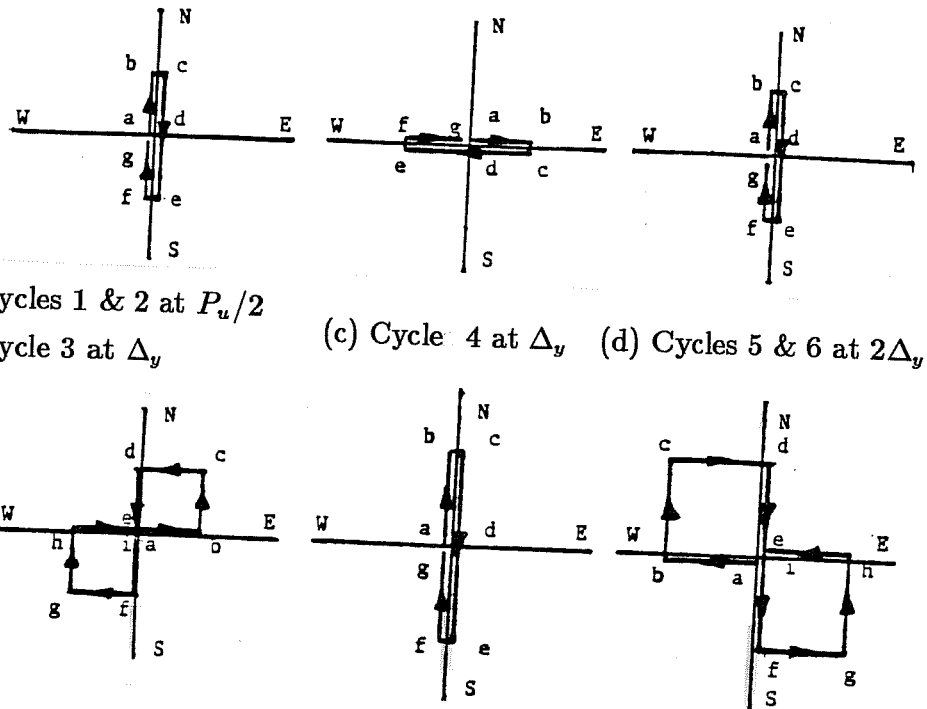

(a) Cycles 1 & 2 at $P_u/2$
(b) Cycle 3 at Δ_y
(c) Cycle 4 at Δ_y
(d) Cycles 5 & 6 at $2\Delta_y$
(e) Cycles 7 & 8 at $2\Delta_y$
(f) Cycles 9 & 10 at $4\Delta_y$ or 0.02 drift
(g) Cycles 11 & 12 at $4\Delta_y$ or 0.02 drift

P_u: calculated ultimate load Δ_y: yield deflection

Fig. 3.1 Bidirectional loading history (U.S.-N.Z.-Japan Cooperative Program)

The third meeting was held in Christchurch, New Zealand, August 10 to 12, 1987. The bidirectional loading tests using the testing methods described above were presented and discussed. Seven Japanese reports were presented.[30-36]

The list of participants in the meetings is given in Appendix C. Japanese participants consisted of researchers from Universities of Tokyo, Kyoto, Hokkaido and Meiji, Osaka Institute of Technology and General Building Research Corporation. The Japanese studies presented in the meetings are outlined hereafter.

3.2 Studies on RC Interior Joints

Various tests were conducted to study the behavior of RC interior (+ shaped) joints under unidirectional and/or bidirectional loading conditions. Some of the test results were analyzed statically using a nonlinear finite element method. The dynamic behavior was examined using hysteretic models simulating force-deformation relations measured in the tests. The studies are outlined below.

3.2.1 Unidirectional Loading Tests.

Hokkaido University. Three series of interior beam-column joint specimens were tested at Hokkaido University.[21,35,36] In the first series[21] six specimens (B1 through B6) were tested to investigate the effect of geometry on joint behavior, as shown in Fig. 3.2. Specimen B1 was the reference test. Specimen B2 had beams of the same width as the columns. Specimen B3 had the standard beam on one side and a smaller and shorter beam on the other side. Specimen B4 was identical to B1 except it had less beam bottom reinforcement. Specimens B5 and B6 were eccentric joints. All specimens were designed to fail in beam flexure. The beam-column joints were laterally reinforced with three ϕ6, (see Appendix B) hoops spaced at 87.5 mm.

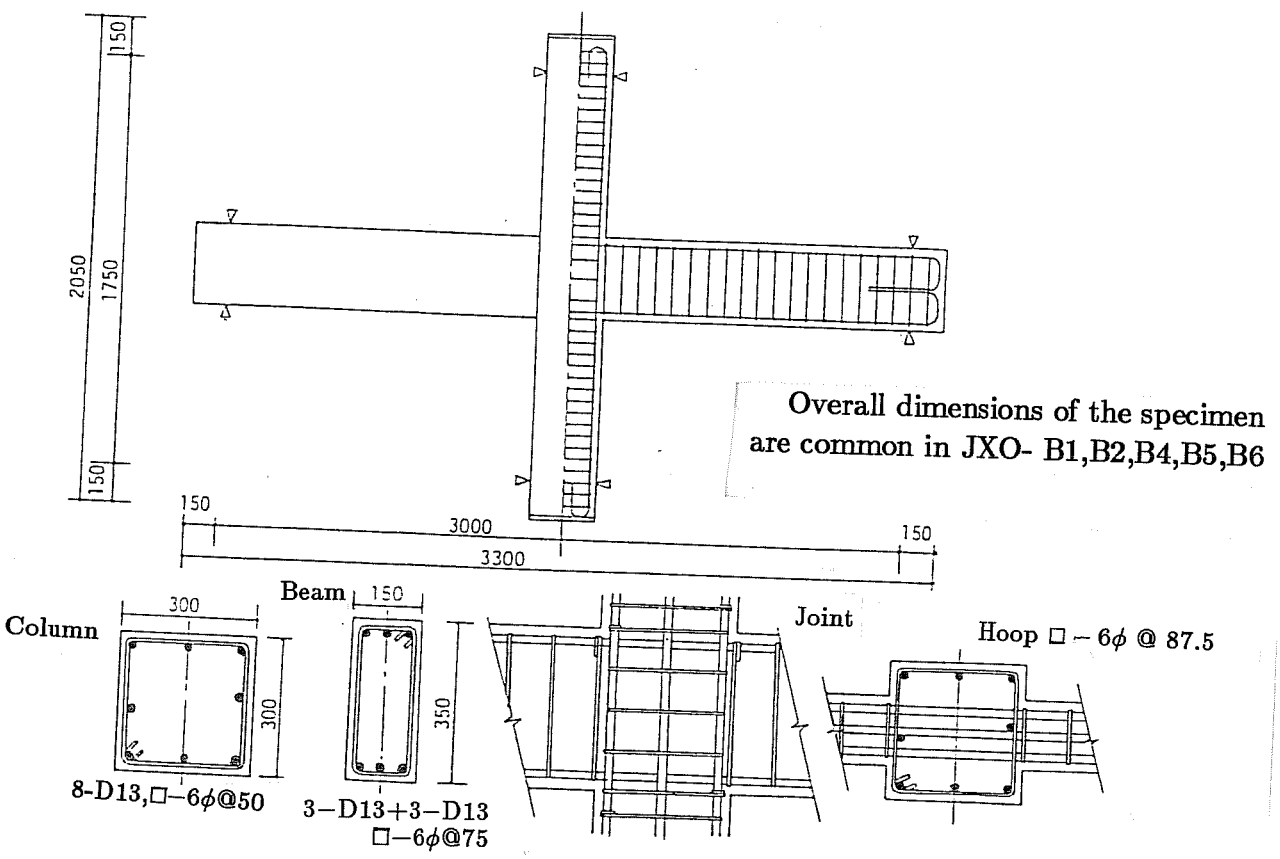

(a) Specimen B1

Fig. 3.2 Details of interior joint specimens

In B4 the bottom beam reinforcement consists of 2- D13.

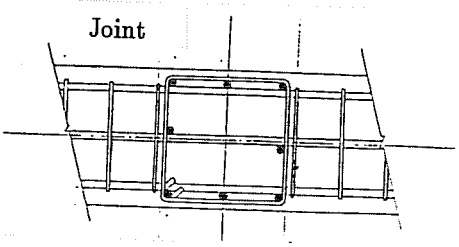

(b) Specimen B2

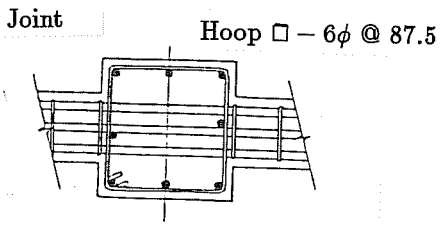

(d) Specimen B4

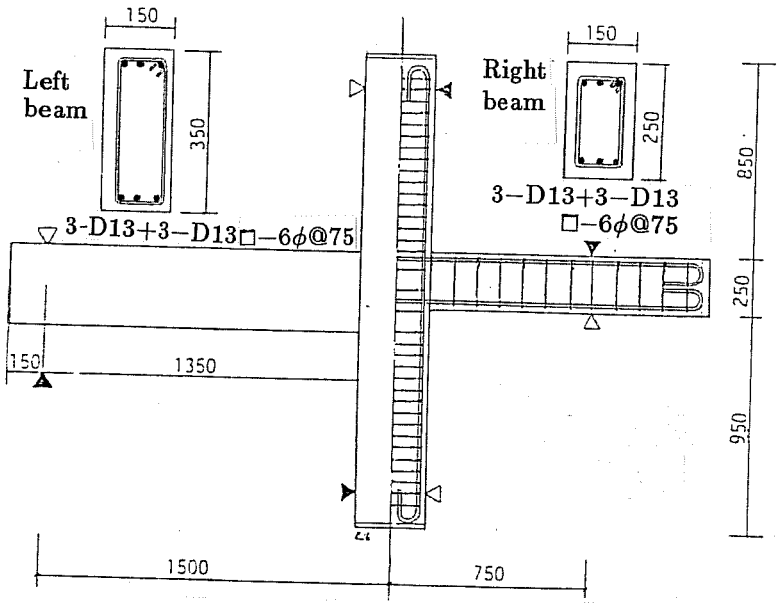

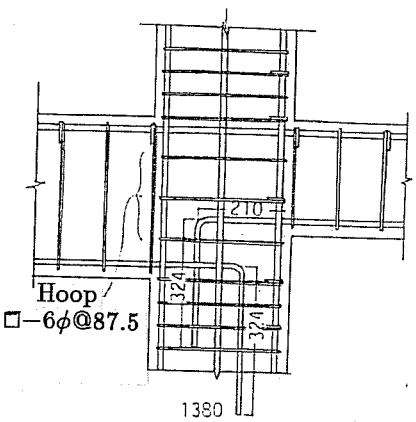

(c) Specimen B3

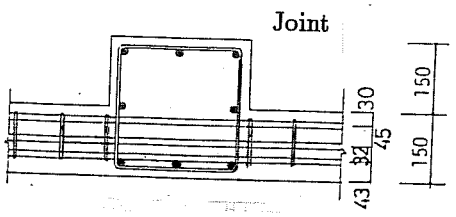

(e) Specimen B5

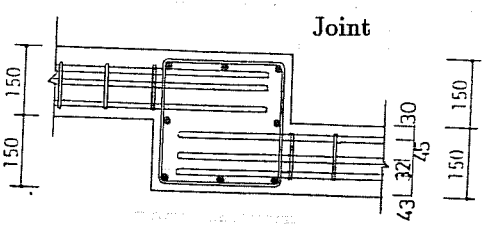

(f) Specimen B6

Fig. 3.2 Continued

Concrete strength ranged from 212 to 276 kgf/cm^2. Bar yield strength was 3780 kgf/cm^2 for longitudinal reinforcement (D13) and 3130 kgf/cm^2 for lateral reinforcement. The loading setup is shown in Fig. 3.3. The beams were deflected equally but in opposite directions. A constant axial load of 31.5 ton was applied to all specimens. Story shear-drift angle relations are shown in Fig. 3.4. Specimens B1, B5 and B6 failed in joint shear after forming plastic hinges at beam ends. Specimens B2, B3 and B4 failed in beam flexure. It was reported that the wide beam specimen (B2) failed in beam flexure, but the narrow beam specimen (B1) filed in joint shear. The eccentric joint specimens (B5 and B6) showed poorer ductility compared with the others, although these specimens reached almost the same maximum load as the others. However, the beam end rotation measured in the eccentric joint specimen B6 showed better hysteresis than that in the standard Specimen B1, as shown in Fig. 3.5. This is probably because the beam bars in B6 were anchored in the joint but those in B1 were continuous through the joint. The shear distortion measured on both sides of the eccentric joint of B5 showed that larger distortion took place on the beam side of the joint than on the other side, as shown in Fig. 3.6.

The second series of unidirectional loading tests at Hokkaido University[35] were intended to improve the hysteretic behavior of interior joints by developing beam plastic hinges at a distance from the column face. This series was aimed at reducing bond deterioration of beam longitudinal bars along their anchorage through the joint. To locate the plastic hinge away from the column face, additional beam bars terminating in 90° hooks at both ends were arranged in the critical region adjacent to the joint, as shown in Fig. 3.7. Specimen B8 had standard details and the beam plastic hinges were expected to form at the column face. Specimens B9 through B11 were detailed so that the critical sections of the plastic hinges were located at $D_b/2$ (175 mm) to D_b (350 mm), D_b = beam depth, from the column face. The additional top bars in Specimen B11 were cranked and extended into the bottom of the beam. The beam critical region was confined with ϕ6 three-leg stirrups spaced at 50 mm. Concrete strength ranged from 24.9 to 25.9 MPa. Bar yield strength was 404 MPa for longitudinal reinforcement (D13) and 377 MPa for lateral reinforcement except in the joint. The joint reinforcement was designed to meet the requirements in New Zealand code[37] and was fabricated with ϕ5 steel bars having a yield strength of 1010 to 1320 MPa.

The specimens were loaded in the same manner as in the first series. All specimens failed in beam flexure as shown in Fig. 3.8. Specimen B8 failed at the region immediately adjacent to the joint, while the other specimens failed at the expected critical sections where the additional beam bars were hooked or bent. Story shear vs drift angle relations are shown in Fig. 3.9. The hysteretic curves for Specimen B8, hinging at the column face, showed considerable pinching after reaching the maximum load in cycle 9. This is probably due to the slippage of the beam bars in the joint. Specimens B9 and B11, hinging at $D_b/2$ and at $D_b/2$ to D_b, respectively, showed stable and spindle-shaped hysteresis loops even in the final cycle, although Specimen B10 with hinging at D_b, showed some pinching as observed for B8.

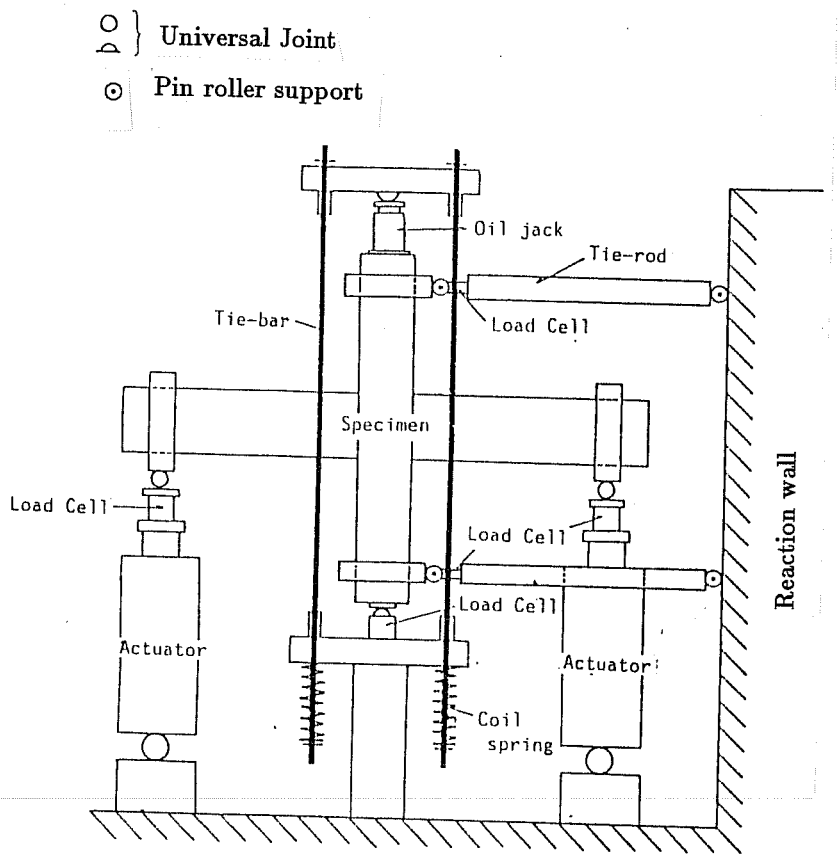

Fig. 3.3 Loading setup

It should be noted that the plastic hinges in B10 were required to undergo the largest rotation and carry the highest shear force at equal story drifts because B10 had the shortest distance form the critical section to the loading point. Beam end rotations measured at the joint face are shown in Fig. 3.10. The rotation for Specimen B8 was much larger than that for the other specimens and showed considerably pinched hysteresis as observed in the story shear-drift angle relation.

Figure 3.11 shows the strain distributions along beam bars for Specimen B9. The maximum tensile strains were observed at the critical section for the main beam bars and at the column face for the additional bars.

The last of the three series at Hokkaido University[36] was conducted to study the effect of lateral reinforcement on the bond behavior of beam longitudinal bars passing through the joint. Four specimens, variations of Specimen B8 in the second series, were designed changing the details of the lateral reinforcement in the joint and/or the beam end critical region, as

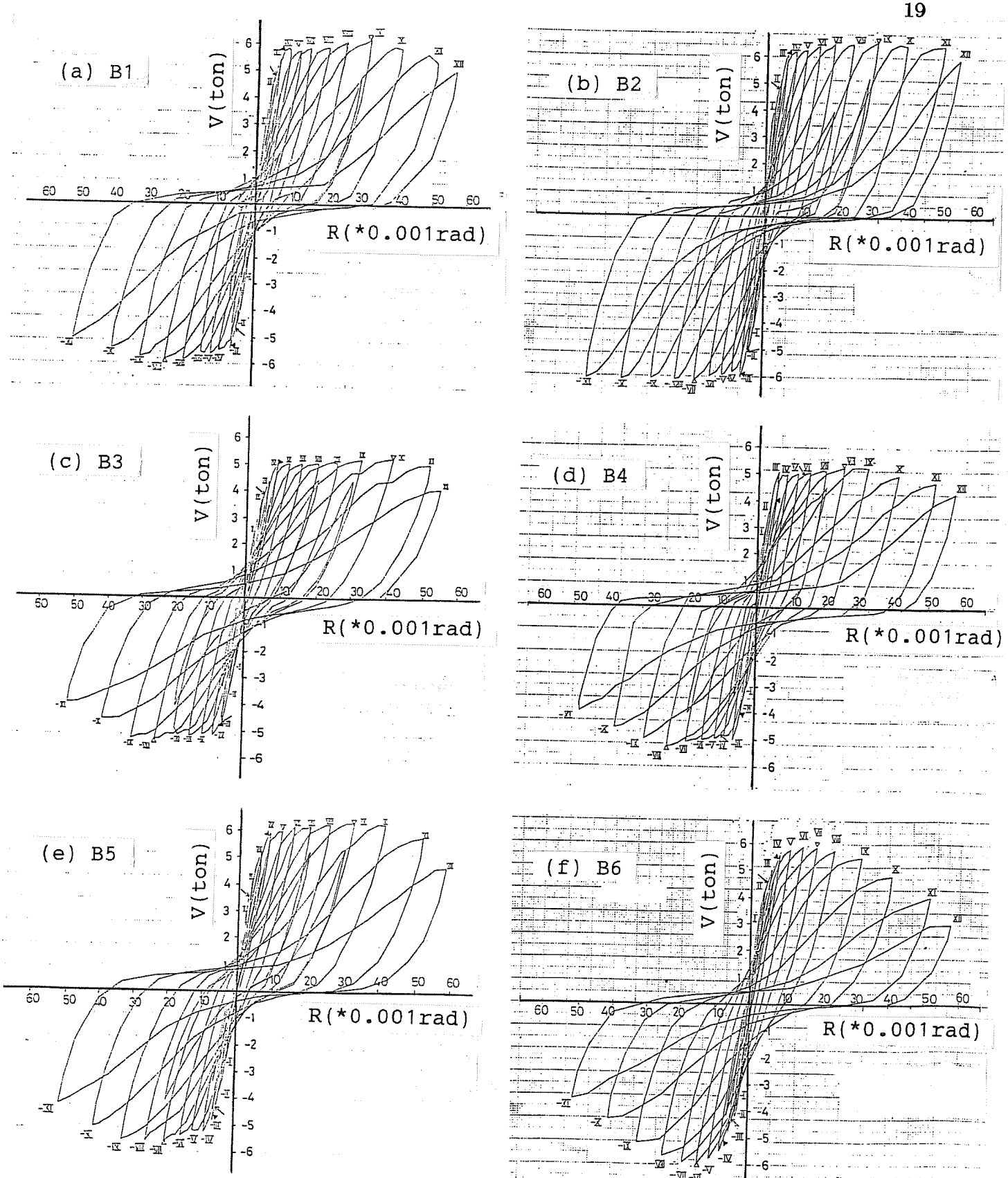

(V: story shear, R: drift angle)

Fig. 3.4 Story shear vs drift angle relations

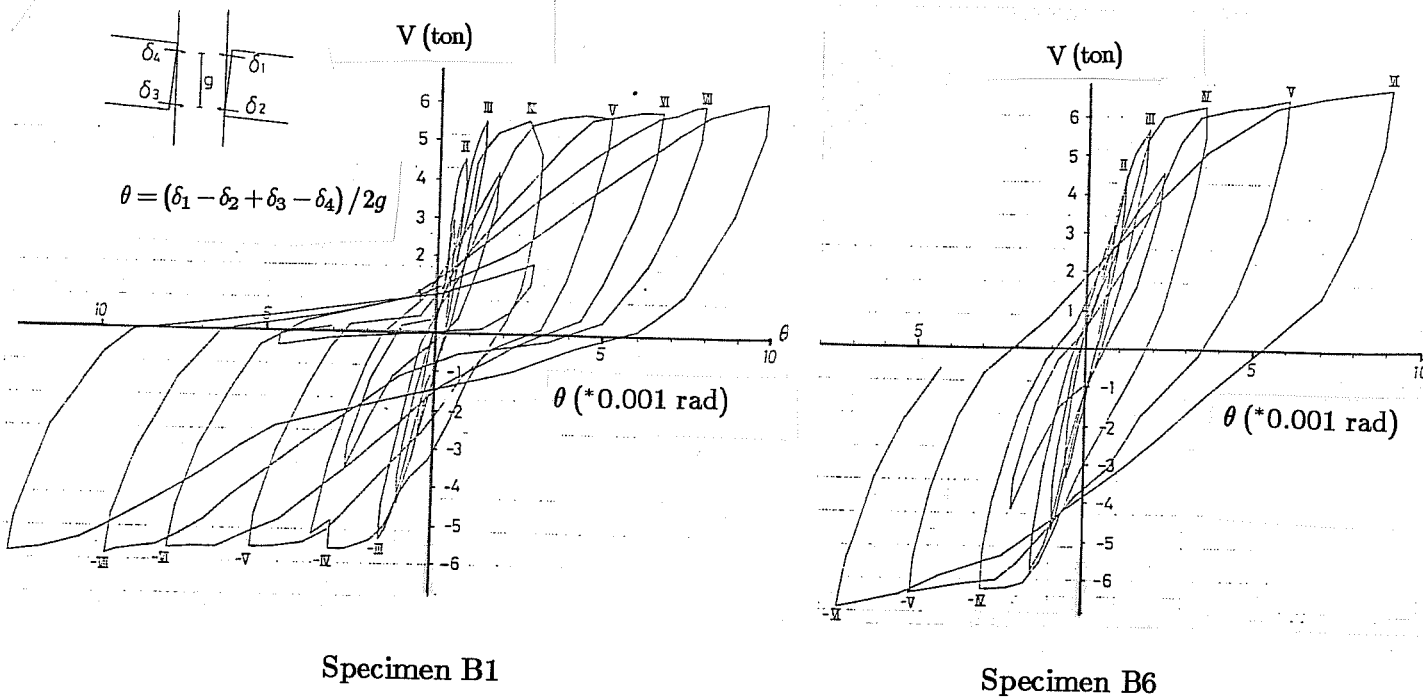

Specimen B1 Specimen B6

Fig. 3.5 Story shear vs beam end rotation

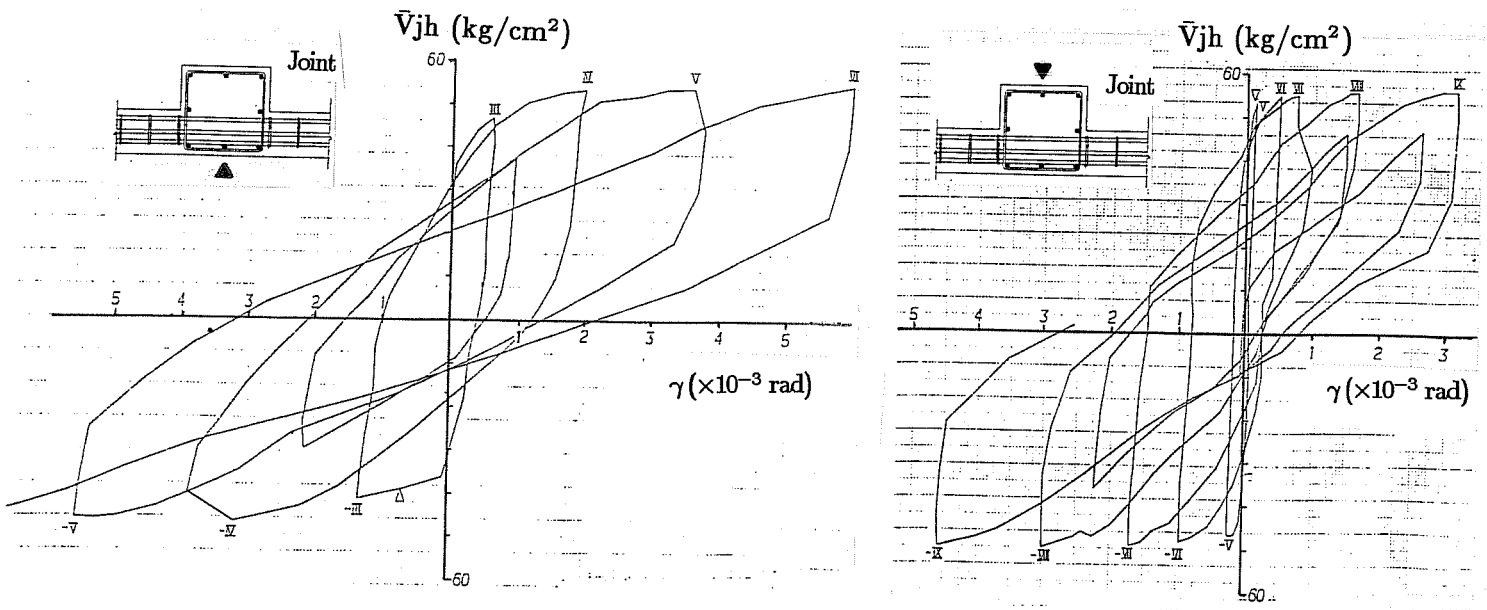

Fig. 3.6 Joint shear stress vs strain for Specimen B5

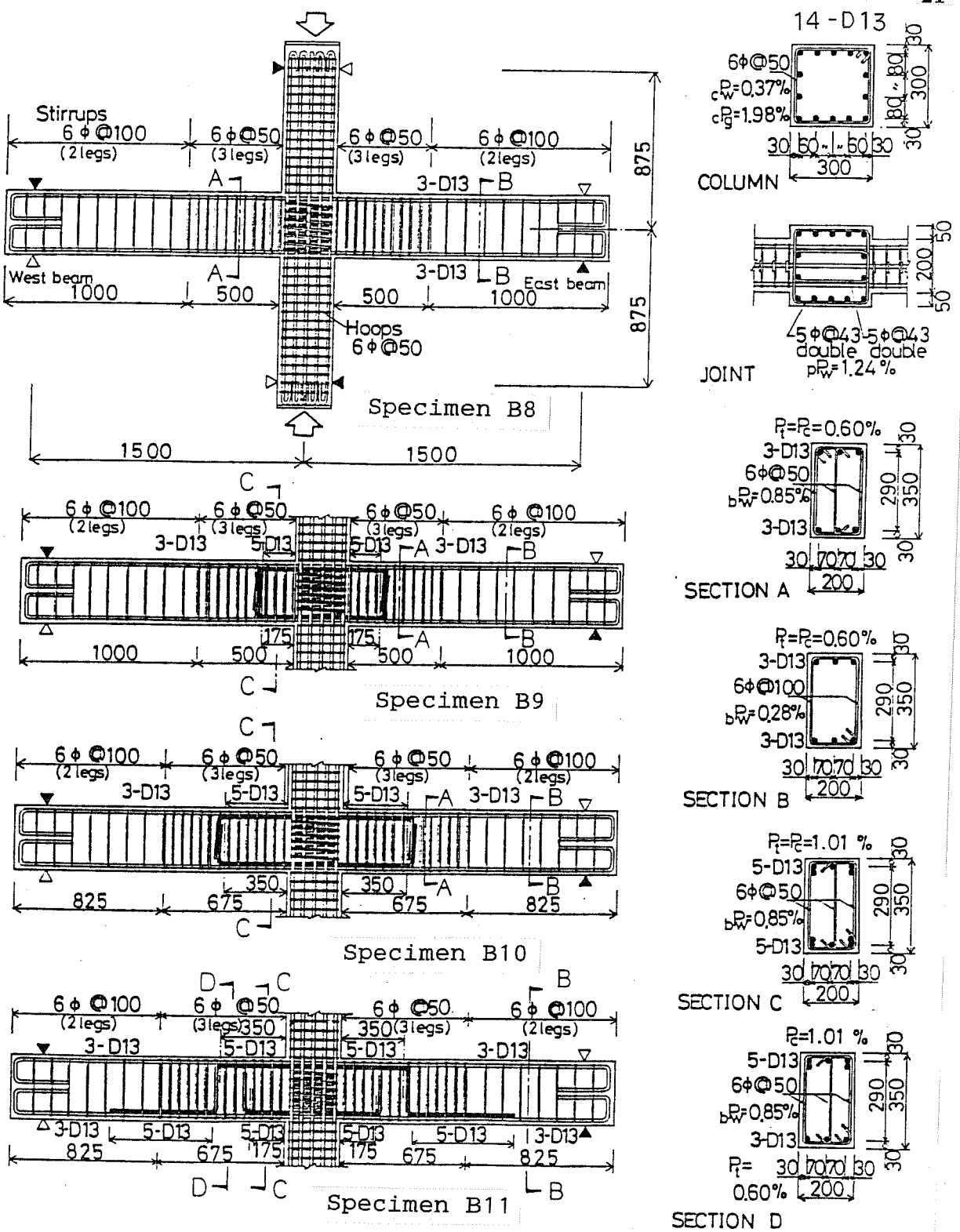

Fig. 3.7 Details of specimens

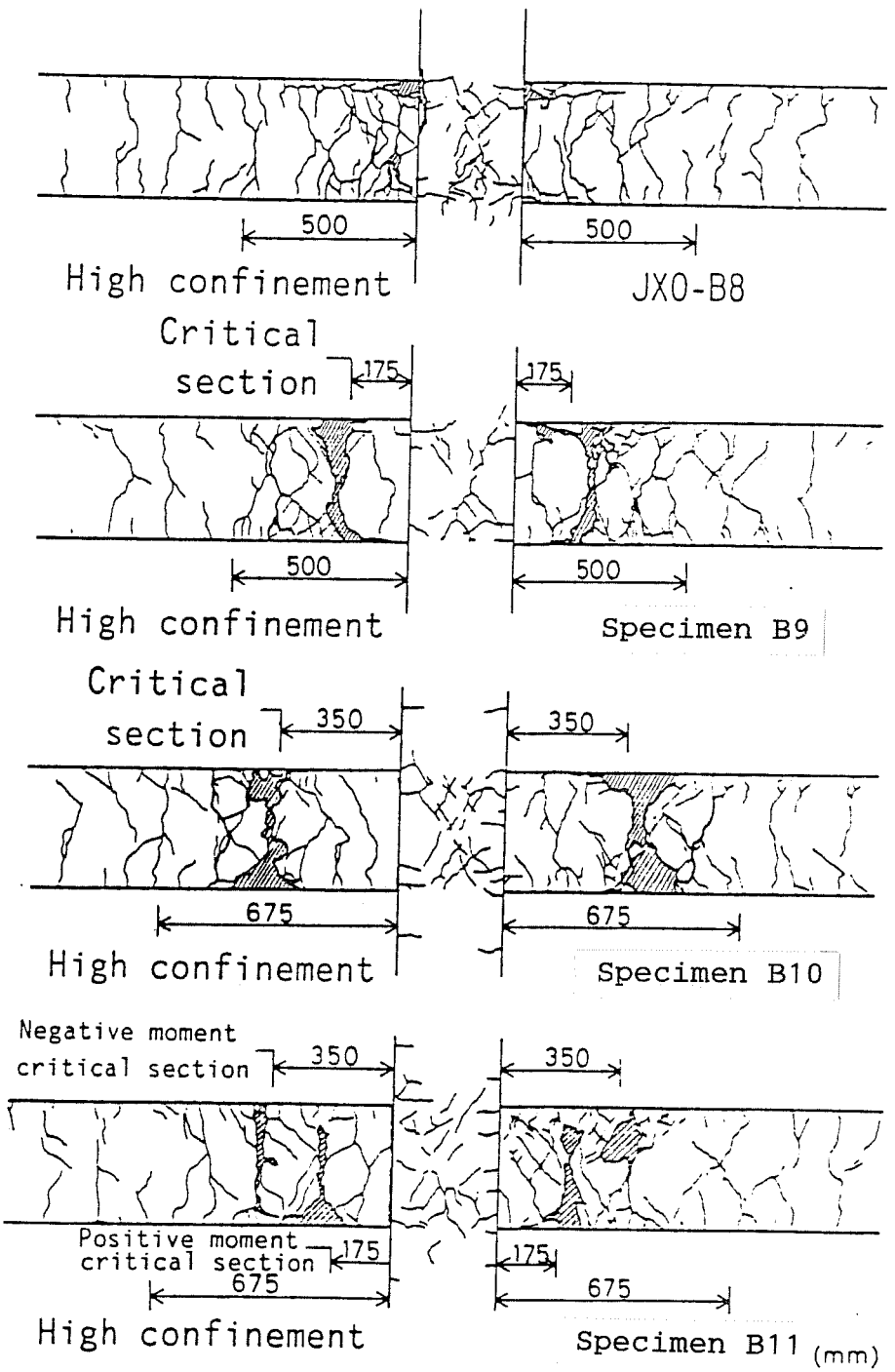

Fig. 3.8 Crack patterns after test

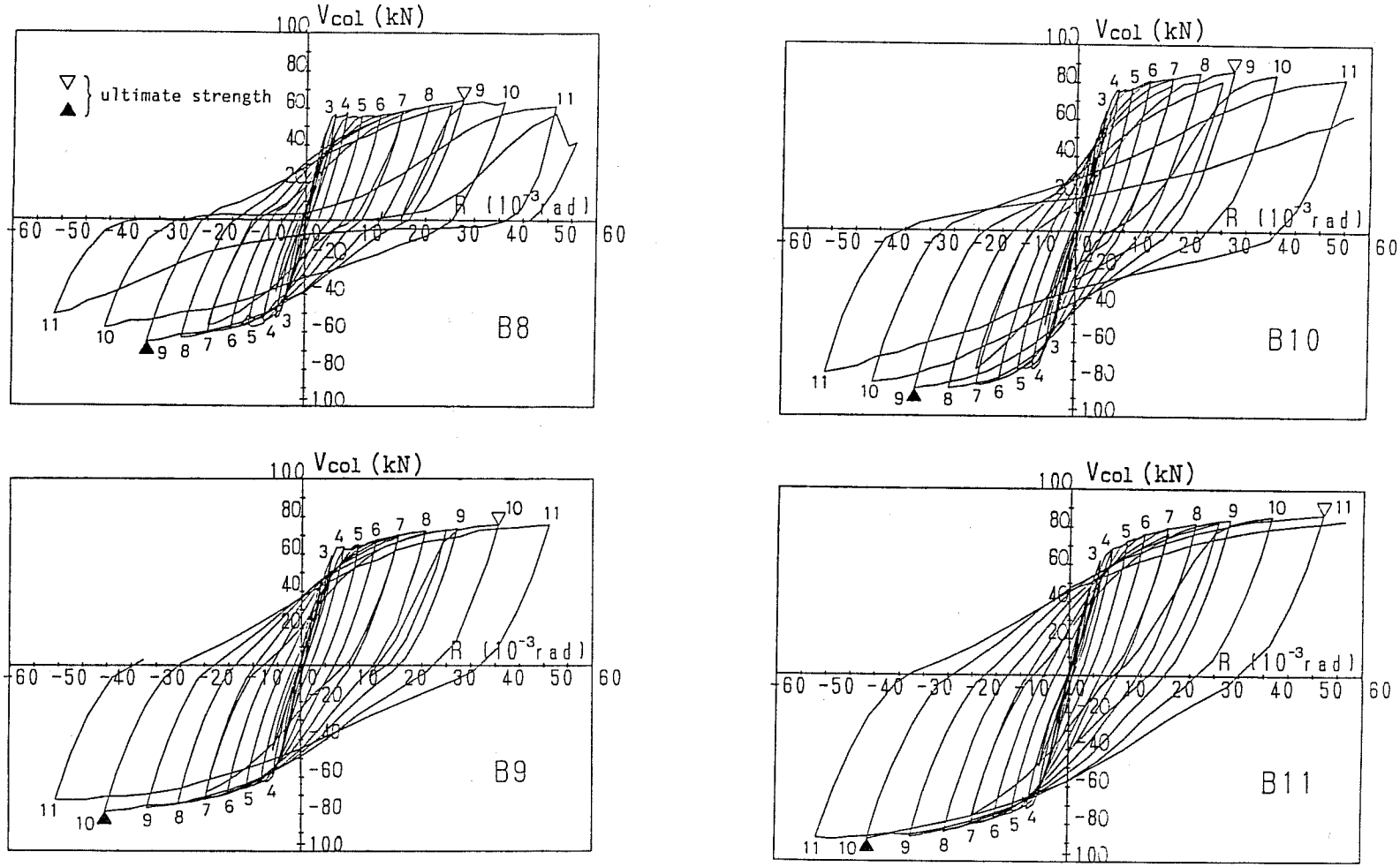

Fig. 3.9 Story shear vs drift angle relations

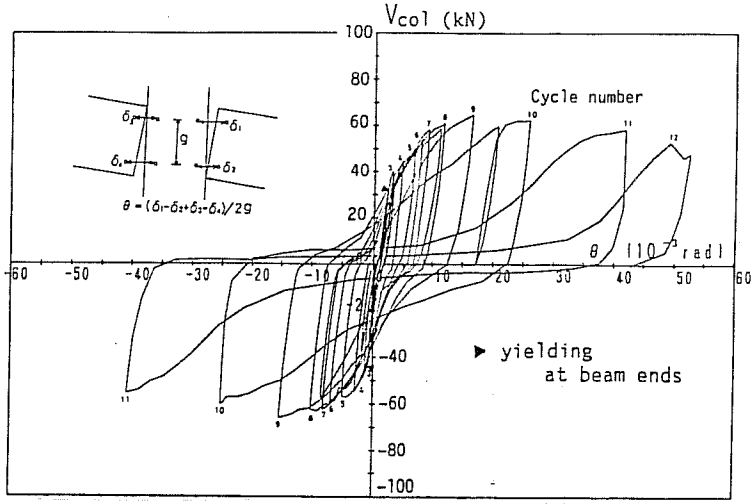

(a) Beam end rotation for Specimen B8

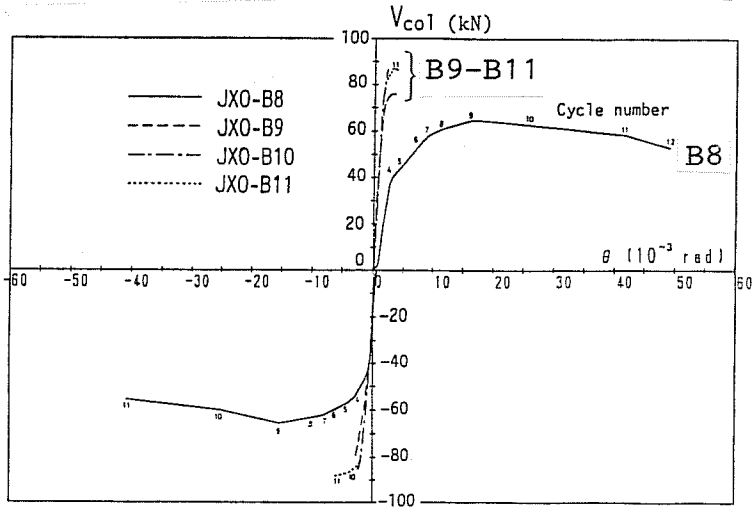

(b) Comparison of envelope curves

Fig. 3.10 Story shear vs beam end rotation

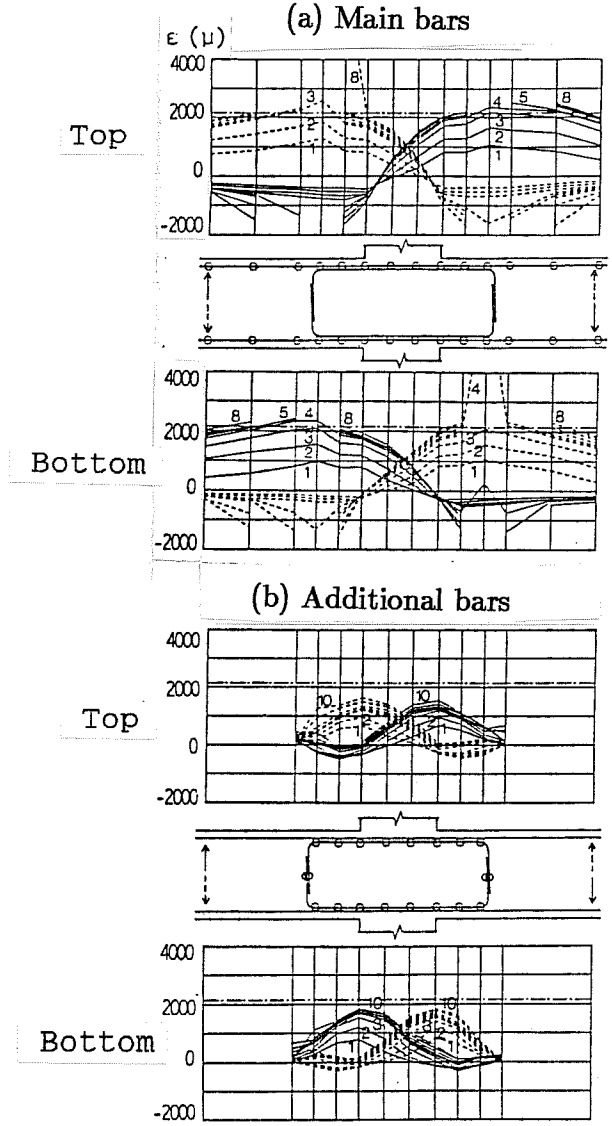

Fig. 3.11 Distributions of beam bar strains (Specimen B9)

shown in Fig. 3.12. The specimens in this series were designated with the combination of two letters representing the amount of joint beam transverse reinforcement, respectively. Specimen B8, designated as HH hereafter, and Specimen B1 in the first series were cited to compare results. Specimen MHUB, a variation of Specimen MH, was fabricated using vinyl chloride pipes to develop unbonded conditions along beam bars within the joint. Concrete strength varied from 26.1 to 28.1 MPa. Bar properties were identical to those in the second series. The same loading apparatus as in the previous two series was used to load the specimens. The column axial load was held constant at 353 kN. All specimens in this series failed in beam flexure as shown in Fig. 3.13.

Many shear cracks formed within the joint of specimens HH and HL with a large amount of joint reinforcement, while a few diagonal cracks opened widely in the joint of Specimen LH with a small amount of joint reinforcement. No shear cracks occurred in the joint of the unbonded specimen MHUB. Story shear-drift angle relations are shown in Fig. 3.14(a). The hysteretic loops became pinched and inverse-S-shaped with a decrease in the amount of the joint lateral reinforcement. The unbonded specimen MHUB showed remarkable pinching of the hysteresis curves and somewhat low strength compared with the other specimens. The joint shear distortion in MHUB was much smaller than that in MH, as shown in Fig. 3.14(b). Figure 3.15 shows slip of the beam bars measured relative to the joint face. Slip in Specimen MHUB was observed at the beginning of loading. Slip in the other specimens began after yielding of the beam bars occurred. The amount of slip, especially during pull-out loading, decreased roughly with increase of the joint lateral reinforcement.

University of Tokyo. Three series of RC interior joint specimens were tested under unidirectional loading at the University of Tokyo.[20,27] All specimens in these series were half-scale interior beam-column subassemblages designed to develop weak-beam strong-column behavior.

The dimensions of members were common to all specimens; beams were 200 mm $\times$ 300 mm, and columns were 300 mm $\times$ 300 mm. The specimens were tested using the loading apparatus shown in Fig. 3.16. The constant vertical load and reversing horizontal load were applied at the top of the column by two actuators. In the first series (S-series), six specimens shown in Fig. 3.17 were tested to study the effect of bond deterioration of beam bars passing through a beam-column joint.[20] Specimen S1 is the standard specimen, in which (a) D13 bars were used as beam longitudinal reinforcement, (b) the columns were subjected to an average axial stress of 60 kgf/cm^2, and (c) the joint was reinforced so that the entire shear could be resisted by shear reinforcement (D6 four-leg hoops spaced at 25 mm). Specimen S2 was subjected to a lighter column axial stress of 20 kgf/cm^2. D10 and D16 bars were used as beam longitudinal reinforcement in Specimens S3 and S4, respectively. Specimen S5 had monolithic spandrel walls above the beams with narrow slits against the column face so that

Variations of Specimens

Amount of Lateral Reinforcement		Beam End Stirrups	
		High ($P_w = 0.85\%$)	Low ($P_w = 0.28\%$)
Joint Ties	High* ($P_w = 1.16\%$)	HH**	HL
	Medium ($P_w = 0.41\%$)	MH (MHUB)	
	Low ($P_w = 0.21\%$)	LH	LH

P_w : Lateral reinforcement ratio
UB : Unbond beam bars
* : Fabricated with high strength steel
** : Specimen B8

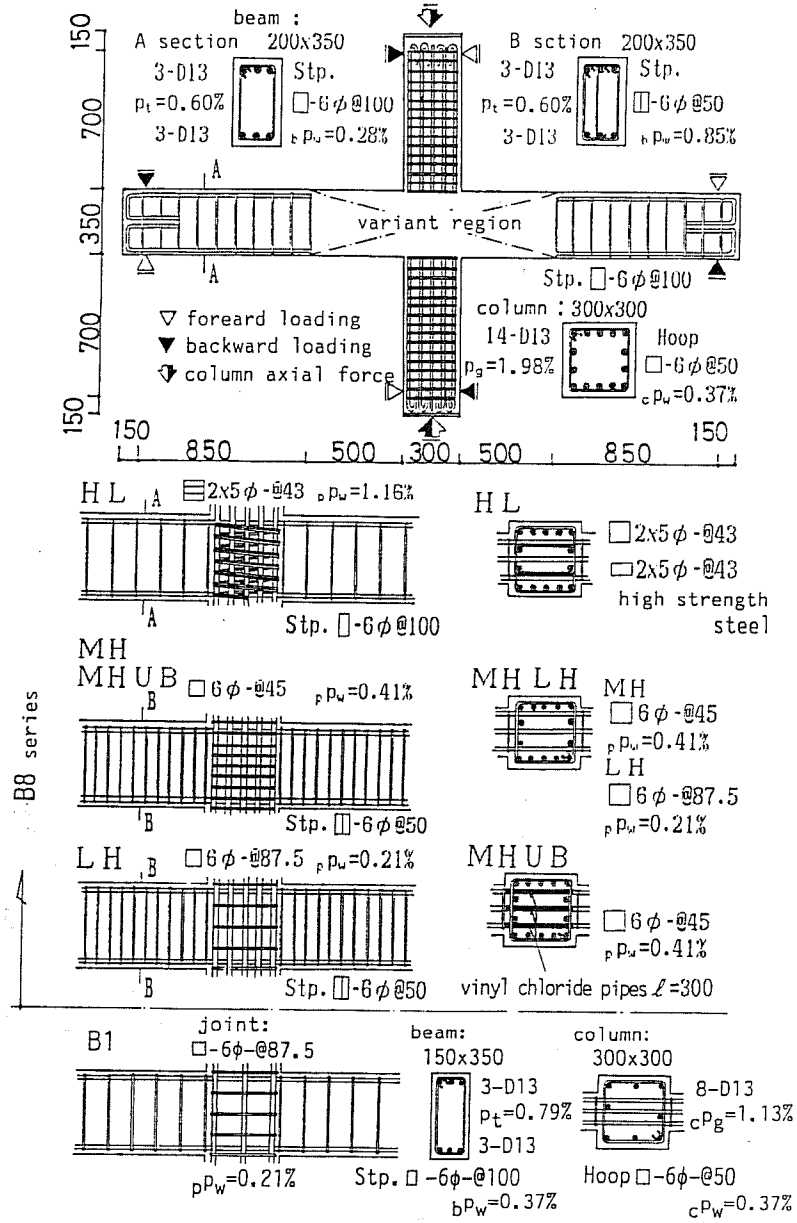

Fig. 3.12 Details of specimens

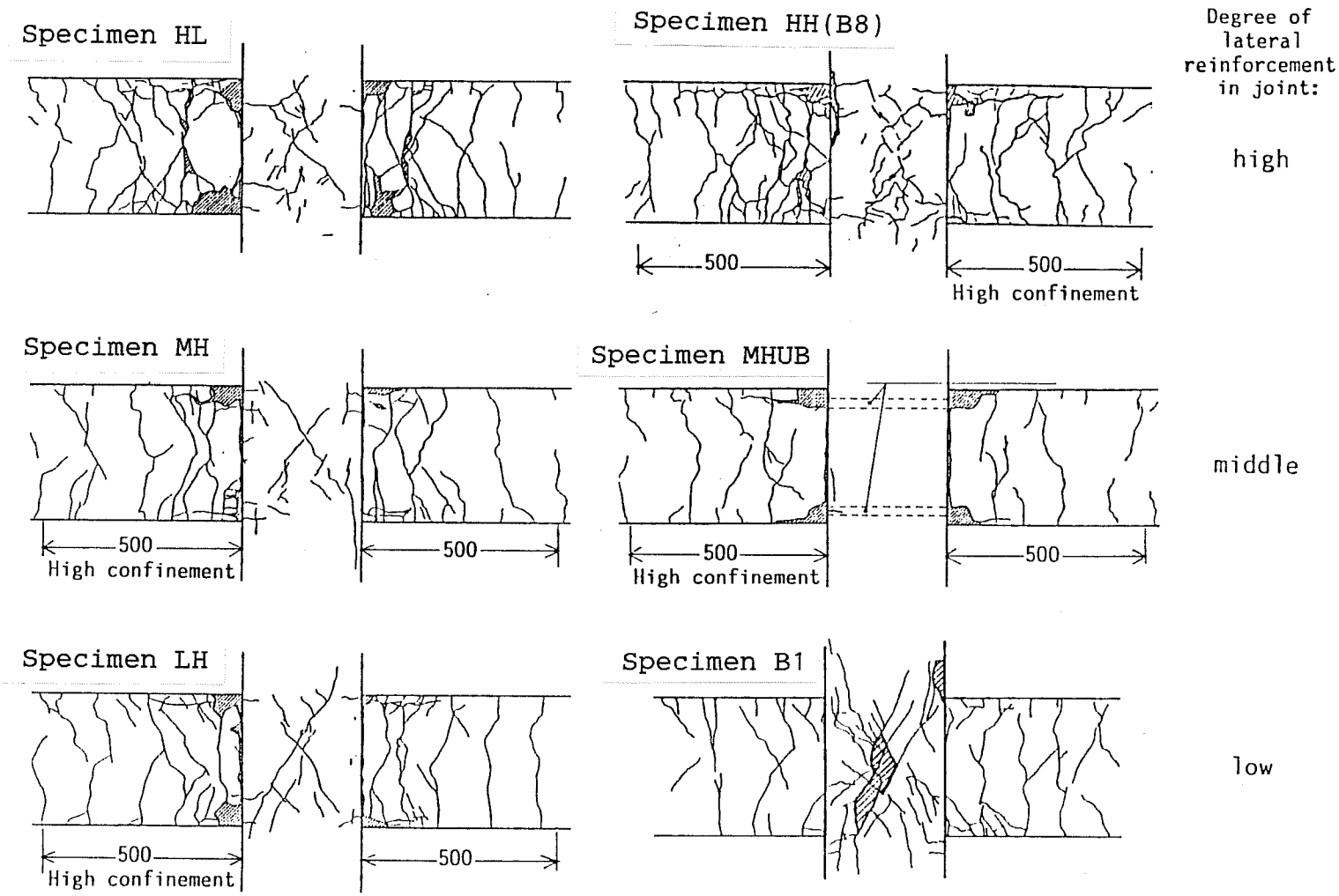

Fig. 3.13 Crack patterns after test

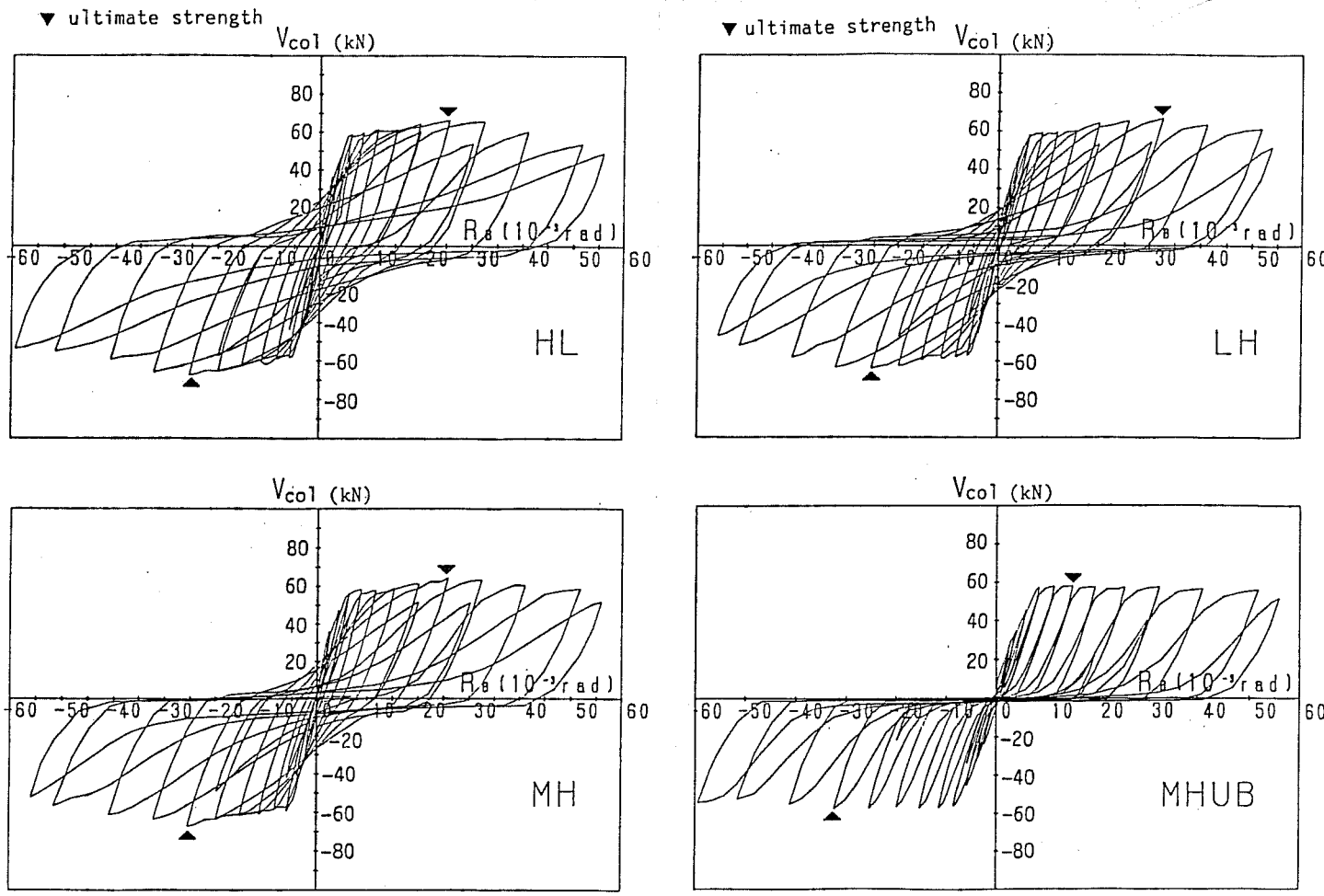

Fig. 3.14 (a) Story shear vs drift angle relations

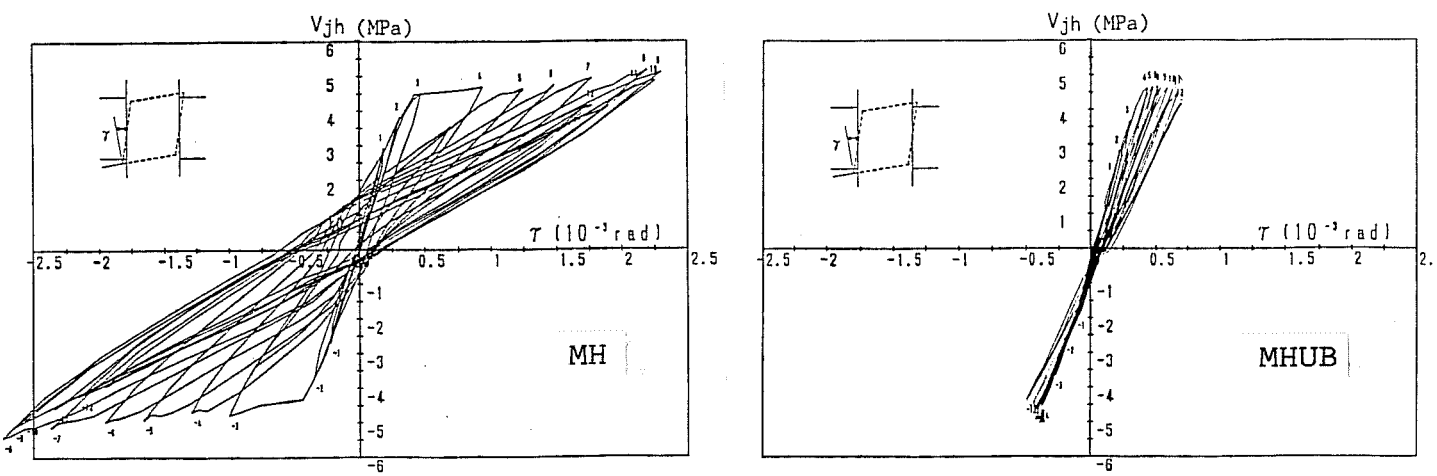

Fig. 3.14 (b) Joint shear stress vs shear distortion

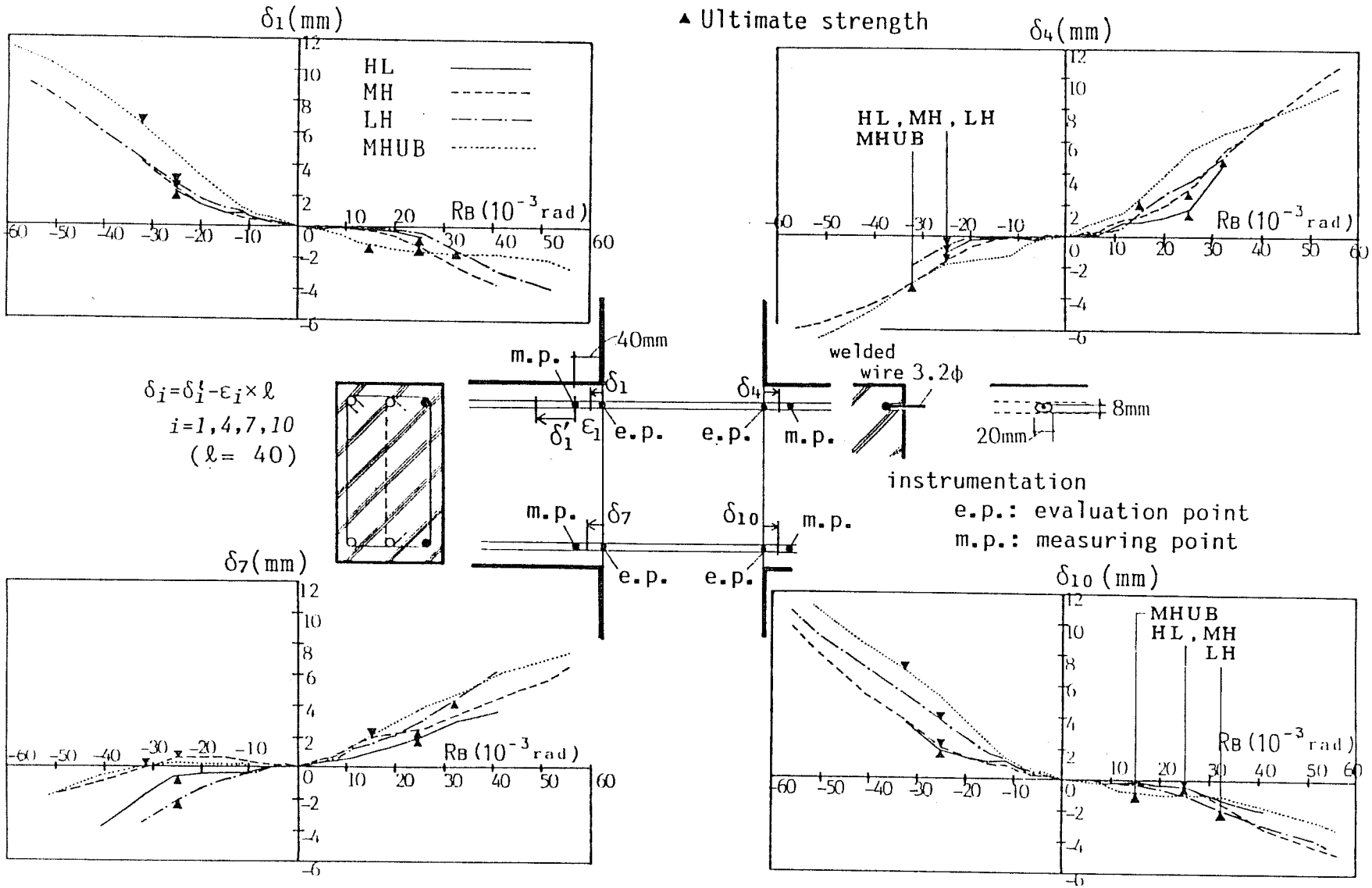

Fig. 3.15 Beam bar slippage vs drift angle relations

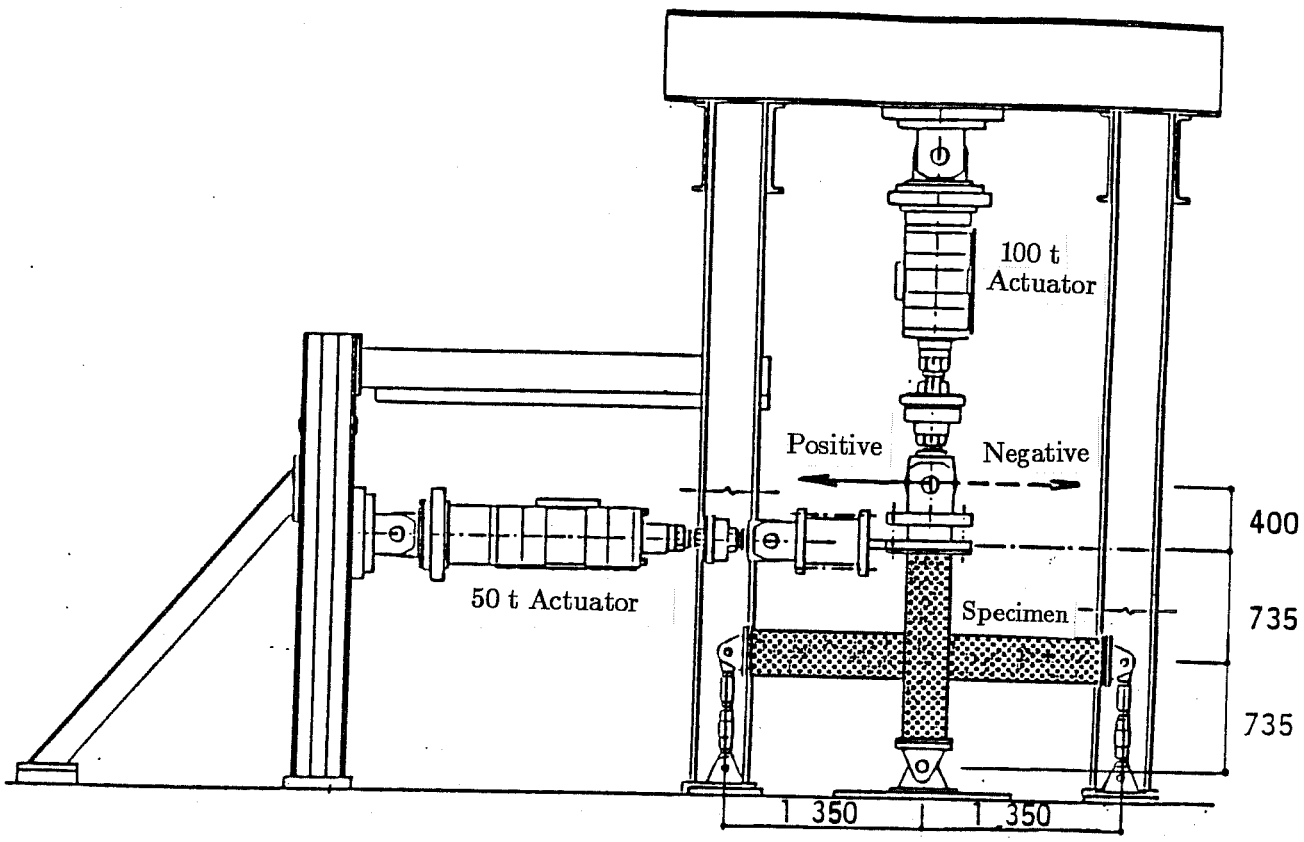

Fig. 3.16 Test specimen in loading setup

beam inelastic deformations were forced to concentrate in the slitted zones. In Specimen S6, the amount of the joint shear reinforcement was significantly reduced to a level commonly used in Japan (D6 two-leg hoops spaced at 50 mm).

The specimens were designed so that the average horizontal shear stress in the joint at flexural yielding of the beams would be less than the diagonal cracking stress calculated by the principal stress analysis. It should be noted that all specimens in this series had transverse beams 300 mm long. Concrete strength was 283 kgf/cm^2 for Specimens S1 through S3 and 256 kgf/cm^2 for S4 through S6. Bar yield strength was 3510 to 4250 kgf/cm^2 for longitudinal reinforcement and 3390 kgf/cm^2 for lateral reinforcement. The crack patterns observed at the end of loading are shown in Fig. 3.18. All specimens developed beam hinges. The story shear-drift relations are shown in Fig. 3.19. The story shear was calculated from the measured load applied by the horizontal actuator corrected for the P-delta effect. Most specimens showed a slip-type hysteresis after yielding except Specimen S2 which was subjected to a lower vertical load. The yield deformation of the specimen defined by strain measurements on beam bars

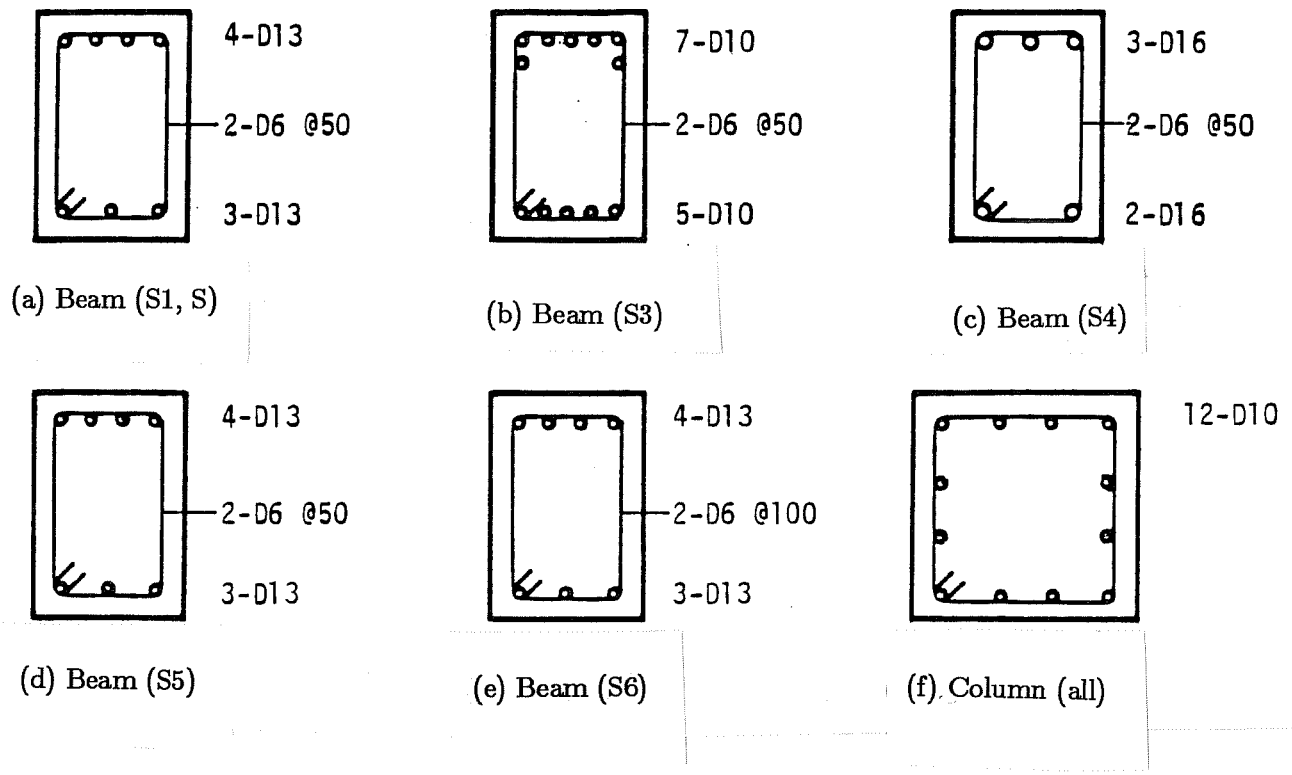

Beam and column sections

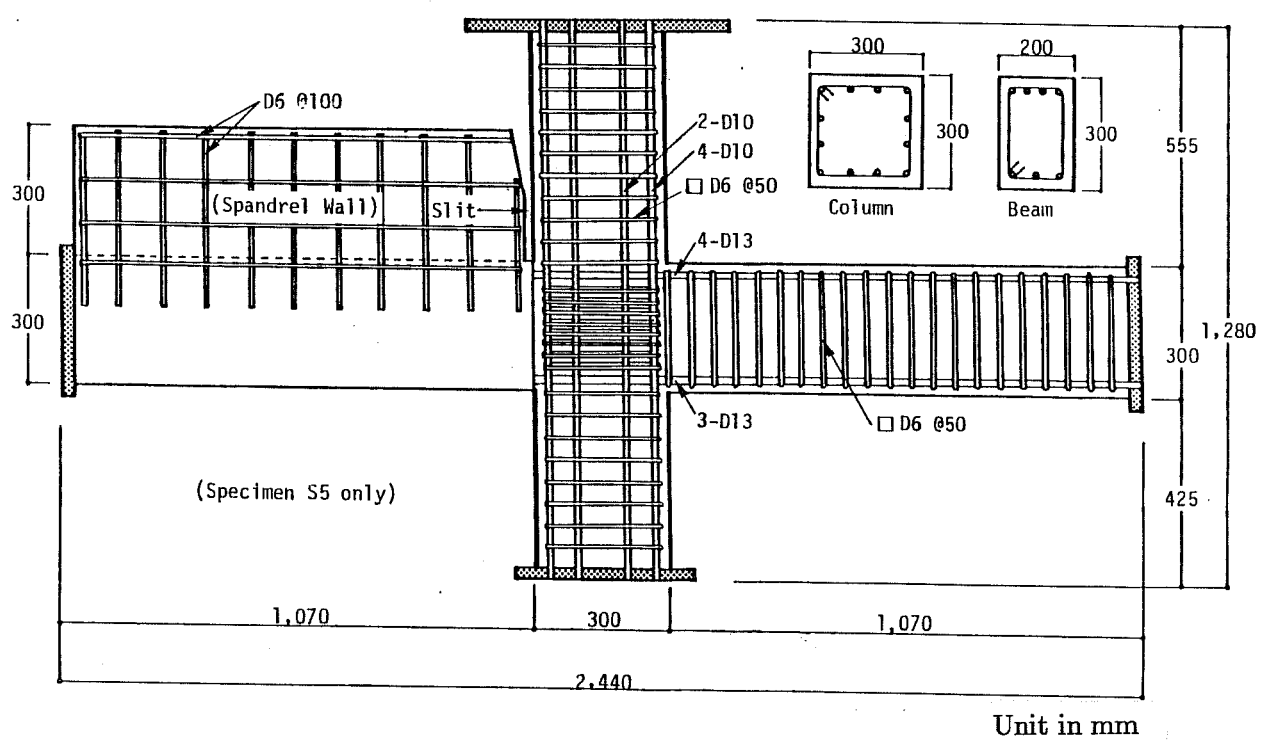

Reinforcement details of Specimens S1,S2,S5 and S6

Fig. 3.17 Details of S-Series specimens

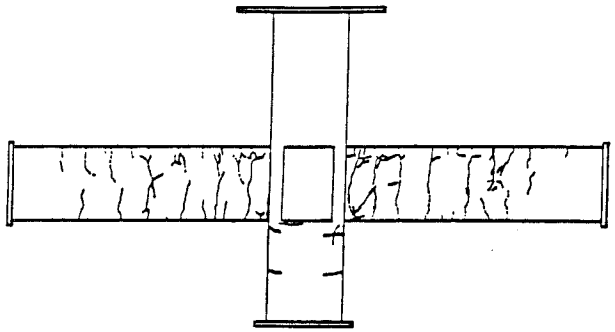

(a) Specimen S1

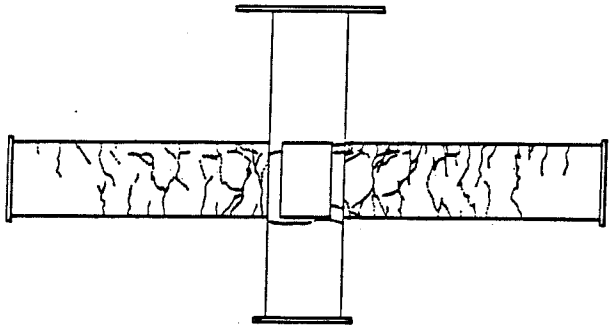

(b) Specimen S2

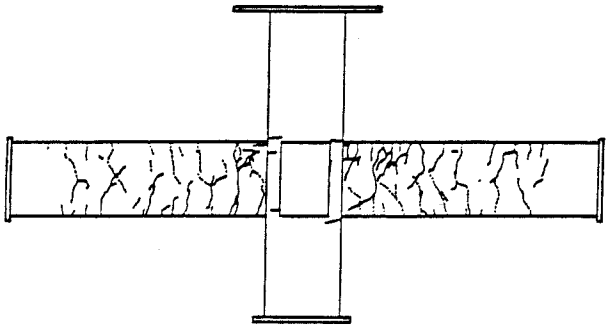

(c) Specimen S3

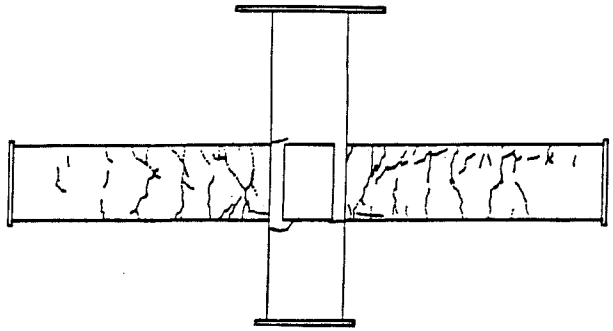

(d) Specimen S4

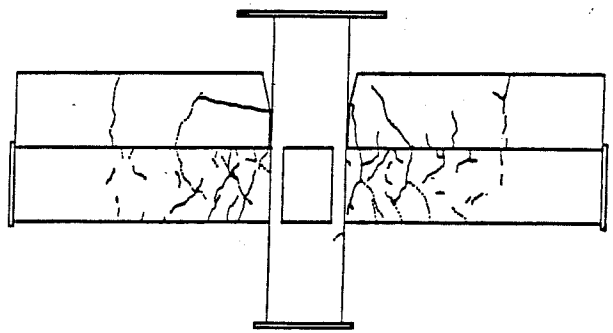

(e) Specimen S5

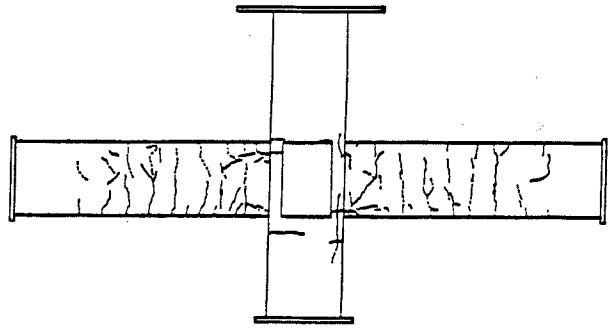

(f) Specimen S6

Fig. 3.18 Crack patterns at end of loading (S– Series)

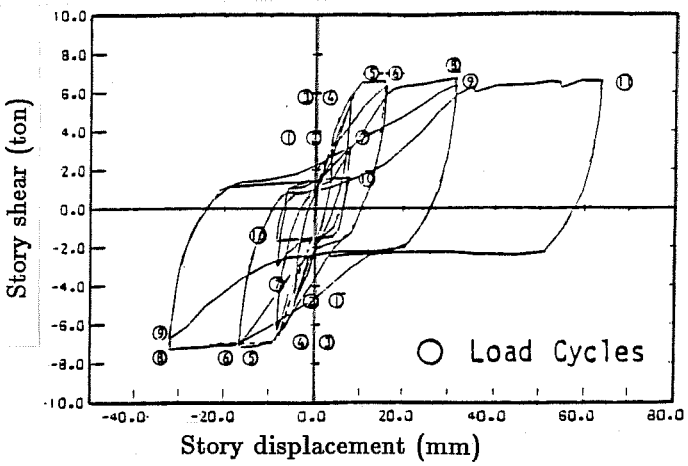

(a) Specimen S1

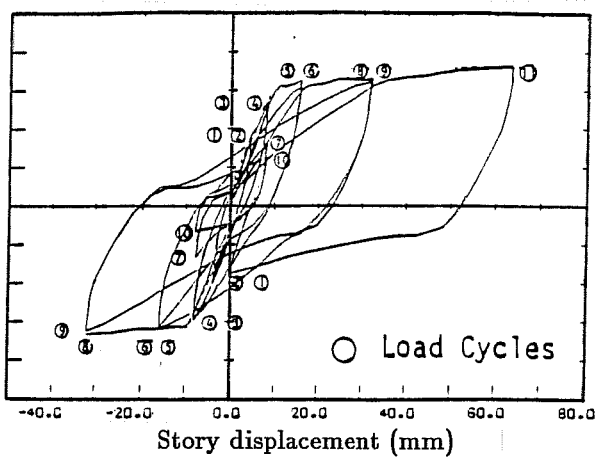

(b) Specimen S2

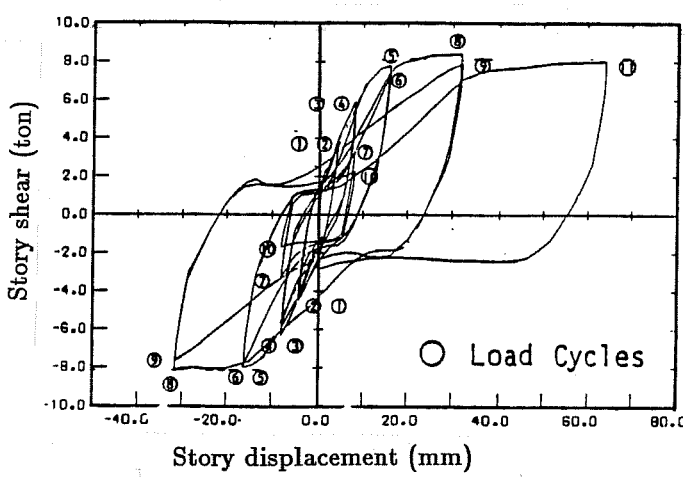

(c) Specimen S3

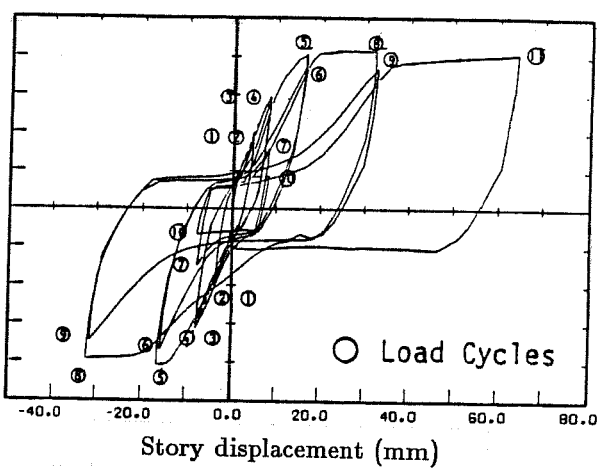

(d) Specimen S4

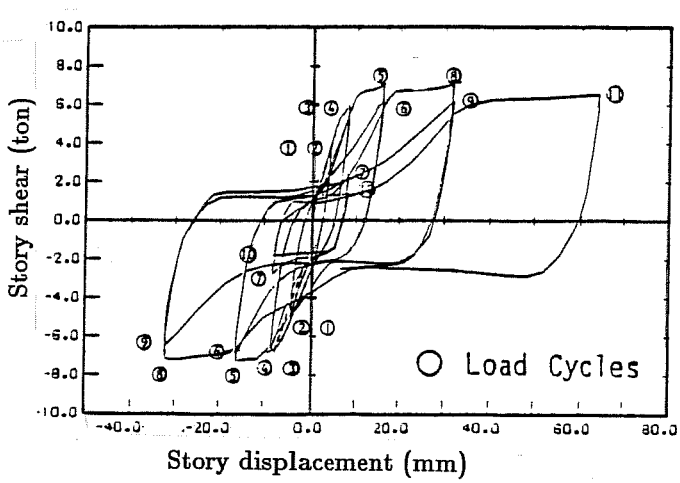

(e) Specimen S5

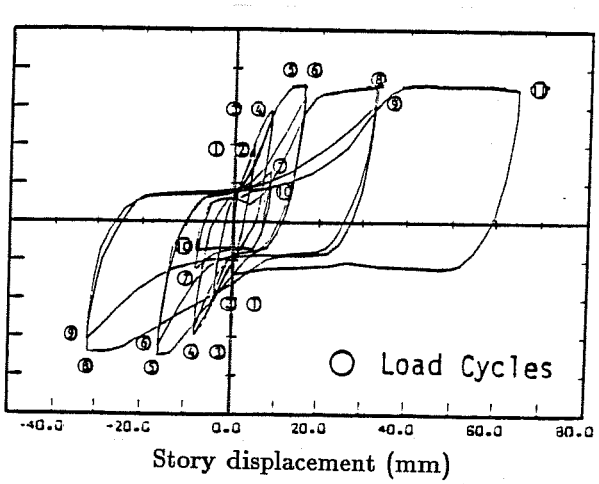

(f) Specimen S6

Fig. 3.19 Story shear vs story drift relations (S–Series)

was much larger than the calculated yield deflection. The axial deformations at the beam top and bottom fibers were measured over a distance of 180 mm from the column face. The bottom fiber was subjected to a more severe stress history than the top fiber, because more reinforcement was placed at the top to simulate the contribution of slab reinforcement to the beam resistance. The axial deformations at the bottom fiber are plotted against the beam shear in Fig. 3.20. All specimens showed a slip-type hysteresis shape after yielding at the beam critical section. Specimen S4 (column width/beam bar diameter = 18.9) clearly showed the slip-type characteristics even prior to flexural yielding of beams, indicating a possible progressive deterioration of bond in the joint. A high axial load does not appear to reduce the bar slip within the joint, because the hysteresis curves for Specimen S1 (axial stress of 60 kgf/cm^2) are similar to those for Specimen S2 (20 kgf/cm^2) except in the final loading cycle.

In the second series (J-series) at the university of Tokyo, six specimens, shown in Fig. 3.21, were tested to study the effect of lateral reinforcement ratio on the joint shear strength.[20] Specimen J1 is the standard specimen, in which (a) the amount of column lateral reinforcement was continued through the joint as often seen in Japanese construction, and (b) the columns were subjected to an axial stress of 20 kgf/cm^2. Specimen J2 modeled U.S. construction, where the amount of confining reinforcement at column ends was continued through the joint. Specimen J3 was provided with approximately 60% of the joint shear reinforcement required by the New Zealand code.[37] Specimen J4 was identical to J1 but subjected to a higher axial stress of 60 kgf/cm^2. In Specimen J5, intermediate longitudinal column reinforcement in the direction of loading was omitted. Specimen J6 was provided with a smaller amount of beam reinforcement to limit the level of joint shear stress to the shear cracking level. All specimens in this series had no transverse beams. Concrete strength ranged from 245 to 293 kgf/cm^2. Bar yield strength was 3530 to 4090 $kgf/cm^2$for longitudinal reinforcement and 3750 $kgf/cm^2$for lateral reinforcement.

Figure 3.22 shows the crack patterns in the joint after reaching a drift angle of 1/23 rad. Shell concrete of Specimens J1 through J5 spalled from the joint face. Only a few cracks were observed in the joint of Specimen J6. Story shear-drift relations are shown in Fig. 3.23. Specimens J1, J2 and J3 with different amounts of joint lateral reinforcement showed similar hysteresis curves. Specimen J5 without column middle reinforcement showed a hysteresis relation very similar to Specimen J1. Specimen J4, subjected to a higher vertical load, showed a larger hysteresis area than Specimen J1. Joint shear distortions are plotted against the story shear in Fig. 3.24. Comparing the relations of Specimens J1 through J3, a large amount of joint reinforcement in Specimen J3 is obviously effective in reducing the joint shear distortion.

In Specimen J4, the vertical load on the column appeared to increase the shear distortion after reaching a drift angle of 1/23, because the joint shear resisting mechanism deteriorated at a faster rate with the normal stress. It should be noted that the slip-type hysteresis observed in the story shear-drift relation for Specimen J6 must have been caused

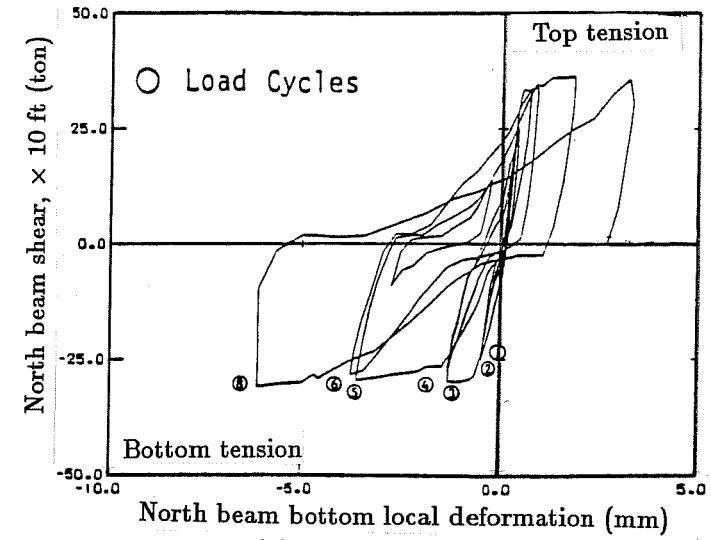

(a) Specimen S1

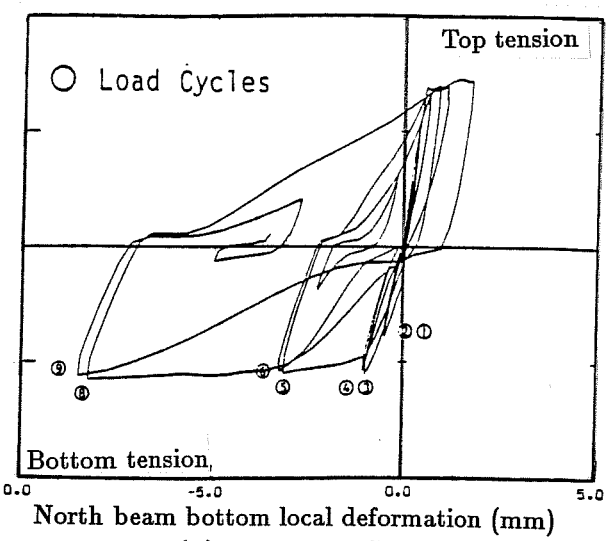

(b) Specimen S2

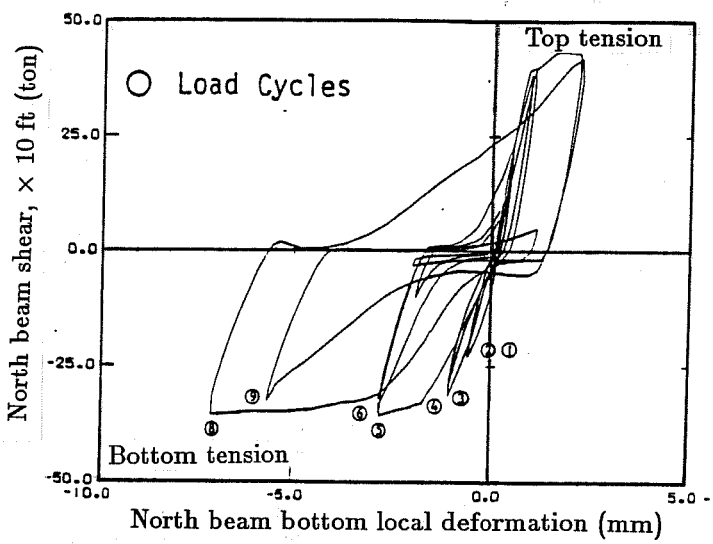

(c) Specimen S3

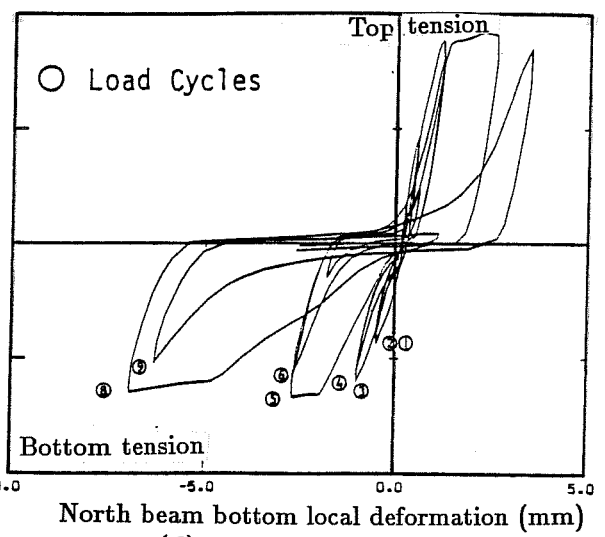

(d) Specimen S4

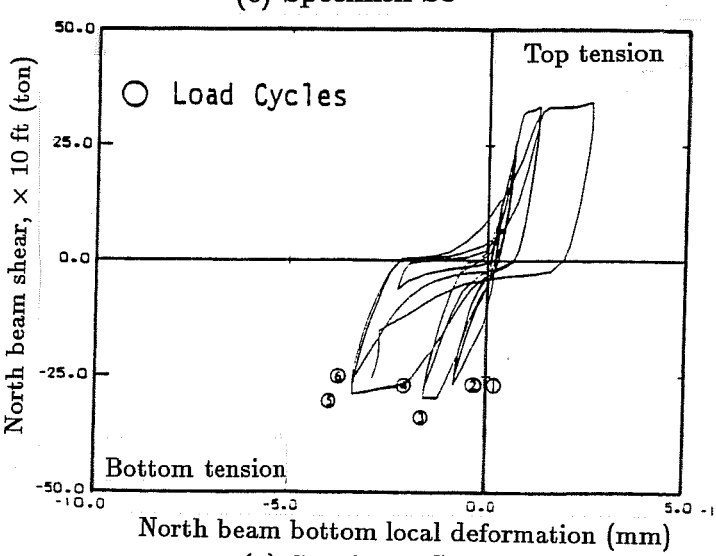

(e) Specimen S5

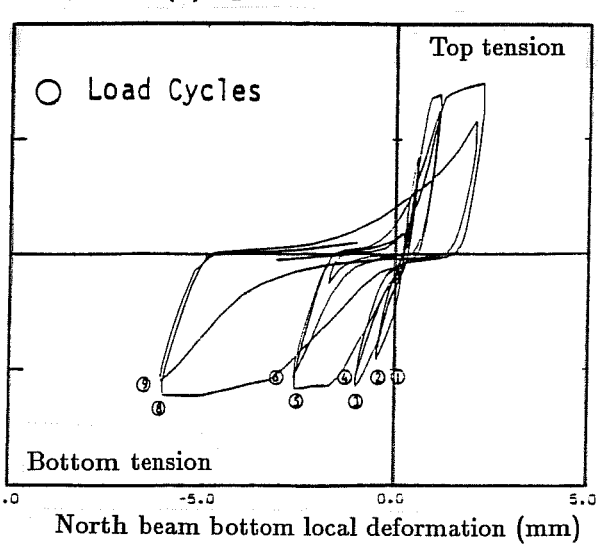

(f) Specimen S6

Fig. 3.20 Beam shear vs bottom fiber axial deformation

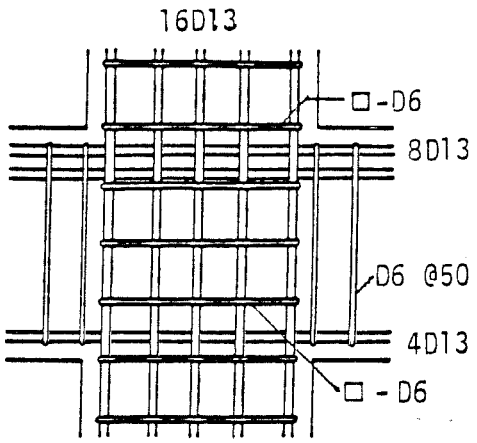

(a) Specimens J1 and J4

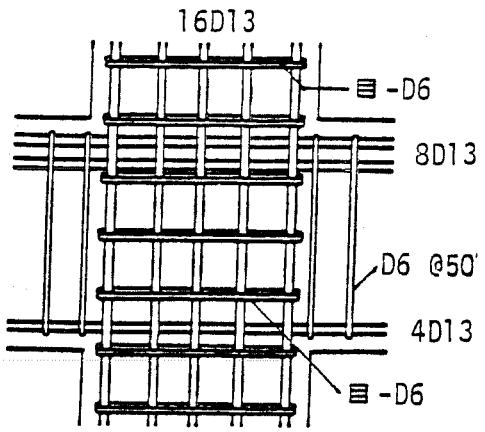

(b) Specimen J2

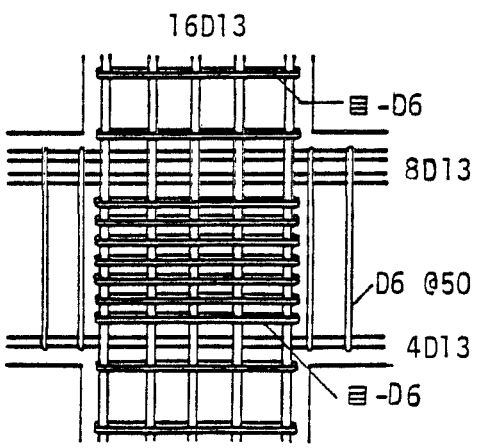

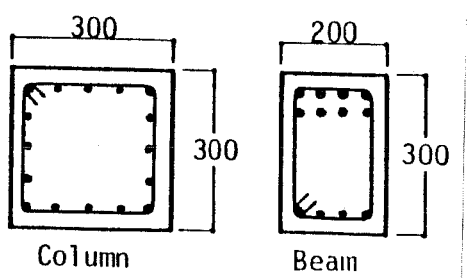

(c) Specimen J3

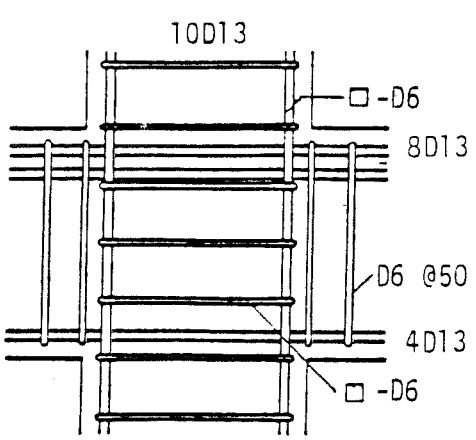

(d) Specimen J2

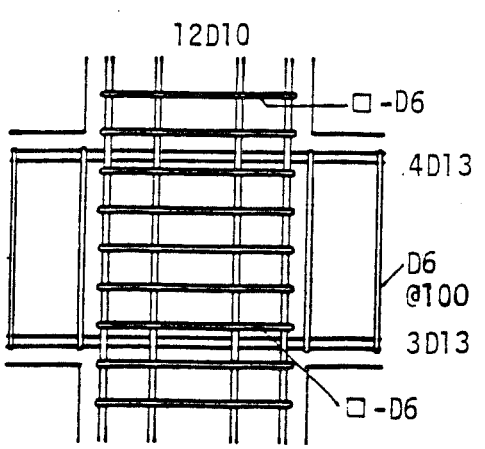

(e) Specimen J6

Fig. 3.21 Details of J-Series Specimens

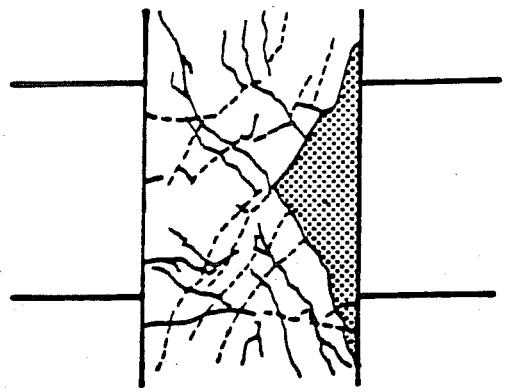

(a) Specimen J1

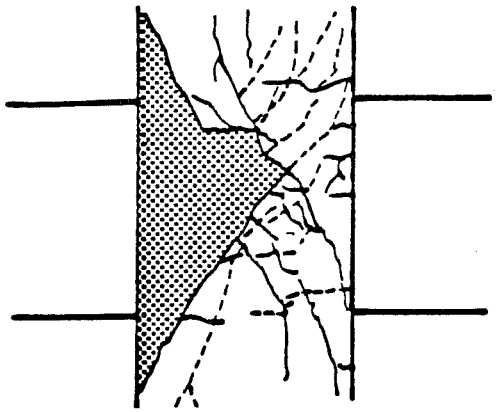

(b) Specimen J2

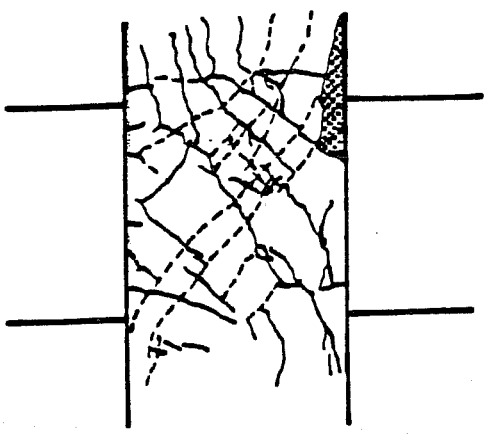

(c) Specimen J3

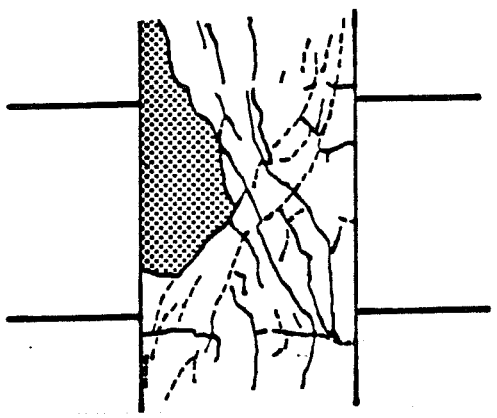

(d) Specimen J4

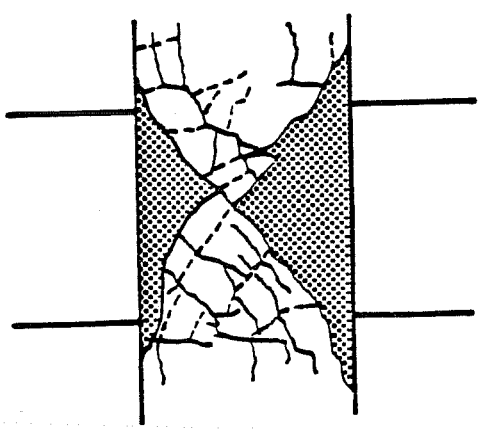

(e) Specimen J5

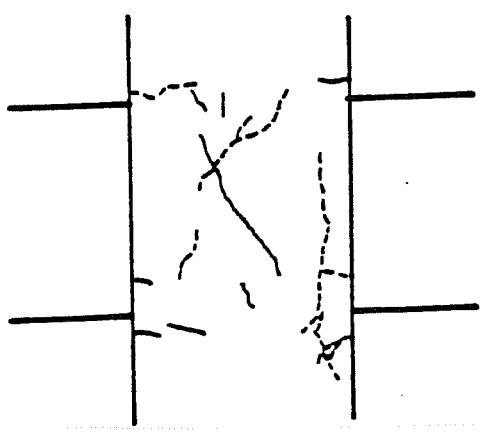

(f) Specimen J6

Fig. 3.22 Crack patterns at 1/23 rad drift (J- Series)

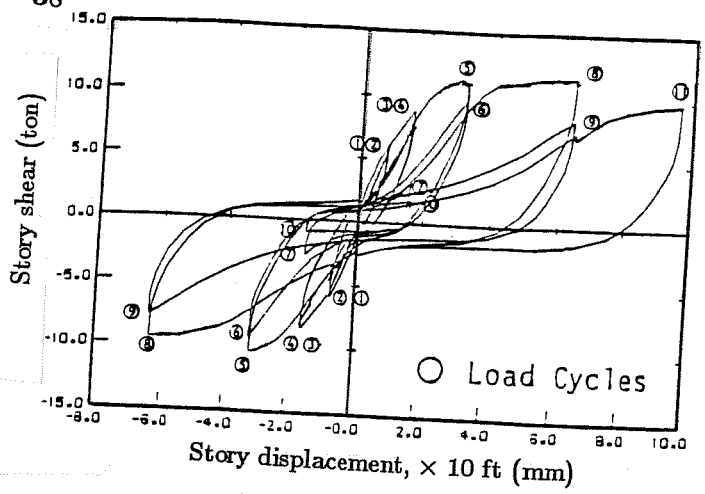

(a) Specimen J1

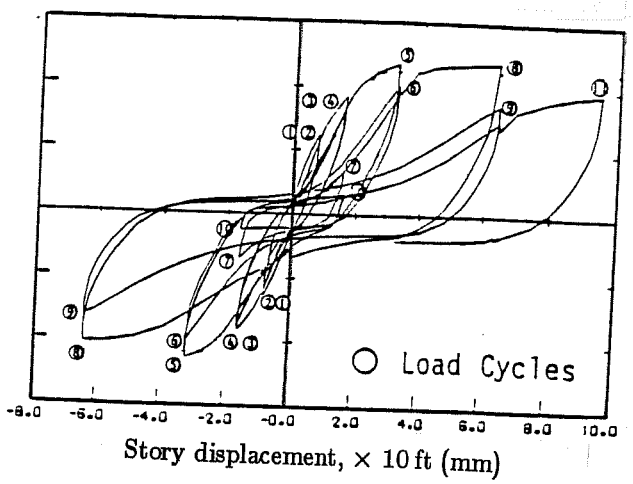

(b) Specimen J2

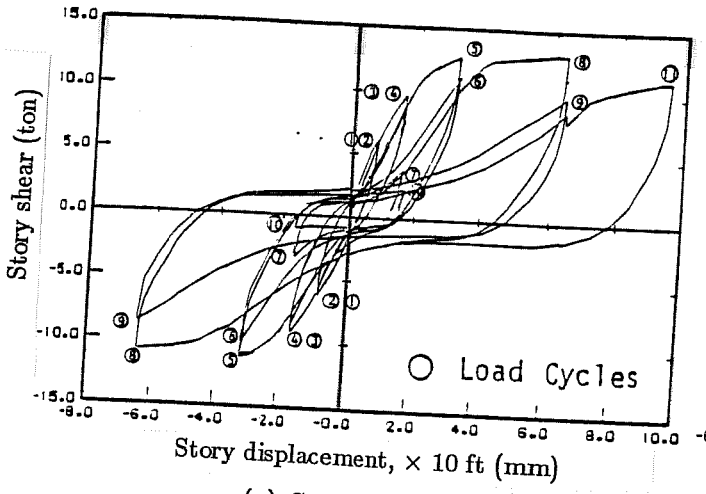

(c) Specimen J3

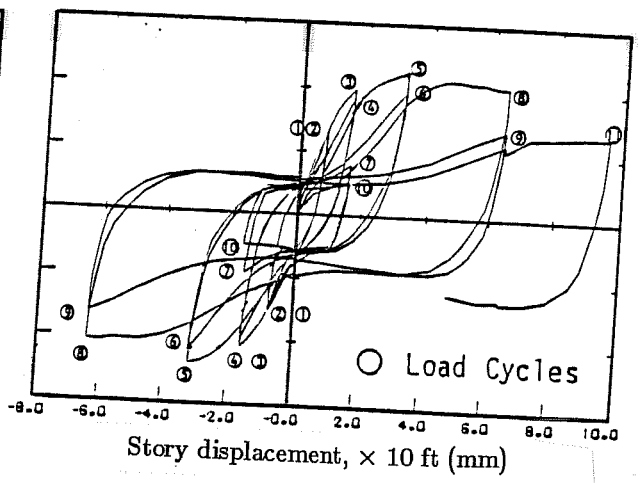

(d) Specimen J4

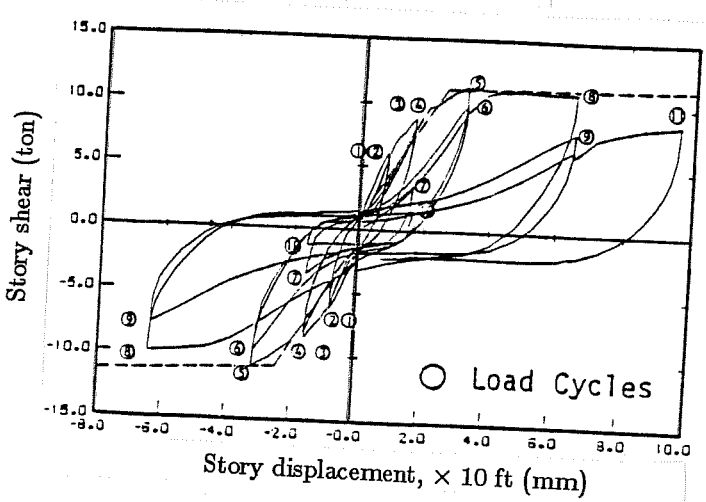

(e) Specimen J5

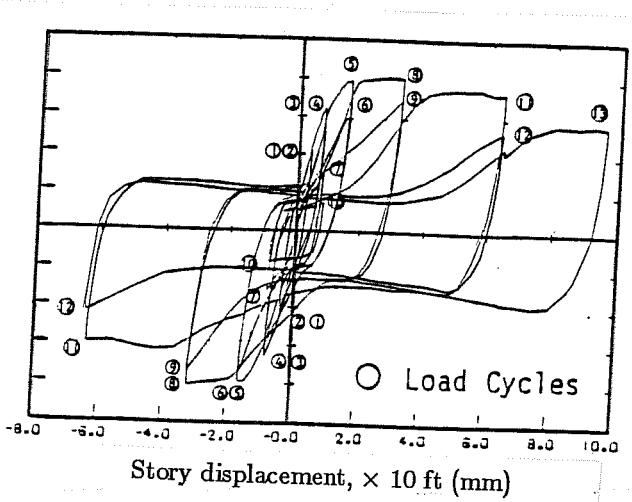

(f) Specimen J6

Fig. 3.23 Story shear vs story drift relations (J-Series)

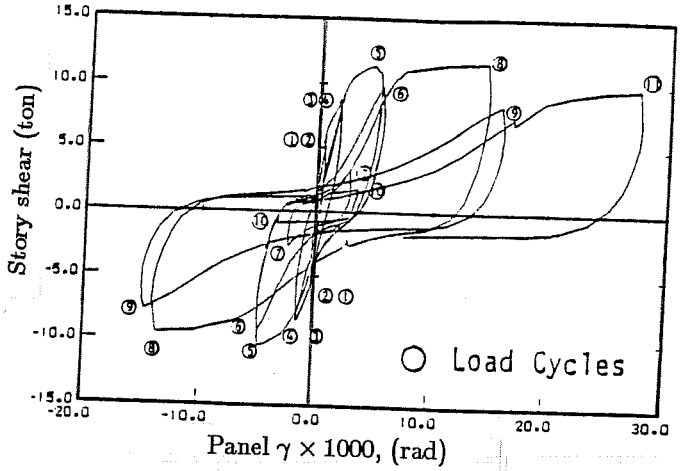

(a) Specimen J1

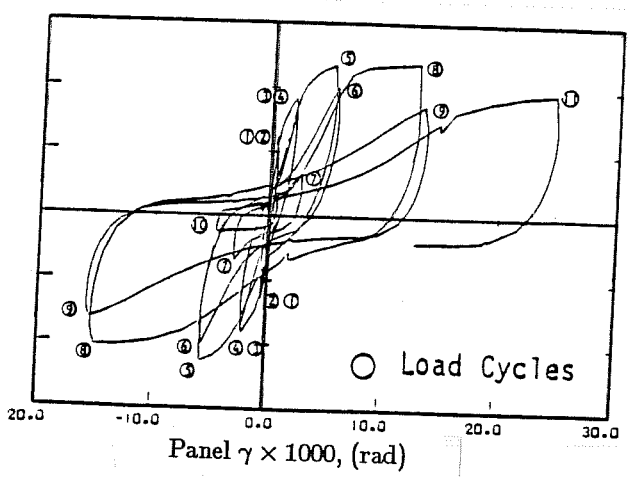

(b) Specimen J2

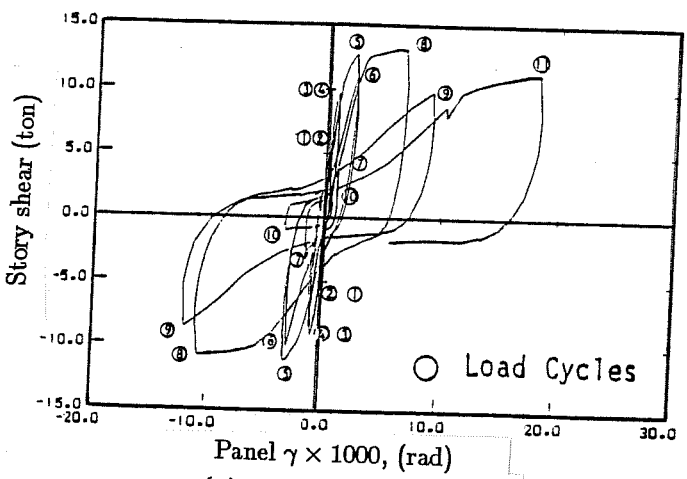

(c) Specimen J3

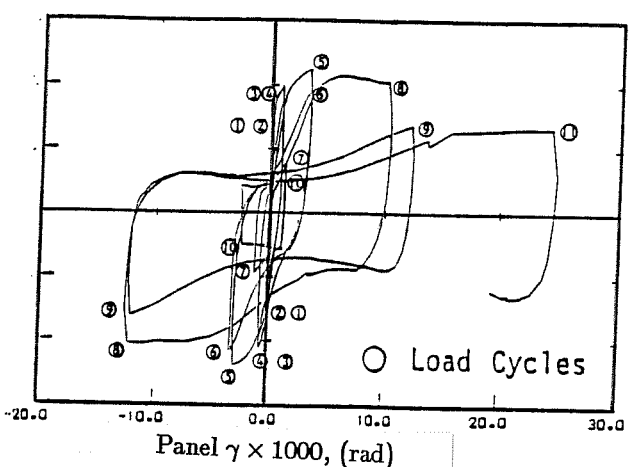

(d) Specimen J4

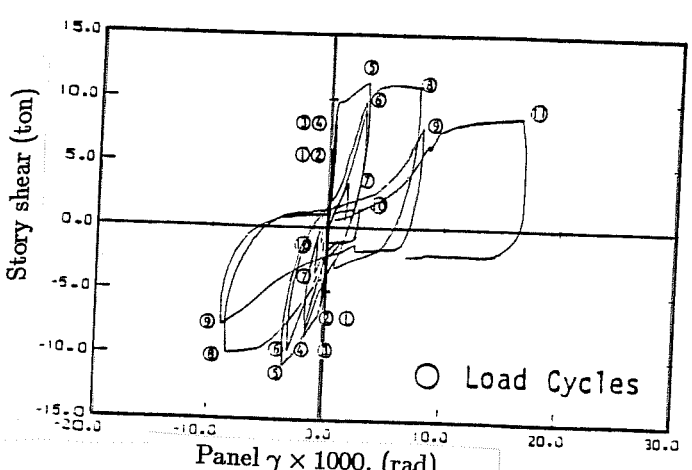

(e) Specimen J5

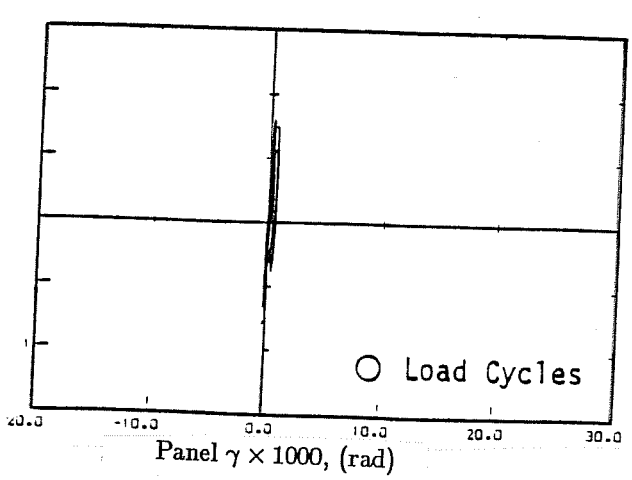

(f) Specimen J6

Fig. 3.24 Story shear vs joint shear distortion (J-Series)

by beam bar slip within the joint because the joint shear distortion was very small in J6. The shear distortion for Specimens J1 through J5 increased after the formation of the beam collapse mechanism even though the shear input to the joint did not increase. This must be due to the change in the shear resisting mechanism as bond deteriorates along the beam reinforcement within the joint.

In the third series (C-series) at the University of Tokyo, three interior specimens were tested to assess the amount of joint lateral reinforcement required to prevent shear deterioration in a beam-column joint when the bond situation was improved for beam longitudinal bars within the joint.[27] The beam bar bond index defined by the following equation was introduced to indicate the bond situation.

$$U_b = f_y \, (d_b/h_c)/2 \tag{8}$$

where f_y = yield strength of beam bars, d_b = diameter of beam bars, and h_c = column depth.

The beam bar bond index corresponding to the requirement in the New Zealand code[37] is approximately 55 kgf/cm^2 and is lower than the values for the specimens in the previous two series; U_b = 67.5 kgf/cm^2 for Specimen S3 with D10 beam bars, 74.3 to 86.6 kgf/cm^2 for those with D13 beam bars (S1, S2, S5, S6 and J1 through J6), and 100.4 kgf/cm^2 for Specimen S4 with D16 beam bars. The three specimens in C-series were designed to limit the beam bar bond index to 55 kgf/cm^2. As shown in Fig. 3.25, the beam and column sections were common for the three specimens but the amount of joint lateral reinforcement was varied. Specimen C1 was a standard specimen modeling usual Japanese practice. Specimen C2 was designed on the basis of ACI 318-83[38] so that the amount of confining reinforcement at column ends was continued through the joint. Specimen C3 was designed on the basis of the New Zealand Code[37] so that the entire shear could be resisted by joint shear reinforcement. All specimens had no transverse beams and were subjected to a column axial stress of 20 kgf/cm^2. Concrete strength was 261 kgf/cm^2. Bar yield strength was 3260 kgf/cm^2 for beam longitudinal reinforcement (the bond index U_b = 52 kgf/cm^2) and 3300 to 3360 kgf/cm^2 for joint lateral reinforcement. Crack patterns observed at the end of loading are shown in Fig. 3.26.

Flexural cracks were distributed uniformly along the beams and concrete spalled from the bottom of beams in the plastic hinge zones. Specimen C1 with the least joint lateral reinforcement was observed to develop wider shear cracks than the other two specimens during loading at a drift angle of 1/23 rad. Story shear-drift relations are shown in Fig. 3.27. The three specimens showed a fat spindle-shaped hysteretic behavior. The contribution of parts of the specimen to the story drift was calculated and is shown in Fig. 3.28. The deflection of beams was dominant in the story drift. Strains in the joint lateral reinforcement are shown in Fig. 3.29. The strains in Specimen C1 exceeded the yield strain at a drift angle of 1/92, although the strains in Specimen C3 stayed less than 0.1% throughout loading.

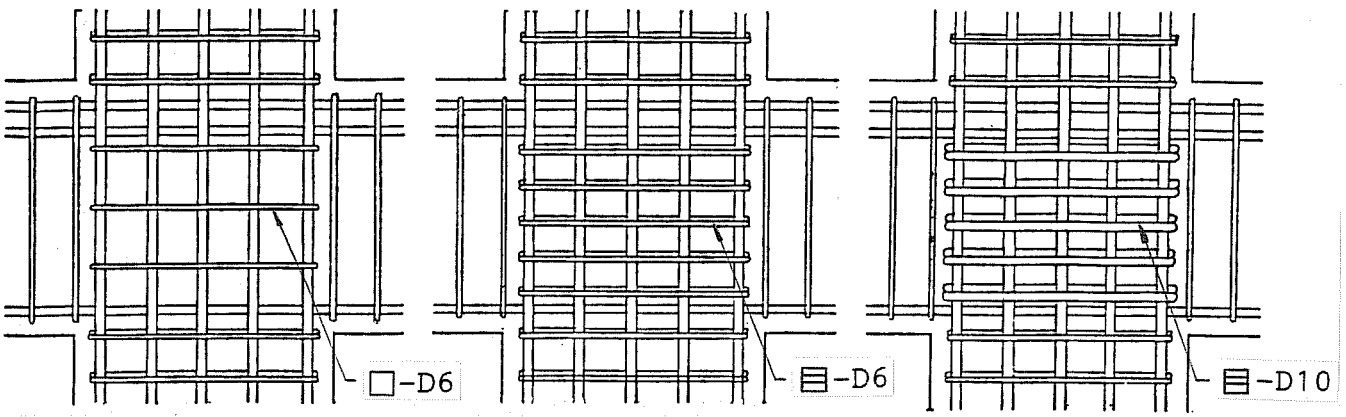

(a) Specimen C1 (b) Specimen C2 (c) Specimen C3

Details of joint lateral reinforcement

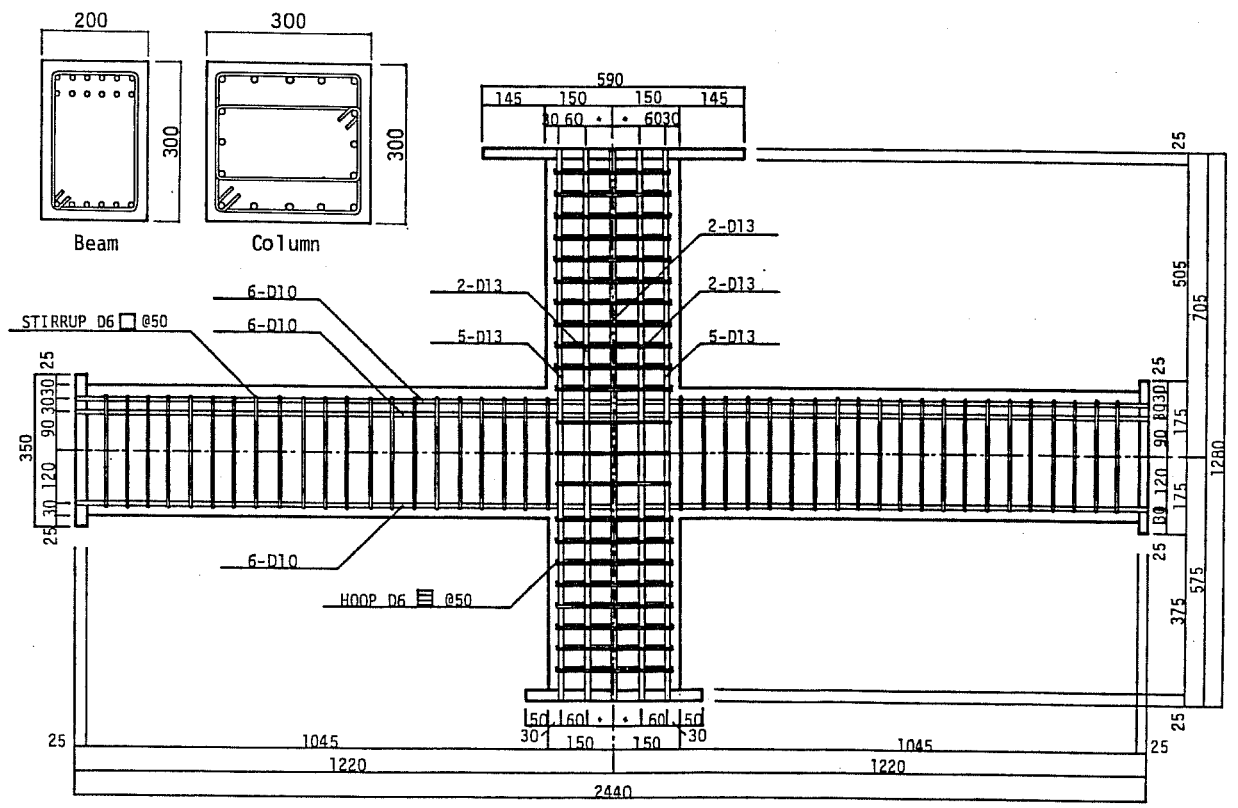

Reinforcement details of Specimen C1

Fig. 3.25 Details of C–Series Specimens

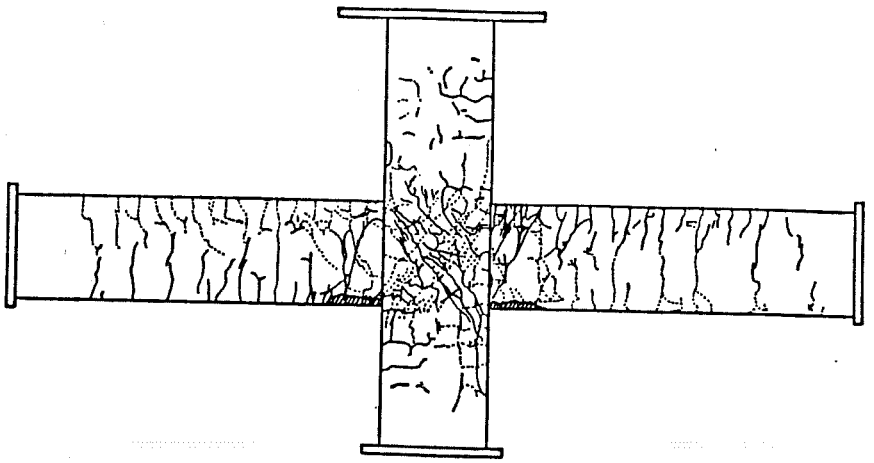

(a) Specimen C1

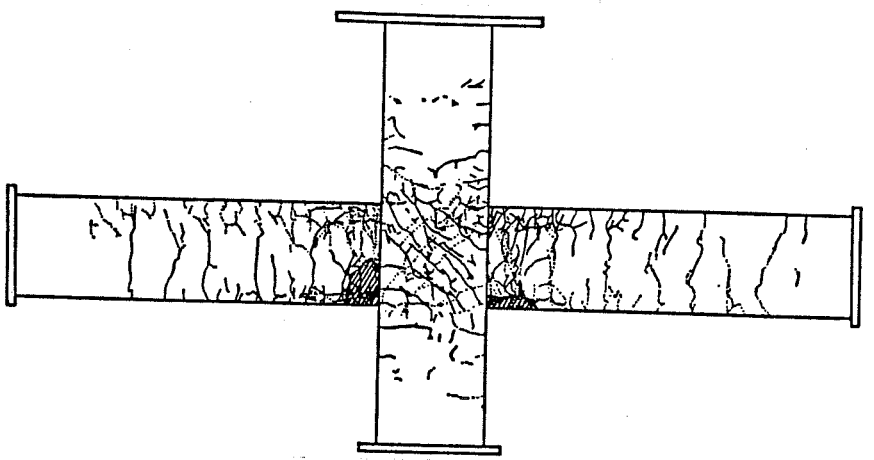

(b) Specimen C2

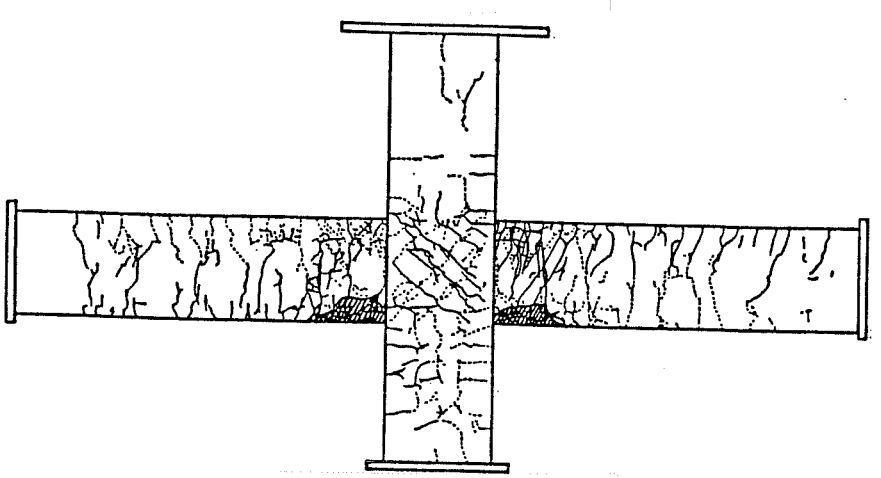

(c) Specimen C3

Fig. 3.26 Crack patterns after test (C–Series)

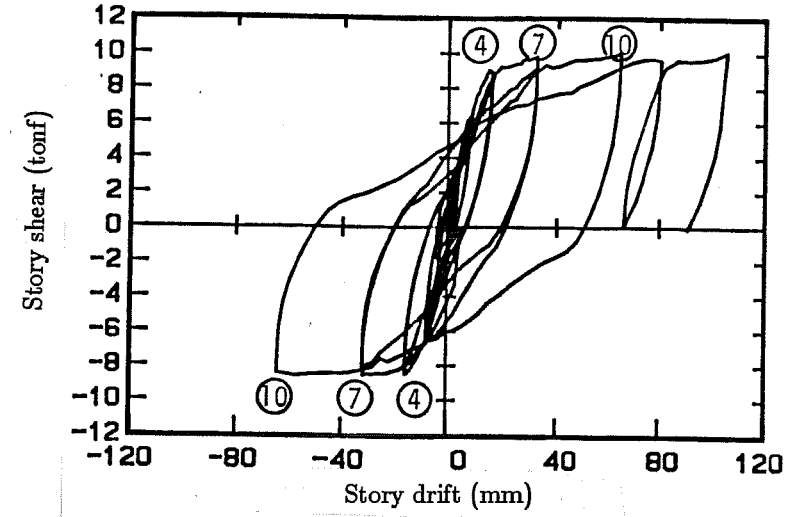

(a) Specimen C1

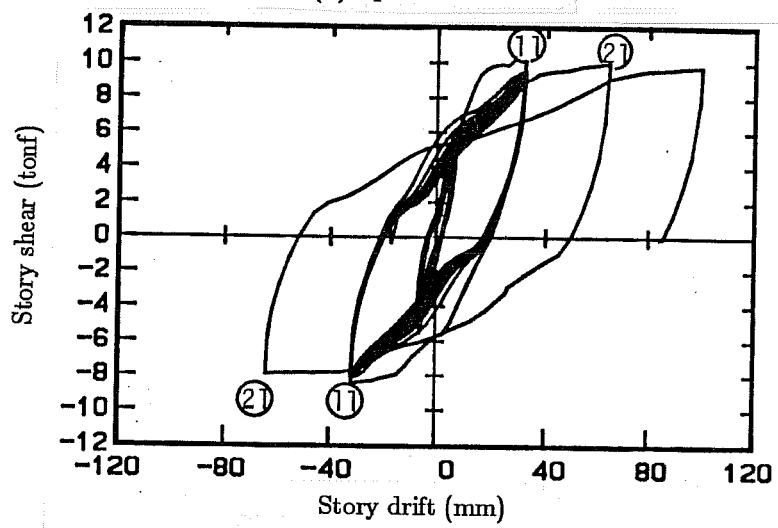

(b) Specimen C2

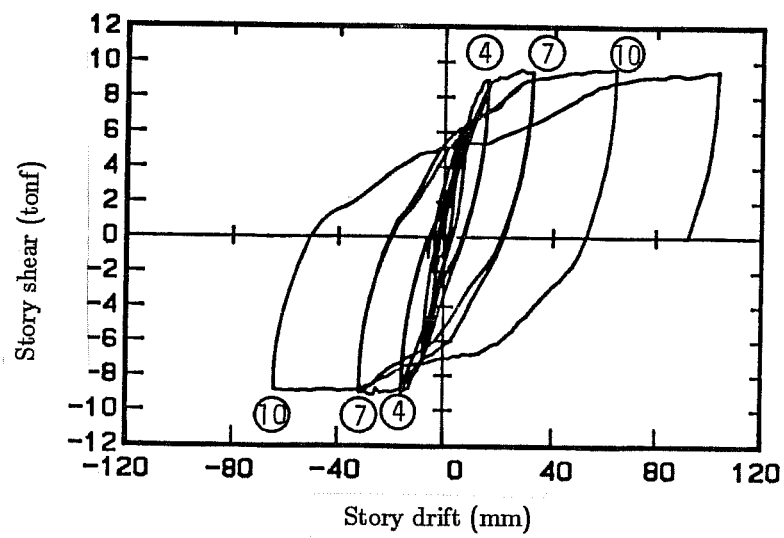

(c) Specimen C3

Fig. 3.27 Story shear vs story drift relations (C–Series)

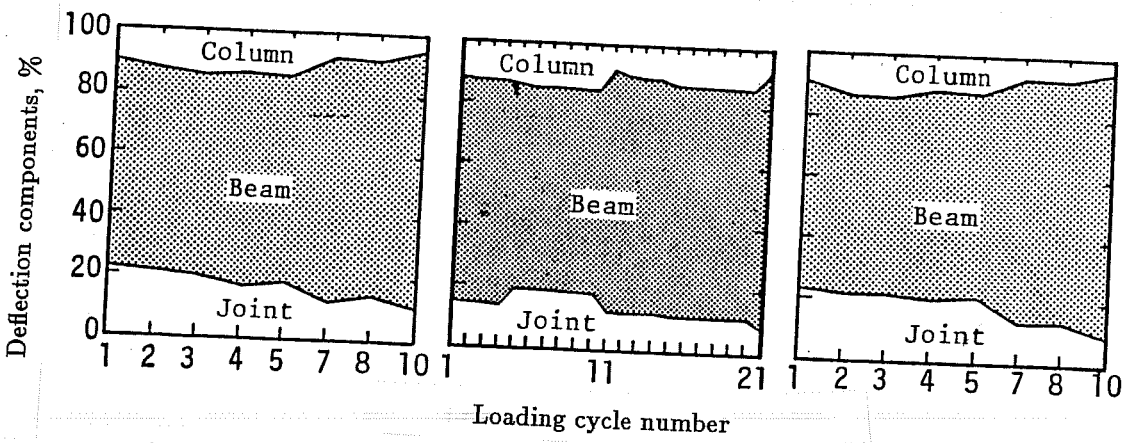

(a) Specimen C1 (b) Specimen C2 (c) Specimen C3

Fig. 3.28 Deflection components of story drift (C–Series)

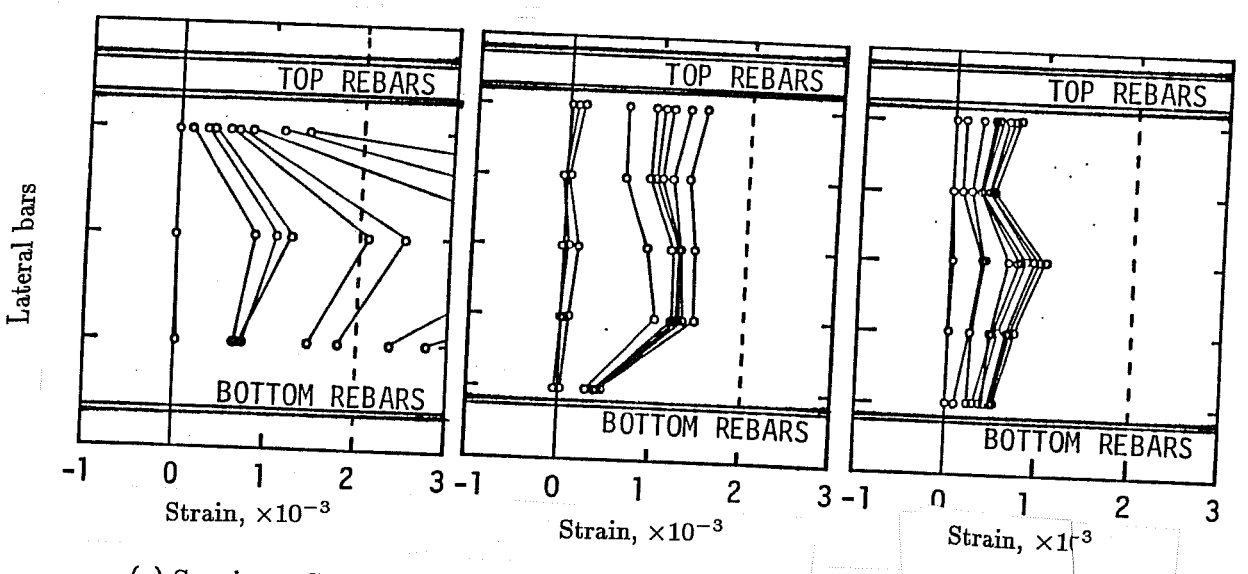

(a) Specimen C1 (b) Specimen C2 (c) Specimen C3

Fig. 3.29 Strains in joint lateral reinforcement (C–Series)

The joint shear resisting mechanism in Fig. 3.30 was discussed by comparing the test results for Specimens J1 and C1, as rearranged in Fig. 3.31.[32] Specimen J1 with D13 beam bars (bond index $U_b = 86.6$ kgf/cm^2) failed in joint shear, while Specimen C1 with D10 beam bars ($U_b = 52$ kgf/cm^2) failed in beam flexure. Although the joint shear stress developed in

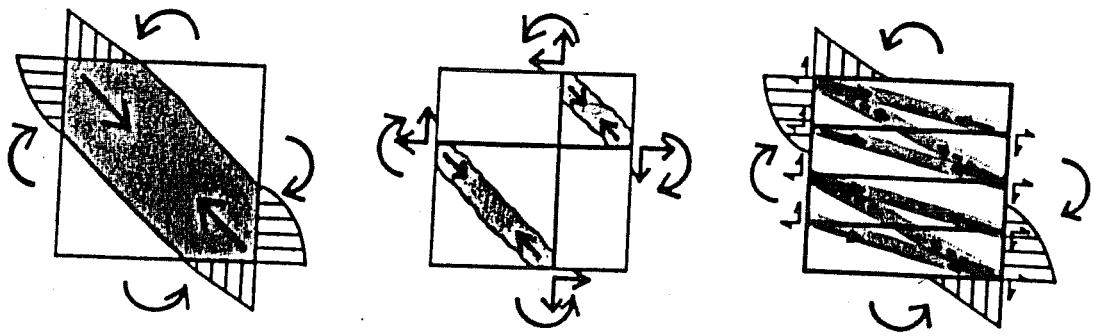

(a) Main strut mechanism (b) Sub-strut mechanism (c) Truss mechanism

Fig. 3.30 Joint shear resisting mechanism

Specimen J1 was approximately 1.25 times higher than that in Specimen C1, the number of joint shear cracks was less in Specimen J1.

Specimen J1 developed shear cracks by the sub-strut mechanism but the shear cracks in the main diagonal became dominant at a large deformation. The sub-strut mechanism was lost with bond deterioration along the beam bars and the forces were concentrated in the main strut. On the other hand, the sub-strut mechanism as well as the main strut mechanism was maintained in Specimen C1 and diagonal compression stresses distributed uniformly in the joint concrete. The role of joint lateral reinforcement in these two series appears different depending on the degree of bond deterioration along the beam bars. In specimens with poor bond (J-series), different amounts of joint lateral reinforcement resulted in little difference in the stains in the joint reinforcement. On the contrary, a larger amount of lateral reinforcement resulted in lower strains in the joint reinforcement in the specimens with lower bond stresses in the beam bars through the joint (C-series).

Chiba University. A series of unidirectional loading tests were conducted at Chiba University.[33] Eight specimens were tested to study the effects of joint shear stress level and beam bar bond on the joint shear resistance. As shown in Fig. 3.32, the specimens were half-scale interior beam-column subassemblages having the same dimensions as in the J- and C-series at the University of Tokyo.

The first four specimens (No. 1 through No. 4) were provided with only one D6 hoop as joint lateral reinforcement. The other four specimens (No. 5 through No. 8) were designed so that half of the entire shear could be resisted by joint lateral reinforcement. D13 and D10 bars were used as beam longitudinal reinforcement to produce poor and good bond conditions, respectively. The beam bar bond index (see Eq. 8) was 54 kgf/cm^2 for the specimens with

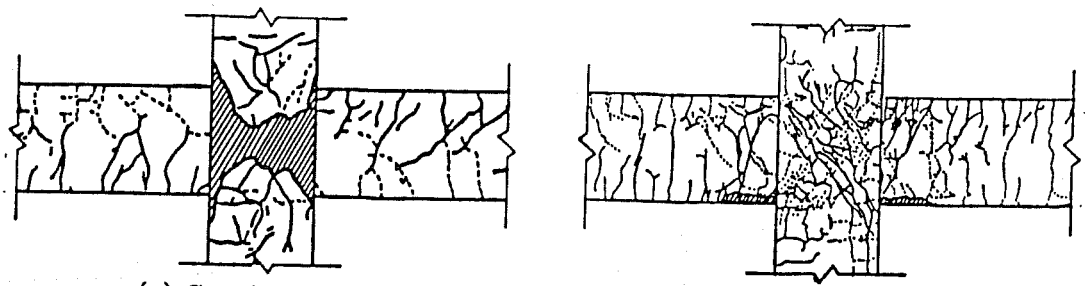

(a) Specimen J1 (b) Specimen C1

Crack patterns after tests

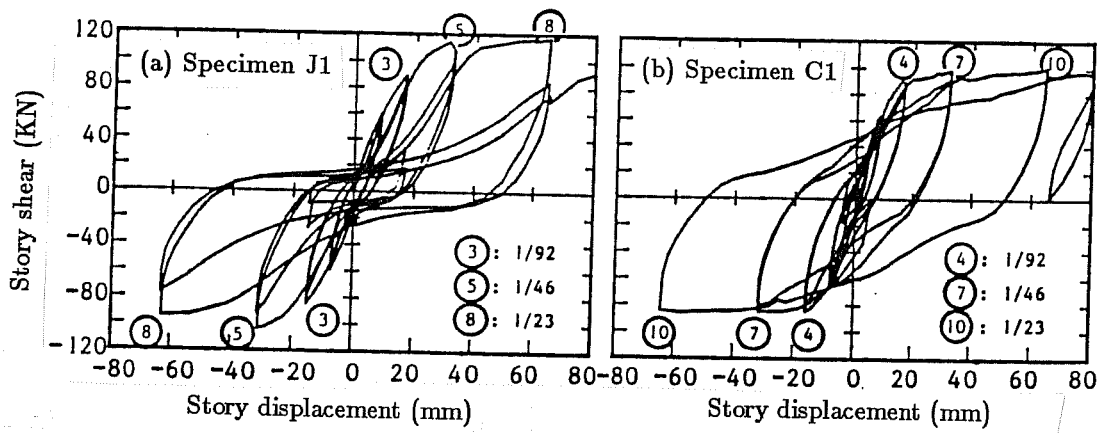

Story shear-story drift relation

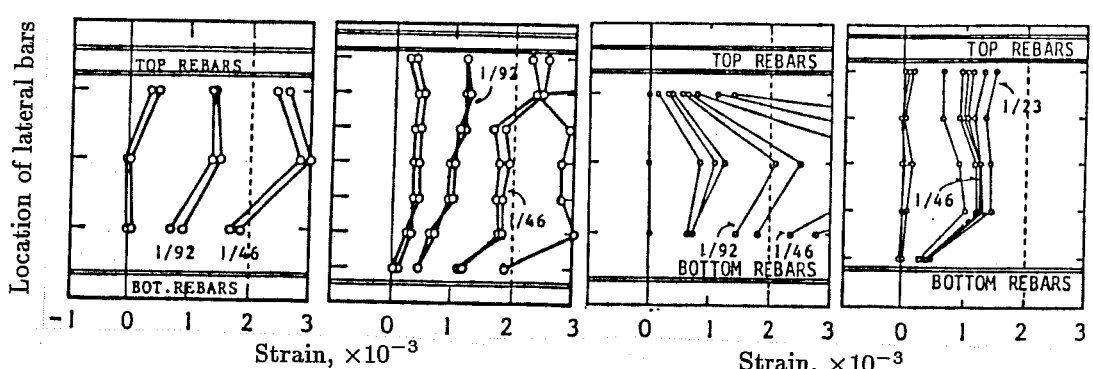

(a) Specimen J1 (b) Specimen J3 (c) Specimen C1 (d) Specimen C2

Strains in joint lateral reinforcement

Fig. 3.31 Comparison of test results

Properties of Specimens

Specimen	No. 1	No. 2	No. 3	No. 4	No. 5	No. 6	No. 7	No. 8
Beam								
Top Bars	12-D10	10-D10	6-D13	5-D13	10-D10	8-D10	5-D13	4-D13
Bottom Bars	12-D10	10-D10	6-D13	5-D13	10-D10	8-D10	5-D13	4-D13
$P_t(\%)$	1.67	1.39	1.49	1.25	1.39	1.11	1.25	1.00
Stirrups	2-D6	2-D6	2-D6	2-D6	2-D6	2-D6	2-D6	2-D6
Column								
Total Bars	18-D13	16-D13	18-D13	16-D13	16-D13	12-D13	16-D13	12-D13
$P_g(\%)$	2.61	2.31	2.61	2.31	2.31	1.72	2.31	1.72
Hoops	2-D10	2-D10	2-D10	2-D10	2-D10	2-D10	2-D10	2-D10
Connection								
Hoops	2-D6	2-D6	2-D6	2-D6	24-D6	16-D6	24-D6	16-D6
$P_w(\%)$	0.10	0.10	0.10	0.10	1.15	0.76	1.15	0.76

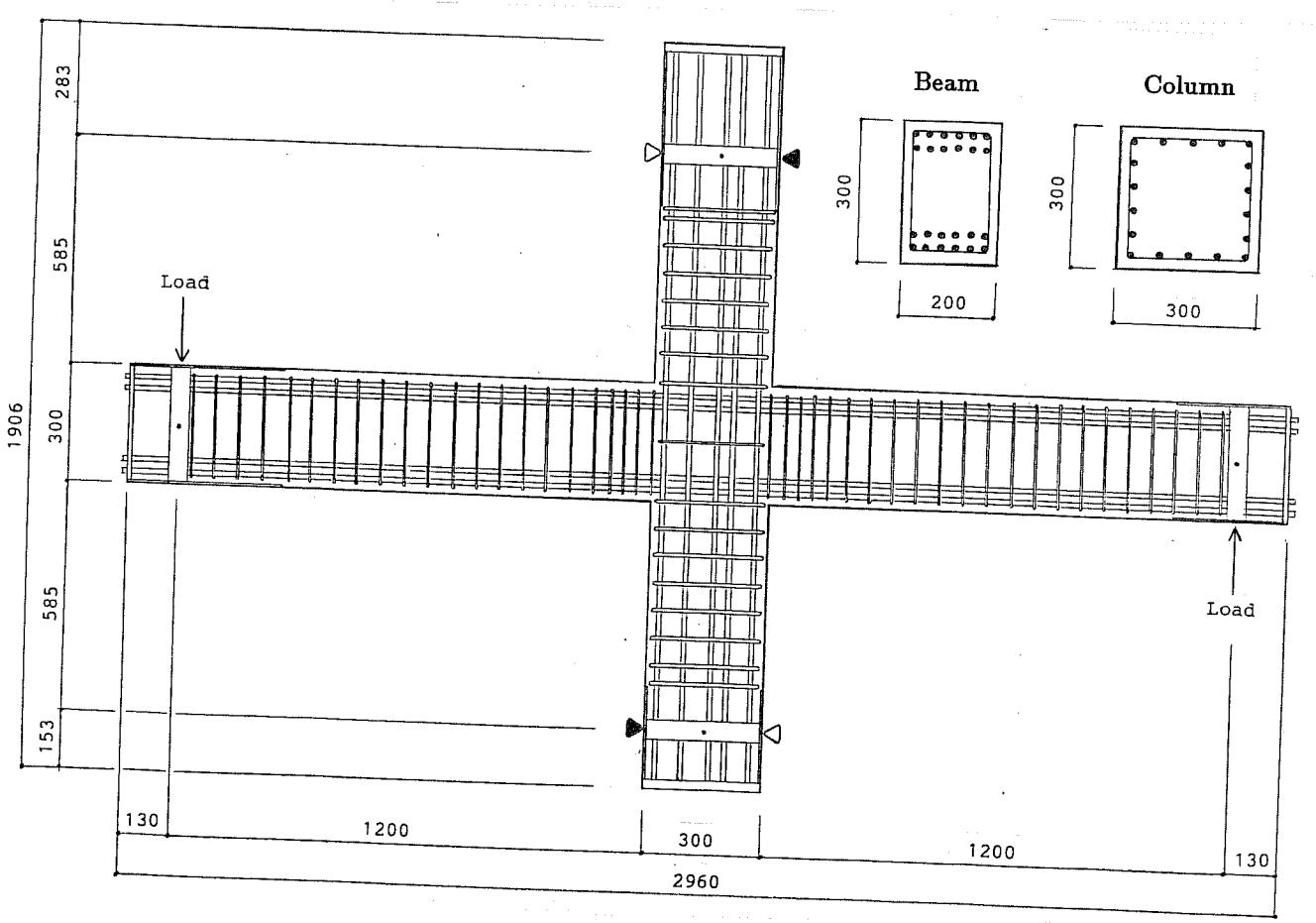

Reinforcement details of Specimen (No. 1-4)

Fig. 3.32 Details of specimens

D10 beam bars and 77 to 83 kgf/cm^2 for those with D13 beam bars. Concrete strength was 335 kgf/cm^2 for Specimens No. 1 through No. 4 and 291 kgf/cm^2 for No. 5 through No. 8. Bar yield strength was 3260 to 3830 kgf/cm^2 for longitudinal reinforcement and 3270 to 3450 kgf/cm^2 for lateral reinforcement. The loading setup is shown in Fig. 3.33. The specimens were subjected to a constant stress of 20 kgf/cm^2 at the column and reversing loads at the beam tips. Figure 3.34 shows final crack patterns and shear crack widths observed in the joint. Specimens with a small amount of joint lateral reinforcement (No. 1 through No. 4) developed wide shear cracks in the joint and eventually failed in joint shear after flexural yielding of the beams. Specimens with a larger amount of joint lateral reinforcement (No. 5 through No. 8) failed in beam flexure. Figure 3.35 shows story shear-drift relations during the loading to a drift angle of 1/26 rad.

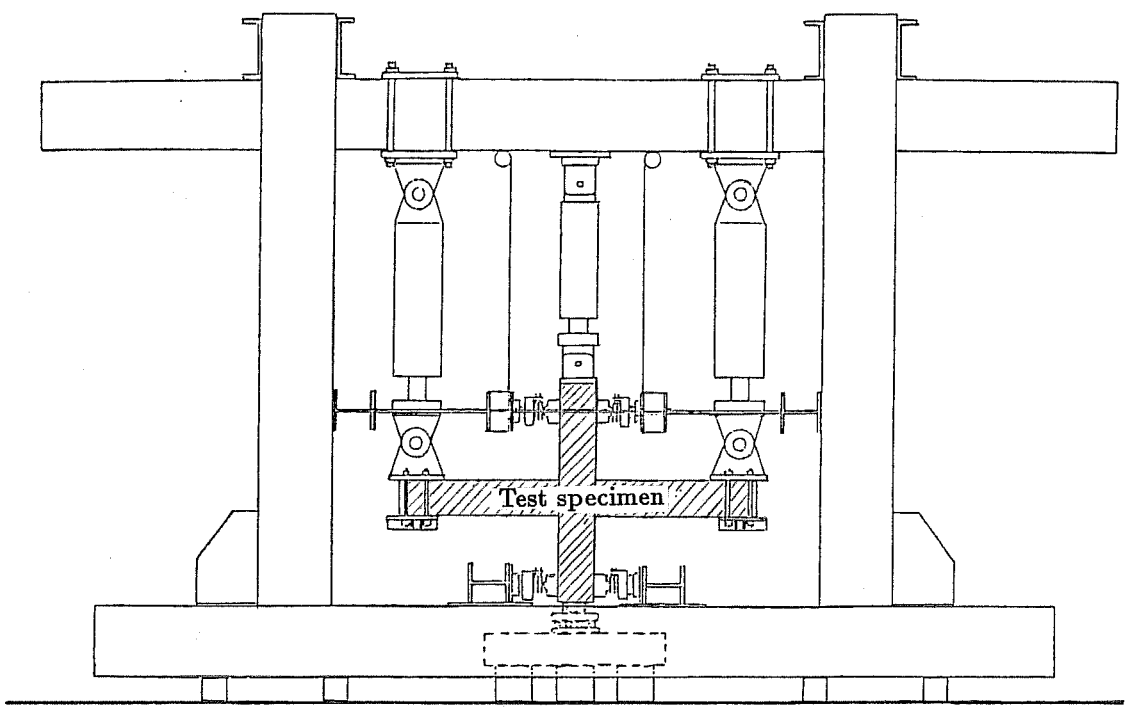

Fig. 3.33 Test specimen in loading setup

Specimen No. 5 with the combination of high joint reinforcement ratio and good beam bar bond showed fat spindle-shaped hysteretic behavior. The other specimens in this figure showed an inverse-S-shaped hysteretic behavior because of the deterioration in the joint shear resisting mechanism for Specimens No 2 and No. 4, and because of the bond deterioration of beam bars within the joint for Specimen No. 7. Joint shear stress-shear distortion relations are shown in Fig. 3.36. A larger amount of joint lateral reinforcement is obviously effective in

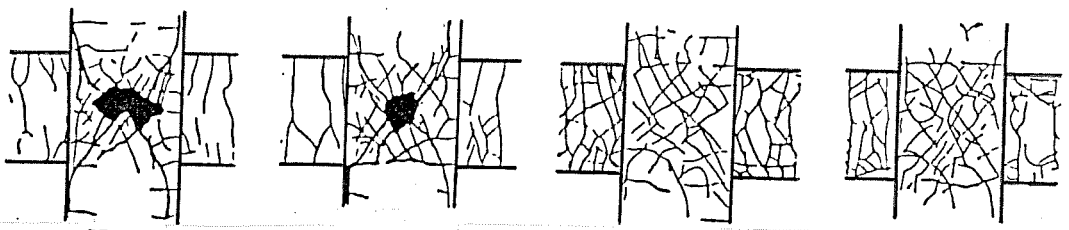

(a) Crack patterns after test

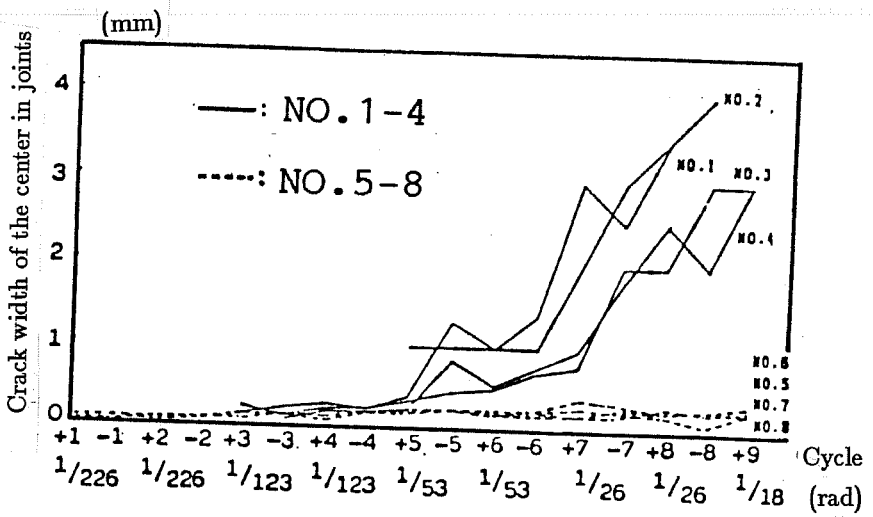

(b) Shear crack width at the center of joint

Fig. 3.34 Joint shear cracks

reducing the shear distortion. It should be noted that Specimen No. 2 with good bond showed a little larger distortion than Specimen No. 4 with poor bond. This tendency is more clearly observed in the test results from Hokkaido University, as shown in Fig. 3.14(b). Strains in joint lateral reinforcement are shown in Fig. 3.37. Specimen No. 5 with good bond showed much larger strains than Specimen No. 7 with poor bond. This is because the joint shear resisting mechanism contributed by lateral reinforcement was affected by the bond situation, as discussed previously.

The conclusions in the preceding studies are summarized as follows:

1. Specimens with a small amount of joint lateral reinforcement (lateral reinforcement ratio: $p_w = 0.1$ to 0.5%) developed beam flexural yielding but failed in joint shear at a drift angle of 2 to 4%.[20,21,33]

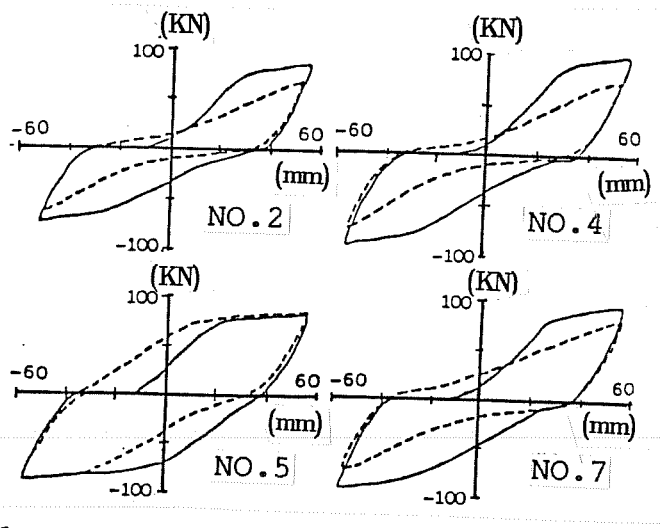

Fig. 3.35 Story shear vs story drift relations during loadings to drift angle of 1/26

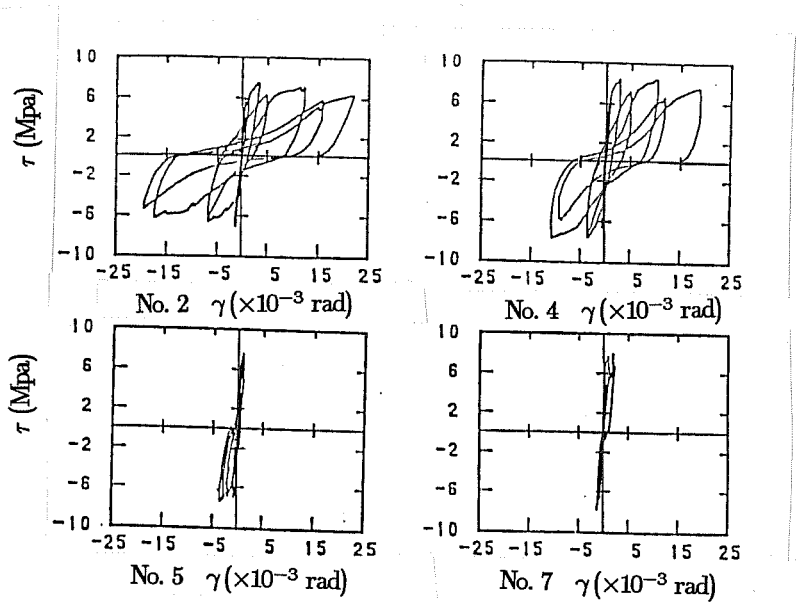

Fig. 3.36 Joint shear stress vs shear distortion

2. A large amount of joint lateral reinforcement (p_w = 0.8 to 1.2%) was effective in (a) preventing joint shear failure,[33] (b) reducing shear crack width and shear distortion,[20,33] and (c) reducing beam bar bond slip within the joint.[36]

3. The joint shear resisting mechanism appeared to be affected by bond along beam longitudinal bars passing through the joint.[32,33,36] A specimen with unbonded beam bars developed no shear cracks in the joint.[36] Joints with good bond developed more

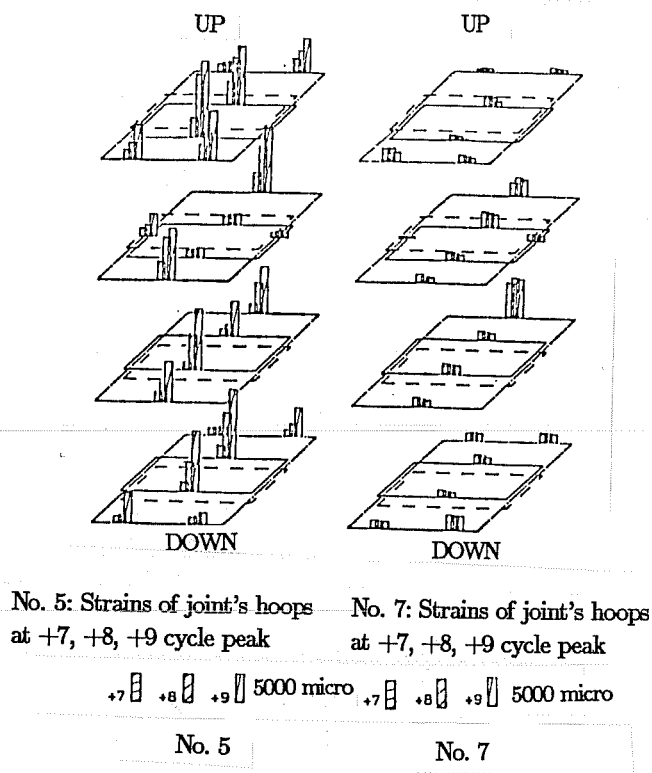

Fig. 3.37 Strains in joint lateral reinforcement

shear cracks,[32] underwent larger shear distortion [33,36] and reached higher strains in the lateral reinforcement[32,33] than those with poor bond.

4. Large-size beam longitudinal bars accelerated bond deterioration within the joint and caused slip-type hysteretic behavior.[20,33] Good spindle-shaped hysteretic behavior was observed for the specimen with a beam bar bond index of 55 kgf/cm^2 or less[27,33] and for the specimen designed to locate the beam critical section at a distance from the column face.[35] Column axial load did not appear to reduce beam bar bond slip.[20]

5. When beams and columns were connected eccentrically to each other, the influence of the eccentricity primarily appeared in the ductility of the specimen rather than in the strength.[21]

3.2.2 Bidirectional Loading Tests.

Hokkaido University. A series of bidirectional loading tests were conducted at Hokkaido University.[28] Four specimens shown in Fig. 3.38 were tested to study the shear resistance of interior beam-column joints in two-way frame structures. The specimens were half-scale interior beam-column-slab subassemblages in which four beams framed into a joint in two directions. The first three specimens (B1-XY, B1-45 and B1-45 PH) were three-dimensional

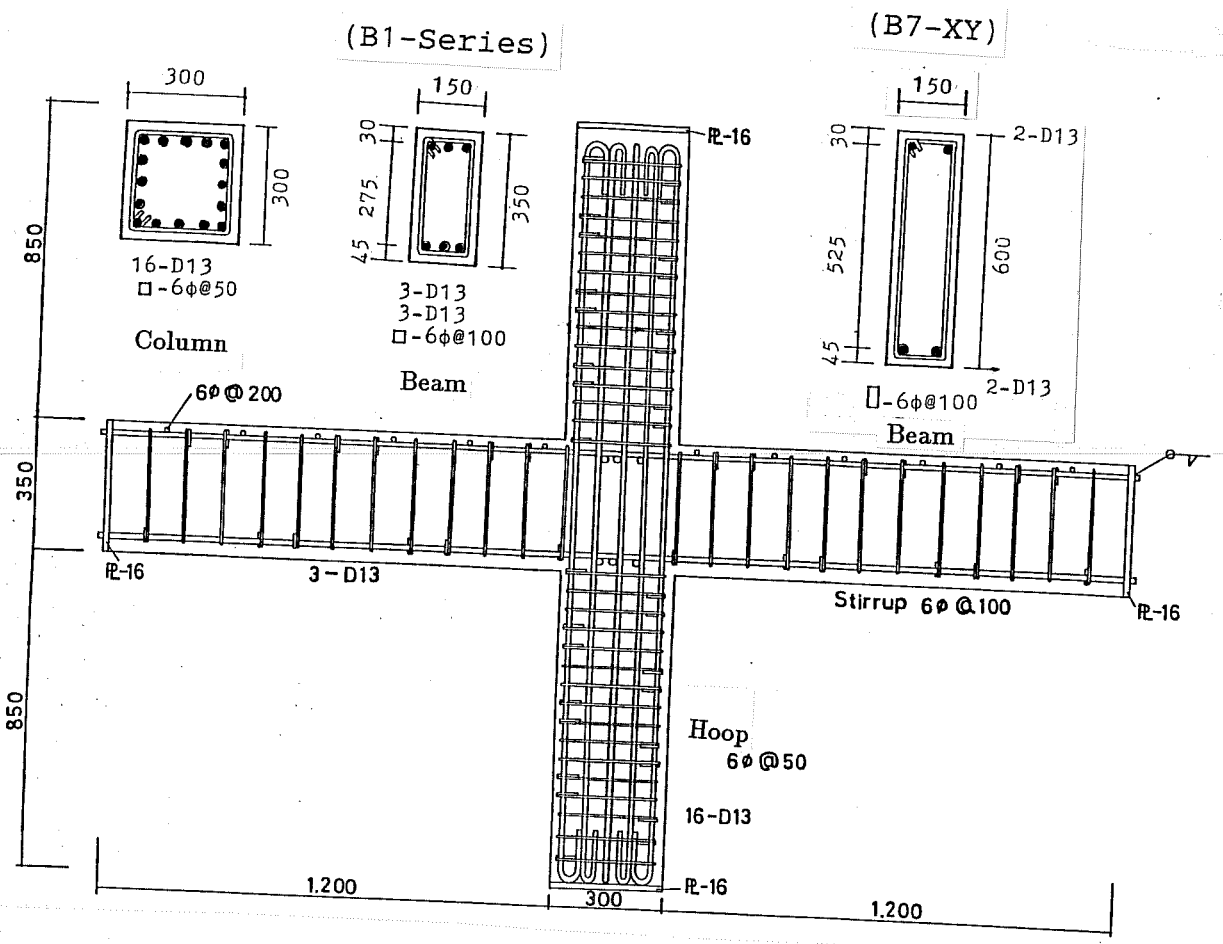

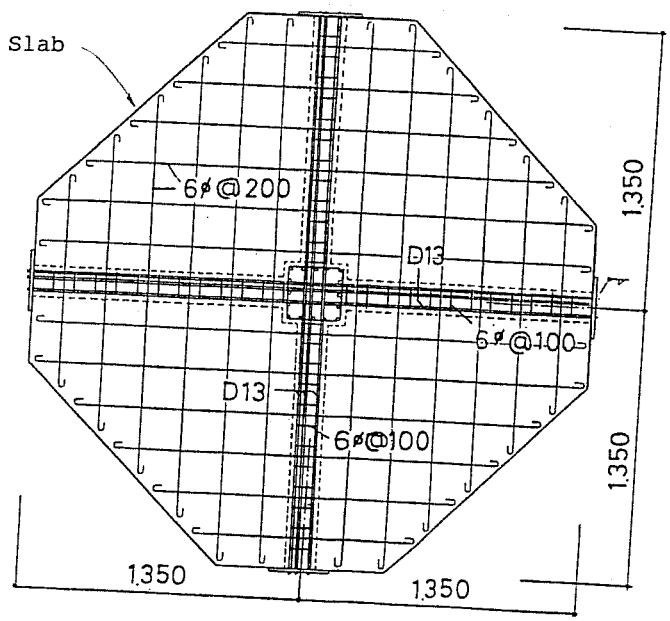

Fig. 3.38 Details of specimens

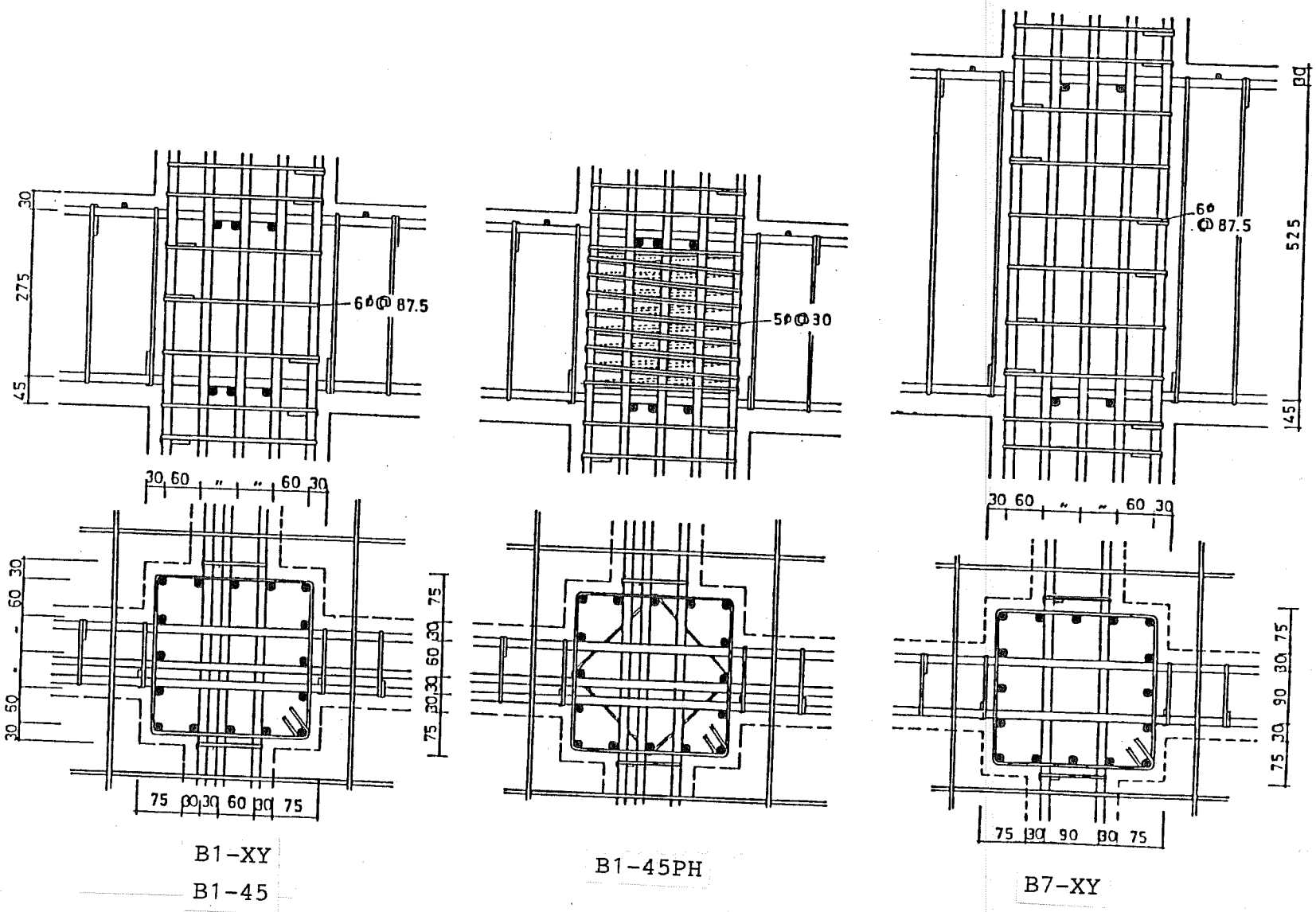

Details of joint lateral reinforcement

(Fig. 3.38 Continued)

variations of Specimen B1 in the unidirectional loading series (see Figs. 3.2 through 3.5). Specimen B1-XY had standard details where the joint was laterally reinforced with $\phi 6$ hoops spaced at 87.5 mm. Specimen B1-45 was identical to B1-XY but loaded differently. Specimen B1-45 PH was designed to meet the requirements of the New Zealand Code[37] as well as ACI 318-83[38] so that the joint was laterally reinforced with a large amount of high strength steel. Specimen B7-XY had an elongated joint because deep beams were used. The slab was 60 mm thick and reinforced with a single layer of $\phi 6$ bars in each direction. Concrete strength ranged from 210 to 278 kgf/cm^2. Bar yield strength was 13600 kgf/cm^2 for the joint lateral reinforcement in Specimen B1-45 PH and 3390 to 3700 kgf/cm^2 for the other reinforcement. The loading setup is shown in Fig. 3.39. Reversing bidirectional loads were applied at the top of the column with two actuators installed in the two orthogonal directions. Specimens B1=XY and B7-XY were loaded in the two directions parallel to the beam longitudinal axes, while Specimens B1-45 and B1-45 PH were loaded in the two directions at an angle of 45° to the beam axes. The bidirectional loading direction was changed alternately at every cycle. A constant column axial stress of 35 kgf/cm^2 was applied to all specimens. Crack patterns at the end of loading are shown in Fig. 3.40. Crushing of concrete was observed at beam ends and joint corners. Flexural cracks in the slab developed at an angle of approximately 45° to the beam axes. Story shear-drift angle relations are shown in Fig. 3.41. All specimens showed inverse-S-shaped hysteresis. The loading at an angle of 45° to the beams (B1-45) resulted in 20% higher story shear than the loading parallel to the beams (B1- XY), indicating biaxial strength less than $\sqrt{2}$ times the uniaxial strength. Specimen B1-45 PH with heavy joint reinforcement showed a little higher strength than Specimen B1-45, but the difference was not as large as expected using Kamimura's equation (Eq. 3). Specimen B7-XY with the oblong joint showed higher story shear than any other specimen, but the horizontal shear measured in the oblong joint was much lower than calculated using Eq. 3. Compared with Specimen B1 in the unidirectional loading series, Specimen B1-XY showed about 30% higher story shear. This difference is attributable to the fact that Specimen B1-XY had transverse beams and a slab while B1 did not.

University of Tokyo. Another series of bidirectional loading tests were conducted at the University of Tokyo.[31] The main variable in this series (K-series) was the bond situation along beam longitudinal bars within the joint. Two interior and one exterior specimen were tested and the results for the interior specimens are described below (see Sec. 3.3.2 for the exterior specimen).

The interior specimens (K1 and K2) were half-scale beam-column-slab subassemblages as shown in Fig. 3.42. The specimens were designed in accordance with Japanese practices in design and construction so that the beam-column joints were provided with a small amount of lateral reinforcement (D6 hoops spaced at 50 mm).

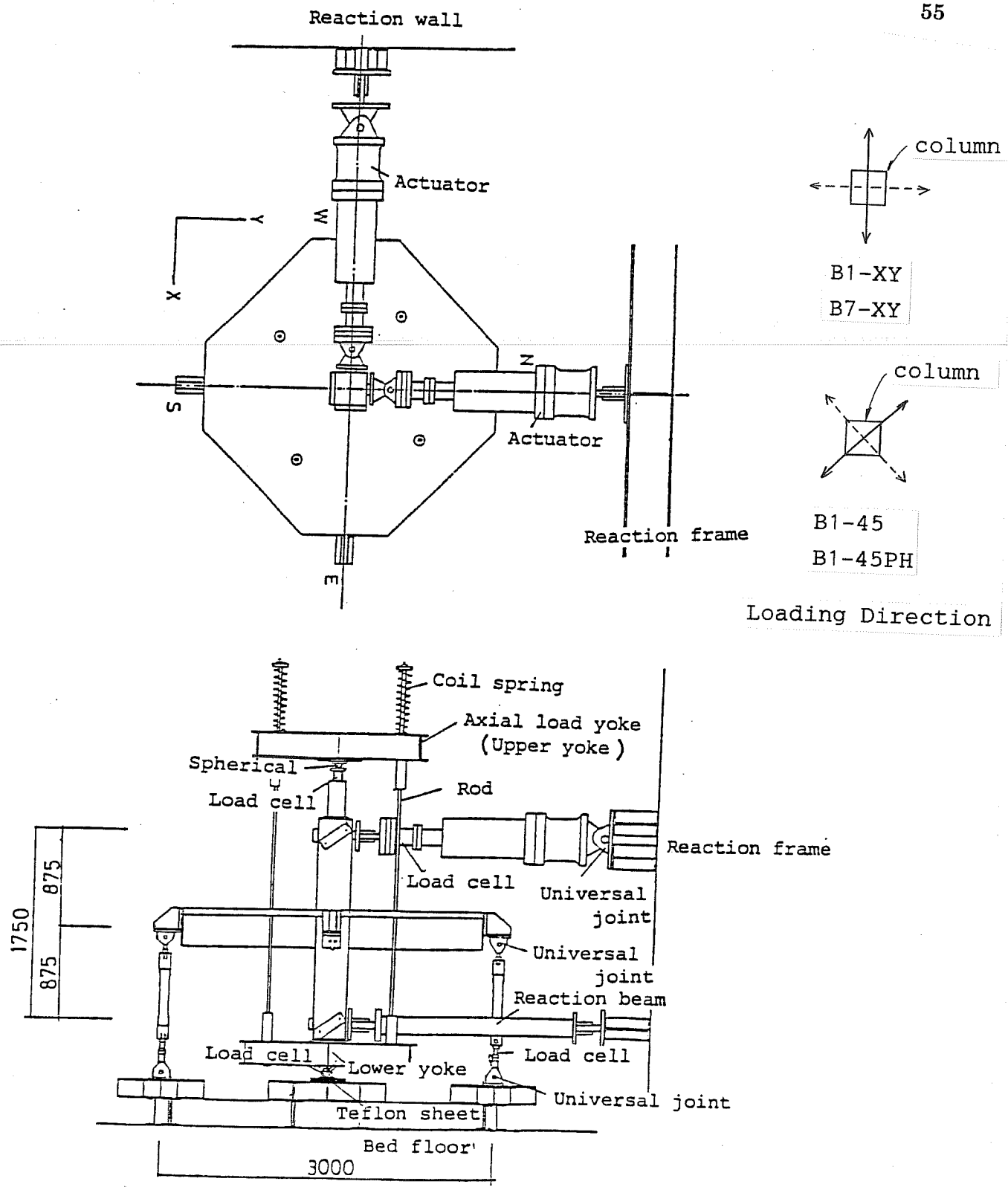

Fig. 3.39 Loading setup

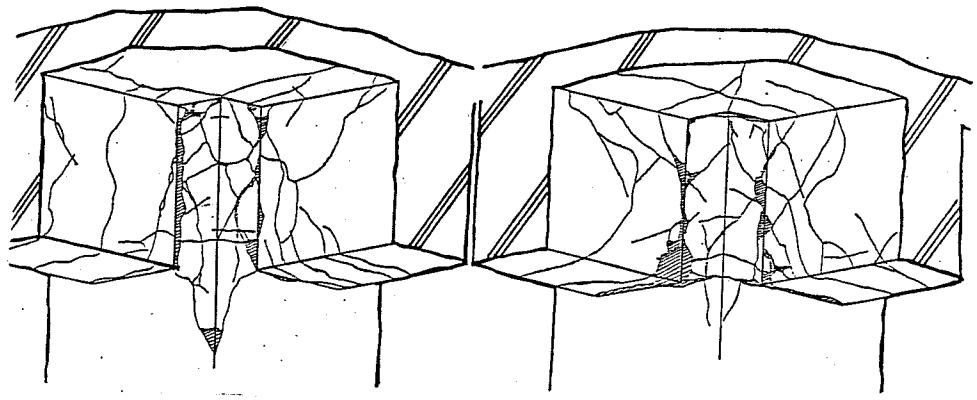

B1-XY

B1-45PH

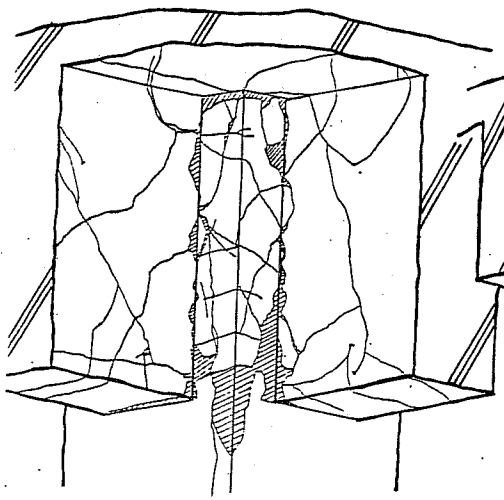

B7-XY

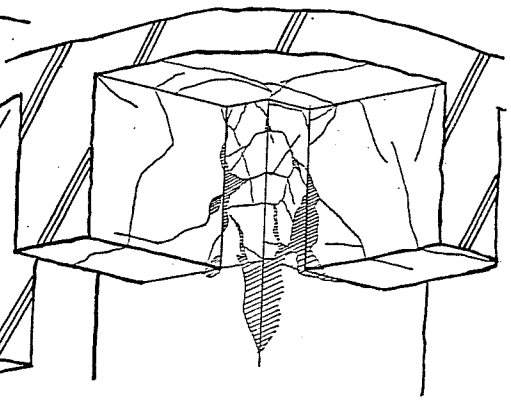

B1-45

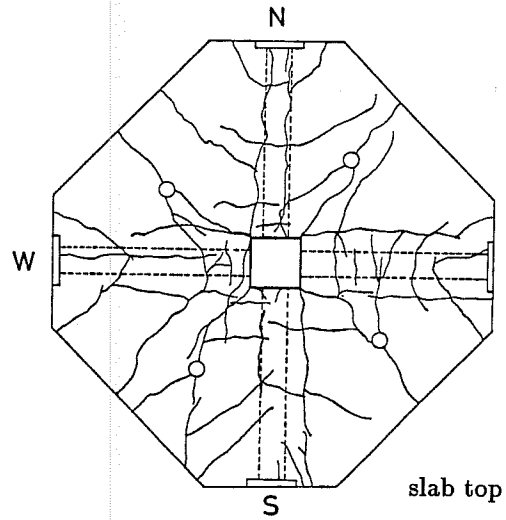

slab top view

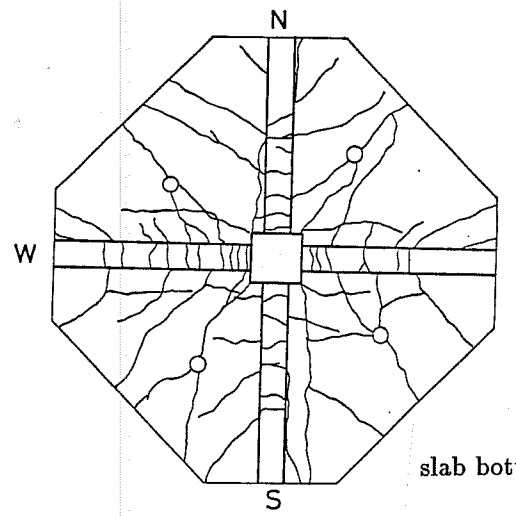

slab bottom view

B1-XY

Fig. 3.40 Crack patterns after test

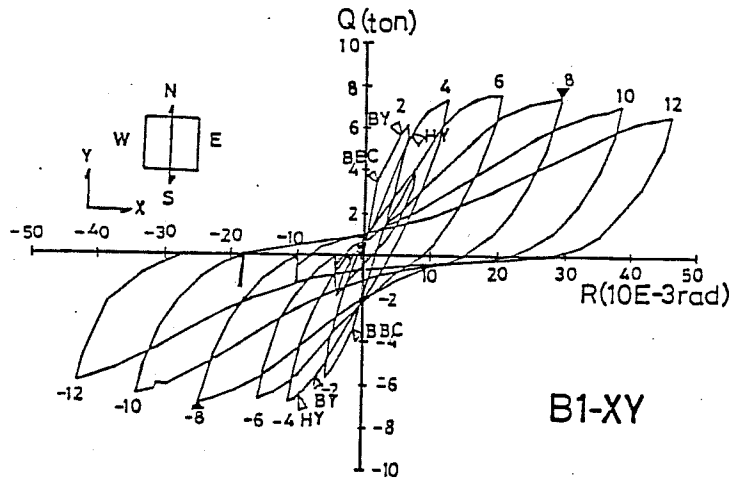

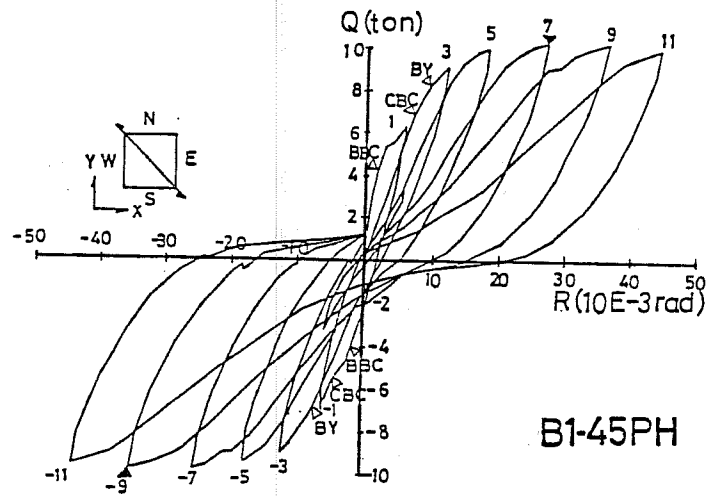

C.B.C: flexural crack in column
B.B.C: flexural crack in beam
B.Y : yielding in beam
H.Y : yielding in hoops of joint
▼ : ultimate strength

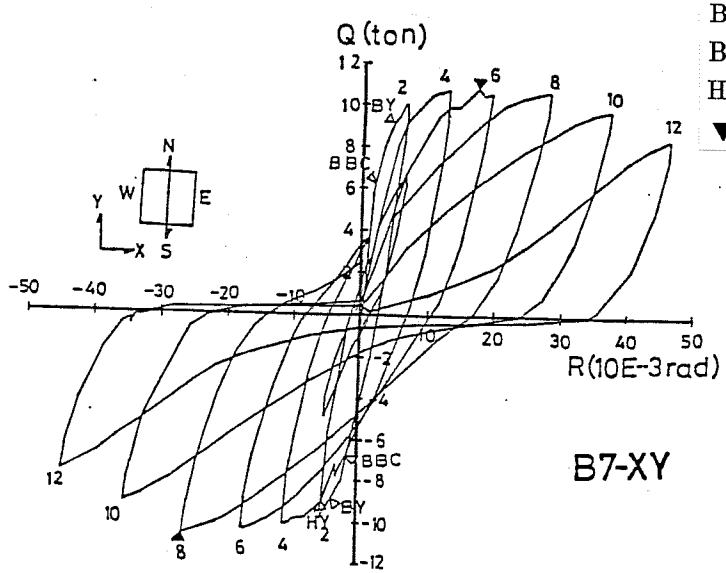

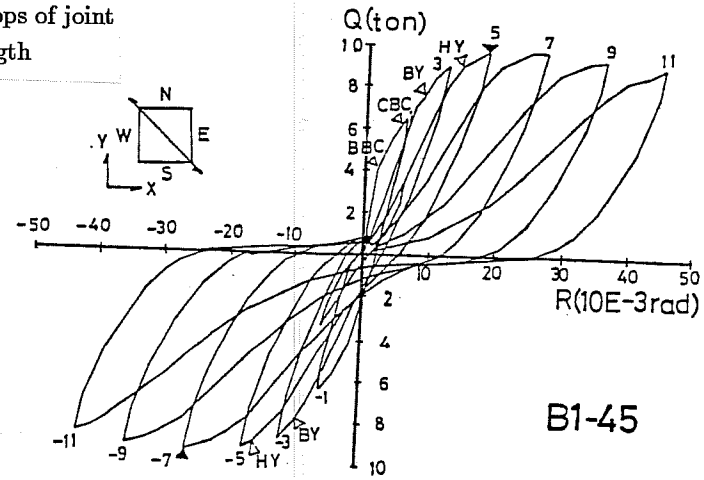

Fig. 3.41 Story shear vs drift angle relations

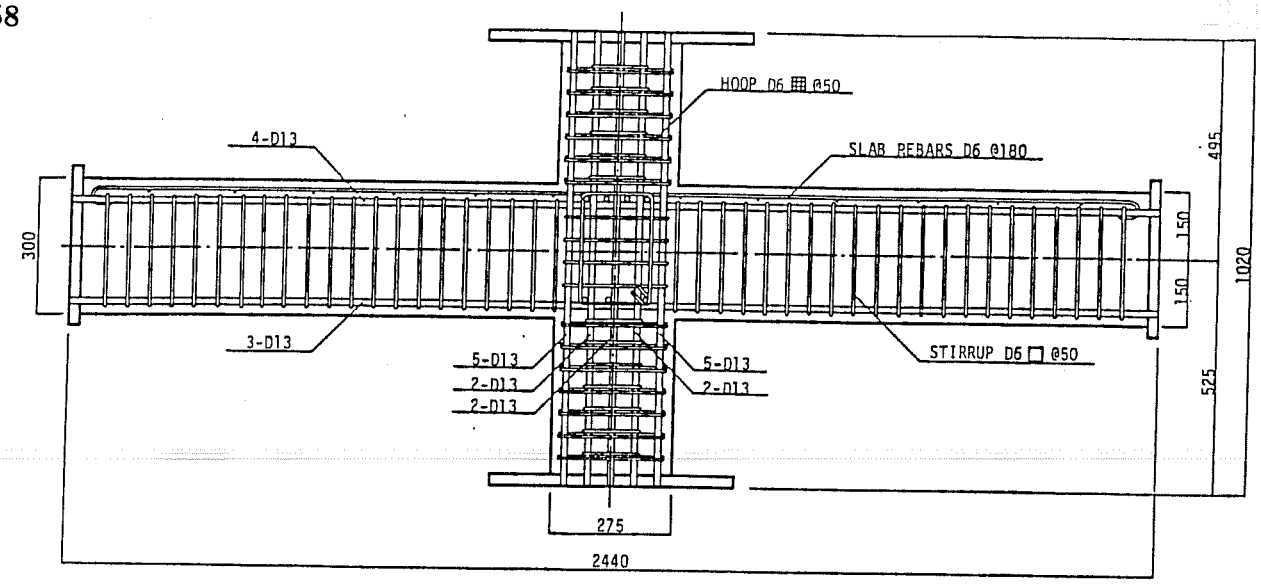

(unit: mm)

(i) Elevation

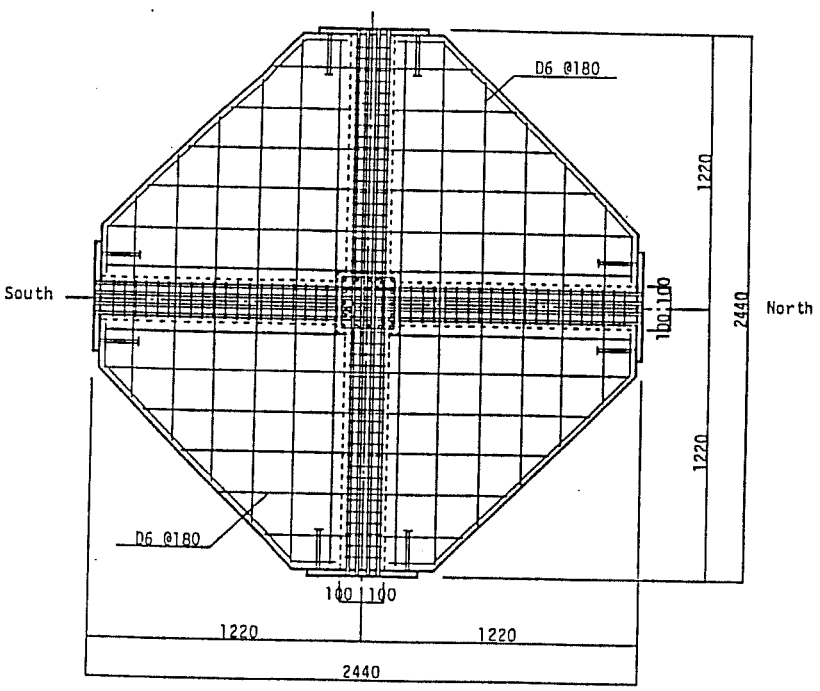

(ii) Plan

(unit: mm)

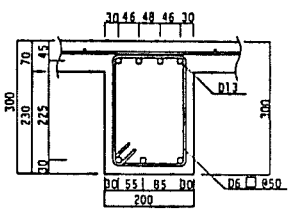

(iii) Longitudinal beam

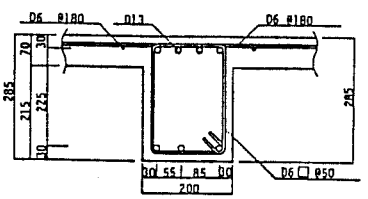

(iv) Transverse beam

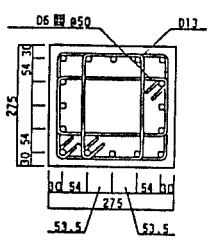

(v) Column

Specimen K1

Fig. 3.42 Details of interior specimens (K– Series)

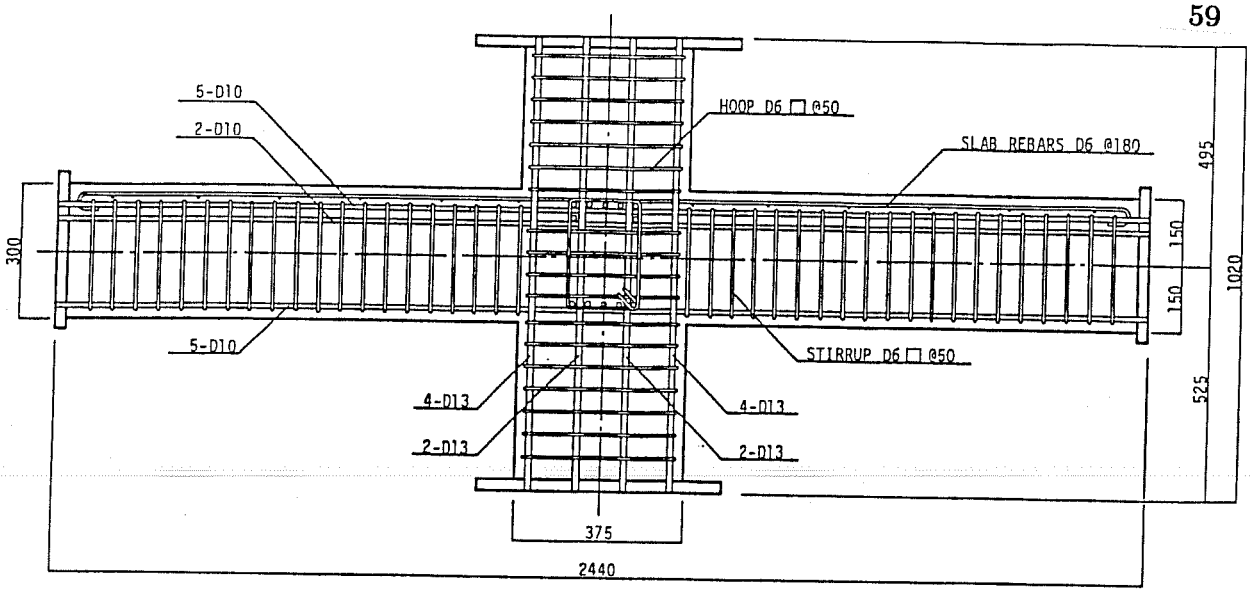

(i) Elevation (unit: mm)

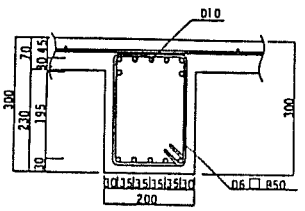

(iii) Longitudinal beam

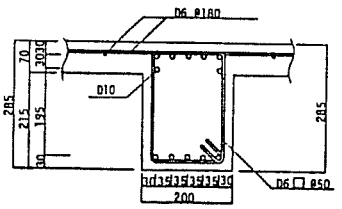

(iv) Transverse beam

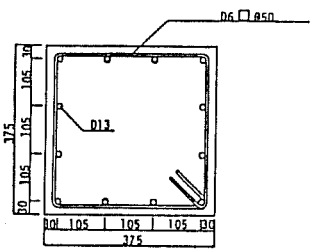

(v) Column

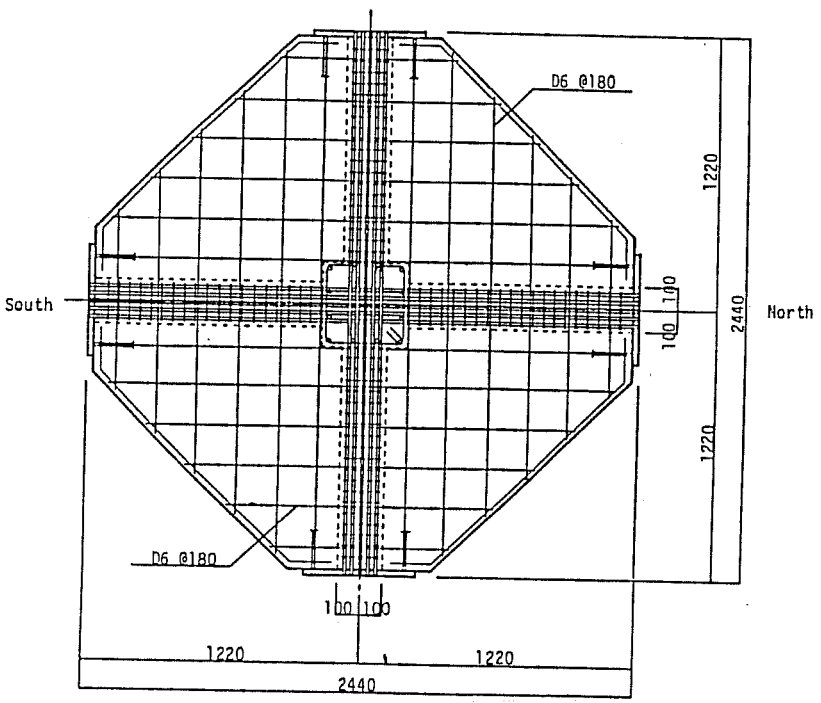

(ii) Plan (unit: mm)

Specimen K2

(Fig. 3.42 Continued)

Beam dimensions were common to the two specimens, but beam longitudinal bars and column depth were varied to develop different bond conditions. The beam bar bond index (Eq. 8) was 102 kgf/cm^2 for Specimen K1 with D13 beam bars passing through the 275 mm-deep column, and 57 kgf/cm^2 for Specimen K2 with D10 beam bars through the 375 mm-deep column. Concrete strength was 244 to 266 kgf/cm^2. Bar yield strength was 4420 to 4460 kgf/cm^2 for longitudinal reinforcement and 4010 kgf/cm^2 for lateral reinforcement. The loading apparatus is shown in Fig. 3.43. A constant axial stress of 20 kgf/cm^2 and reversing bidirectional horizontal loads were applied at the top of the column with three actuators. The bidirectional loading followed the displacement history shown in Fig. 3.1. Crack patterns at the end of loading are shown in Fig. 3.44. Specimen K1 developed a single and wide concentrated crack at the critical section of the beams. Specimen K2 developed fine flexural cracks distributed along the beams. The shell concrete spalled in the four corners near and within the joint of Specimen K1 but did not in Specimen K2. Story shear-story drift relations are shown in Fig. 3.45. The vertical segments as observed between points A and B in the relations resulted from the biaxial interaction of the resistances in which the loading in one direction reduced the story shear in the other direction while the story drift was held constant. Compared with the good spindle-shaped hysteresis for Specimen C2 in the unidirectional loading series (Figs. 3.25 through 3.29), hysteresis for Specimens K1 and K2 showed considerable pinching. The pinching phenomenon was more pronounced for Specimen K1 than for Specimen K2 because the bond deterioration along beam bars occurred in Specimen K1. However, the pinching observed in Specimen K2 could be attributed to the existence of the slab rather than to bond deterioration because the bond situation in Specimen K2 (bond index $U_b = 57$ kgf/cm^2) was equivalent to that in Specimen C2 ($U_b = 52$ kgf/cm^2).

Deflection components of the story drift are shown in Fig. 3.46. The component contributed by the joint shear distortion remained almost constant up to a drift angle of 1/25 rad and showed no sign of joint shear failure. The beam deformation of Specimen K2 contributed more of the story drift than in Specimen K1 because K2 had bigger and stiffer columns than K1. Figure 3.47 shows beam deflection components contributed by deformations within various regions of the beam. The deflection component within the region immediately adjacent to the joint (Region 1) included the deformation caused by the pull-out of the beam bars from the joint and reached about 70% of the total beam deflection for Specimen K1.

On the contrary, the component within Region 1 stayed at 50% of the beam deflection for Specimen K2, indicating much less pull-out deformation because of the better bond conditions along beam bars. Slab bar stresses were calculated from measured strains assuming the Ramberg-Osgood stress-strain hysteresis relation and are shown in Fig. 3.48. The stresses increased with drift. Strains in joint lateral reinforcement are shown in Fig. 3.49. The lateral reinforcement appeared to confine the joint concrete, because the strains increased during the bidirectional loading. Specimen K1 developed larger strains than Specimen K2 at the same story drift, probably because the joint of Specimen K1 was subjected to higher shear stresses.

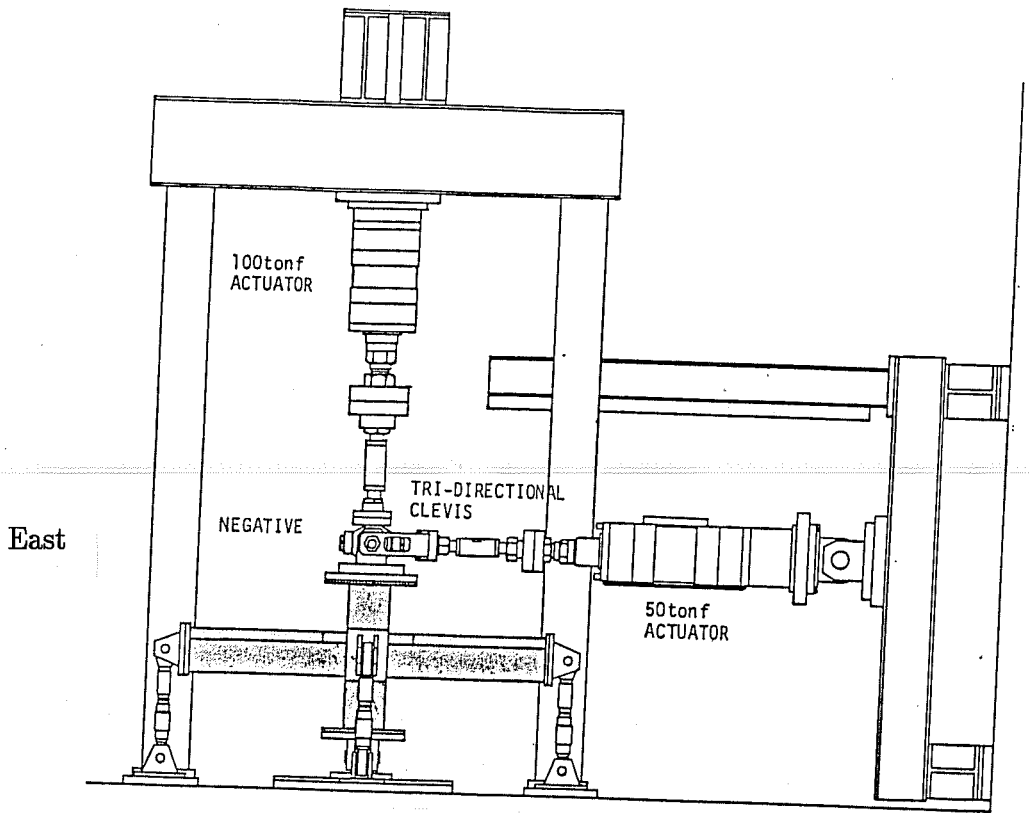

(a) East–west direction

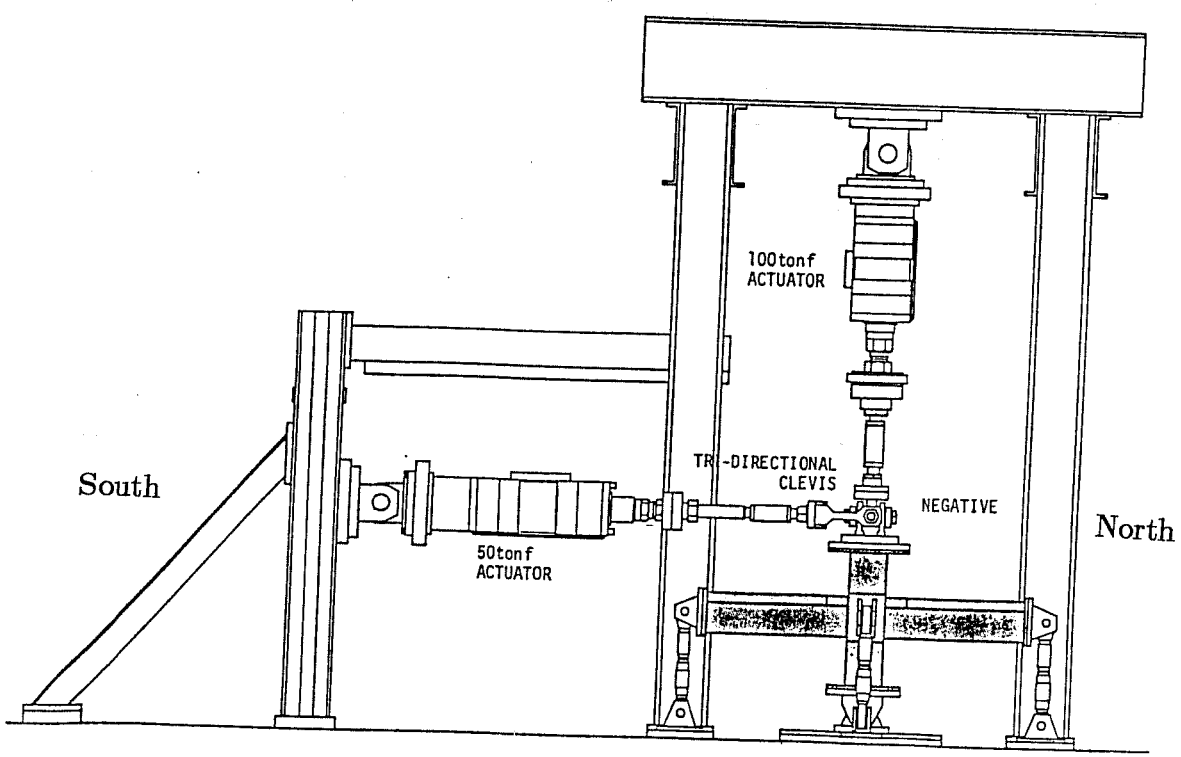

(b) South–north direction

Fig. 3.43 Loading apparatus (K–Series)

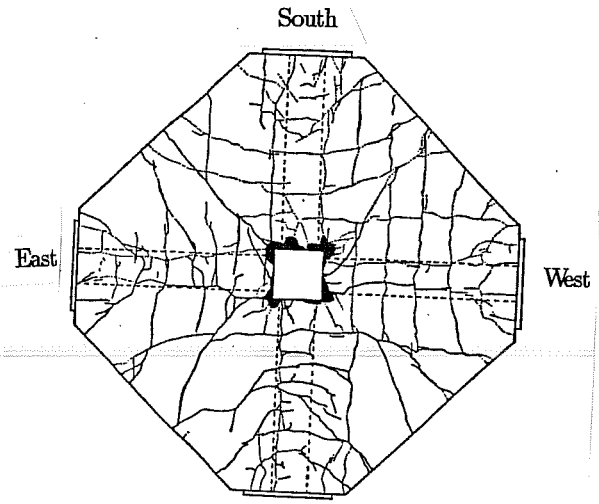

(i) Top view

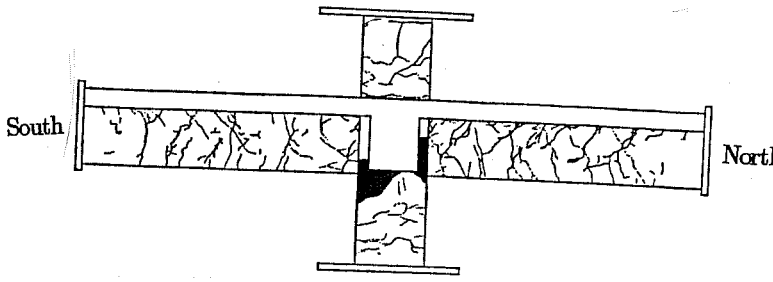

(i) North–south direction

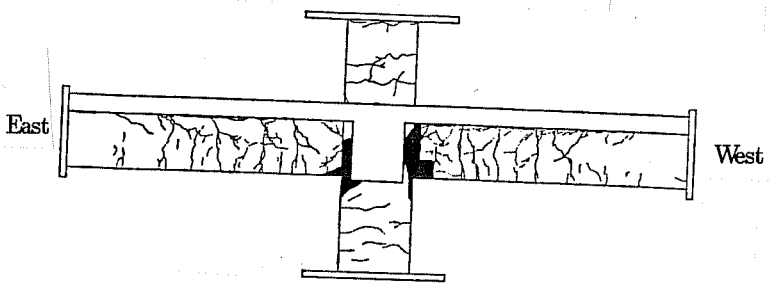

(ii) East–west direction

Specimen K1

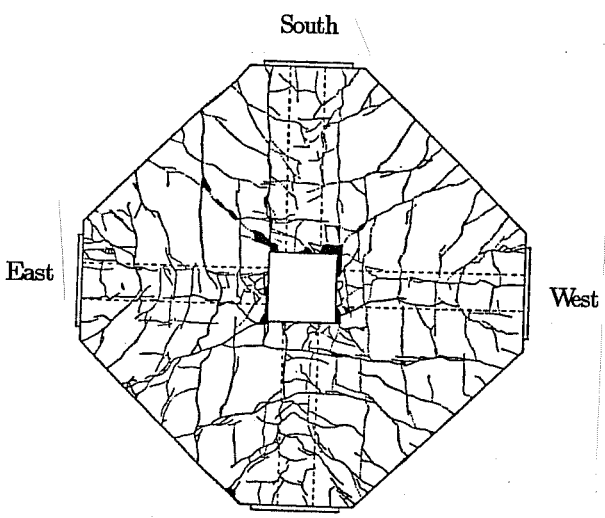

(i) Top view

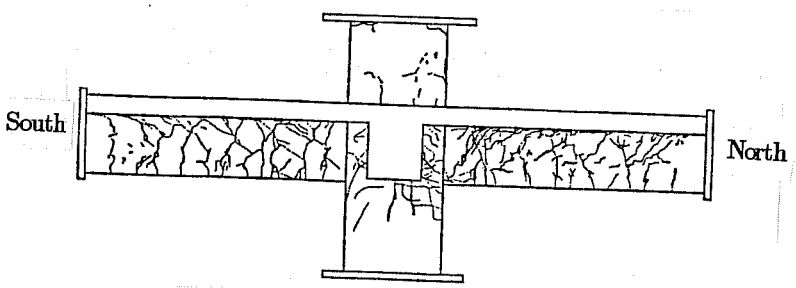

(i) North–south direction

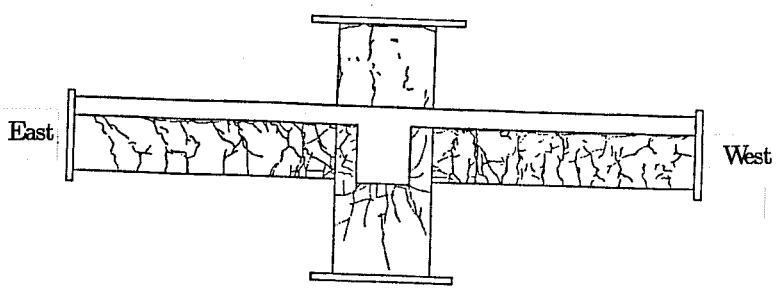

(ii) East–west direction

Specimen K2

Fig. 3.44 Crack patterns after test (K-Series)

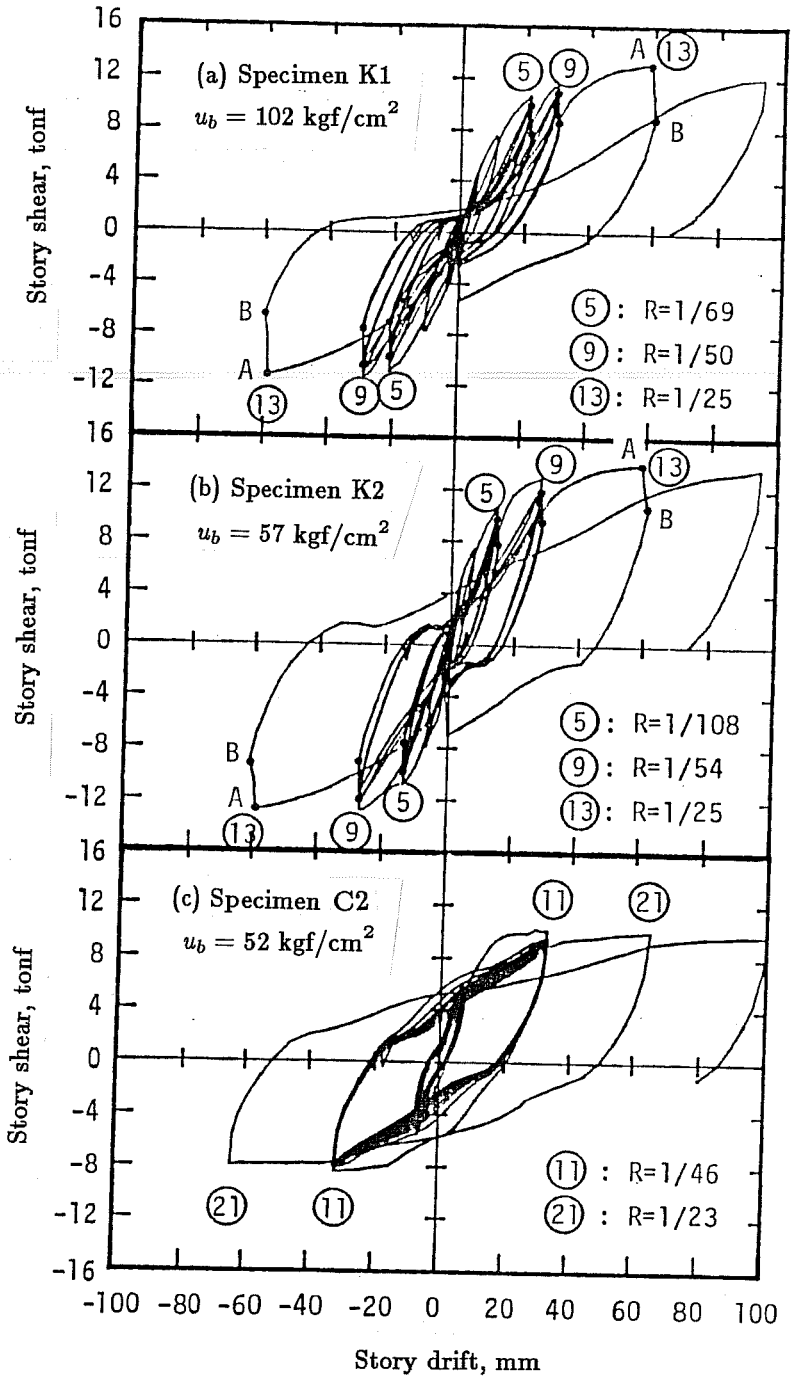

Fig. 3.45 Story shear vs story drift (North–south direction)

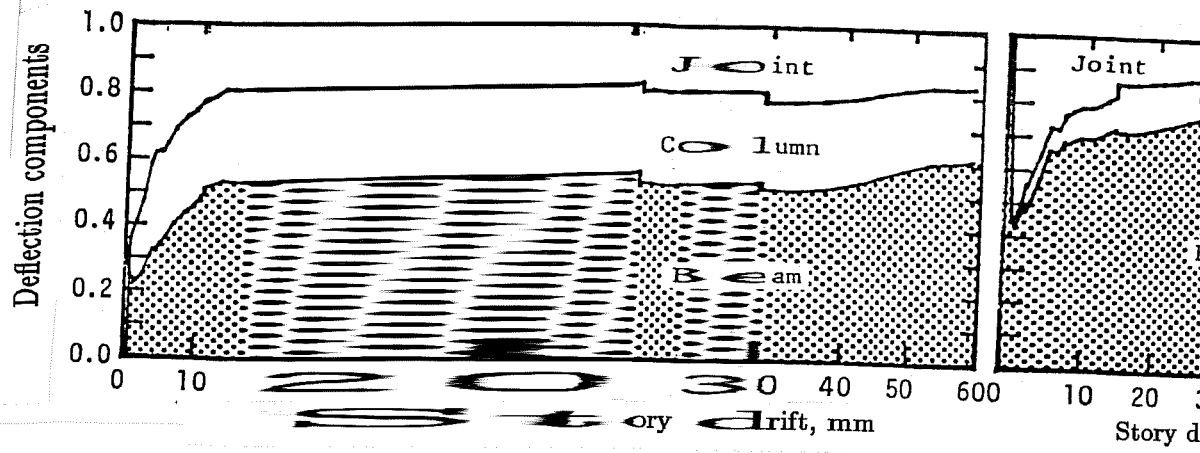

(a) Specimen K1 (b) Specim

Fig. 3.46 Deflection components of stor

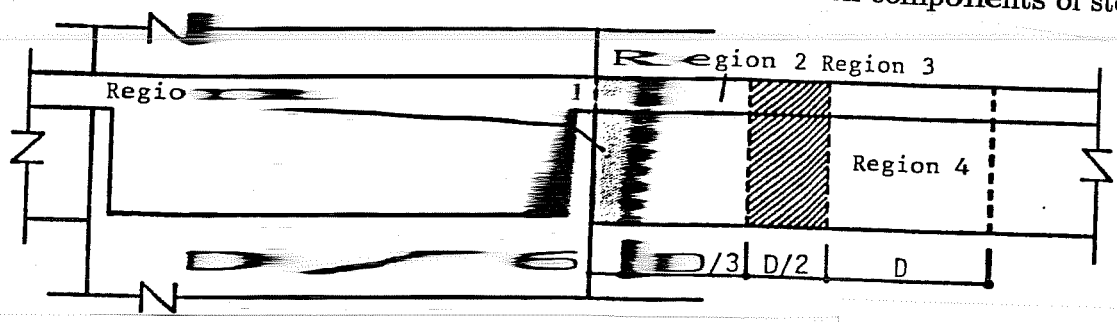

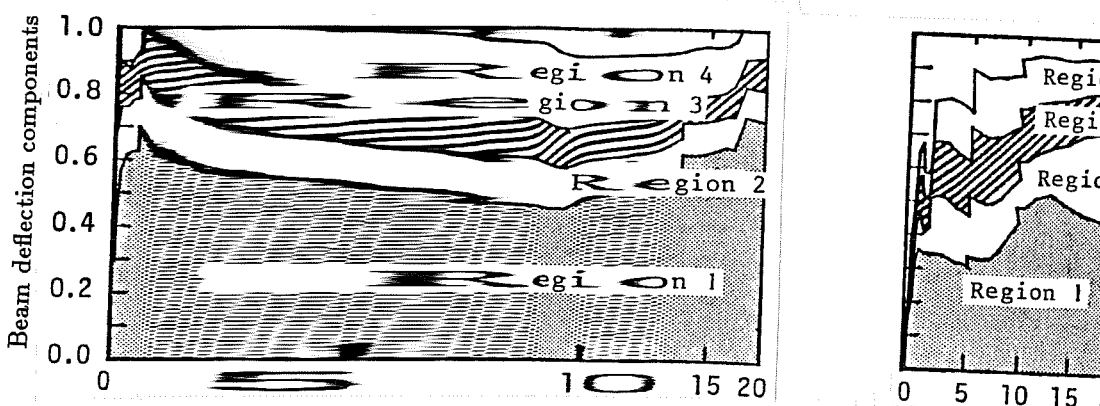

(a) Specimen K1 (b) Specimen K

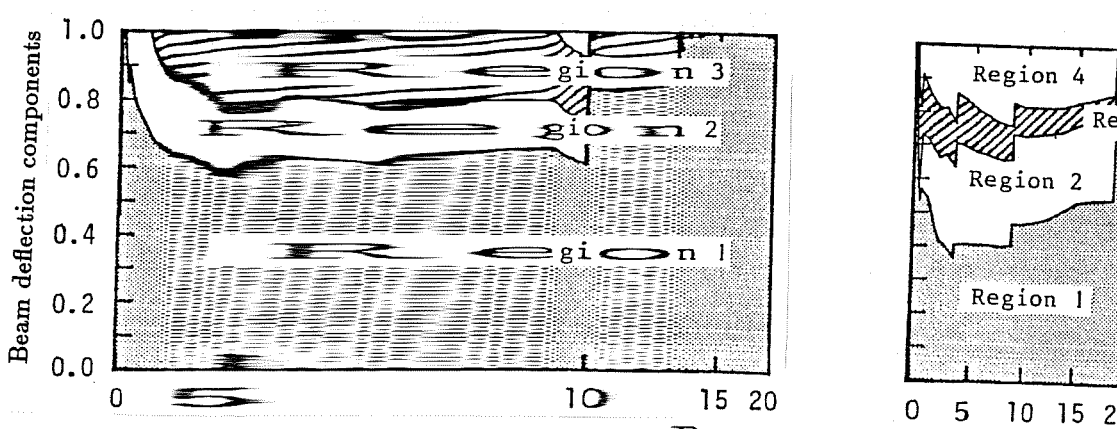

(a) Specimen K1 (b) Specimen K

Fig. 3.47 Contribution of local rotation to beam d

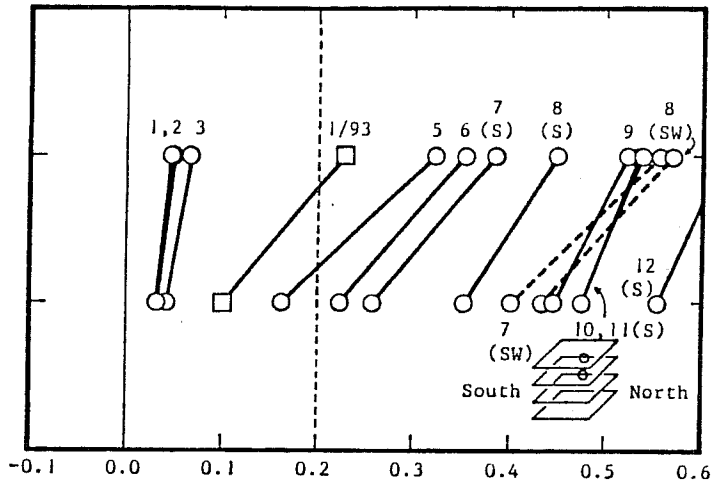

(a) Lateral bars parallel to north-south direction

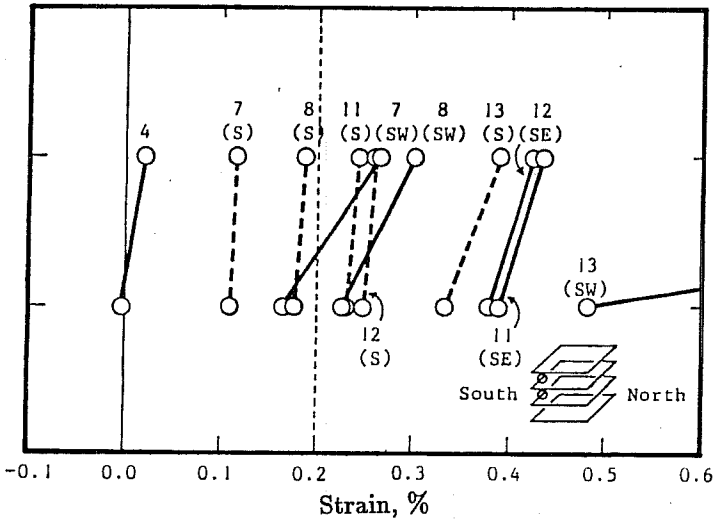

(b) Lateral bars parallel to east-west direction

Specimen K1

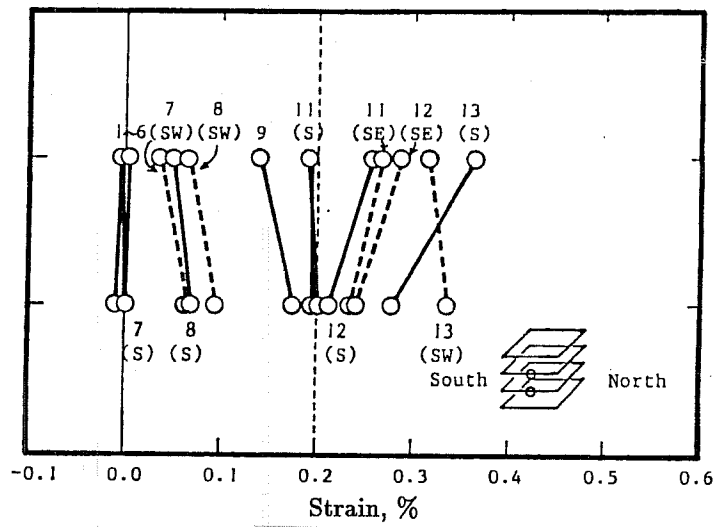

(a) Lateral bars parallel to north-south direction

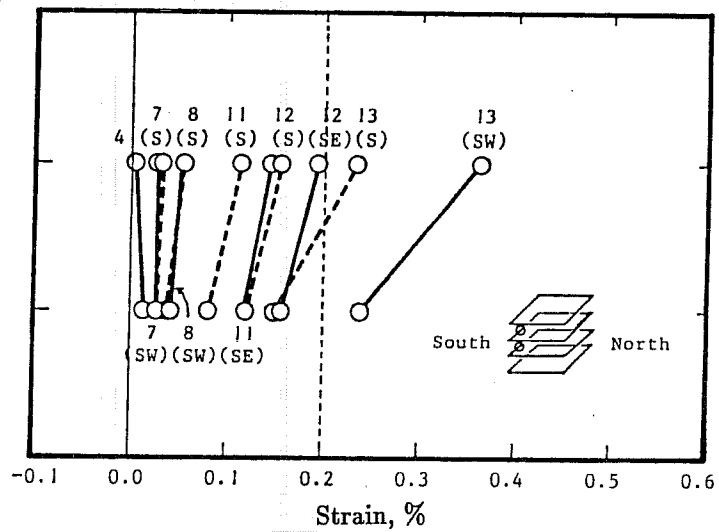

(b) Lateral bars parallel to east-west direction

Specimen K2

Fig. 3.49 Strains in joint lateral reinforcement

From the test results described above, the following conclusions were drawn:

1. The three-dimensional specimens did not fail in joint shear, although they developed high shear stresses in the joint. This is probably because the joint was confined by transverse beams and a slab.[31]

2. The specimens showed pinching hysteresis in the story shear-drift relation.[28,31] The pinching phenomenon observed in the specimen with good bond conditions was probably caused by the slab which raised the neutral axis above the beam top reinforcement in positive bending and thus delayed crack closing when the loading was reversed.[31]

3. The slab width contributing to the beam flexural resistance increased with the beam deformation.[31]

3.2.3 Nonlinear Finite Element Analysis. The inelastic behavior of interior beam-column joints was statically analyzed using the nonlinear finite element method.[18,34] The analysis was aimed mainly at studying the effect of different bond conditions along beam longitudinal bars within the joint. As shown in Fig. 3.50(a), the analytical model was a two-dimensional interior beam-column-joint subassemblage composed of triangular concrete elements, bar elements, bond-link elements and crack-link elements. The bond-link element modeled the bond slip of the beam longitudinal bars assuming the bond stress-slip relation shown in Fig. 3.50(c). The crack-link element shown in Fig. 3.50(b) was placed at the potential crack surface whose location was predetermined by referring to test results. Four specimens (J1, J1′, J2 and J3) were analyzed and compared with test results.[39,40] As shown in Fig. 3.51, the dimensions were the same in all the specimens but the bond conditions along beam bars were varied. Figure 3.52 shows the analytical load-displacement relations in comparison with the test results. The analytical hysteresis curves for Specimens J1 and J2 with poor bond conditions exhibited inverse-S-shaped loops as observed in the test results. On the other hand, Specimen J3 with good bond conditions showed stable spindle-shaped hysteresis in both analytical and experimental results. Principal stress distributions in joint concrete are shown in Fig. 3.53. The diagonal compressive strut formed in Specimens J1 and J2 but did not clearly in Specimen J3. Specimen J1, which failed in joint shear in the test, developed compressive failure of concrete at the center of the joint in the analysis. Shear stresses carried by concrete were calculated and are shown in Fig. 3.54. The stresses in specimens which failed in the joint (J1 and J1′) were much higher than those in the beam-failure-type specimens (J2 and J3) and reached about 50% of the compressive strength of concrete.

3.2.4 Dynamic Response Analysis. Nonlinear earthquake response of frame structures was analyzed to study the effect of beam bar slip within the joint.[27,32] The structural model is a plane frame in which (a) an inelastic rotational spring is placed at member

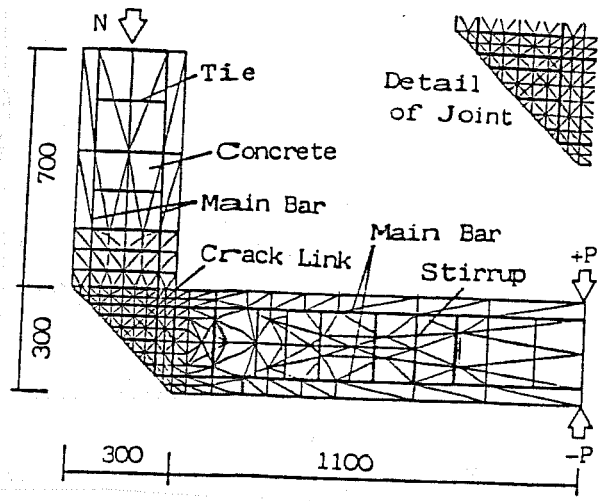

(a) Analytical model

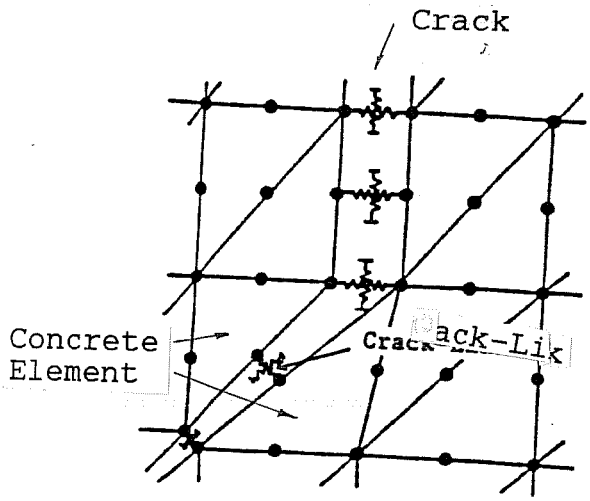

(b) Crack-link element

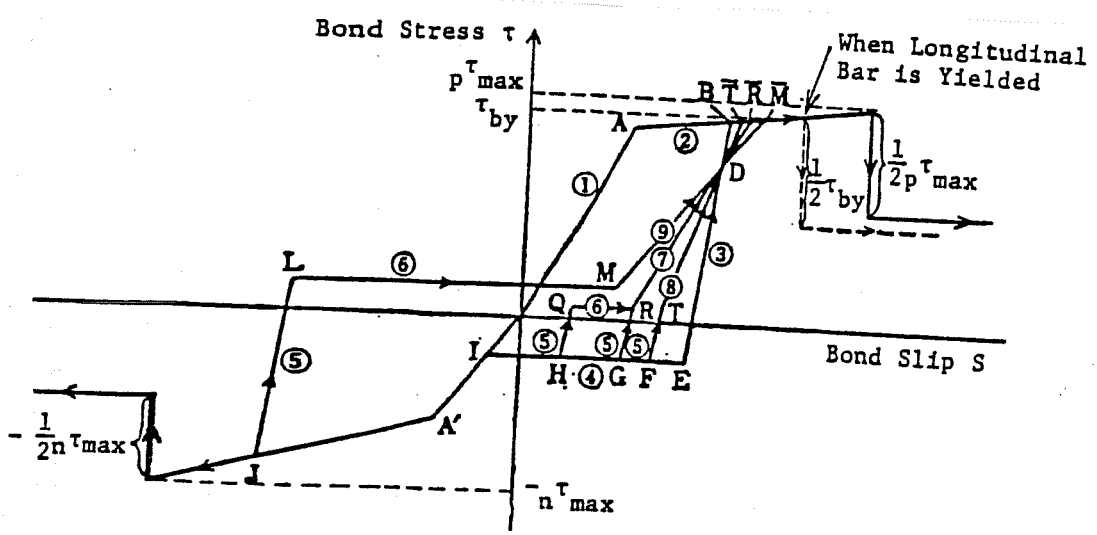

(c) Bond stress-slip relation for bond-link element

Fig. 3.50 Finite element models for beam-column joint

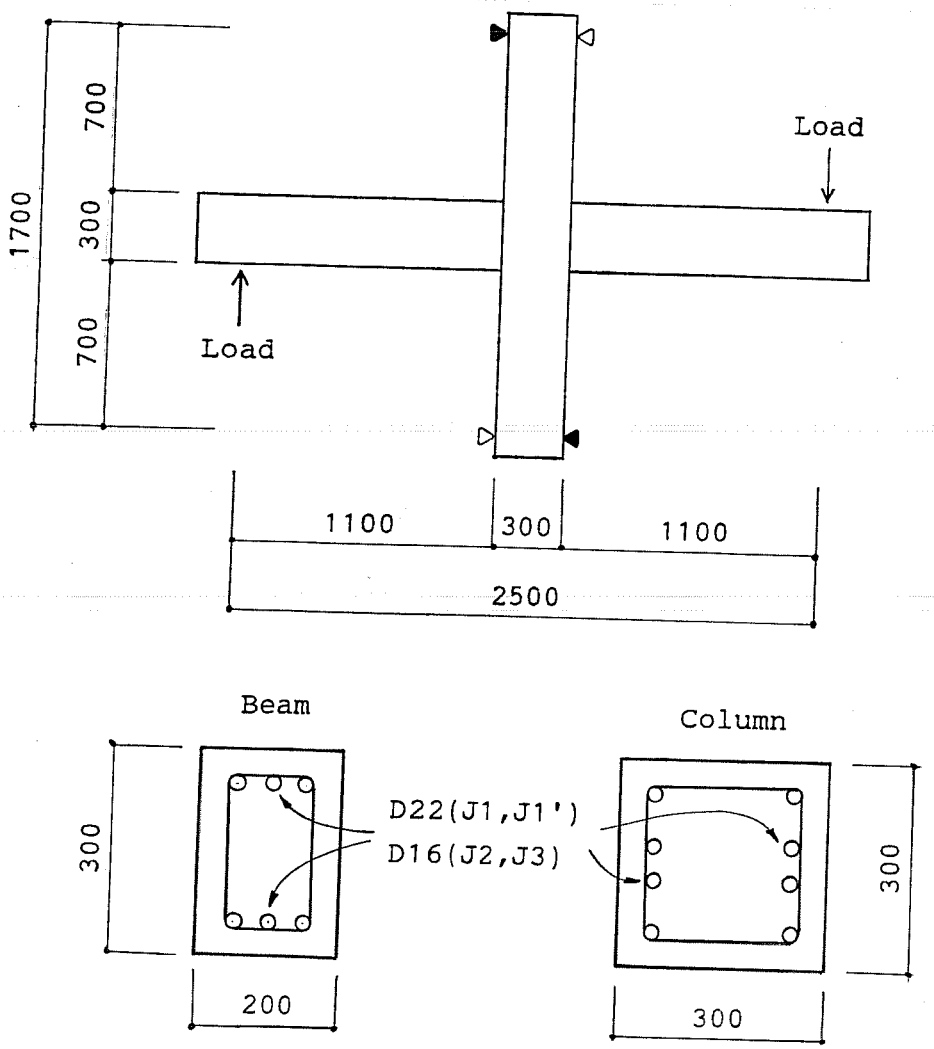

Specimen Variations

Specimen	J–1	J–1′	J–2	J–3
Failure Mode	Joint Failure Bond Deterioration	Joint Failure	Bond Deterioration after Beam Yielding	Beam Yielding
Bond of Beam Longitudinal Bars	Poor	Good	Poor	Perfect
Middle Longitudinal Bars of Column (SD35)	–	D-22	–	–

Fig. 3.51 Properties of specimens in FEM analysis

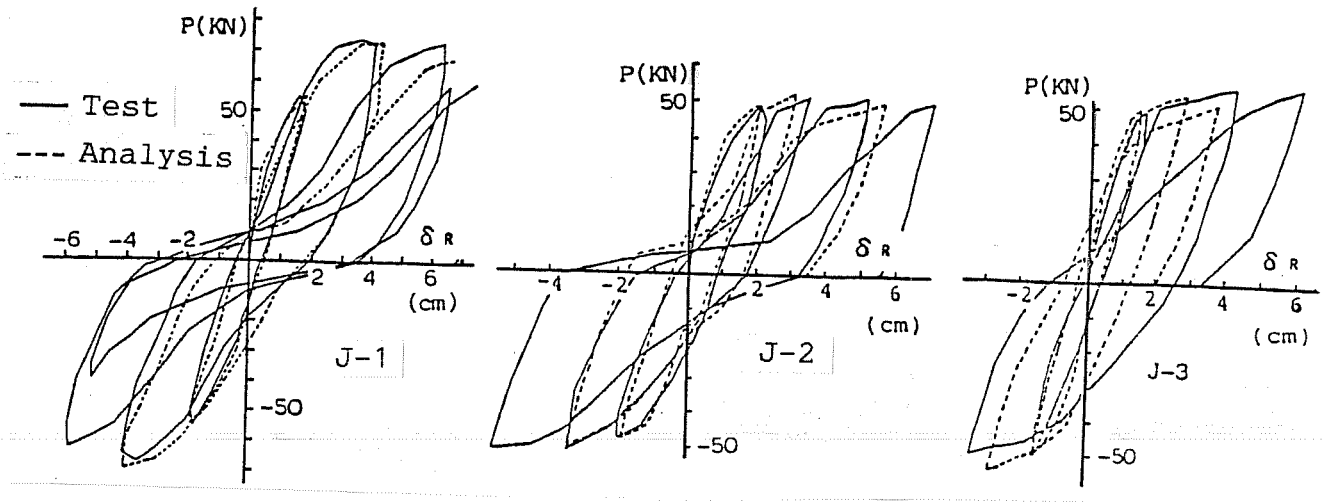

Fig. 3.52 Load vs story displacement relations

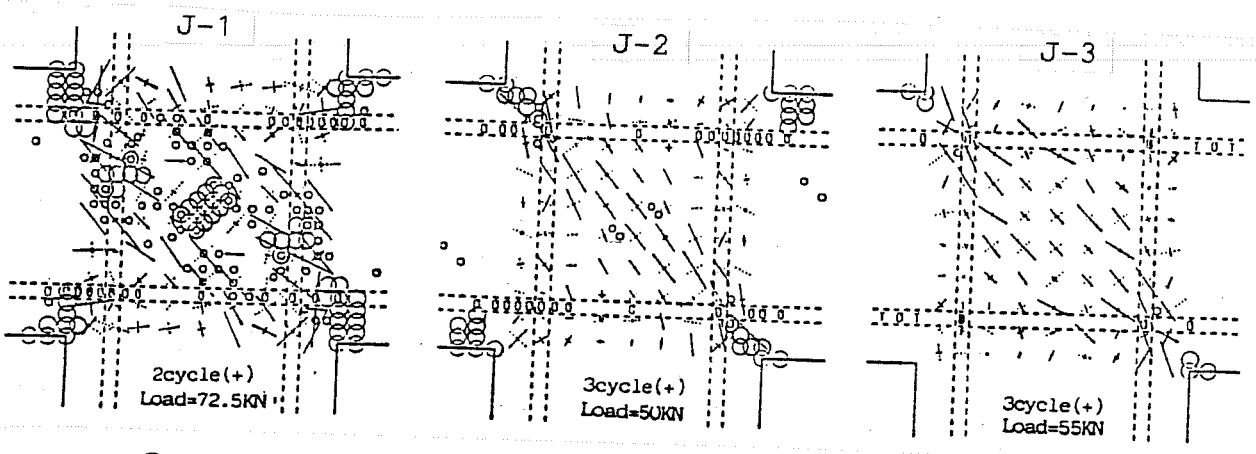

○: Compression failure 0: Bond failure o: Strain softening

Fig. 3.53 Principal stresses in joint

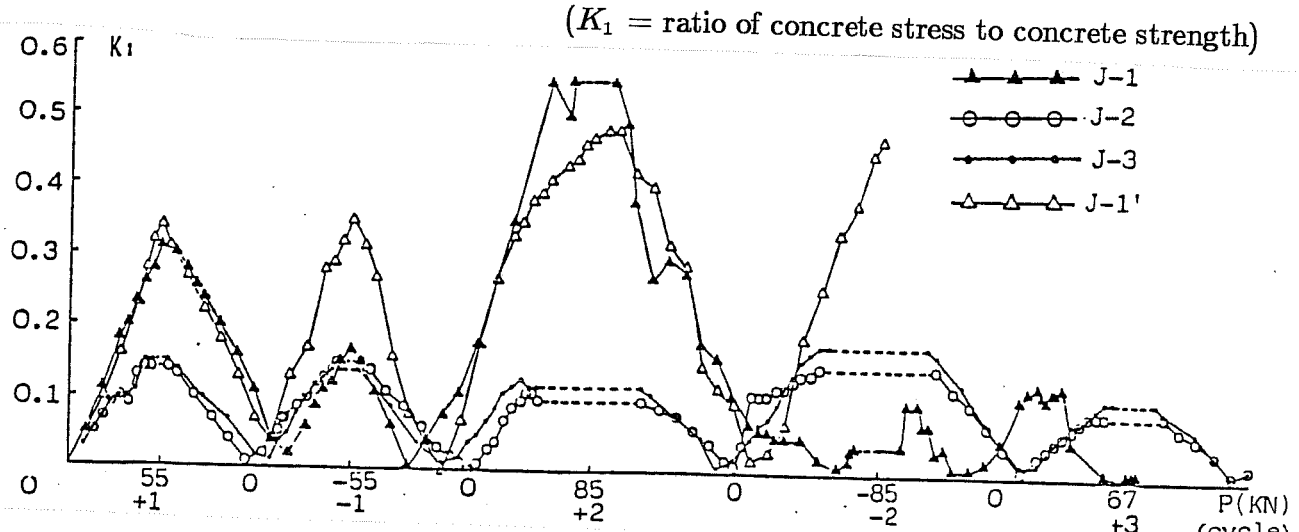

Fig. 3.54 Joint shear stress carried by concrete

ends, (b) beam-column joints are rigid, (c) a mass is lumped at each floor level, and (d) a floor slab acts as a rigid diaphragm so that all joints at a floor displace equally in the horizontal direction.

Different hysteresis models were assigned to the inelastic rotational springs as shown in Fig. 3.55(a). A Takeda-slip model simulated the pinching hysteresis due to the bond deterioration along beam bars within the joint and a Takeda model simulated the spindle-shaped hysteresis for beams and columns with good bond conditions. The response analysis was carried out on one total frame[27] and three substructure frames[32] as shown schematically in Fig. 3.55(b). The total frame modeled an eight-story office building with four 6m-long spans. The three substructure frames, removed from an arbitrary frame by cutting off the beams framing into an interior joint at their inflection points, had four stories, seven stories and sixteen stories, respectively. The frames were fixed at their base and subjected to several horizontal ground motions such as El Centro 1940 NS record, Taft 1952 S69E record and so on.

The ground motion records were scaled so that the maximum response rotation would reach a ductility factor of four. Figure 3.5(b) shows horizontal displacement histories at the roof level. The structures with beam bar slip in the joint (Takeda-slip model) showed larger displacements than those without bar slip (Takeda model). However, the beam bar slip did not increase rotational ductility factors at beam ends, as shown in Fig. 3.57. It should be noted that the yield deflection at the beam end with the Takeda-slip model was greater than that with the Takeda model because of the additional deformation due to the bar slip. That is why the attained ductilities were comparable for the two hysteresis models. The substructure frames were analyzed with two Takeda-slip models having different h_{eq} values (h_{eq} = equivalent viscous damping ratio). A change in the h_{eq} value from 0.15 to 0.10 did not affect the response ductilities. It is important to note that the h_{eq} value is a measure of the hysteretic energy dissipating capability. According to the test results at the University of Tokyo (S–, J– and C–series), the h_{eq} values tend to decrease with the increase of beam bar bond index U_b as shown in Fig. 3.58.[32] If $h_{eq} = 0.10$ at a drift angle of 1/50 is allowable, the required ratio of column depth to beam bar diameter is obtained by substituting the bond index $U_b < 1.6\sqrt{f'_c}$ into Eq. 8. The result is shown in Fig. 3.59.[32]

3.3 Studies on RC Exterior Joints

RC exterior (⊢-shaped) joints generally have the following details in Japan.

1. Beam bottom bars as well as top bars are bent down and anchored into a lower column, as seen in the typical details shown in Fig. 3.60a.
2. Bent bar development length is specified in terms of total length L as shown in Fig. 3.60(b) and Table 2.1.

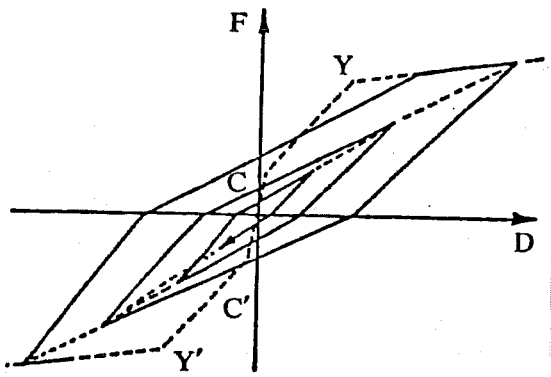

Takeda model

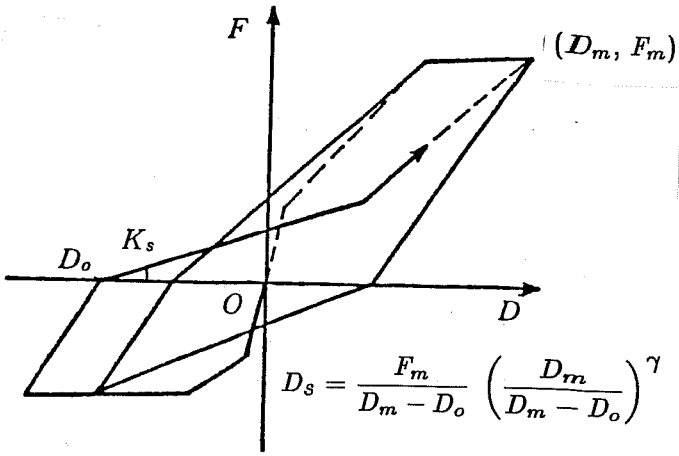

Takeda-slip model

(a) Hysteresis models

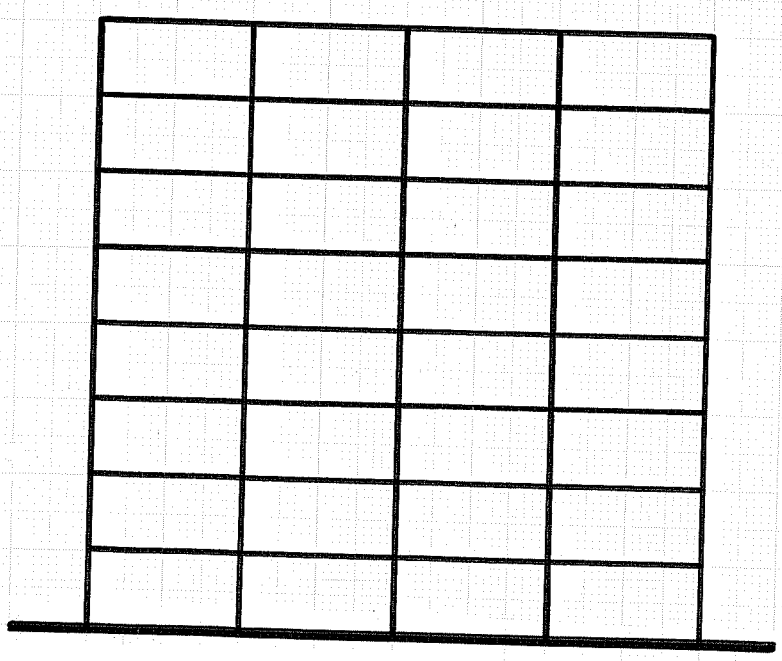

Total frame

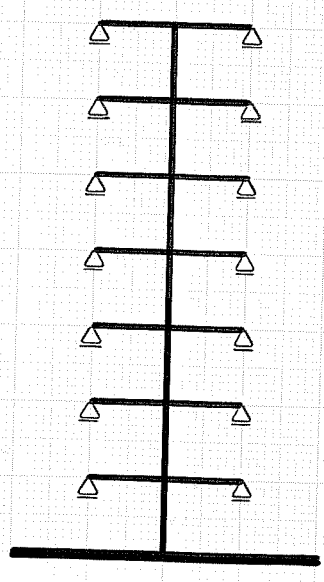

Substructure frame

(b) Frame structures

Fig. 3.55 Structural models in dynamic response analysis

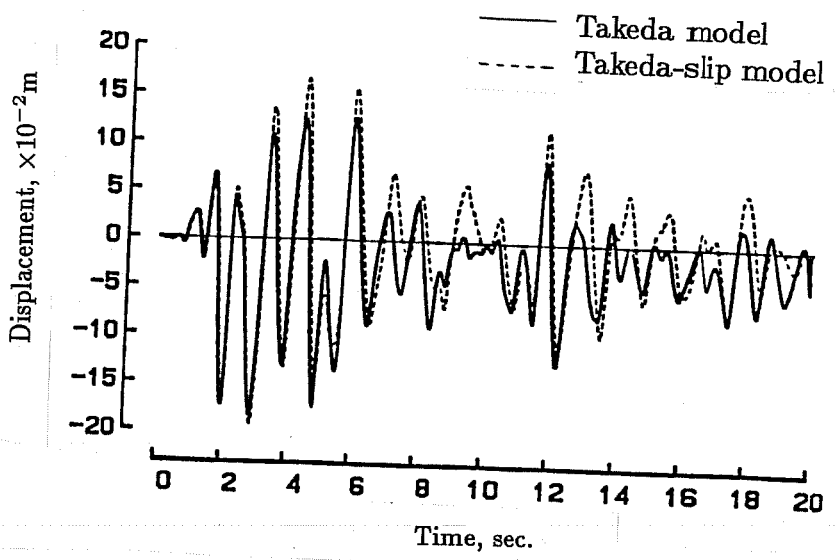

(El Centro 1940 NS Record)

(a) Total frame

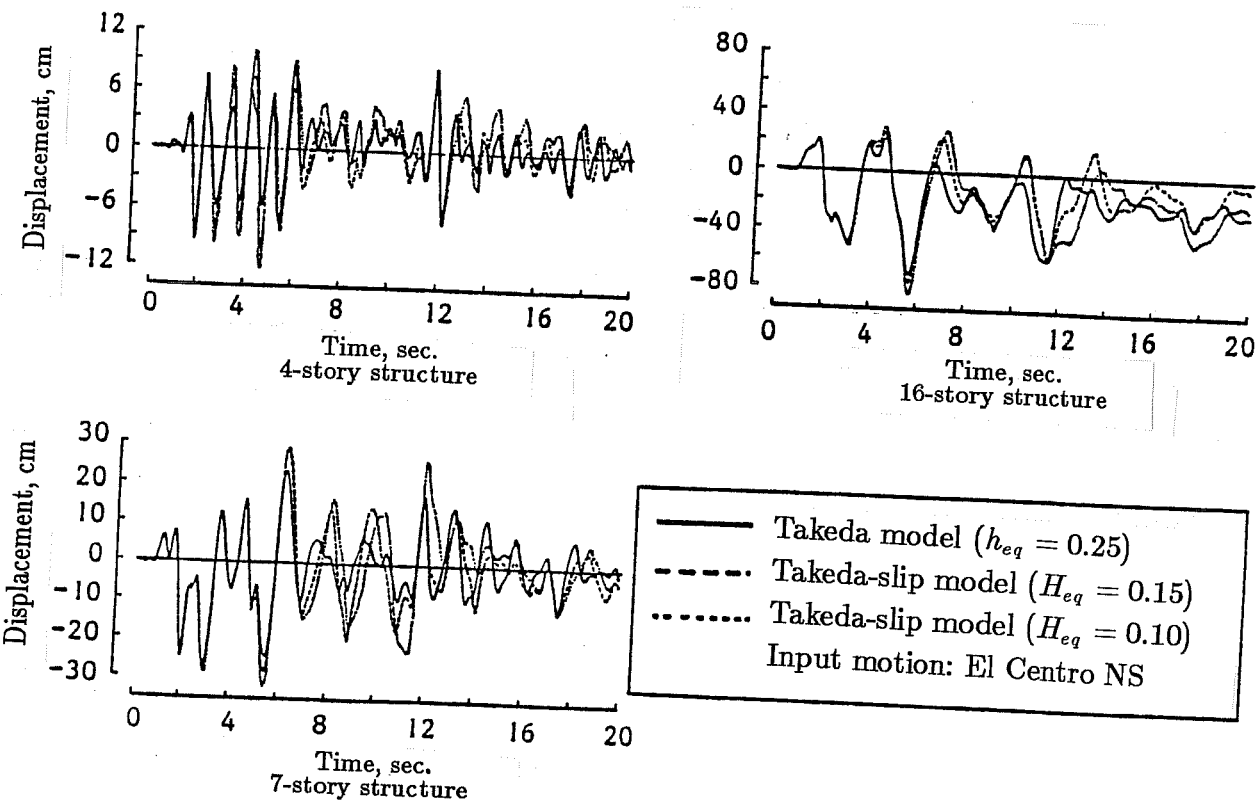

(b) Substructure frames

Fig. 3.56 Displacement response history at roof level

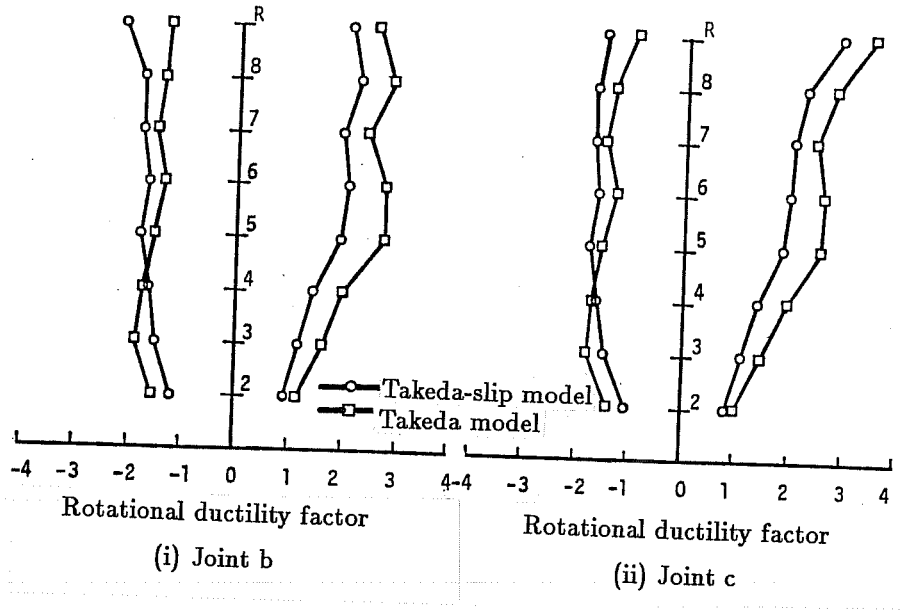

(a) Total frame

(El Centro 1940 NS Record)

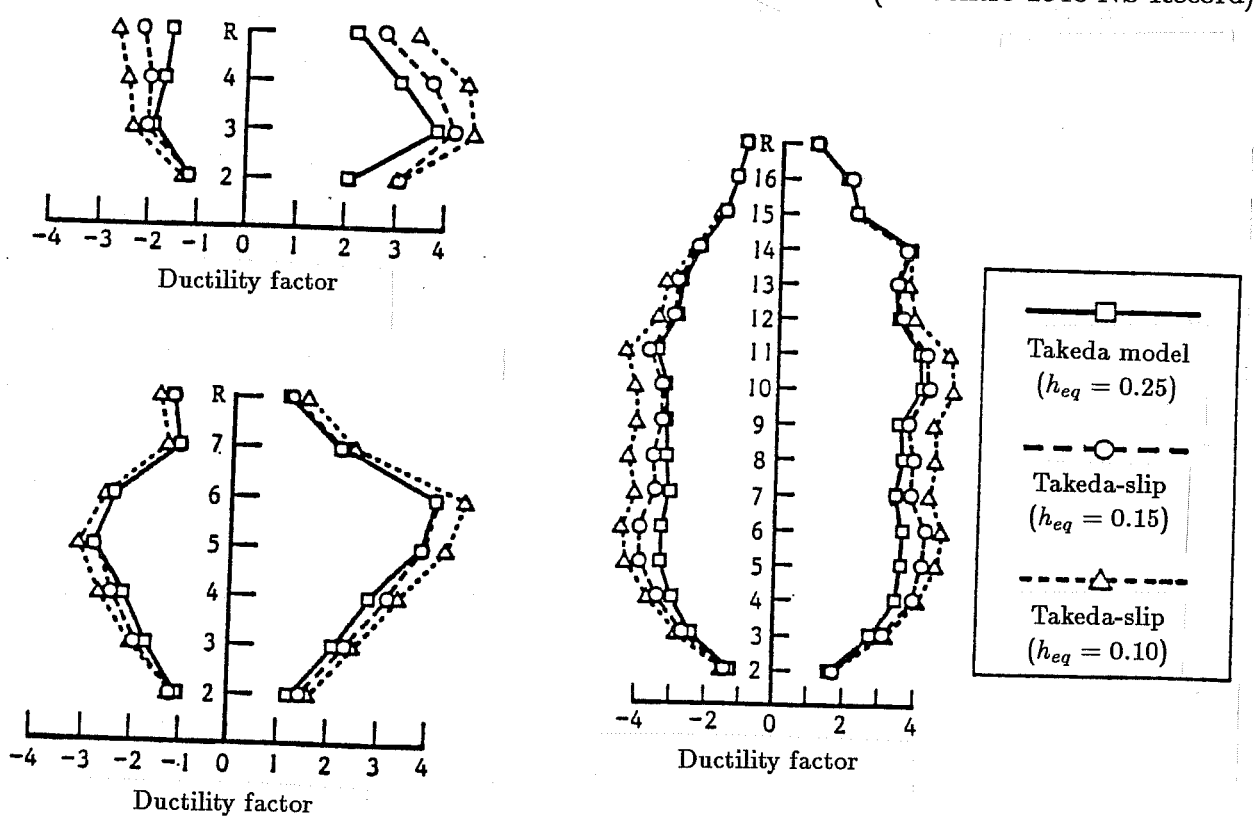

(b) Substructure frames

Fig. 3.57 Attained ductility factors at beam ends

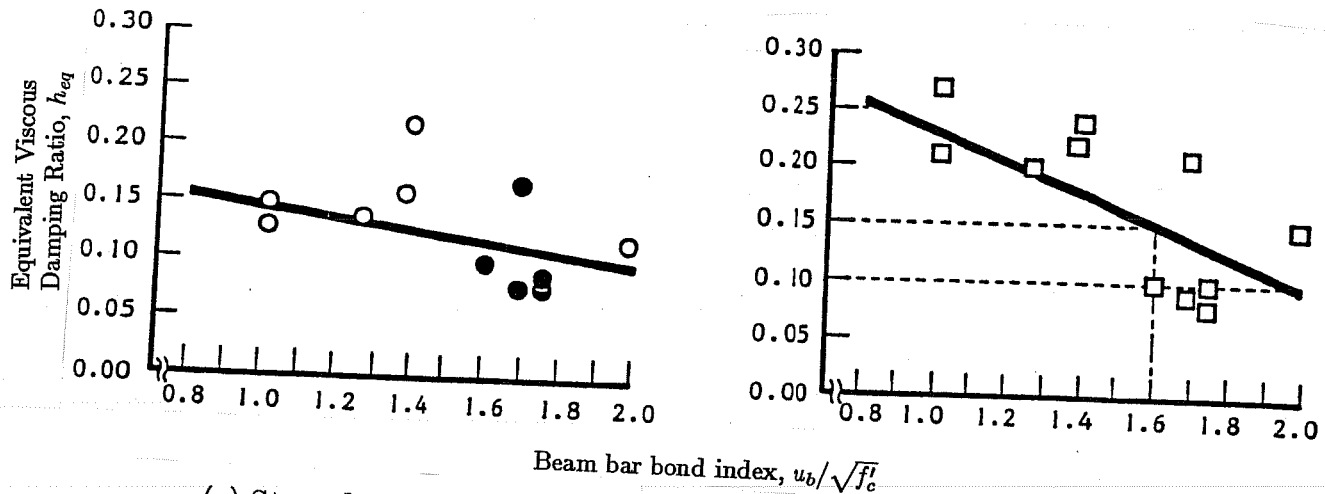

(a) Story drift angle of 1/92

(b) Story drift angle of 1/46

Fig. 3.58 Equivalent viscous damping ratio-beam bar bond index

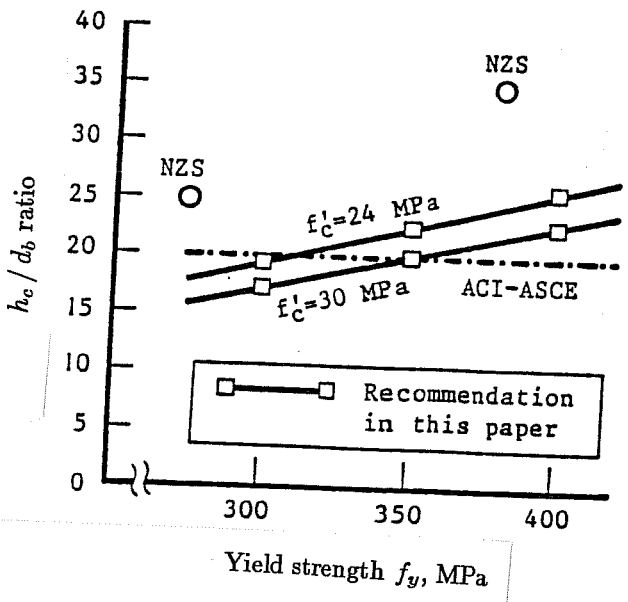

Fig. 3.59 Required ratio of column depth to beam bar diameter

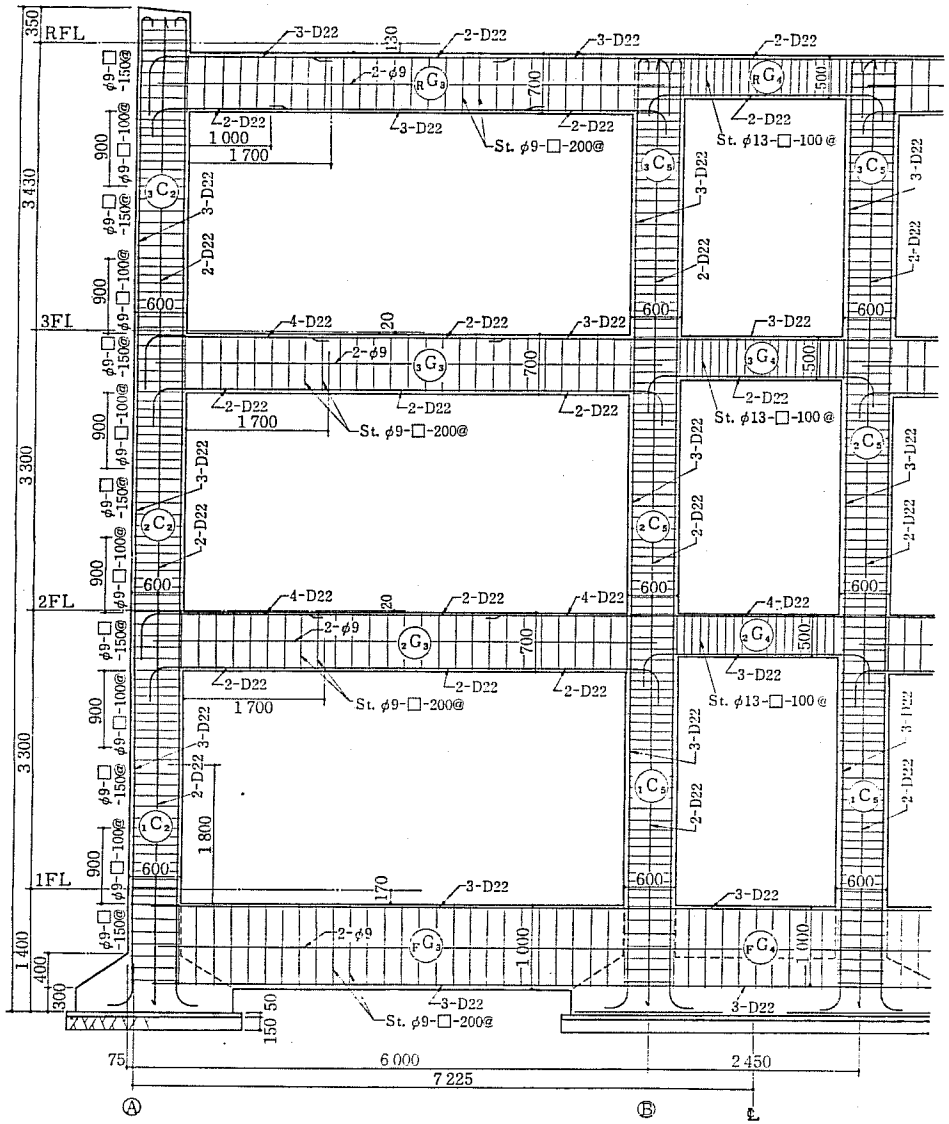

(a) Typical details

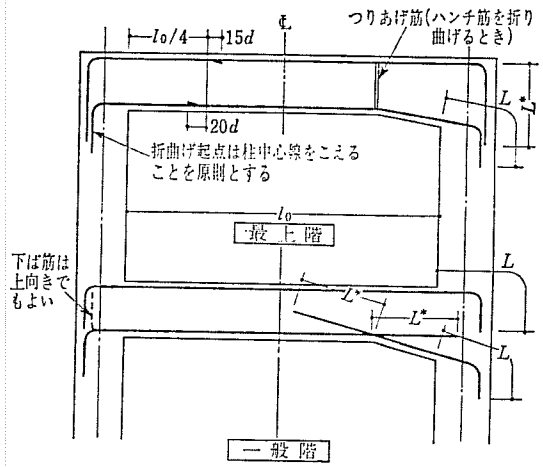

L：定着の長さ(2項)
$L^* = L + 5d$

L: Total development length

(See Table 2.1)

(b) Bent bar development

Fig. 3.60 Reinforcement details in Japanese practice

Generally in Japan, concrete is placed up to the top of a slab in one operation so that columns, walls, beams and slabs in a story are cast all at once. In such a construction procedure, the bent-down anchorage is more suitable for beam bottom bars than the bent-up anchorage, because it alleviates the congestion of reinforcement in the exterior joint and eases the on-site reinforcing work. However, the bent-down anchorage is occasionally provided with insufficient straight embedment length between column face and start of bend because the AIJ standard[3] specifies not the embedment length but the total development length.

Various series of seismic tests were conducted to study the behavior of RC exterior joints under unidirectional and/or bidirectional loading conditions. A number of specimens had the details described above and the problems associated with them were pointed out from the test results. The outline of the studies is described below.

3.3.1 Unidirectional Loading Tests.

Kyoto University. Two series of exterior beam- column joint specimens were tested under unidirectional loading conditions at Kyoto University.[19,24] In the first series, emphasis was on the interaction between beam bar anchorage capacity and joint shear strength.[19] In this series, sixteen specimens shown in Fig. 3.61 were fabricated changing the details of beam bar anchorage, the amount of joint lateral reinforcement and the amount of beam longitudinal reinforcement. The beam bars were anchored using three different typical methods; i.e., (1) mechanical anchorage with steel plates and nuts using threaded deformed bars (Type-S), (2) 90° hook anchorage based on ACI 318 code where top bars were bent down and bottom bars were bent up (Type-U), and (3) 90° hook anchorage based on Japanese practice where both top and bottom bars were bent down (Type-R). Concrete strength is given as F_c values in Fig. 3.61. Bar yield strength was 3950 kgf/cm^2 for beam longitudinal reinforcement and 3000 kgf/cm^2 for joint lateral reinforcement.

The specimens were subjected to cyclic loading at the beam tip as shown in Fig. 3.62. The specimens with beam tensile reinforcement of four D19 bars failed in joint shear and those with two D19 bars failed in bond. Thus all specimens showed distinct deterioration in strength and stiffness. The load-displacement relations varied widely depending on the anchorage details and the amount of joint lateral reinforcement, as shown in Fig. 3.63. The specimens with bent-down bottom bars (Type-R) apparently showed lower strength in positive bending (negative loading) than the others. The joint shear strength calculated using Eq. 2 resulted in good agreement with the measured maximum loads when the joint effective depth was assumed to be the development length (ℓ_{dh} in Fig. 3.61). Figure 3.64 shows the crack patterns and the assumed shear resisting mechanism. When the development length was reduced as shown in Fig. 3.64(a) to (c), the compressive strut was steeper and narrower. When the beam bottom bars were bent down and were in tension as shown in Fig. 3.64(d) and (e), they did not provide stable support to the compressive strut at the bend, thus Type-R specimens showed lower strength in positive bending than in negative bending. However, extra hoops around the bent-down anchorage were effective in equalizing the behavior in the

NO.	SPECIMEN*1 DESIGNATION	BEAM REINFORCEMENT TOP	BOTTOM	SHEAR	COLUMN REINF.	JOINT REINF.	ANCHORAGE OF BEAM REINF. ANCHORAGE TYPE	DEVELOP. LENGTH (mm)	SIDE COVER (mm)	FC (kg/cm²)
1	S40	4-D19	4-D19	2-φ9@50	6-D22	NONE	PLATE	300	60.5	248
2	S41	4-D19	4-D19	2-φ9@50	6-D22	2-φ9@100	PLATE	300	60.5	248
3	S42	4-D19	4-D19	2-φ9@50	6-D22	2-φ9@50	PLATE	300	60.5	248
4	U40L	4-D19	4-D19	2-φ9@50	6-D22	NONE	U-SHAPED	228	60.5	248
5	U41L	4-D19	4-D19	2-φ9@50	6-D22	2-φ9@100	U-SHAPED	228	60.5	272
6	U42L	4-D19	4-D19	2-φ9@50	6-D22	2-φ9@50	U-SHAPED	228	60.5	307
7	U41S	4-D19	4-D19	2-φ9@50	6-D22	2-φ9@100	U-SHAPED	152	60.5	272
8	U42S	4-D19	4-D19	2-φ9@50	6-D22	2-φ9@50	U-SHAPED	152	60.5	307
9	U20L	2-D19	2-D19	2-φ9@100	4-D19	NONE	U-SHAPED	228	60.5	272
10	U21L	2-D19	2-D19	2-φ9@100	4-D19	2-φ9@100	U-SHAPED	228	60.5	307
11	U21S	2-D19	2-D19	2-φ9@100	4-D19	2-φ9@100	U-SHAPED	152	60.5	272
12	U22S	2-D19	2-D19	2-φ9@50	4-D19	2-φ9@50	U-SHAPED	152	60.5	307
13	R41L	4-D19	4-D19	2-φ9@50	6-D22	2-φ9@100	LL-SHAPED	228	60.5	221
14	R42S	4-D19	4-D19	2-φ9@50	6-D22	2-φ9@50	LL-SHAPED	152	60.5	221
15	R21L	2-D19	2-D19	2-φ9@100	4-D19	2-φ9@100	LL-SHAPED	228	60.5	221
16	R21*S	2-D19	2-D19	2-φ9@100	4-D19	2-φ9@100	LL-SHAPED	152	60.5	221

*1 SPECIMEN DESIGNATION

U41L

- Development length L:ldh=12db=228mm, S:ldh= 8db=152mm
- Joint reinforcement 0:none reinf., 1:φ9 hoops @100, 2:φ9 hoops @50
- Number of beam reinforcement (2or4) per layer
- Anchorage type of beam reinforcement

S:straight bar anchoraged with steel plate in far face side of column (PLATE)
U:90 deg. bent bar anchorages in joint core for both top and bottom bars (U-SHAPED)
R:90 deg. bent bar anchorages in the same direction for top and bottom bars (LL-SHAPED)

DEVELOPMENT LENGTH : ldh

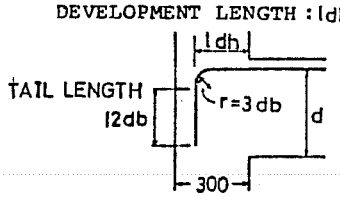

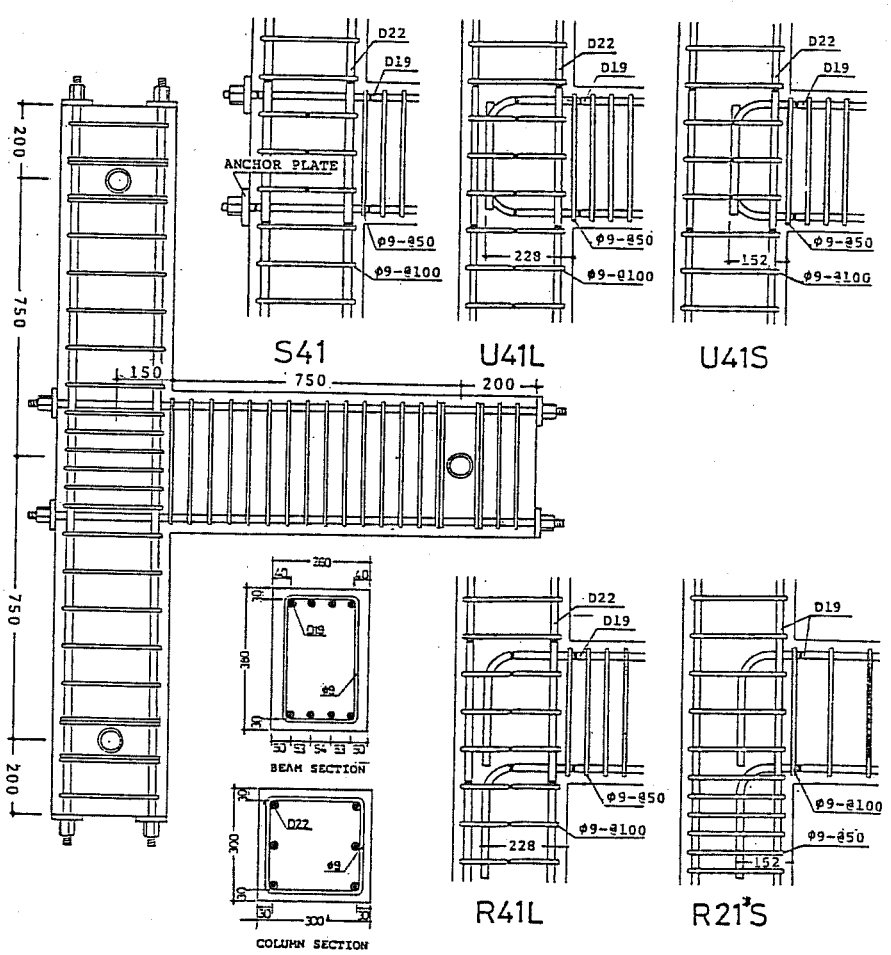

Fig. 3.61 Details of specimens

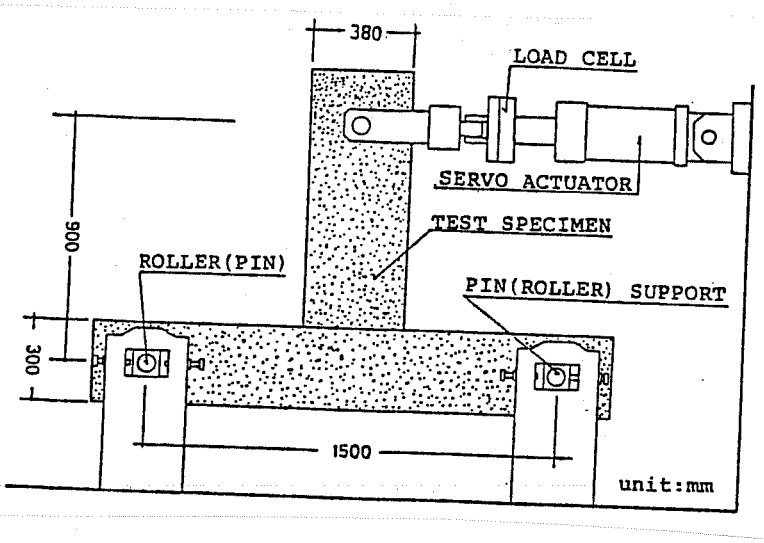

Fig. 3.62 Loading setup

two directions, because Specimen R21*S shown in Fig. 3.61 improved the poor behavior in positive bending. Figure 3.65(a) shows the total joint shear force and the portions contributed by concrete and lateral reinforcement. Deterioration in the joint shear strength was caused mainly by concrete degradation as seen in Specimens S41 and U41L. Deterioration was delayed by using a larger amount of joint lateral reinforcement as seen in Specimens S42 and U42L, although shear carried by the concrete decreased with an increase in the lateral reinforcement. It should be noted that joint shear in the unreinforced specimens (S40 and U40L) was different from the concrete contribution in the reinforced specimens (S41, S42, U41L and U42L), as seen in Fig. 3.65b.

In the second series at Kyoto University, ten specimens shown in Fig. 3.66 were tested to study the effect of joint lateral reinforcement on the behavior of exterior beam-column joints.[24] The main variables in this series were the amount and the arrangement of lateral reinforcement in and at the joint where beam longitudinal bars were anchored. The specimens were fabricated with the same dimensions and tested using the same loading system as in the first series. Beam tensile reinforcement was two D19 bars for Type-A specimens and four D19 bars for Type-B specimens. The top and bottom beam bars terminated in a 90° downward bend with a development length of $12d_b$, a bend radius of $3d_b$ and tail extension length of 12 d_b, where d_b = bar diameter. Concrete strength was 295 kgf/cm^2 for Type-B specimens except B101 and 326 kgf/cm^2 for the other specimens. Bar yield strength was 3400 to 4000 kgf/cm^2 for longitudinal reinforcement and 3100 kgf/cm^2 for lateral reinforcement. Test results are shown in Figs. 3.67 through 3.69. Type-A specimens, detailed with a smaller amount of beam tensile reinforcement, formed a plastic hinge at the beam end and failed in beam flexure. The load- displacement relations were dominated by beam deflection

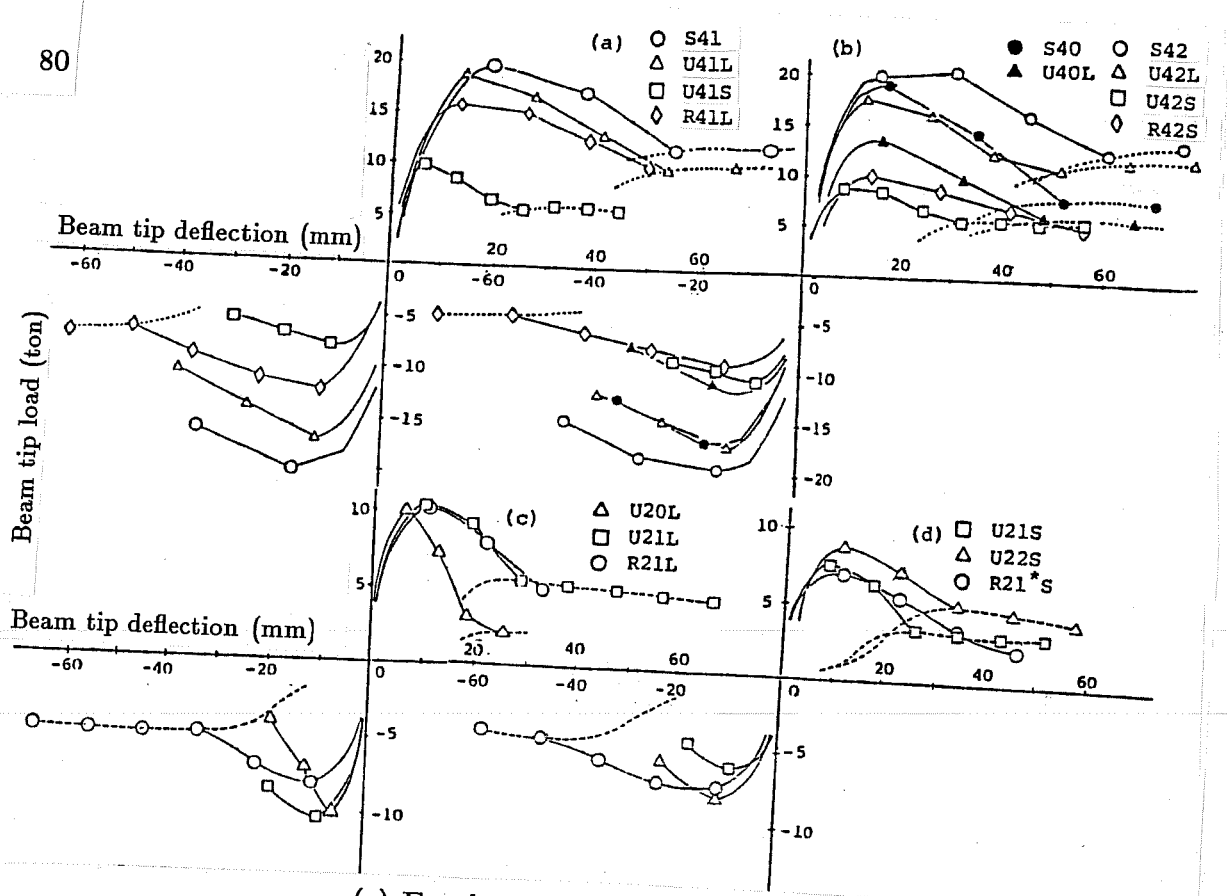

(a) Envelopes of load-displacement curves

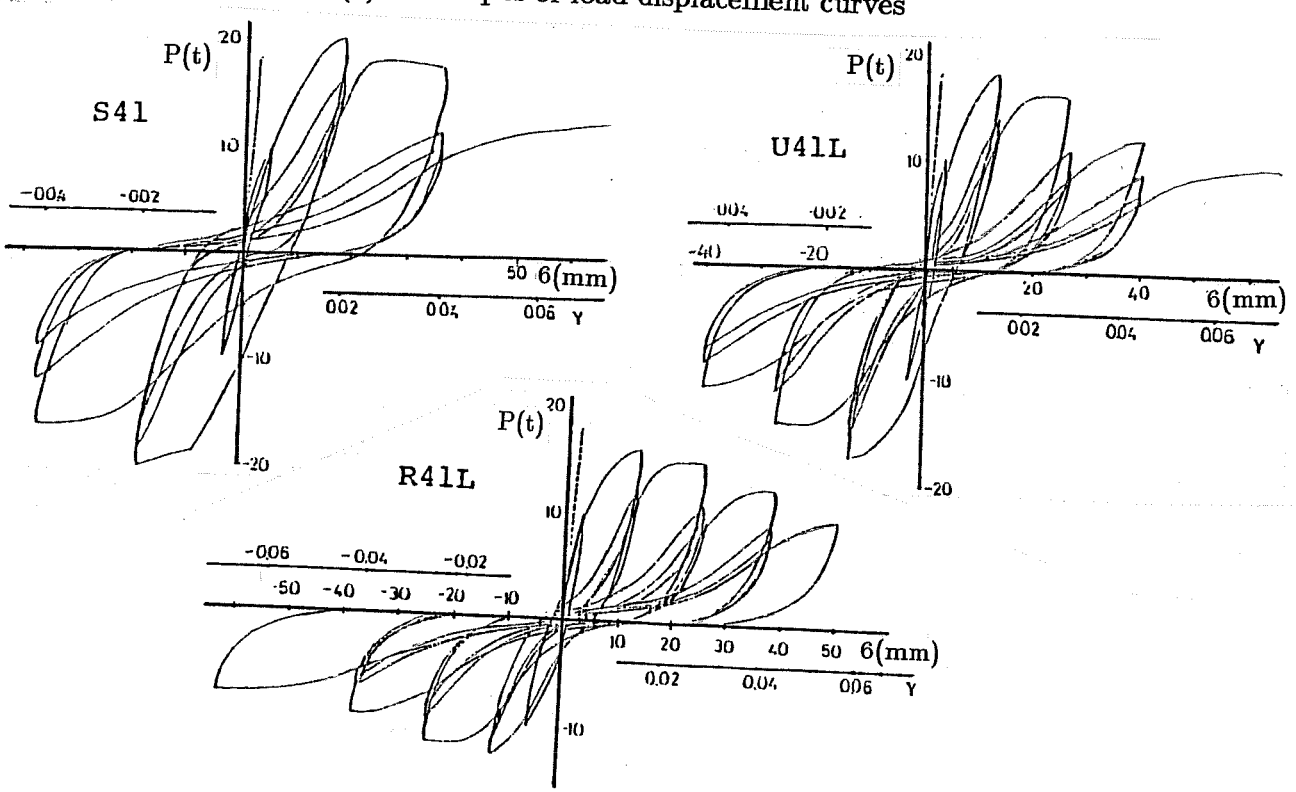

(b) Load-displacement hysteresis

Fig. 3.63 Beam tip load vs displacement relations

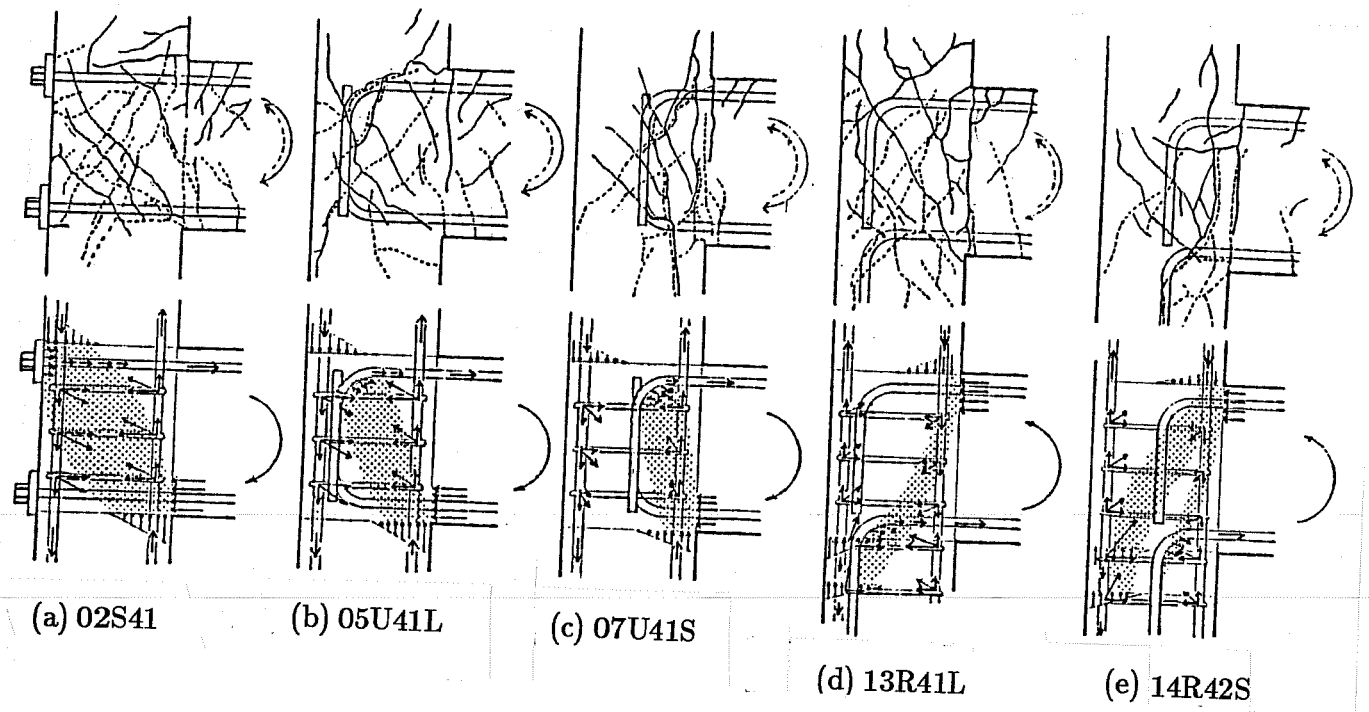

Fig. 3.64 Crack patterns and probable shear transfer

and showed pinching in the hysteresis curves. The pinching behavior is likely due to slip deformation along the beam bar anchorage and partly to the sliding shear deformation in the plastic hinge zone. Specimens with lower lateral reinforcement (A111 and A*111) showed deterioration in strength particularly in positive bending (upward loading), while those with higher lateral reinforcement (A122 and A132) showed stable load-displacement relations in both directions. On the contrary, Type-B specimens, detailed with a larger amount of beam tensile reinforcement, developed flexural yielding of the beam except for B101 and failed in joint shear. Specimen B101 failed before yielding of beam bars. The joint developed wide diagonal cracks and the load-displacement relations showed distinct deterioration in strength and stiffness. A large part of the displacement was contributed by joint shear distortion. The following design criteria for shear strength of exterior joints were derived from the nominal joint shear stresses measured at maximum load and at the displacement of $3\delta_y$ ($\delta_y = 12$ mm for Type-B specimens):

$$V_j/(B \cdot \ell_{dh}) \leq k\sqrt{F_c} \tag{9}$$

$k = 3$ for elastic joint

$k = 2$ for inelastic joint

where V_j = joint shear (kgf), B = column width (cm), ℓ_{dh} = beam bar development length (cm) and F_c = concrete strength (kgf/cm^2).

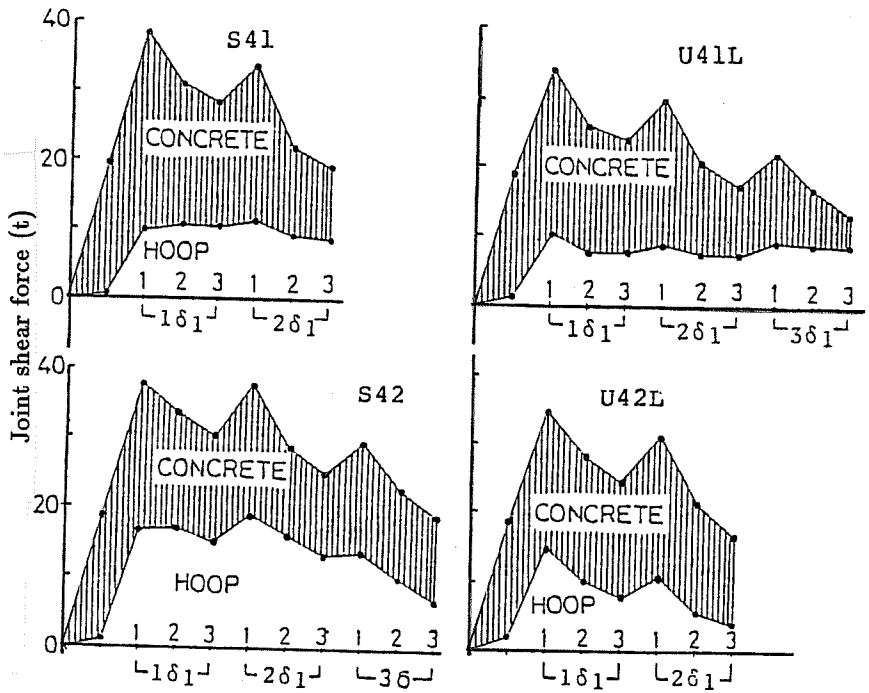

(a) Joint shear at peak displacement

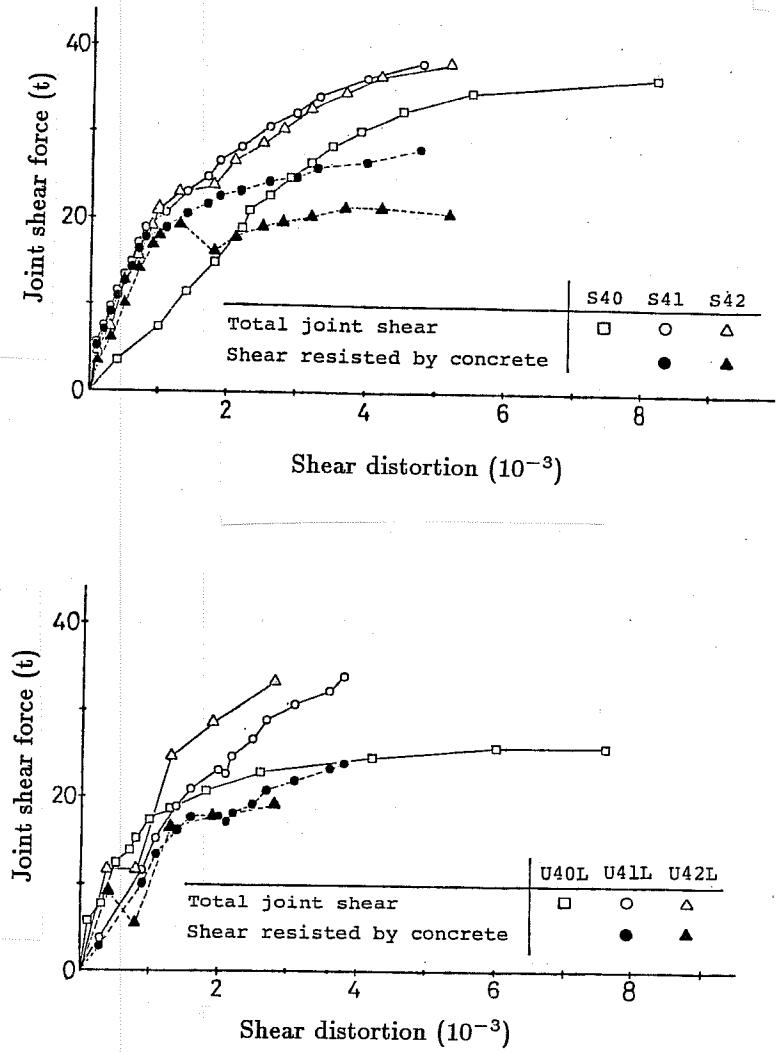

(b) Joint shear carried by concrete

Fig. 3.65 Joint shear force

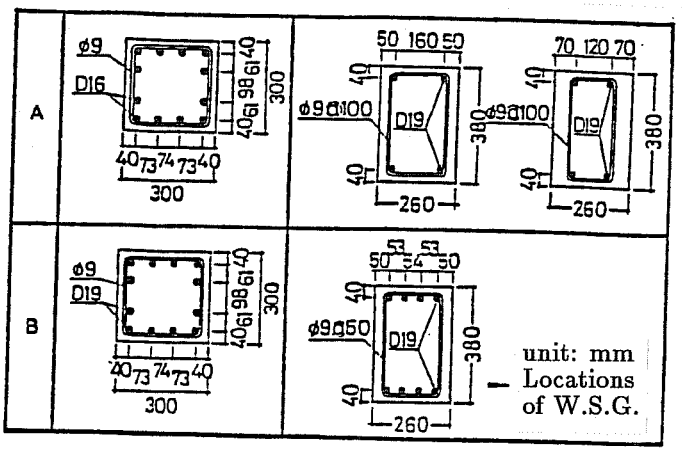

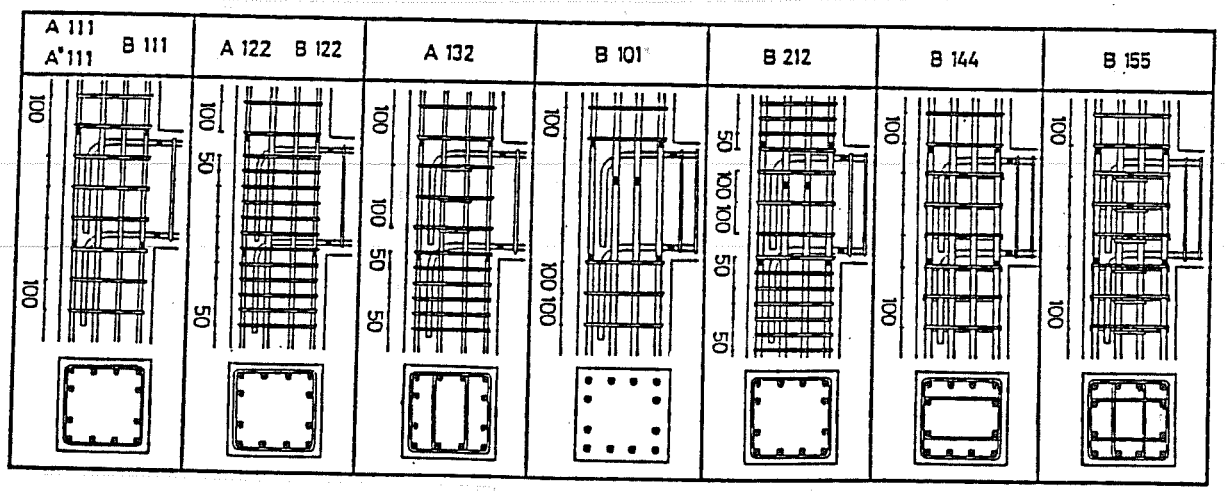

Specimen Designation

A 1 1 1
- Lower-column hoop: 0: none; 1:2−ϕ9@100; 2:2−ϕ9@50; 3:2−ϕ9@100 + cross tie; 4:4−ϕ9@100; 5:4−ϕ9@100 + cross tie
- Joint hoop
- Upper-column hoop
- Test type of specimen: A: Specimen with 2D19 beam bars in tension; B: Specimen with 4D19 beam bars in tension

Fig. 3.66 Details of specimens

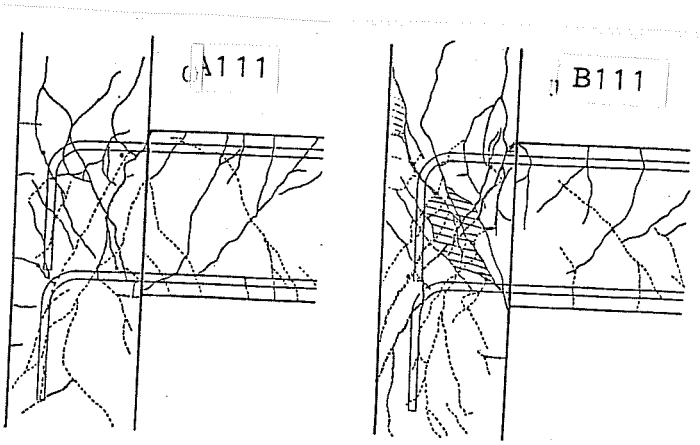

Fig. 3.67 Final crack patterns

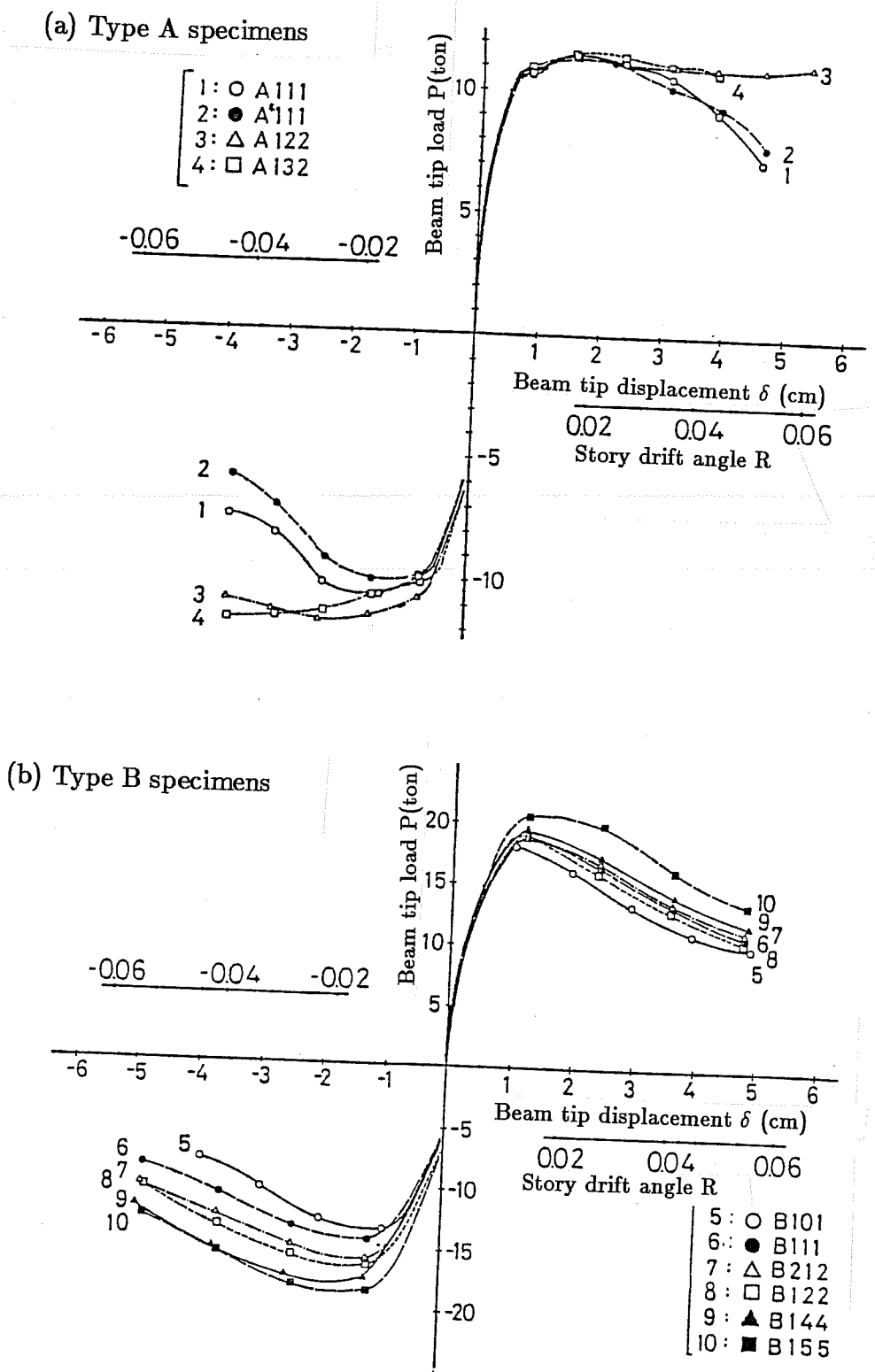

Fig. 3.68 Envelopes of beam tip load-displacement curves

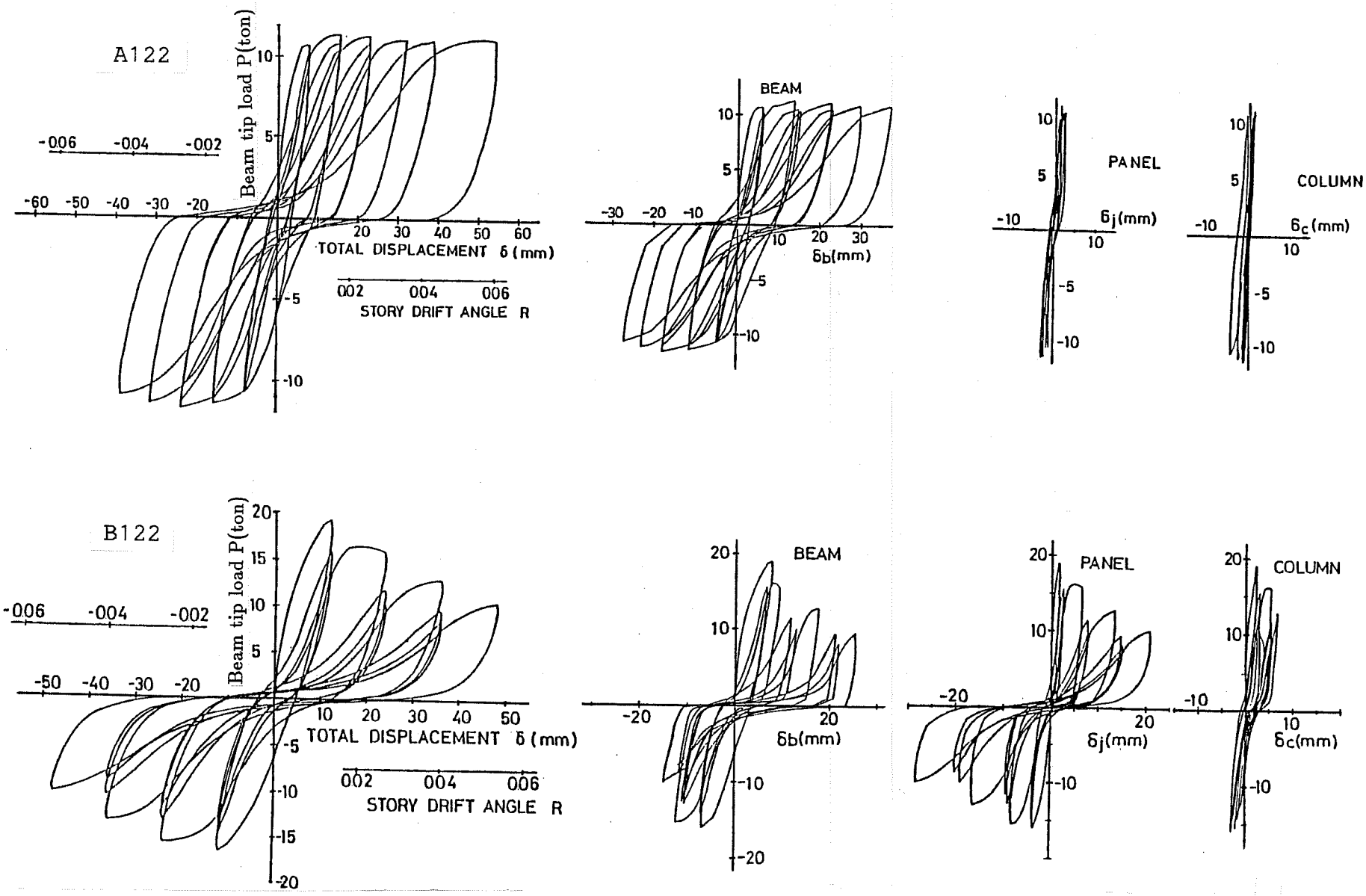

Fig. 3.69 Load vs displacement and deformation components

Osaka Institute of Technology

Another series of unidirectional loading tests were conducted at Osaka Institute of Technology.[25] Twenty-three specimens were tested to study the effect of various factors on the anchorage strength of beam bars terminating in 90° bent-down hooks. The factors studied in this series were the length of bar lead embedment between column face and start of bend, the amount of lateral reinforcement and the level of column axial load. As shown in Fig. 3.70, beam and column dimensions were common to all specimens. Two D16 bars were used as beam longitudinal reinforcement at the top (Type-A) and at the bottom (Type-U) and were bent down into a lower column with a total development length of $30d_b$ (d_b = bar diameter) and a bend radius of $3d_b$. Concrete strength ranged from 245 to 362 kgf/cm^2. Bar yield strength was 3330 to 4320 kgf/cm^2 for longitudinal reinforcement and 1740 to 2350 kgf/cm^2 for lateral reinforcement. The specimens were tested using the loading apparatus shown in Fig. 3.71. The anchorage strength of 90° hooked bars is largely dependent on the lead embedment length as shown in Fig. 3.72(a). The bottom bars showed lower anchorage strength than the top bars for the same embedment length. Figure 3.72(b) shows bar slip-displacement relations. The bar slip decreased with the increase of the lead embedment length for the top bars (Type-A) but did not for the bottom bars (Type-U). Variations of Specimens A2 and U4 were fabricated with various details of lateral reinforcement and were tested as shown in Fig. 3.73. The test results indicated that lateral reinforcement, particularly at the bend portion, was effective in increasing the anchorage strength. Specimens A2, A4, U2 and U4 were fabricated in triplicate and were tested under various axial loads as shown in Fig. 3.74. The test results showed that the anchorage strength increased with the axial load. However, rapid deterioration was observed in the anchorage strength under high axial loads.

The following conclusions were derived from the unidirectional loading tests on exterior beam-column joints described earlier.

1. Specimens with beam bottom bars terminating in 90° bent-down hooks showed poor behavior in strength and ductility when the bars were in tension.[19,24,25] Lateral reinforcement placed around the bent-down anchorage improved the behavior of specimens which failed in bond[19] and in beam flexure[24] but did not increase the joint shear strength.[24]

2. Lateral reinforcement in exterior joints appeared to delay deterioration of the joint concrete and maintain the integrity of the joint.[19,24]

3. The beam bar development length should be used as the joint effective depth for evaluating the shear strength of exterior joints.[19,24]

4. The anchorage strength of 90° bent-down beam bars was largely dependent on the lead embedment length, although the total development length was kept constant.[25]

5. The beam bar anchorage strength was increased by the lateral reinforcement at the bend portion and by the column axial load.[25]

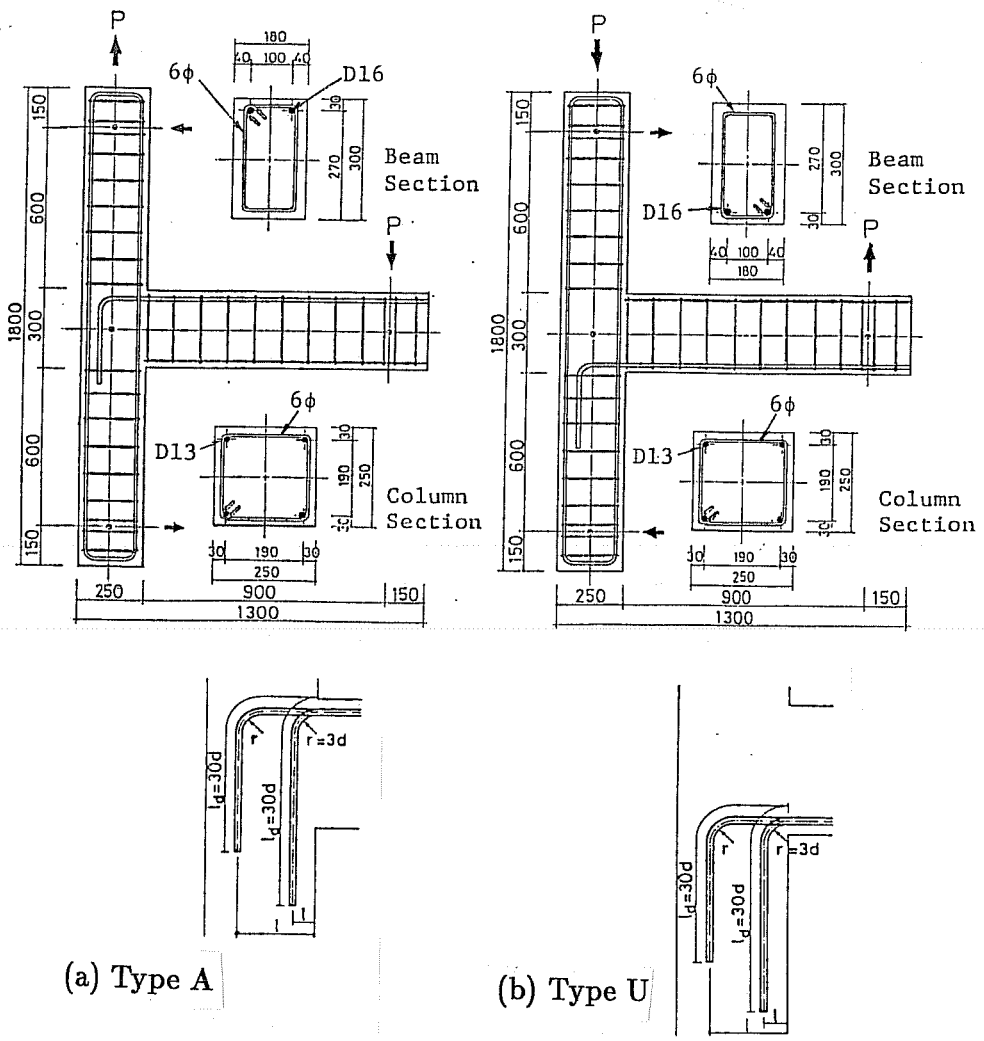

Fig. 3.70 Details of specimens

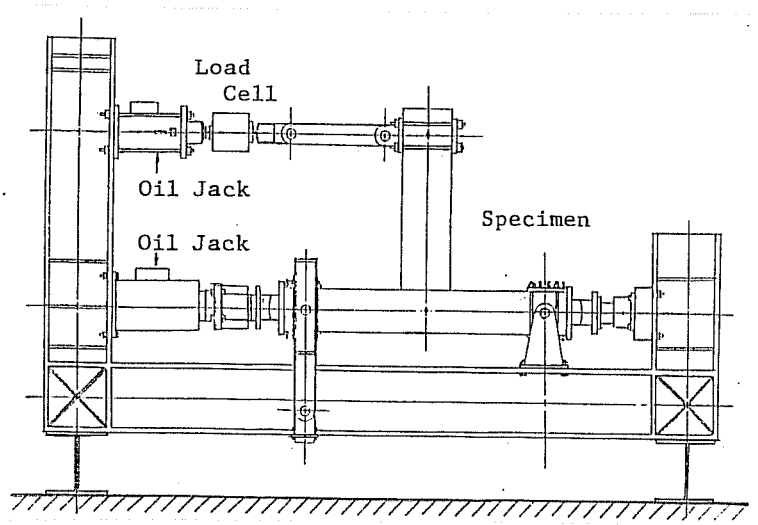

Fig. 3.71 Loading apparatus

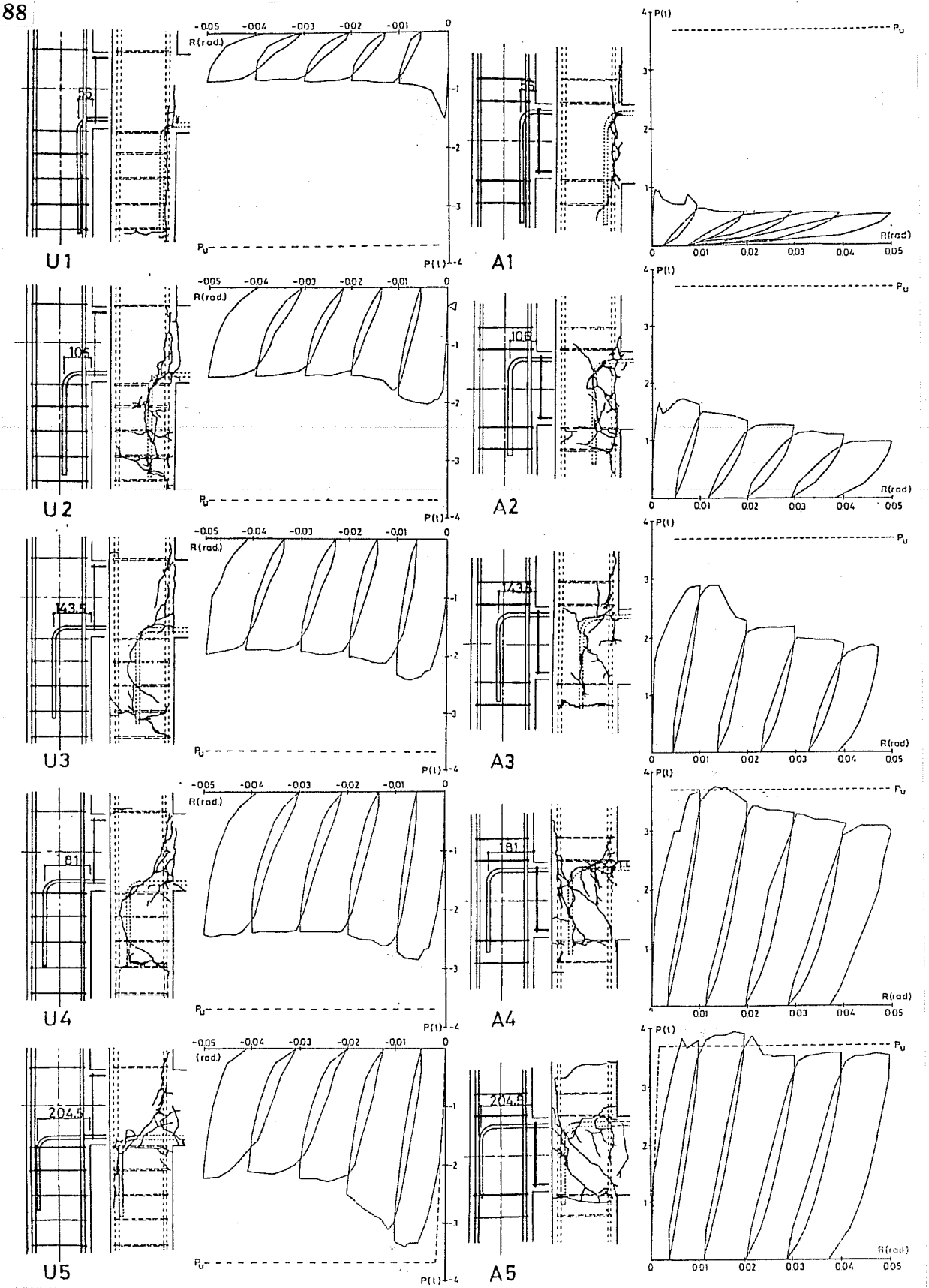

(a) Load-deflection relations and crack patterns

Fig. 3.72 Tests for effect of lead embedment length

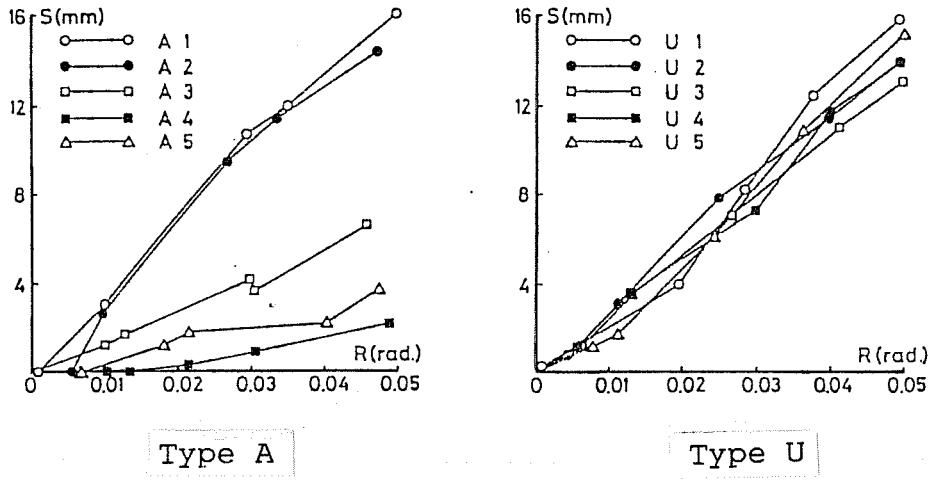

(b) Bar slip-deflection relations

(Fig. 3.72 Continued)

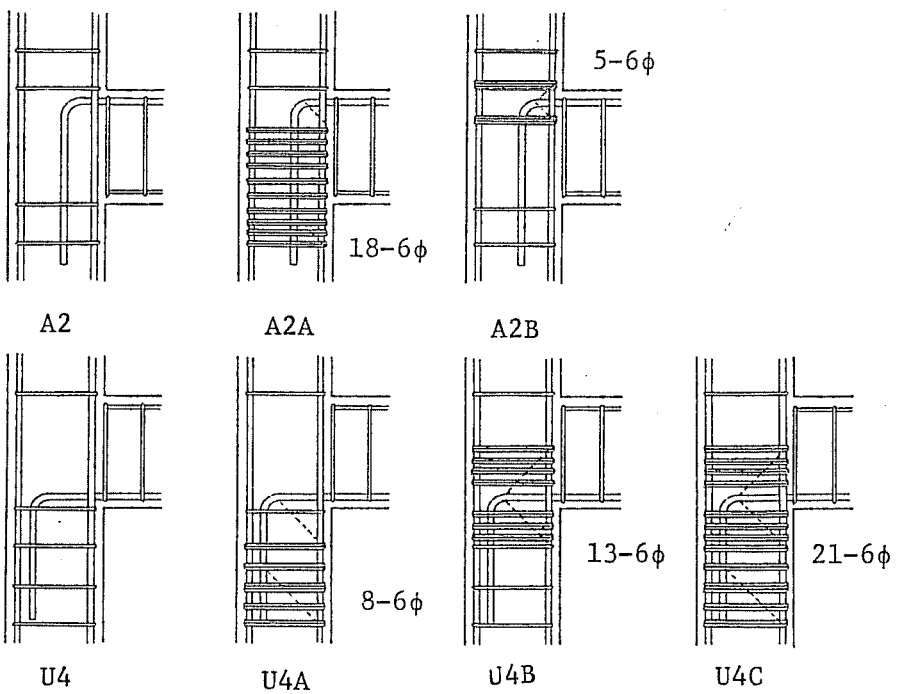

(a) Details of lateral reinforcement

Fig. 3.73 Tests for effect of lateral reinforcement

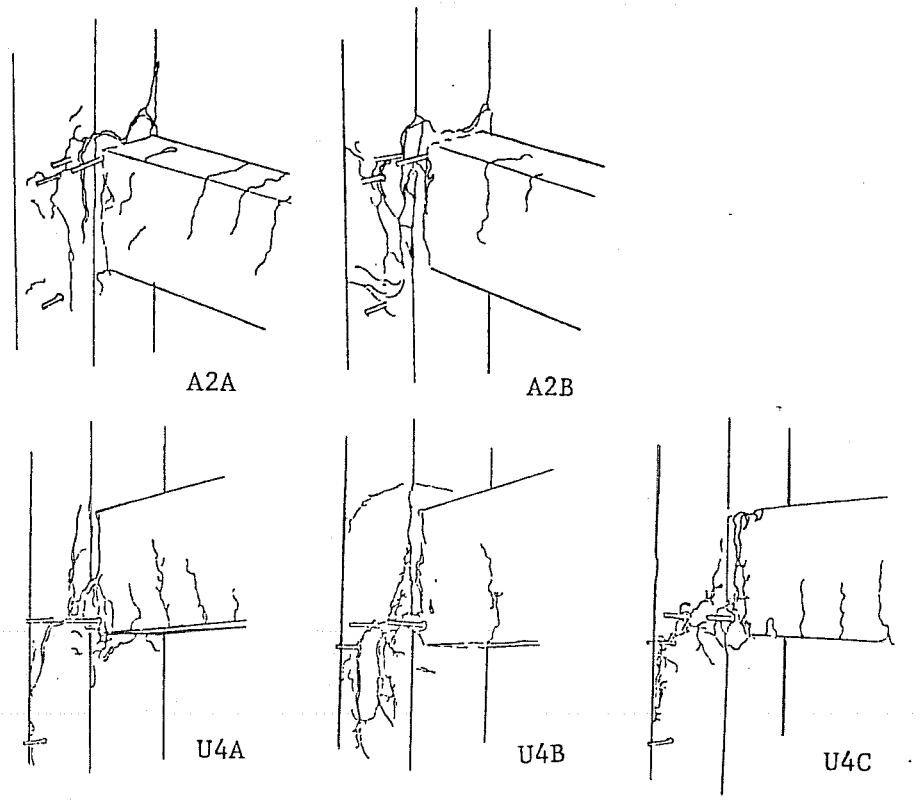

(b) Crack patterns at the end of loading

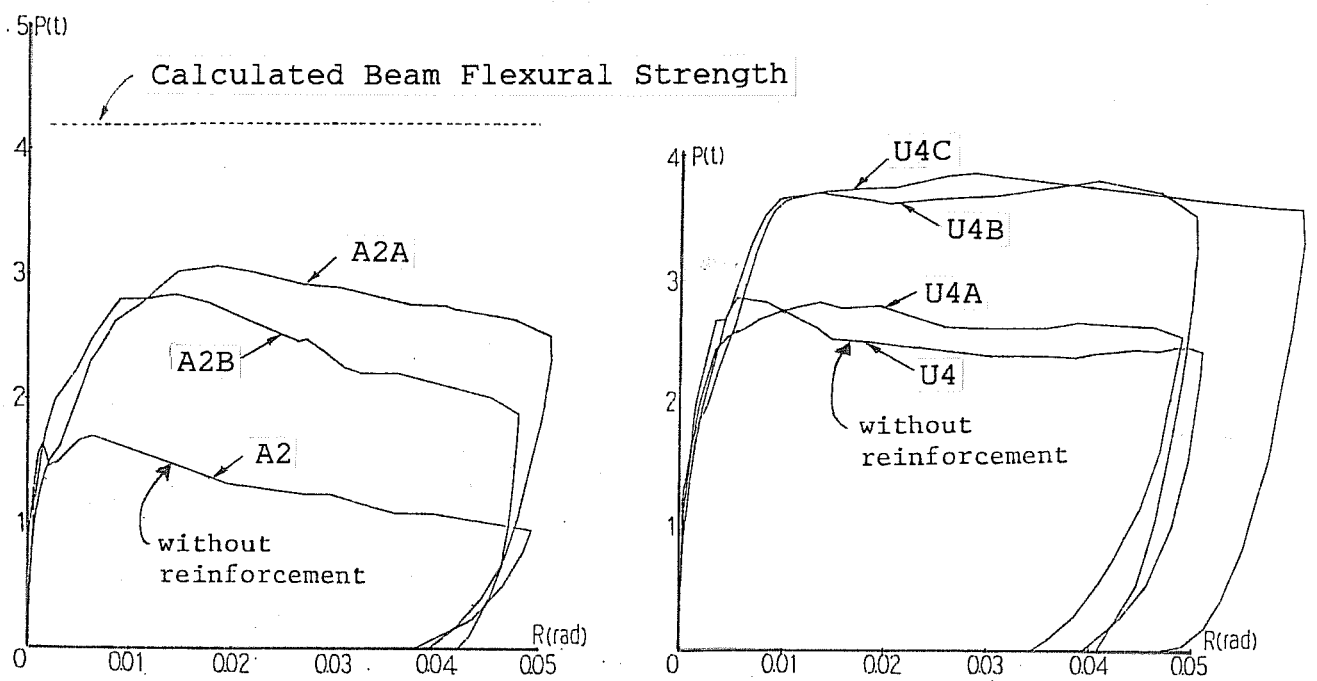

(c) Envelopes of load-deflection curves

(Fig. 3.73 Continued)

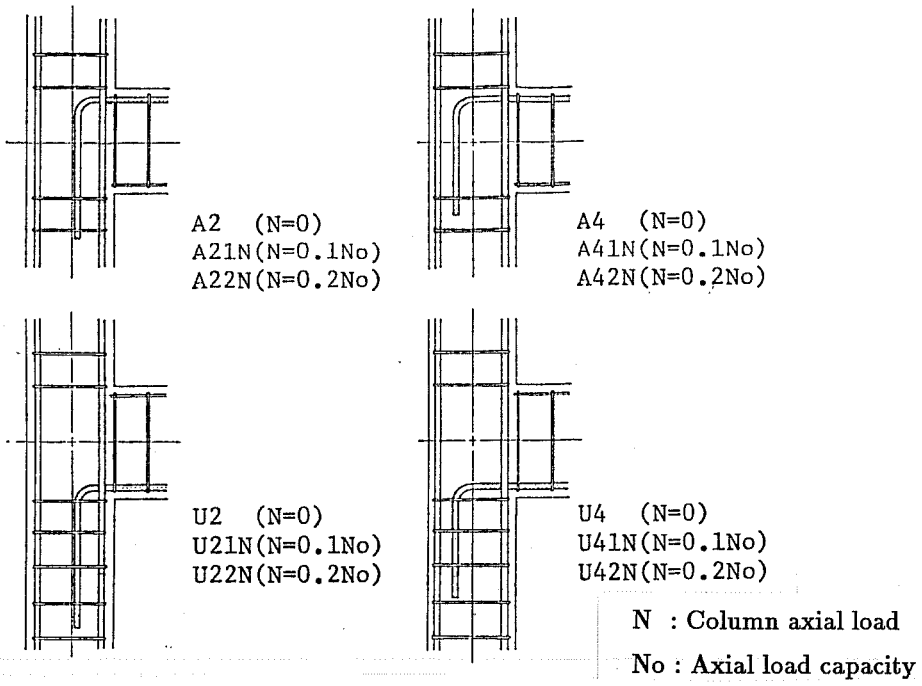

(a) Details of specimens

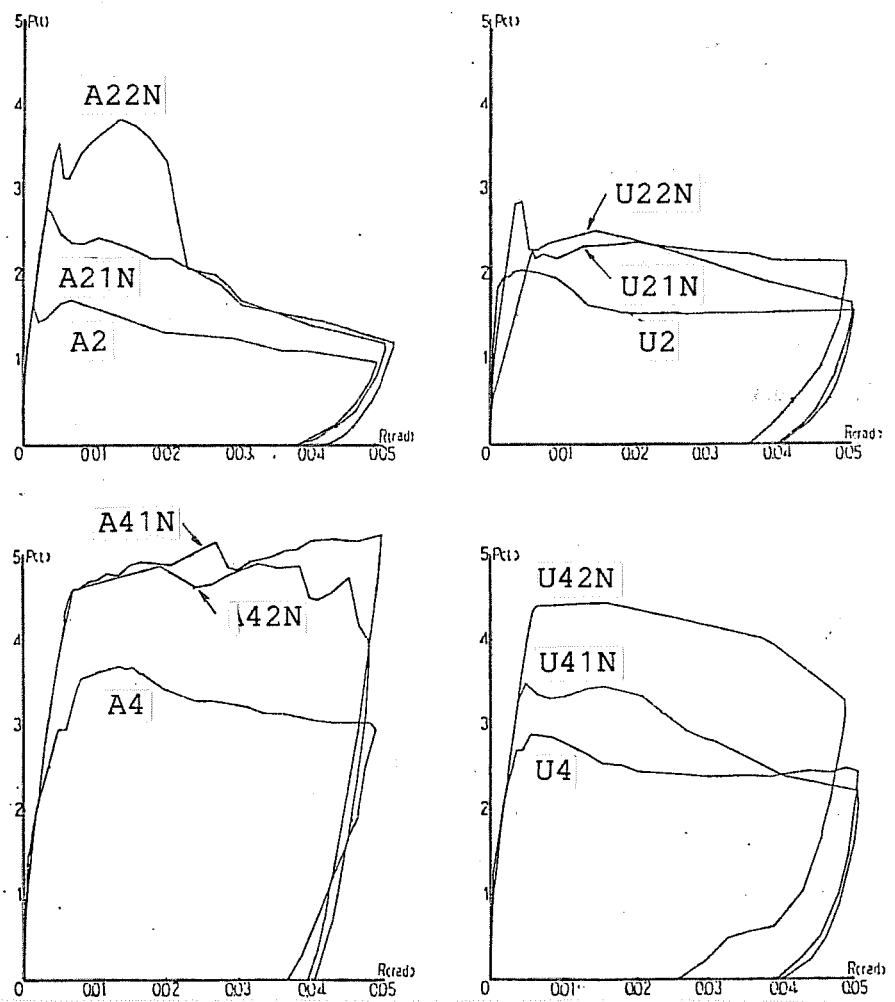

(b) Envelopes of load-deflections curves

Fig. 3.74 Tests for effect of column axial load

3.3.2 Bidirectional Loading Tests.

University of Tokyo. The bidirectional loading tests (K-series) at the University of Tokyo included an exterior joint specimen.[31] As shown in Fig. 3.75, Specimen K3 was a 1/2-scale exterior beam-column-slab subassemblage in which one longitudinal beam and two transverse beams framed into the joint. Beam longitudinal bars in the transverse direction were developed continuously through the joint and those in the longitudinal direction were anchored within the joint where the top bars were bent down and the bottom bars were bent up at a right angle. The joint was laterally reinforced with D6 hoops spaced at 55 mm. The slab was 70 mm thick and reinforced with D6 bars spaced at 180 mm in a single layer. The slab bars in the longitudinal direction terminated in 90° hooks within the transverse beams. Concrete strength was 200 kgf/cm^2. Bar yield strength was 4460 kgf/cm^2 for beam longitudinal reinforcement and 4010 kgf/cm^2 for joint lateral reinforcement. Bidirectional loading (Fig. 3.1) was applied to the specimen using the loading apparatus in Fig. 3.43, as in the tests of interior Specimens K1 and K2 described previously. Crack patterns are shown in Fig. 3.76. The transverse beams developed torsional cracks near the column during loading in the longitudinal direction but did not fail in torsion. The joint developed diagonal shear cracks in the transverse direction but did not fail in shear. Figure 3.77 shows story shear-drift relations in comparison with calculations based on various slab widths. The story shear calculated with the entire slab width showed good agreement with the test at a drift angle of 1/69 rad or larger. Figure 3.78 shows stress distributions in slab bars at loading peaks under positive bending (solid lines) and negative bending (broken lines). The slab bars in the longitudinal direction developed compressive stresses near the column and tensile stresses near the free edges under positive bending. Under negative bending, the slab bars within the entire slab width yielded in tension at a drift angle of 1/25 rad in both directions. The transverse beams were horizontally deflected by the tensile force in the slab, particularly under negative bending. Figure 3.79 shows joint shear stresses measured for Specimen K3 as well as for the other specimens tested at the University of Tokyo. Specimen J1, a two-dimensional interior joint specimen without slab, failed in joint shear at a shear stress of $0.25f'_c$ (f'_c = concrete strength), although Specimens K1 and K3 in the transverse direction sustained joint shear stresses of $0.37f'_c$ and $0.35f'_c$, respectively. The transverse beams and the slab confined the joint of the K-series specimens.

As tabulated in this figure, the maximum joint shear under bidirectional loading was less than $\sqrt{2}$ times the larger of the maximum shears measured in the two directions. This is due to the bidirectional interaction of resistances where loading in one direction lowered the shear force in the other direction.

Kyoto University. A series of bidirectional loading tests were conducted at Kyoto University.[30] Eight one-third scale specimens were tested to study the effect of bidirectional

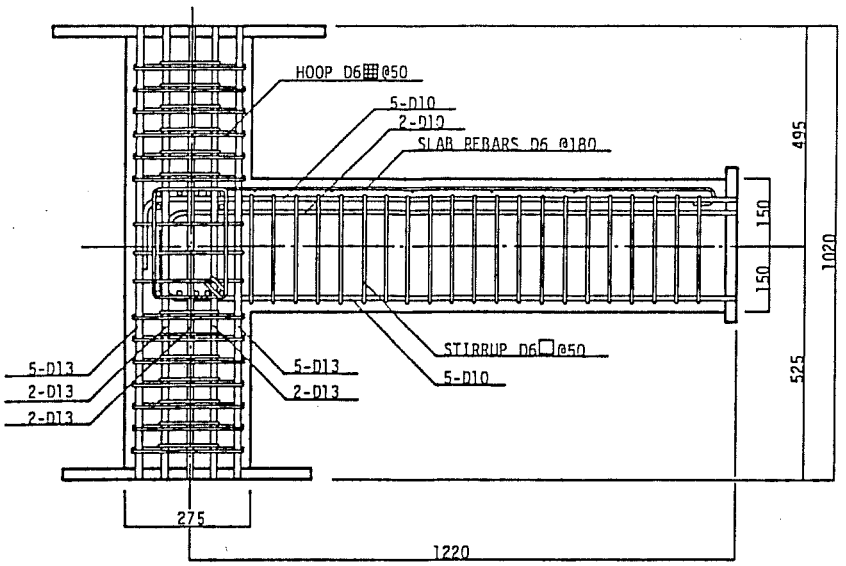

(i) Elevation (unit: mm)

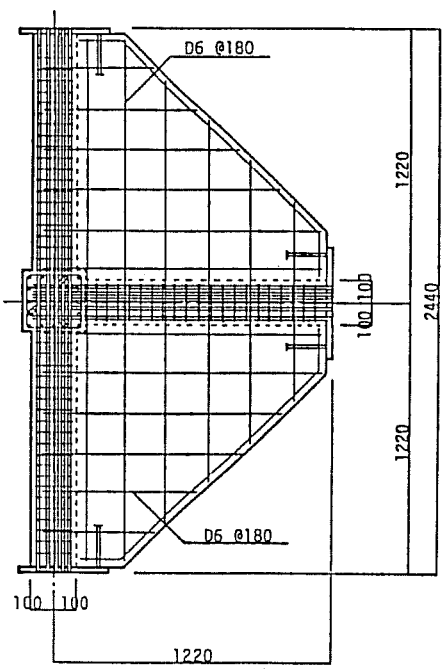

(ii) Plan (unit: mm)

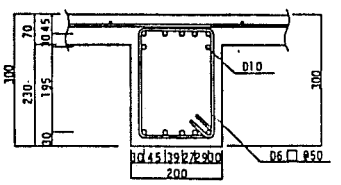

(iii) Longitudinal beam

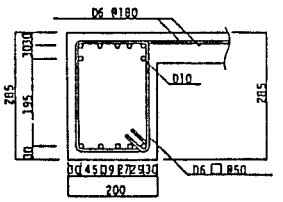

(iv) Transverse beam

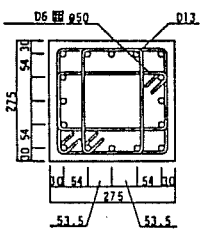

(v) Column

Fig. 3.75 Details of Specimen K3

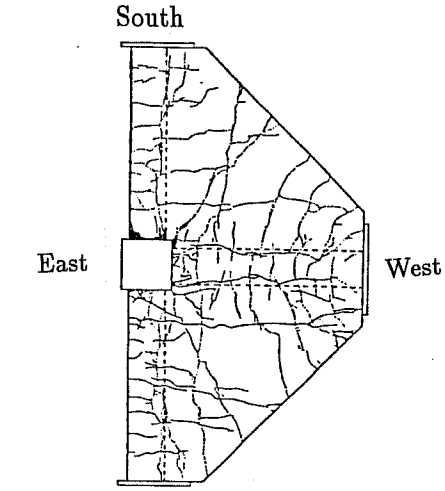

(i) Top view

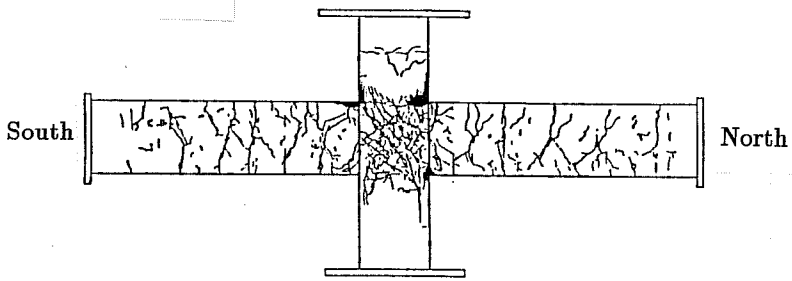

(i) North–south direction

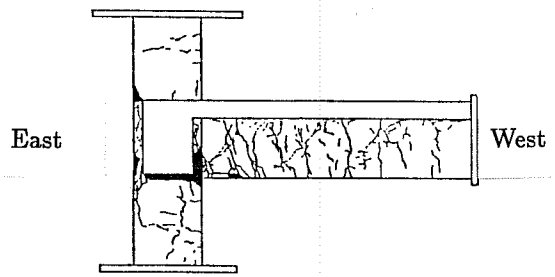

(ii) East–west direction

Fig. 3.76 Crack patterns after test

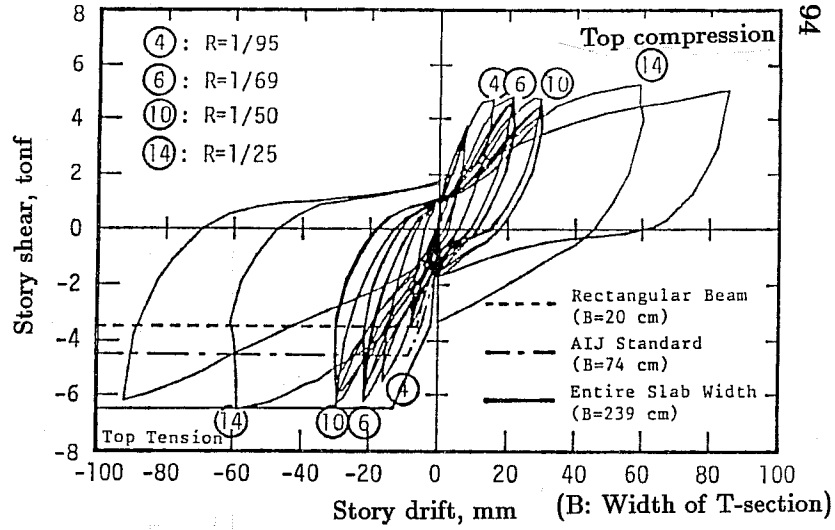

(a) Longitudinal direction (E -W)

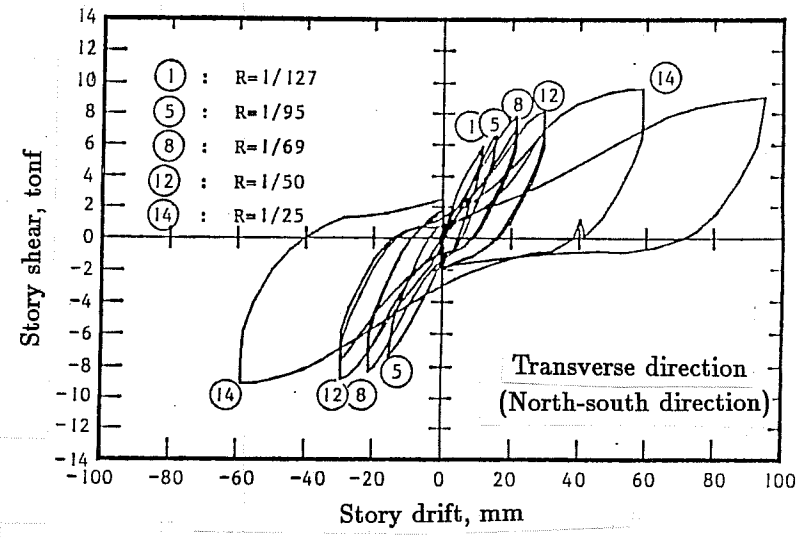

(b) Transverse direction (N-S)

Fig. 3.77 Story shear–story drift relations

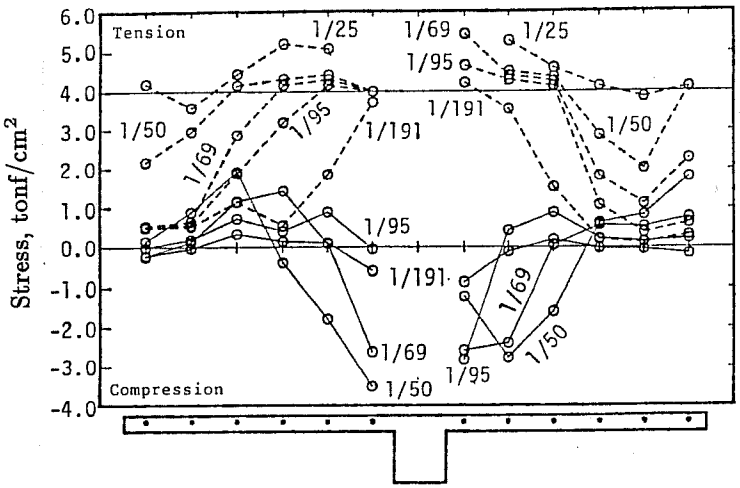

(a) Longitudinal direction

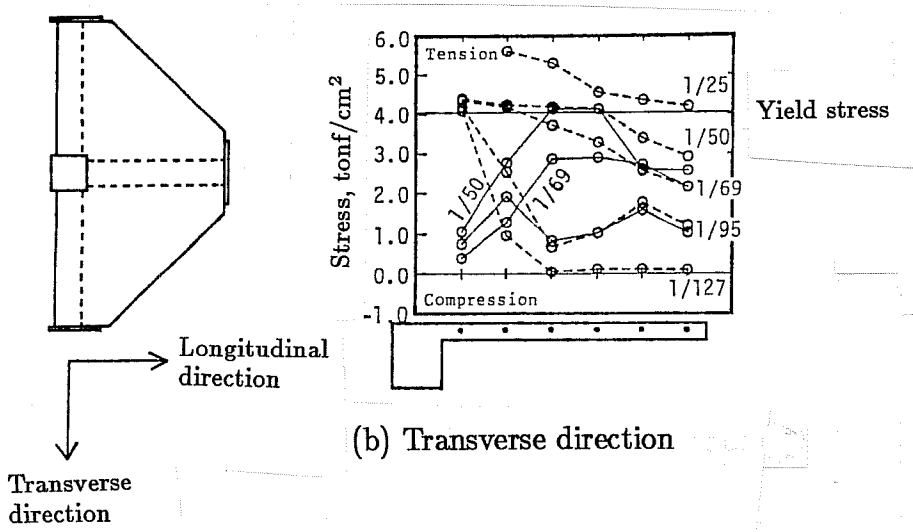

(b) Transverse direction

Fig. 3.78 Stress distributions of slab bars

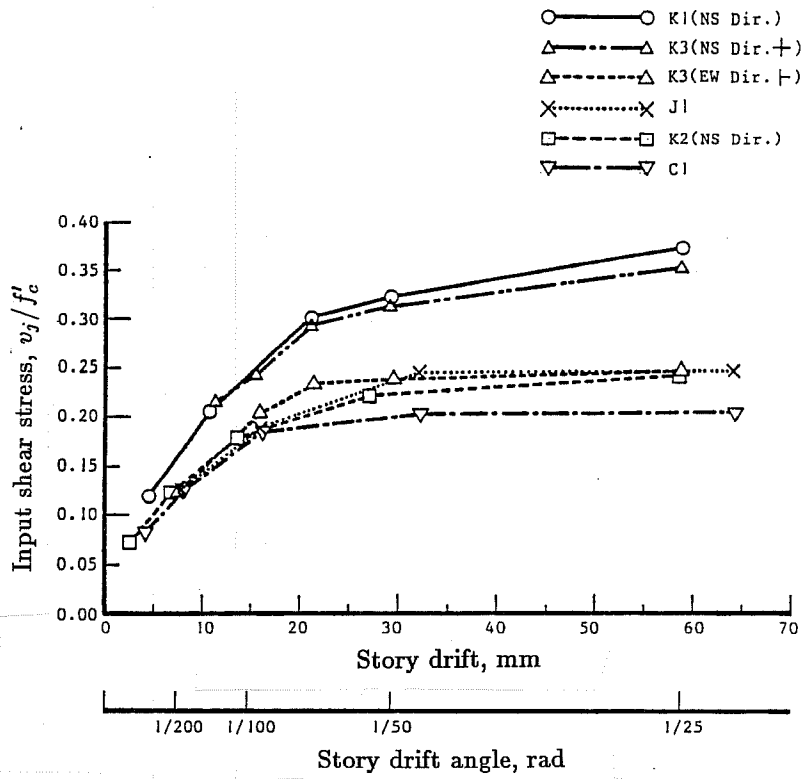

(a) Joint shear stress–story drift relations

(b) Maximum joint shear forces

Specimen	Input shear (longi. dir.) tonf(kN)	Input shear (transv. dir.) tonf(kN)	Resultant shear tonf(kN)	Shear stress divided by f'_c
K1	40.9(401)	52.9(519)	66.8(655) [88.3]*1	0.36
K2	50.7(497)	58.0(569)	77.1(756) [54.8]*1	0.22
K3	45.8(449)	16.6(163)	48.7(478) [64.4]*1	0.32

*1: Resultant shear stress in kgf/cm². The gross section of a column was used for the effective joint area to resist shear.

Fig. 3.79 Joint shear forces

load reversals on the behavior of exterior joints in two-way frame structures. Specimens GOO and OBO were two-dimensional beam-column subassemblages without a slab. Six specimens were three-dimensional beam-column subassemblages, five with a slab (GBS1 through GBS4 and GBSU) and one without a slab (GBO). One main (longitudinal) beam and two transverse beams framed into the joint, as shown in Fig. 3.80. The beam and column sections were common to all specimens. All specimens except GBSU were detailed conforming to Japanese practice so that both top and bottom beam bars terminated in 90° bent-down hooks in the longitudinal direction and the joints were reinforced with a nominal amount of lateral reinforcement (D6 hoops spaced at 70 mm).

Specimens GBS1 through GBS4 were fabricated identically and loaded differently. Specimen GBSU was a variation of GBS1 in which beam bottom bars in the longitudinal direction were bent up at a right angle within the joint and the joint was reinforced with twice the amount of lateral reinforcement (D6 hoops spaced at 35 mm). Specimen GBO was a three-dimensional subassemblage without a slab. Specimen GBO was a three-dimensional subassemblage without a slab. Specimen GOO had the main beam only, while Specimen OBO had transverse beams only. Concrete strength ranged from 294 to 465 kgf/cm^2. Bar yield strength was 3760 to 3930 kgf/cm^2 for beam longitudinal reinforcement and 3740 kgf/cm^2 for joint lateral reinforcement. Figure 3.81 shows the loading program. The specimens were subjected to a constant axial load of 10 tons at the column. Reversing loads were applied at the beam tips. Specimens GOO and OBO were loaded uniaxially in the direction of the beam, while the other specimens were loaded in the two directions alternately (GBO, GBS1 and GBS2) and/or simultaneously (GBS3, GBS4 and GBSU). The loading history for Specimens GBS3 and GBSU followed the bidirectional displacement path shown in Fig. 3.1. Figure 3.82 shows story shear-drift relationships. The three-dimensional specimen (GBO) showed relations similar to those for the two- dimensional specimens (GOO and OBO). GOO and OBO failed in joint shear at the final stage but GBO did not.

Specimens GBS1 and GBS2 with a slab showed higher story shear than Specimen GBO without a slab, because slab reinforcement contributed to the beam flexural resistance. Specimens GBS3 and GBS4, loaded in two directions simultaneously, showed biaxial interaction of the story shear strength in which the loading in one direction lowered the story shear strength in the other direction. The hysteresis loops for these specimens, particularly for Specimen GBS4, appeared fatter than those for the specimens loaded in the two directions alternately (GBS1 and GBS2). Figure 3.83 shows joint shear-strain relations. The shear strain measured in the NS direction for Specimen GBO was smaller than that for Specimen GOO because the joint in GBO was confined by transverse beams in the EW direction. Simultaneous bidirectional loading deteriorated the joint shear resistance more markedly than alternate bidirectional loading because Specimens GBS3 and GBSU showed larger strains that Specimens GBS1 and GBS2. It should be noted that no great difference was observed in the strain behavior, particularly in the NS direction, between Specimen GBS3 with poor details

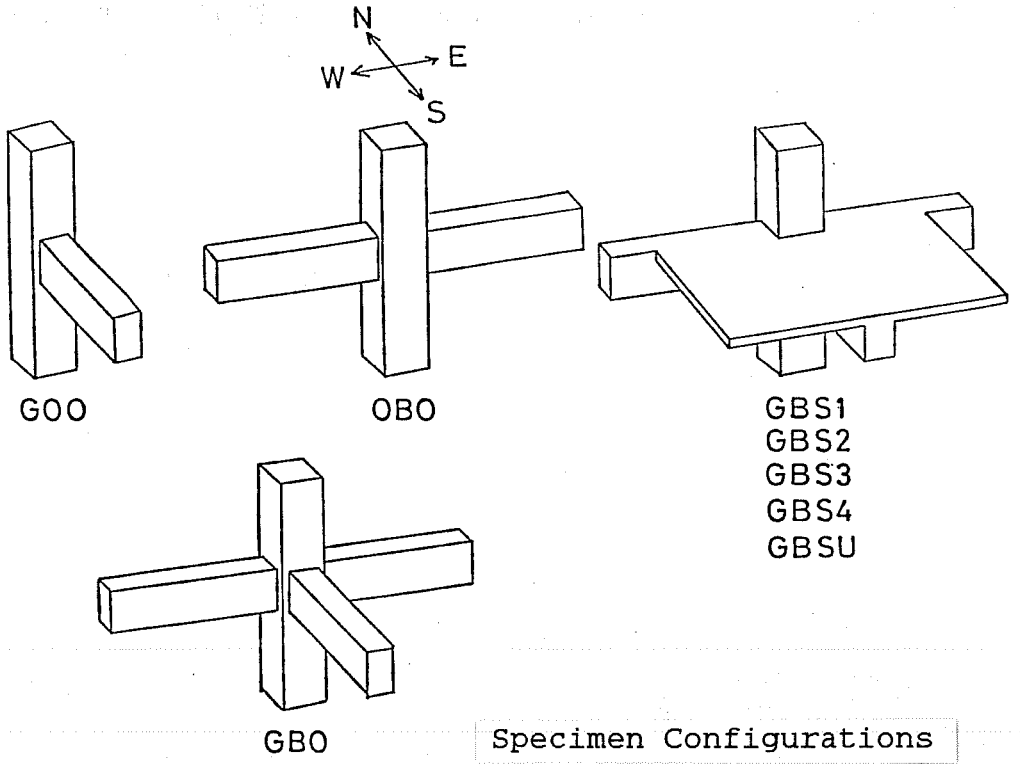

Specimen Configurations

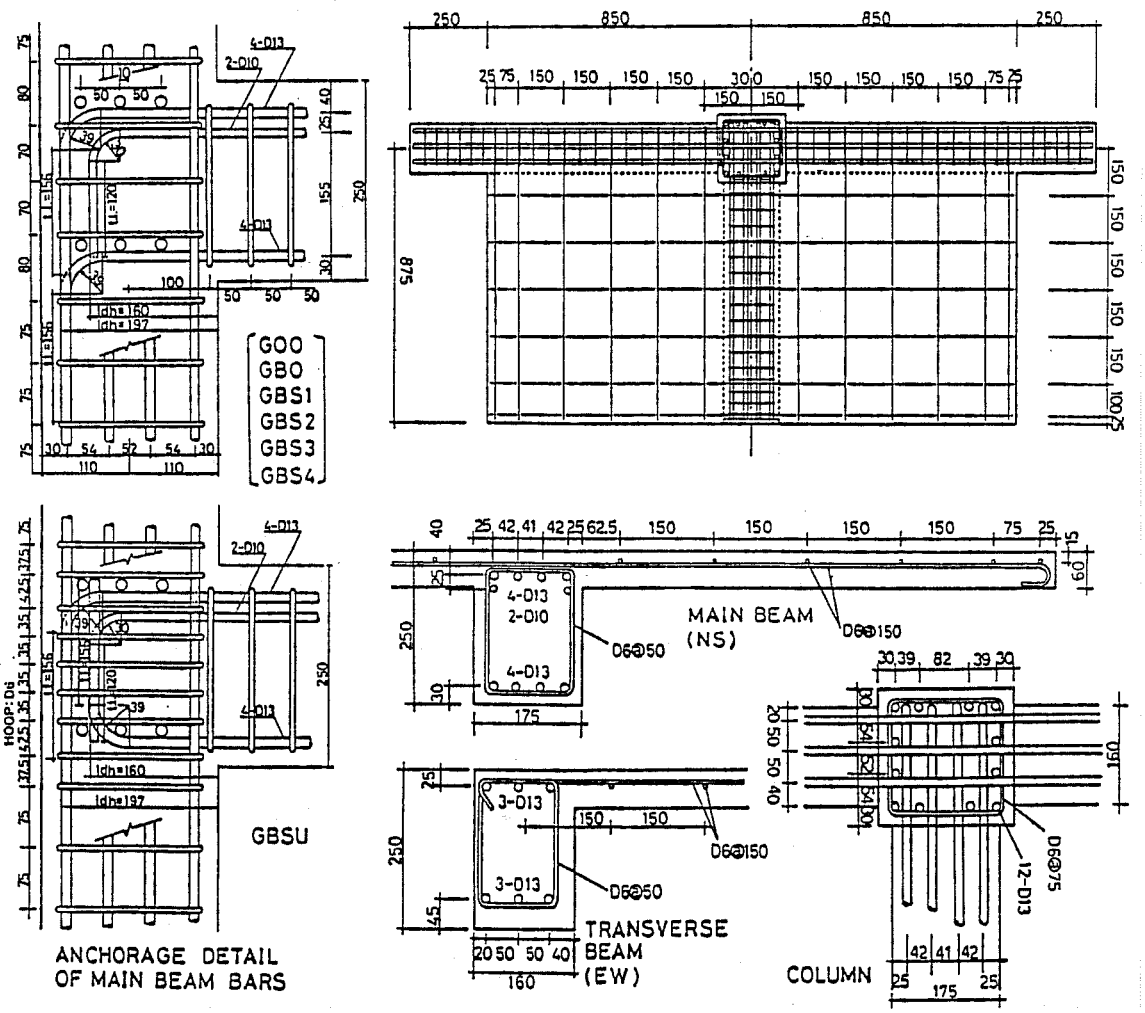

Fig. 3.80 Details of specimens

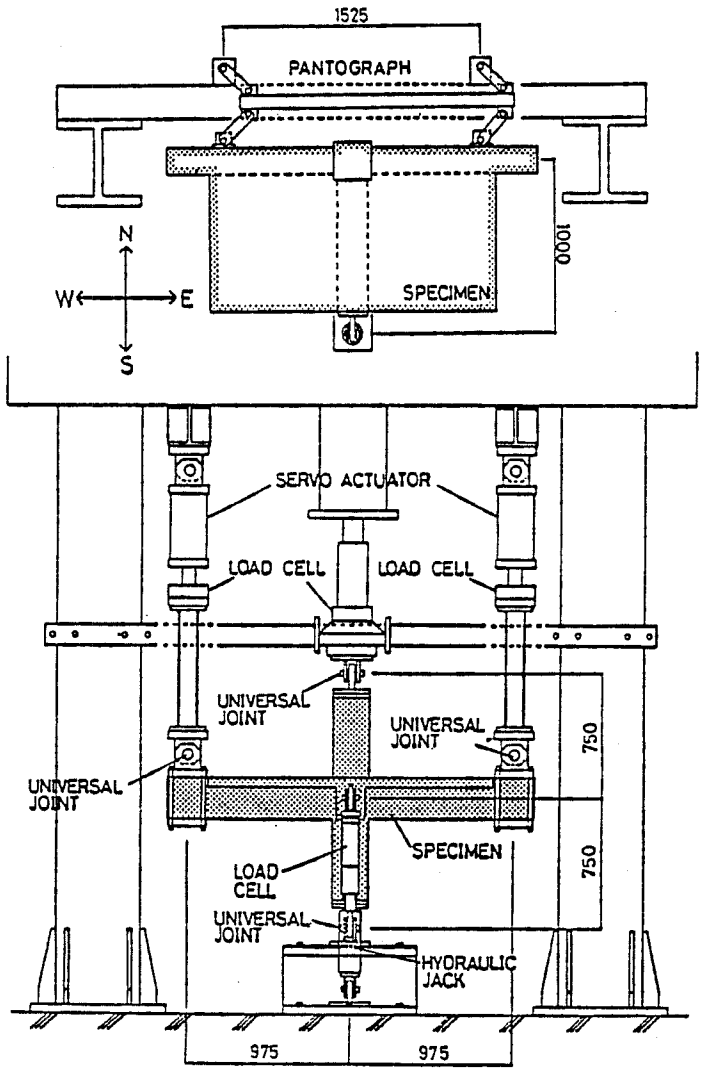

(a) Test setup

GOO	EW NS 2.5-5-5-10-10-20-20-40-40
OBO	EW 2.5-5-5-10-10-20-20-40-40 NS
GBO	EW NS 2.5-5-5-10-10-20-20 5-10-20 20-40
GBS1	EW NS 2.5-3.5-5-5-10-10-20-20 5-10-20 20-40
GBS2	EW 2.5-5-5-10-10-20-20 20-40 NS 2.5-5-10-20
GBS3	EW NS 2.5 2.5 (5) * 10 10 20-20 (20) (20) 40 (40)
GBS4	EW NS 2.5 2.5 (5) * (10) (20) (40)
GBSU	EW NS 2.5 2.5 (5) 10 10 20-20 (20) (20) 40 (40)

Note: numbers indicate peak deflection levels at beam- end for each cycle

* Bi-directional loading patterns

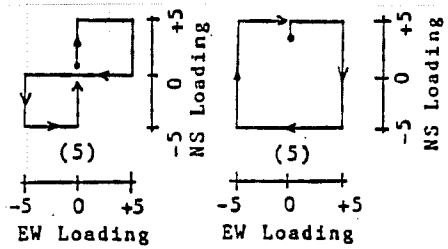

(b) Loading history

Fig. 3.81 Loading program

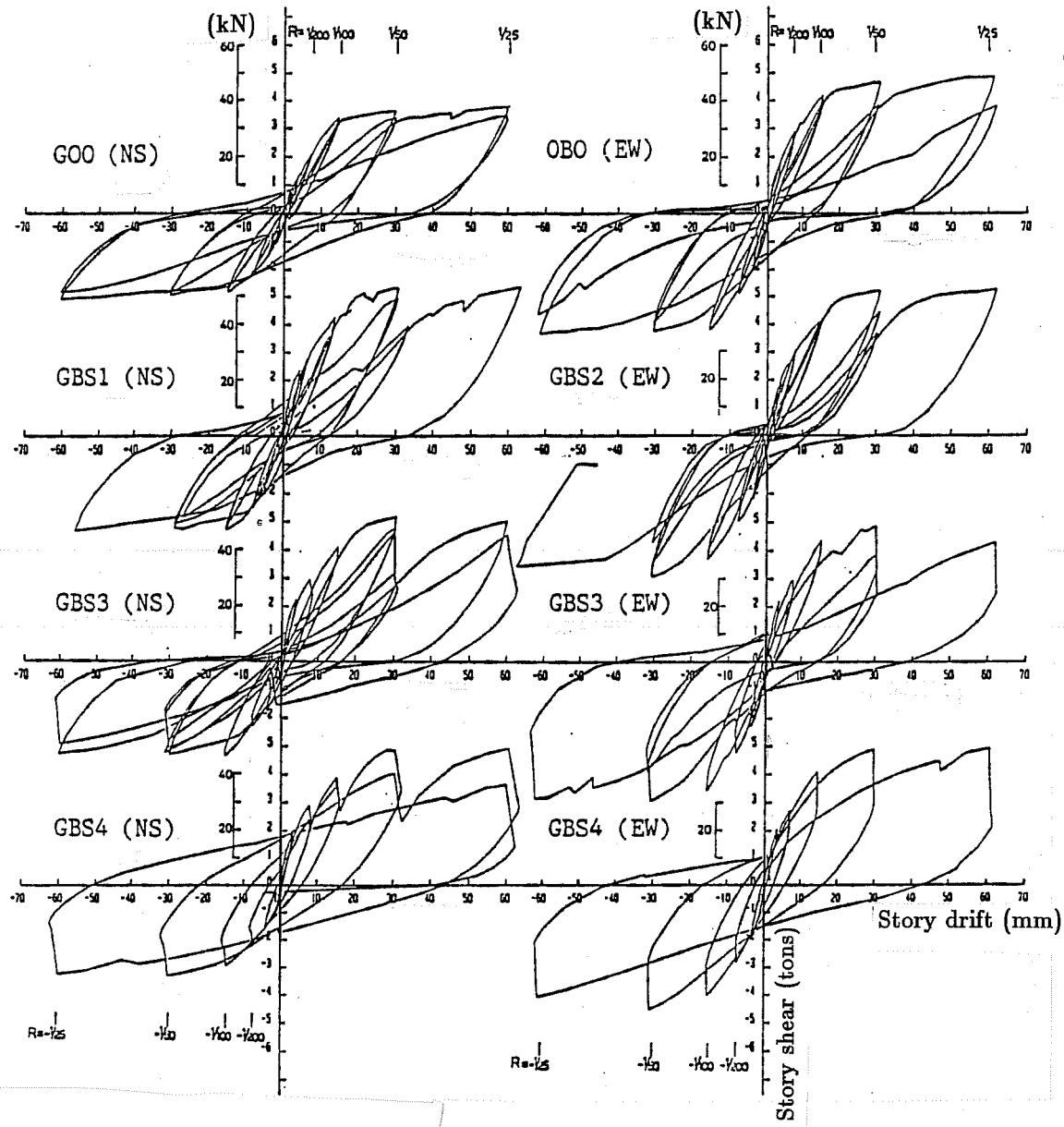

(a) Hysteresis curves

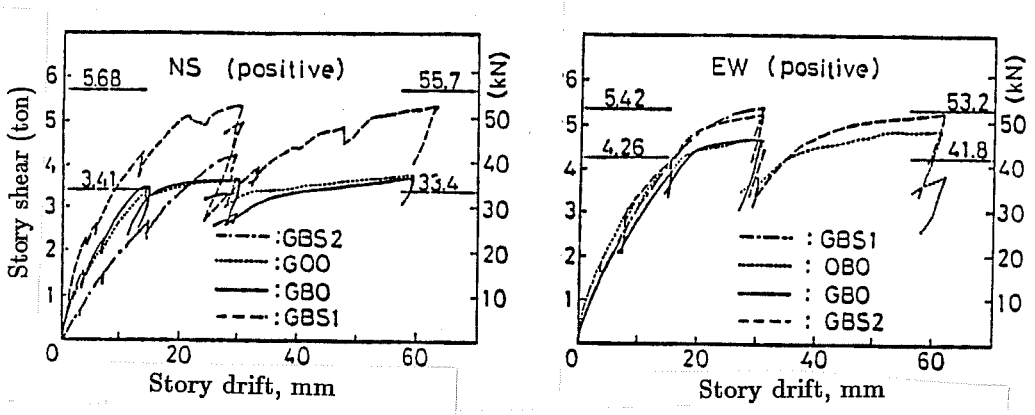

(b) Envelopes of hysteresis curves

Fig. 3.82 Story shear-story drift relations

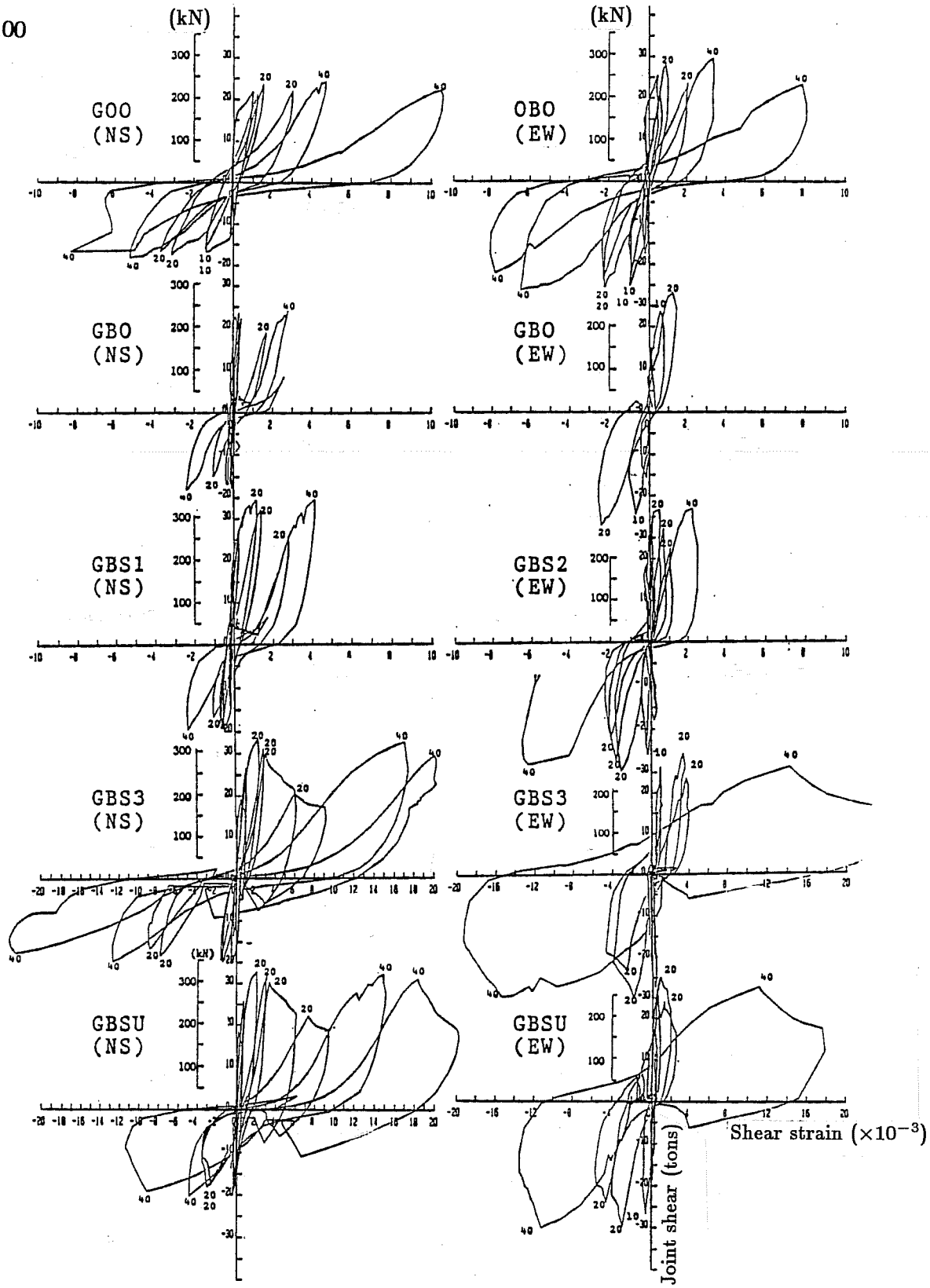

Fig. 3.83 Joint shear force-shear strain relations

from Japanese practice and Specimen GBSU with improved details. This indicates that the compressive strut mainly governed the shear resisting mechanism of the exterior joint and an increase in the amount of joint lateral reinforcement from 0.4 to 0.8% did not improve the joint behavior. Simultaneous bidirectional loading increased not only the joint shear strain but also the column deflection because the loading caused crushing of the corner concrete in and at the joint and reduced the biaxial moment capacity of the column as well as producing bond deterioration along column bars within the joint.

The following conclusions were indicated from the bidirectional loading tests described above.

1. Specimens loaded in two directions simultaneously show biaxial interaction of story shears.[30,31]
2. Transverse beams framing into both sides of an exterior joint are effective in confining the joint.[30] However, the effect of a transverse beam framing into one side of an interior joint is uncertain; i.e., one specimen sustained a higher joint shear stress than the plane specimen [31] in one case but not in the other.[30]
3. Slab reinforcement increased story shear by contributing to beam flexural strength.[30,31] The entire slab width should be regarded effective at a large deformation.[31]
4. The increase of joint lateral reinforcement from 0.4 to 0.8% did not affect the overall behavior of exterior joints.[30]

3.4 Studies on SRC Joints

SRC (Steel Reinforced Concrete) structures are extensively used to construct medium-to-high-rise buildings in Japan. A beam-column joint in an SRC structure has steel panels dividing joint concrete into several parts. The steel panels come from steel skeletons in beams and columns framing into the joint, as shown in Fig. 3.84(a).[41] The joint is provided with a nominal amount of two-leg hoops placed at a wide spacing. The hoops must pierce the steel panels in the joint, as shown in Fig. 3.84(b). Therefore, multi-leg hoops or ties are seldom used in actual SRC construction. With regard to the hysteretic behavior, SRC structure response lies somewhere between structural steel and reinforced concrete (RC) structures, depending on the size of the steel skeleton. Figure 3.85 illustrates the difference in the hysteretic behavior among the joints with various materials.[4] The steel concrete joint is an average of ductile steel and brittle concrete joint response. According to the AIJ Standard for SRC structures,[4] the shear strength of SRC joints is defined by superimposing the steel panel strength on the reinforced concrete strength. However, the reinforced concrete in SRC joints showed a little higher shear strength than RC joints as shown in Fig. 3.86.[22] It should be noted that the concrete in SRC joints is confined by steel flanges.

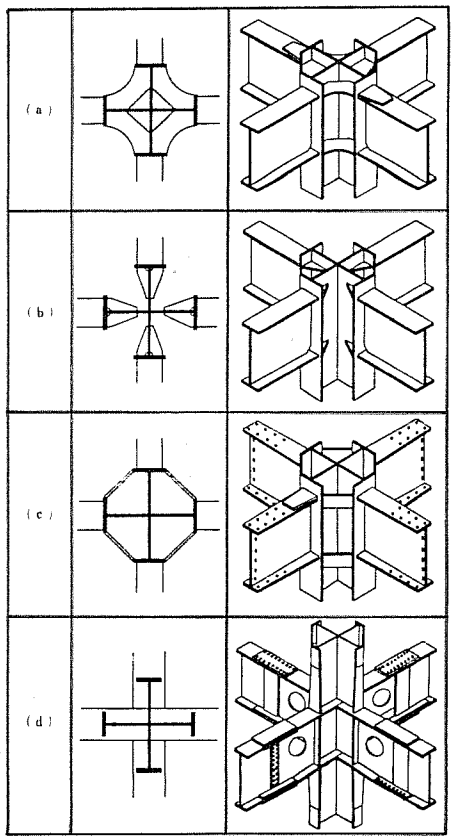

(a) Steel skeleton in joint

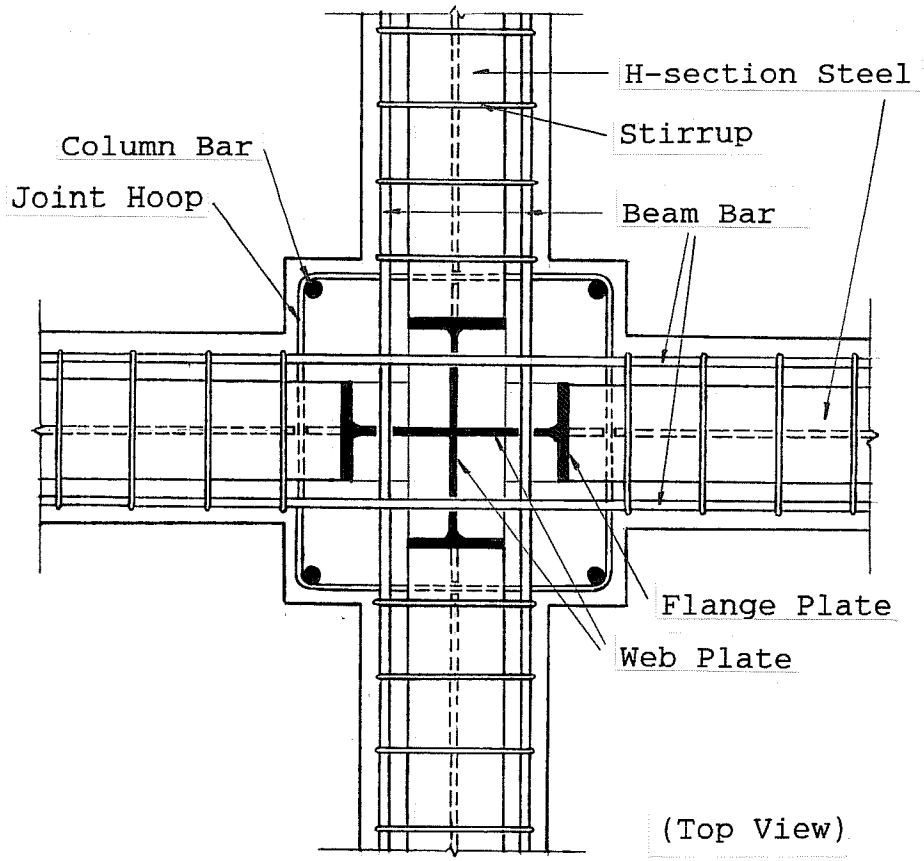

(b) Joint details

Fig. 3.84 Details of steel reinforced concrete (SRC) joint

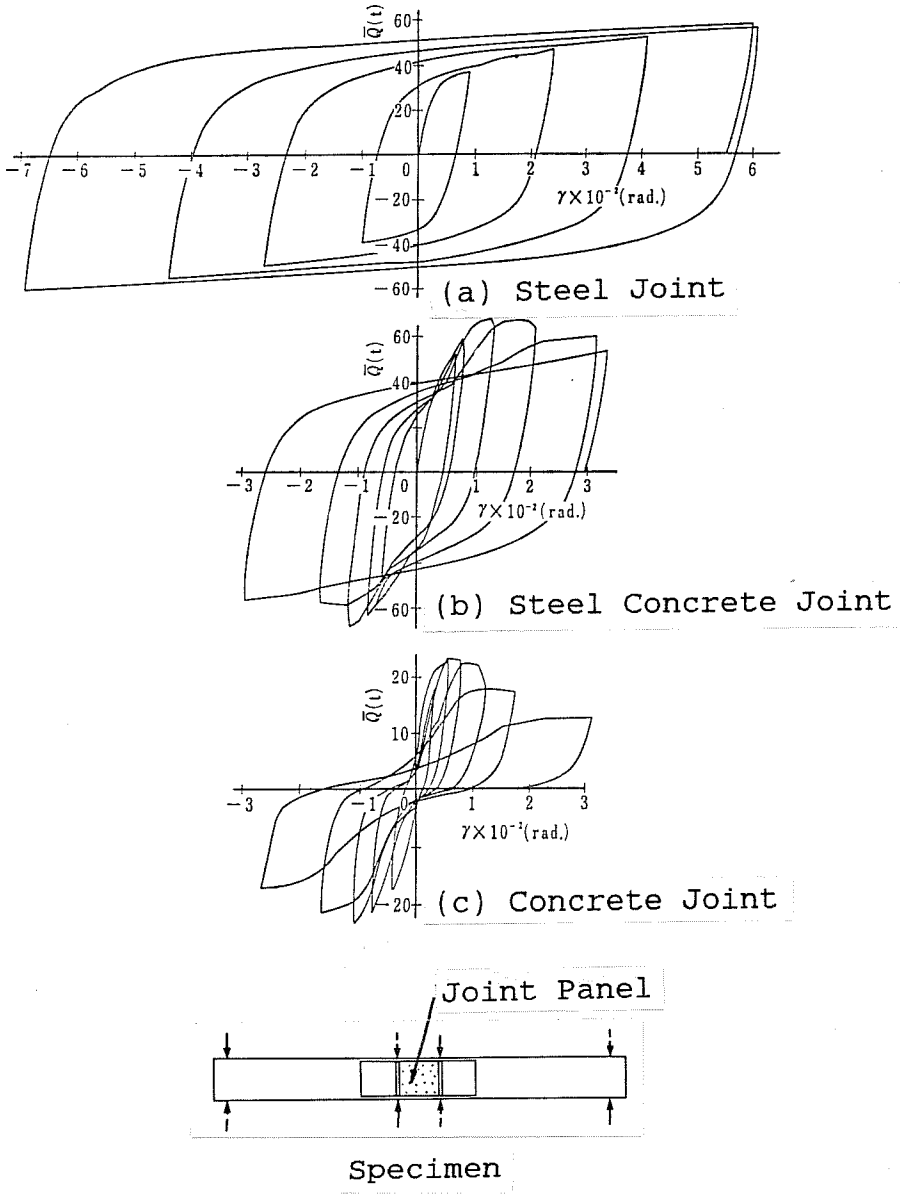

Fig. 3.85 Hysteretic behavior of various joints

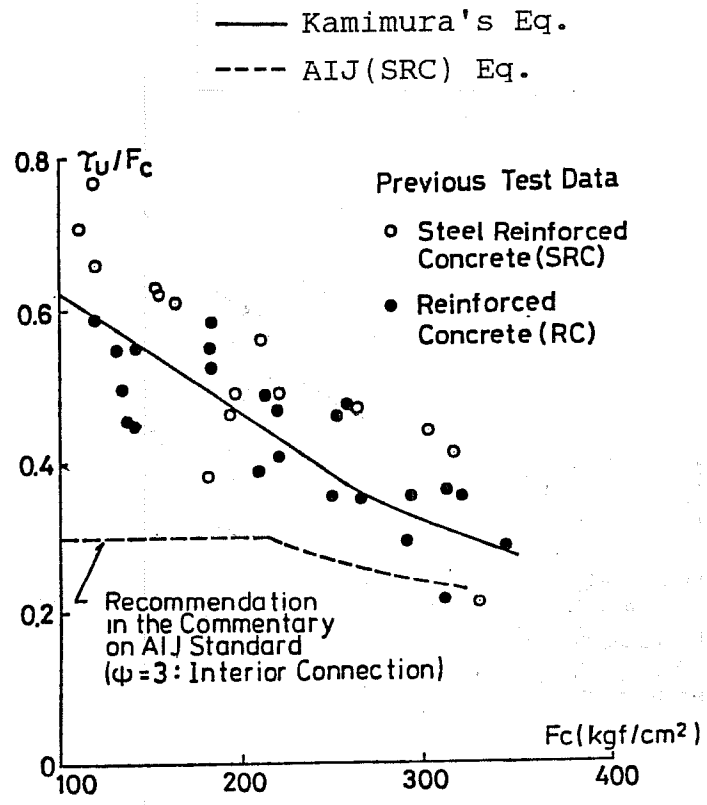

Fig. 3.86 Joint shear stress carried by concrete

A series of unidirectional loading tests were conducted on various SRC joint specimens under monotonic and cyclic loading conditions.[22] The main variables in this series are joint type (interior, exterior or corner) and beam-to-column-width ratio ($B_b/B_c = 0, 0.6, 0.8$ and 1.0). Specimen details are shown in Fig. 3.87. The SRC specimens were not provided with joint lateral reinforcement. Some steel specimens, fabricated with steel skeletons only, were tested and used as a reference to establish concrete behavior in the SRC tests. Crack patterns are shown in Fig. 3.88. The joint failure mode changed from diagonal tension to diagonal compression as the specimen type changed from a corner joint to an interior joint, or as the value of B_b/B_c increased. Although the specimens failed in joint shear, the load-displacement relations showed stable hysteresis loops (Fig. 3.89). No deterioration was observed in the strength until the joint shear strain reached 2% or so. Joint shear stresses carried by concrete were calculated by taking the difference in the stresses between the steel and the SRC specimens and are shown in Fig. 3.90. The column width was used as the joint width in this calculation. The shear cracking strength was hardly affected by the joint type and the value of B_b/B_c. However, the ultimate shear strength apparently increased with the value of B_b/B_c and the effective joint width could be defined as $(B_b + B_c)/2$. The ultimate strength was the highest for the interior joints and the lowest for the corner joints. The strength ratio relative to an interior joint was 0.52 for the corner joints and 0.64 for the exterior joints.

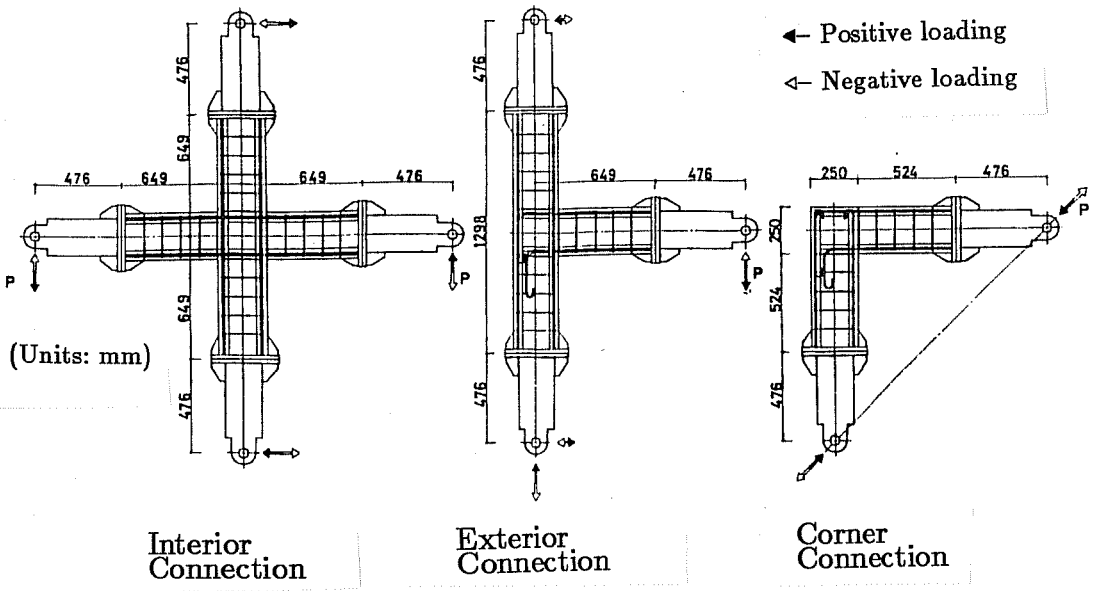

(a) Dimension and loading of test specimens

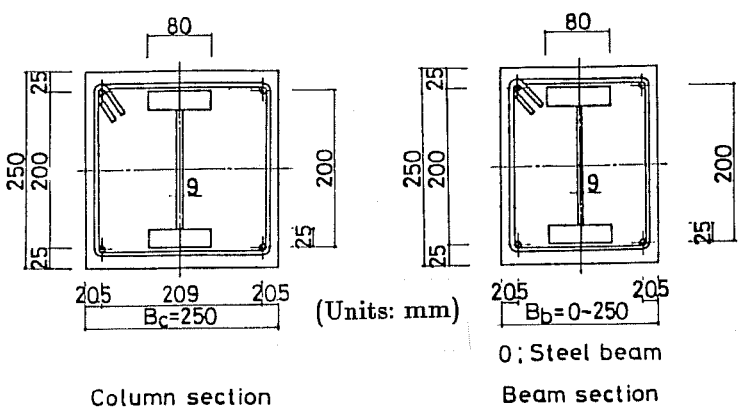

(b) Cross sections of test specimens

Fig. 3.87 Details of SRC joint specimens

Repeated Loading			Monotonic Loading			B_b/B_c
Interior Connection	Exterior Connection	Corner Connection	Interior Connection	Exterior Connection	Corner Connection	
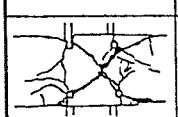	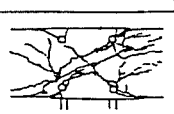	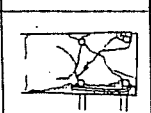	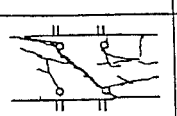	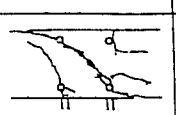	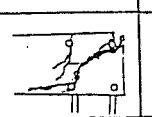	0
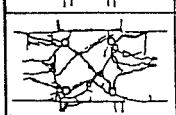	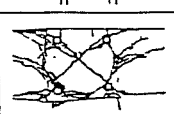	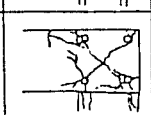	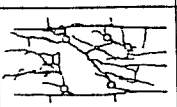	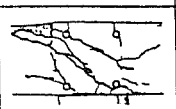	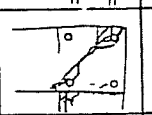	0.6
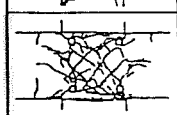	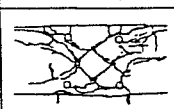	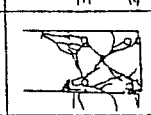	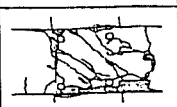	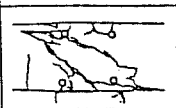	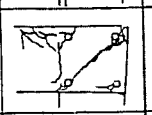	0.8
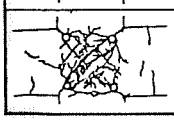	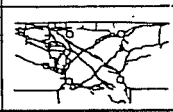	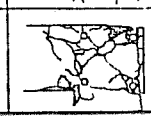	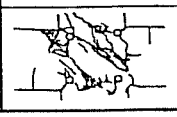		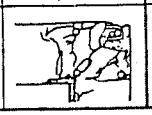	1.0

Fig. 3.88 Crack patterns

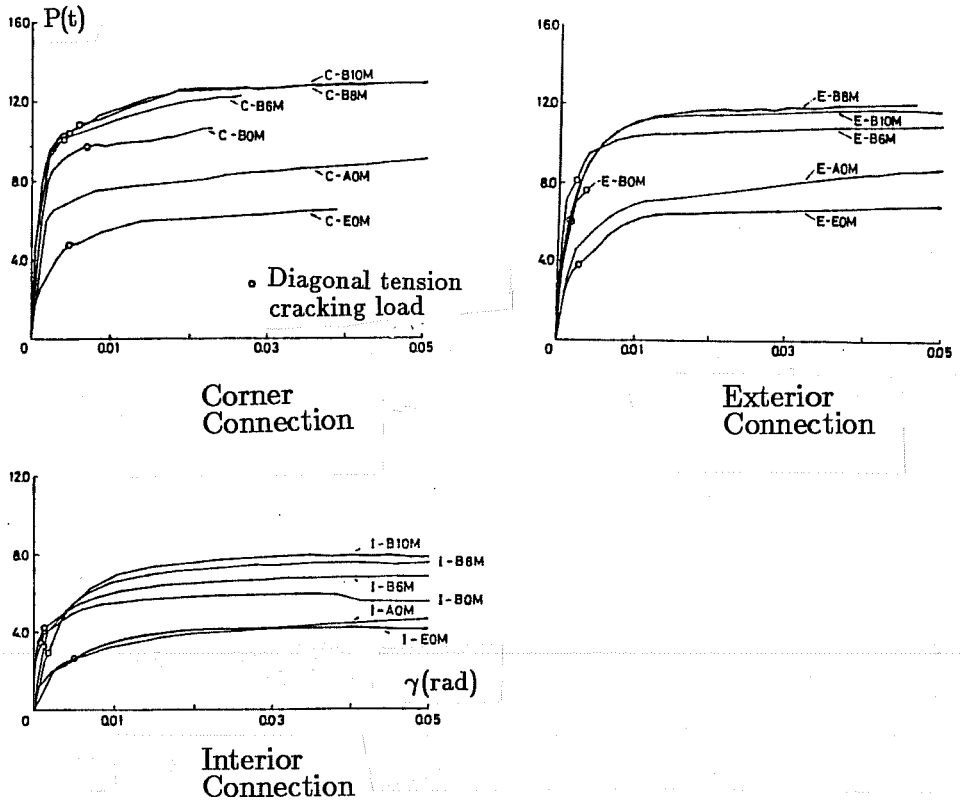

(a) Load-displacement response to monotonic loading

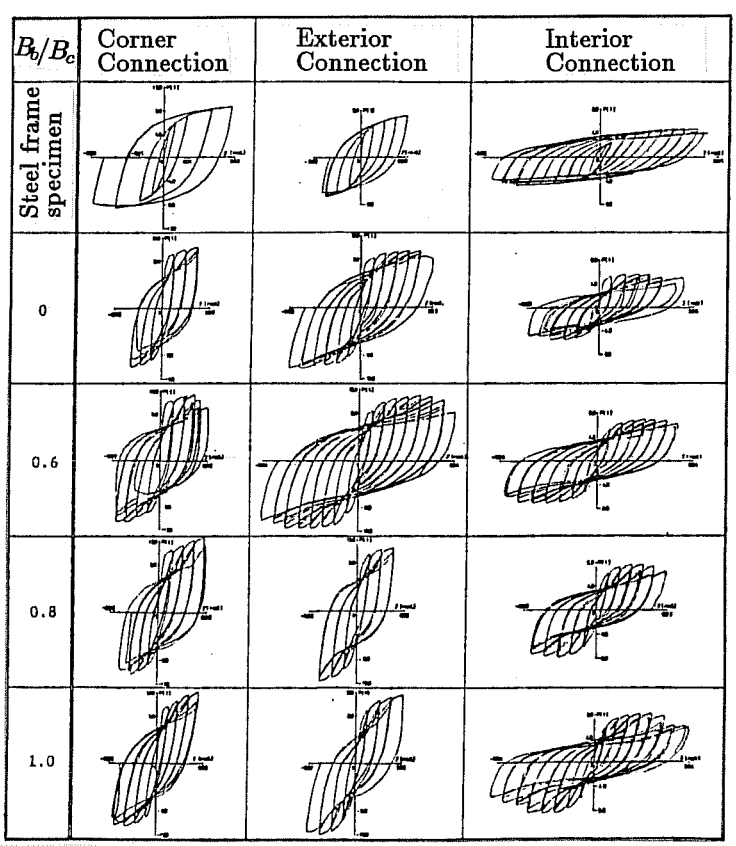

(b) Load-displacement response to repeated cyclic loading

Fig. 3.89 Load-displacement relations

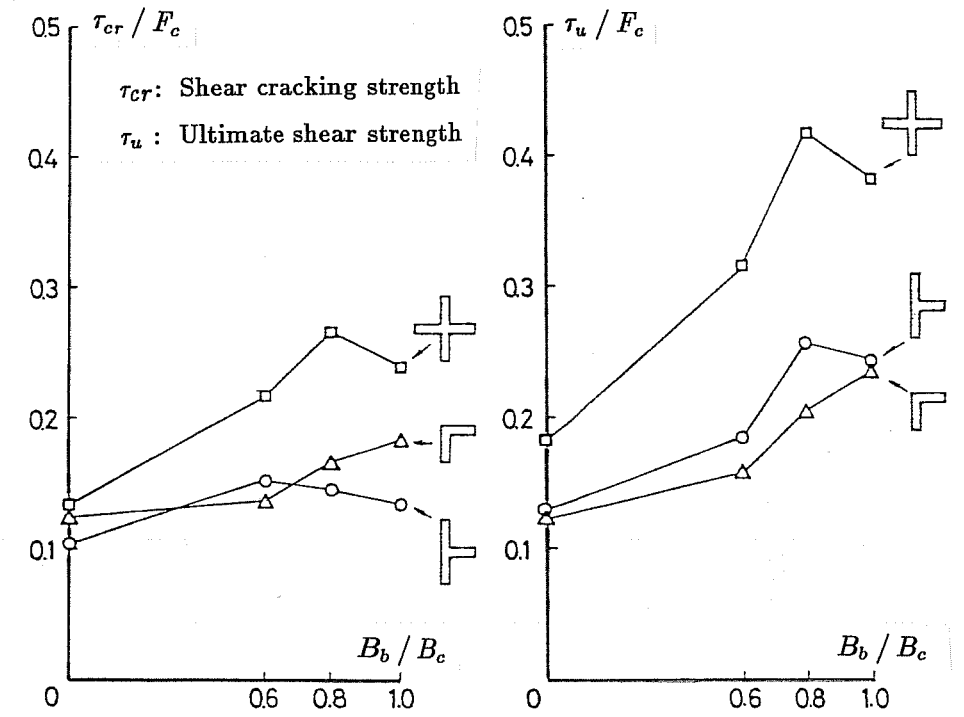

(a) Monotonic loading

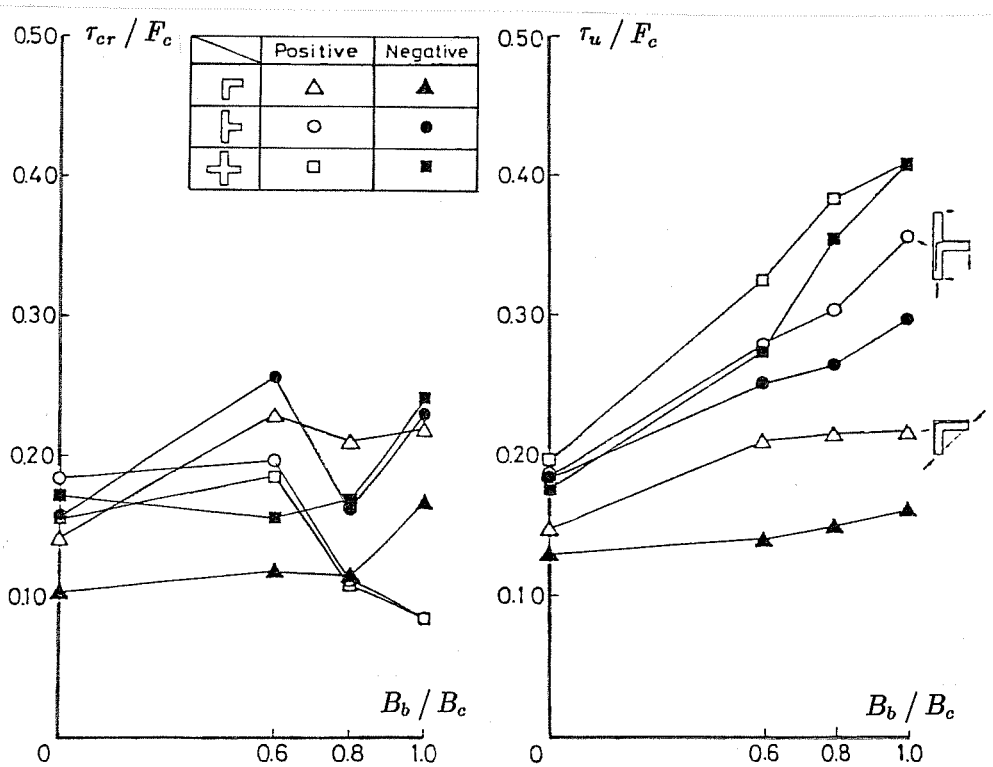

(b) Cyclic loading

Fig. 3.90 Shear strength of concrete panel

blank page 108

4. OTHER RECENT STUDIES ON RC JOINTS IN JAPAN

4.1 Shear Cracking Strength

Shear cracking strength of reinforced concrete beam-column joints generally increases with a column axial stress. According to the principal stress analysis, the shear cracking strength is given by the following equation:

$$\frac{{}_p\tau_c}{\sqrt{F_c}} = \beta^2 + \beta\frac{\sigma_o}{\sqrt{F_c}}, \beta = \frac{F_t}{\sqrt{F_c}} \tag{10}$$

where ${}_p\tau_c$ = shear cracking strength, F_c = compressive strength of concrete, F_t = tensile strength of concrete, and σ_o = column axial stress in kgf/cm^2. As shown in Fig. 4.1, the above equation with $\beta = 1.6$ gave the average of the test results for interior joints[9] but somewhat overestimated the value for exterior joints without transverse beams.[42]

4.2 Effect of Transverse Beams on Joint Behavior

4.2.1 Elastic Behavior. Transverse beams, framing into the joint at a right angle to the loading direction, tend to increase the shear cracking strength of the joint. As shown in Fig. 4.1(b), exterior joints with transverse beams showed a little higher cracking strength than those without transverse beams.[42] The same tendency was observed in interior joint tests.[9]

Figure 4.2 shows joint shear stress-strain relations for specimens with normal-weight concrete (solid lines) and those with light-weight concrete (broken lines).[9] Joints with transverse beams were stiffer than those without transverse beams.

4.2.2 Inelastic Behavior of Interior Joints. Various tests were conducted to study the effect of transverse beams on the behavior of interior joints. Figure 4.3 shows one series.[43] Specimen No. 1 without transverse beams failed in joint shear after yielding of the beams and showed deterioration in strength and stiffness. Specimens No. 4 and No. 5 with transverse beams on both sides of the joint failed in beam flexure and showed good spindle-shaped hysteresis in the load-displacement relations. It should be noted that Specimen No. 5 with wider transverse beams showed more stable hysteresis than Specimen No. 4 with narrower transverse beams.

Another two series of interior joint tests are shown in Figs. 4.4 and 4.5.[44] The main variable was the number of transverse beams; i.e., zero for JO-type, one for JE-type and two for JI-type. As shown in Fig. 4.4, the specimens in the first series (JO-0, JE-0 and JI-0) were not provided with joint lateral reinforcement and failed in joint shear. No great difference was observed in the behavior between Specimen JO-0 without transverse beams and Specimen JE-0 with one transverse beam. However, Specimen JI-0 with transverse beams on both

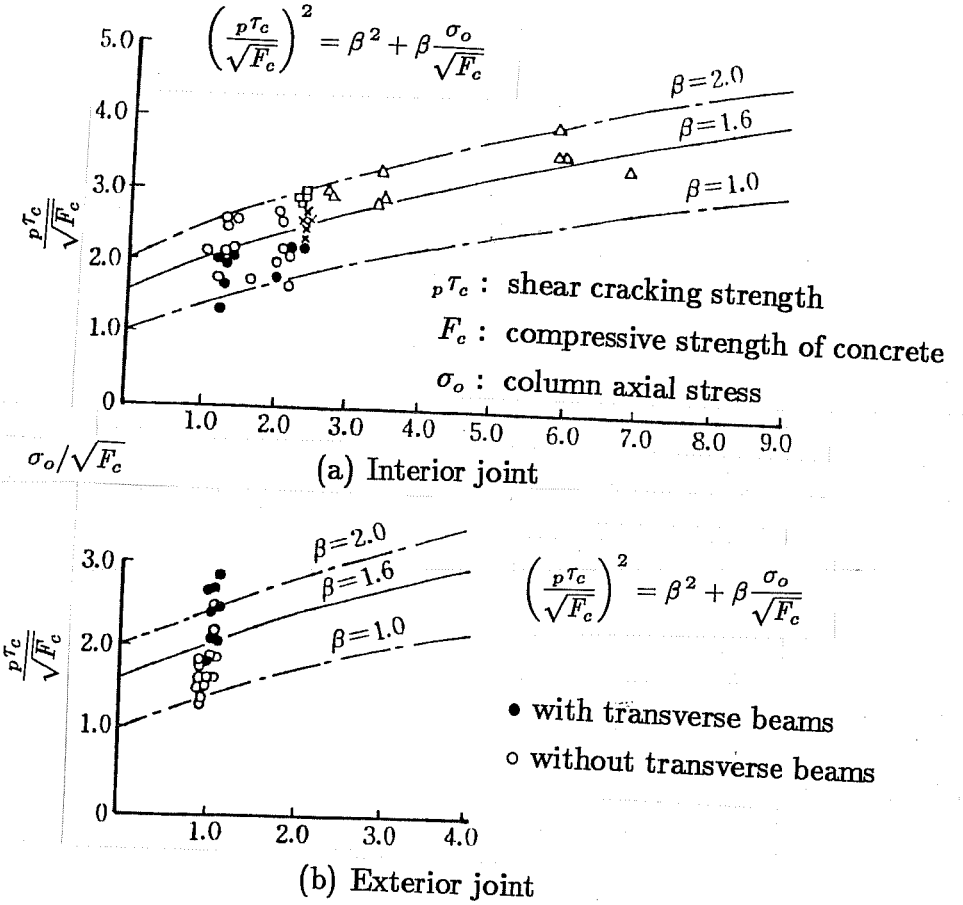

Fig. 4.1 Shear cracking strength in interior and exterior joints

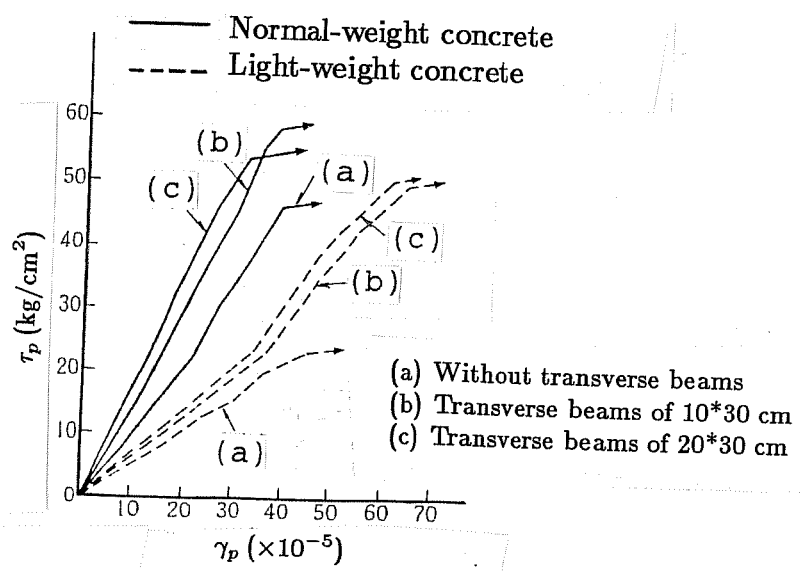

Fig. 4.2 Joint shear stress-strain relations

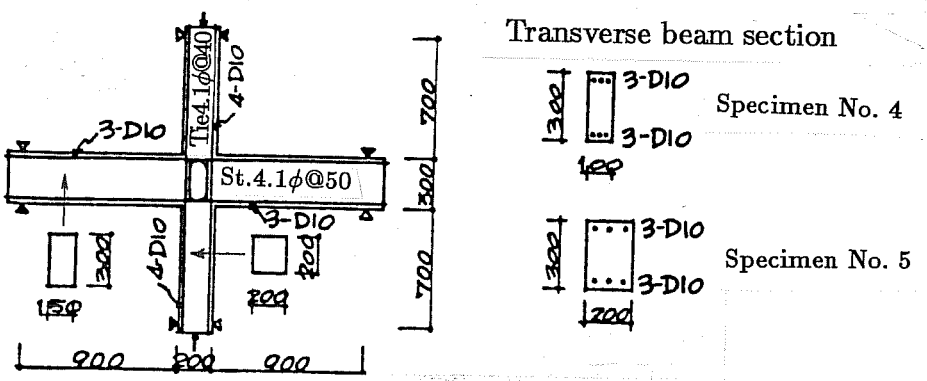

(No transverse beams in Specimen No. 1)

(a) Specimen details

Specimen No. 1 | Specimen No. 4 | Specimen No. 5

(b) Load-displacement relations

Fig. 4.3 Test of interior joints with transverse beams

sides of the joint showed higher strength and better ductility than the others, indicating the confining effect of transverse beams on the joint resistance. In the second series, the beam and column dimensions were the same in the specimens but the amount of lateral reinforcement was varied. Specimens JO-1, JE-1 and JI-1 were not provided with joint lateral reinforcement, but Specimens JO-2, JE-2 and JI-2 were laterally reinforced with $\phi 4$ hoops spaced at 40 mm in the joint (lateral reinforcement ratio: $p_w = 0.4\%$) as shown in Fig. 4.5. Compared with specimens without transverse beams (JO-1 and JO-2), the specimen with one transverse beam showed higher strength when the joint was not reinforced (JE-1) and almost the same strength when the joint was reinforced (JE-2). The specimens with transverse beams on both sides showed the highest strength without deterioration. The joint lateral reinforcement was effective in increasing the strength over that of the specimen without transverse beams and in delaying deterioration in strength compared with the specimen with one transverse beam. However, no great difference was observed in the behavior between the reinforced and unreinforced joints with transverse beams on both sides.

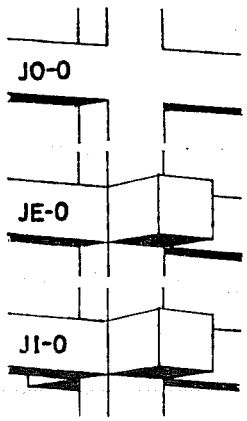

(a) Joint variations

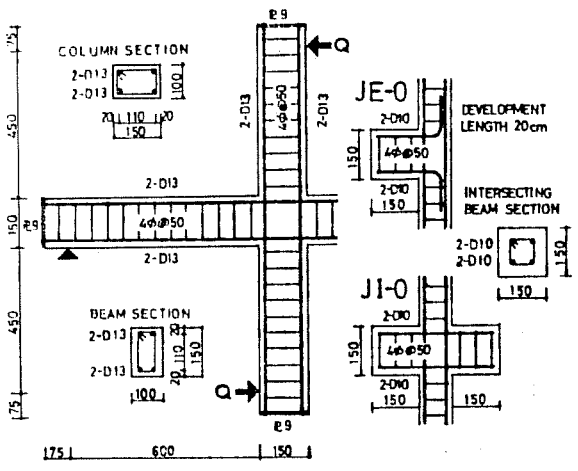

(b) Specimen details

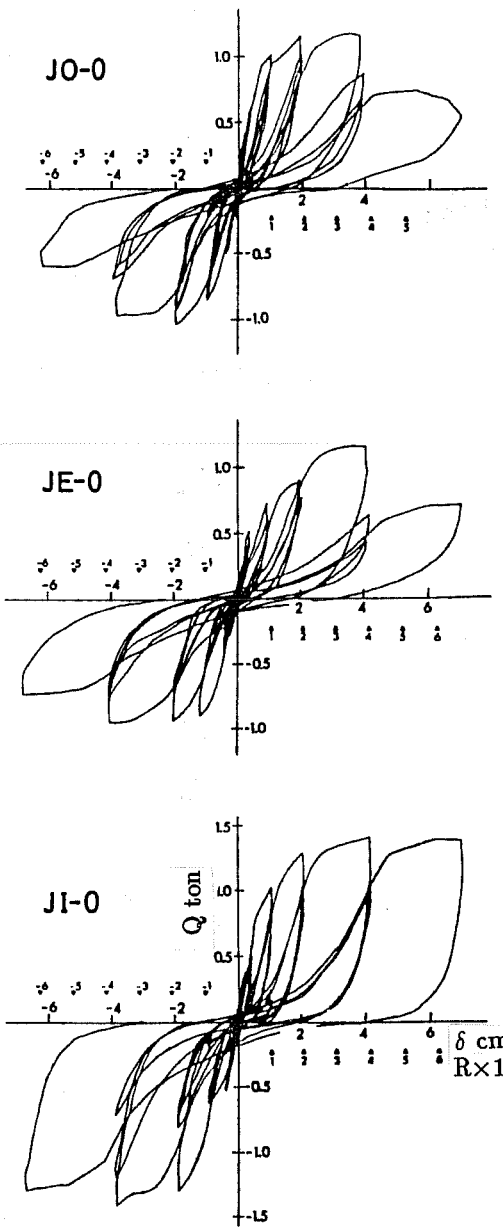

(c) Load-displacement relations

Fig. 4.4 Test of interior joints with transverse beams

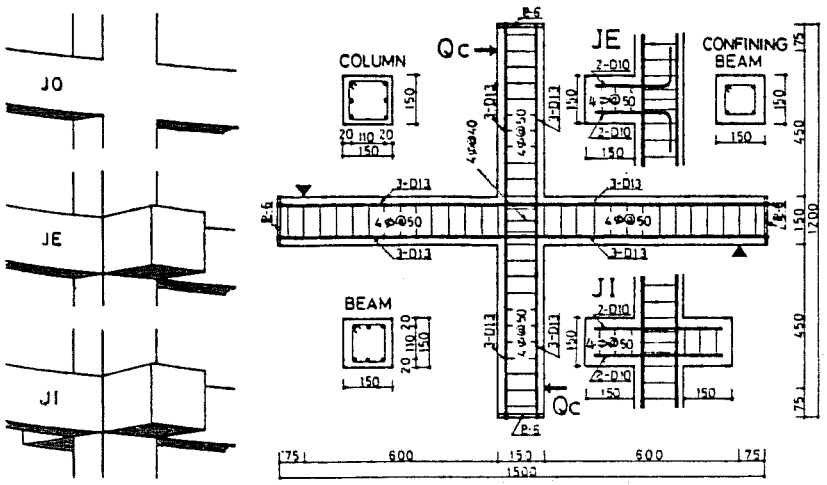

Specimen details

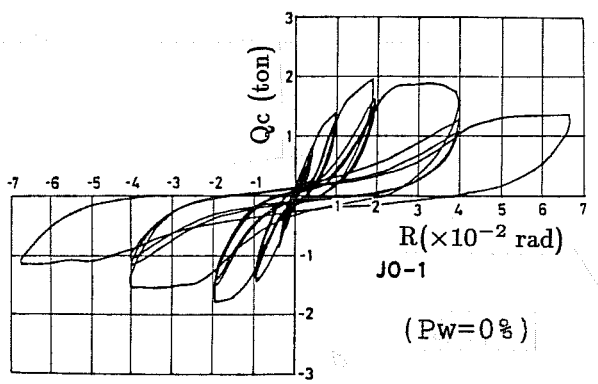

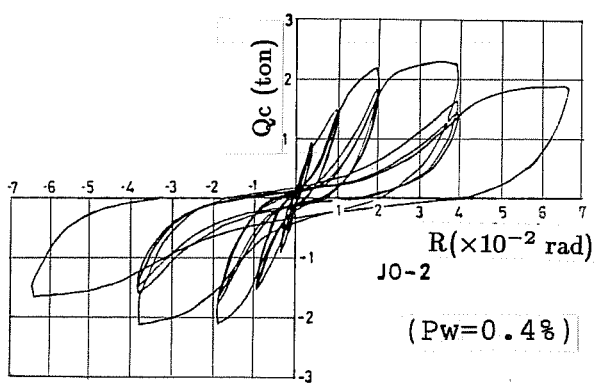

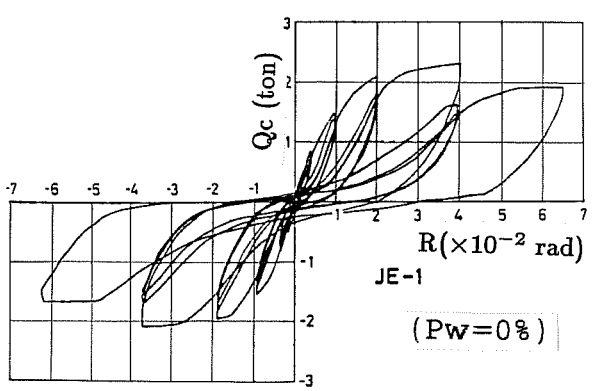

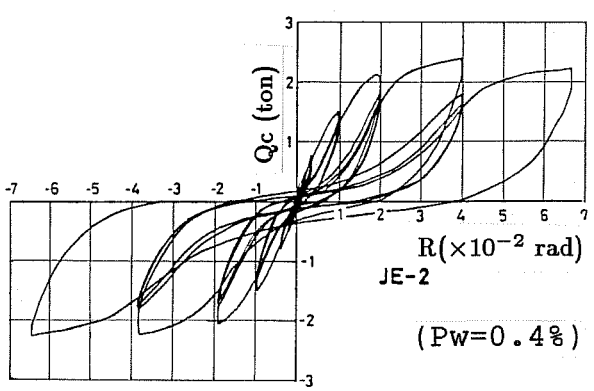

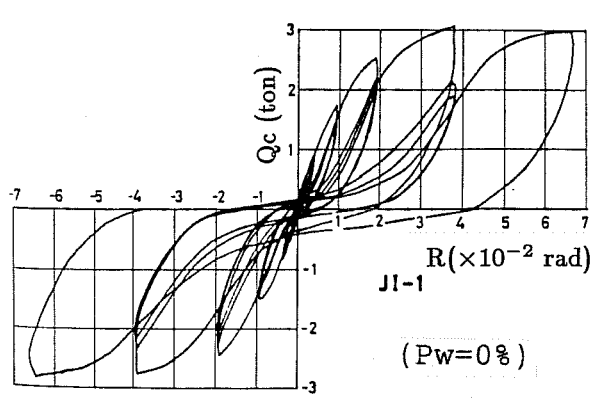

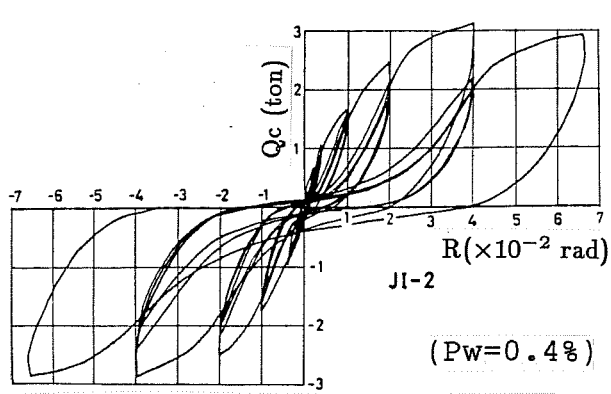

(Pw: joint reinforcement ratio)

Fig. 4.5 Test of interior joints with transverse beams

The other series of interior joint tests are shown in Fig. 4.6.[45] The main variable in this series was also the number of transverse beams. The specimens modeled beam-column joints in high-rise buildings where heavily reinforced beams framed into columns. Specimen J1 without transverse beams developed wide shear cracks in the joint and showed deterioration in strength. On the contrary, Specimens J2 and J3 with transverse beams showed stable load-deflection relations and reached 10% higher strength than Specimen J1. The transverse beam on one side of the joint appeared to be as effective in confining the joint as beams on both sides, because Specimen J2 showed nearly the same behavior as Specimen J3.

4.2.3 Inelastic Behavior of Exterior Joints. Various series of exterior joint specimens were tested to study the effect of transverse beams on the joint behavior as shown in Fig. 4.7.[42,46] The specimens were cast with light-weight concrete. Four D19 bars were used as beam tensile reinforcement and anchored with a total development length of 23 to 27 times the bar diameter (about 70% of the AIJ specification). The beam bottom bars terminated in bent-down anchorage for Type-H and in bent-up anchorage for Type-P. The hysteretic curves show the beam moment-rotation relations in comparison with calculations (broken lines). All specimens showed slip-type hysteresis because of insufficient development length of beam bars. Type-H specimens showed lower strength and stiffness in negative (upward) loading (bottom bars in tension) than in positive (downward) loading (top bars in tension), but Type-P specimens did not. Specimens without transverse beams did not reach the calculated strength and showed large deterioration in resistance. Transverse beams appeared effective in delaying deterioration rather than in increasing the strength or in improving the slip-type hysteresis. It should be noted that the poor behavior of Type-H specimens in negative loading was not improved by the transverse beams.

4.2.4 Bond Behavior of Beam Bars. The bond behavior of beam longitudinal bars within the joint is influenced by transverse beams. Figure 4.8(a) shows average bond stresses along beam bars within interior joints.[45] The bond stresses were calculated from strain measurements in the test of interior joints shown in Fig. 4.6. Bond stresses did not reach the value of $4\sqrt{F_c}$ (see Sec. 2.2) in the test. The specimens with transverse beams (J2 and J3) apparently developed larger bond stresses than the specimen without transverse beams (J1). Figure 4.8(b) shows the bond stress-bar stress relations measured in loading cycles 1 through 6 for exterior joints.[42] The specimen with transverse beams showed larger bond stresses than the specimen without transverse beams.

4.3 Effect of Lateral Reinforcement on Joint Behavior

4.3.1 Normal Strength Reinforcement. Several series of +–shaped and ×–shaped specimens were tested to study the effect of joint lateral reinforcement on the behavior of interior joints, as shown in Fig. 4.9.[47,48] Specimens P-2 and KX-3 were not provided with

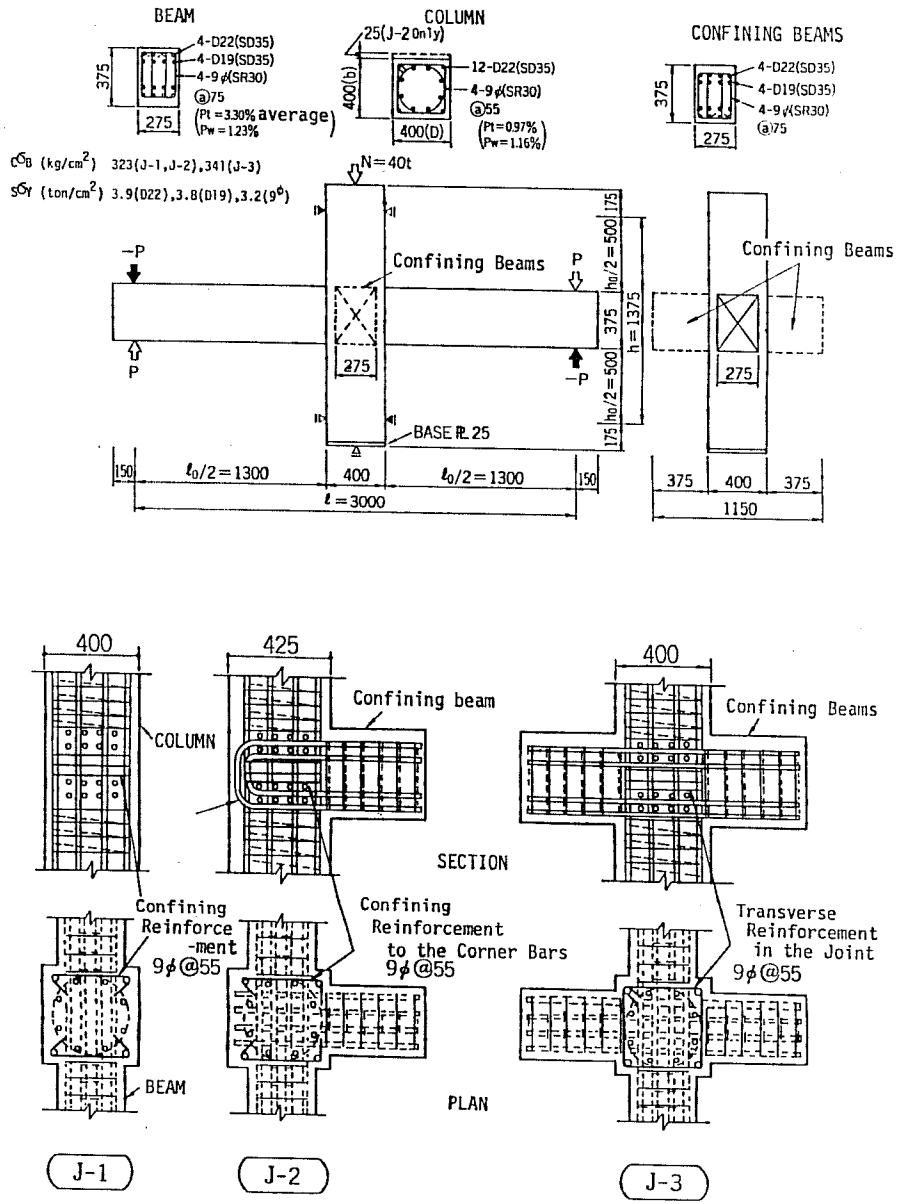

(a) Specimen details

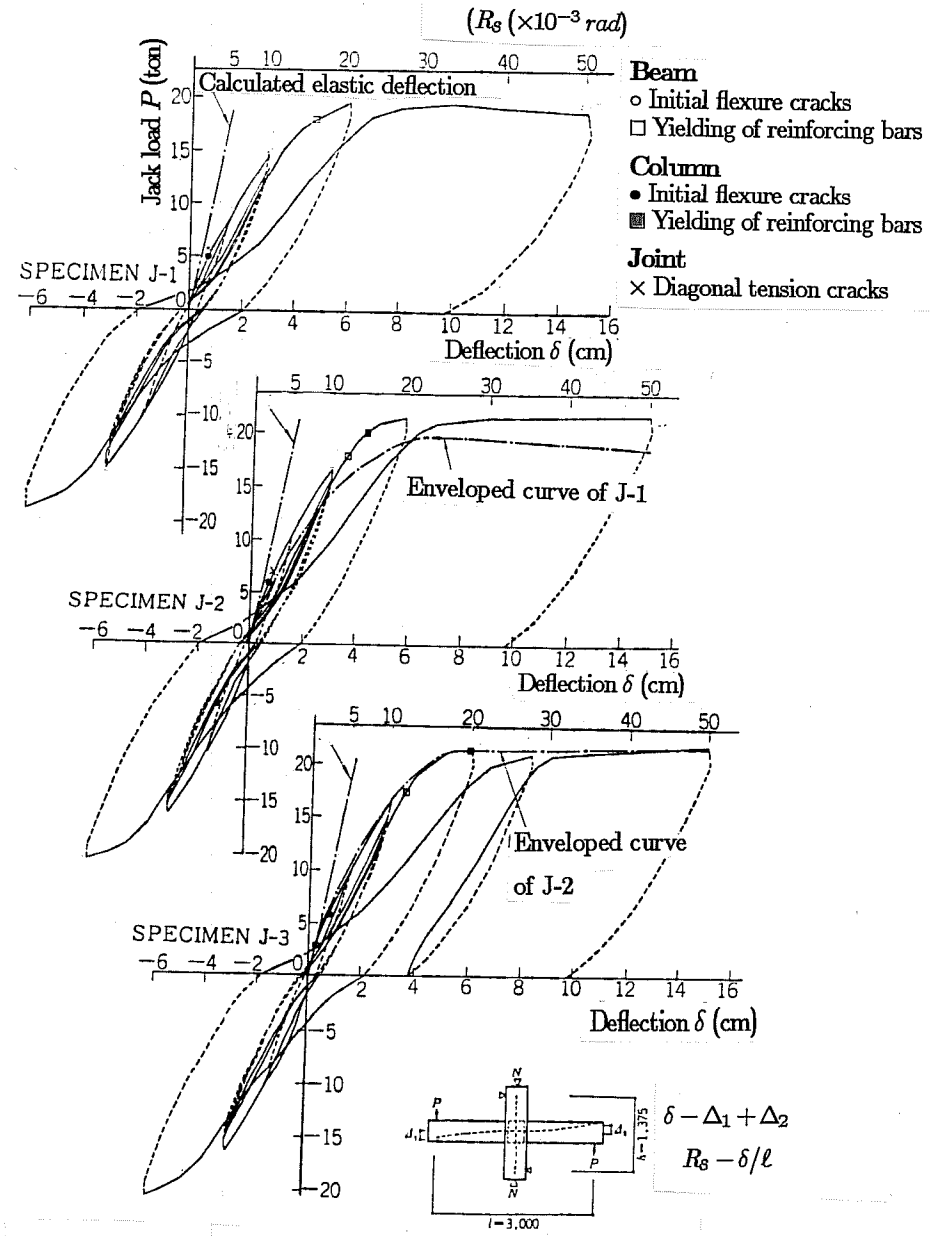

(b) Load-deflection relations

Fig. 4.6 Test of interior joints with transverse beams

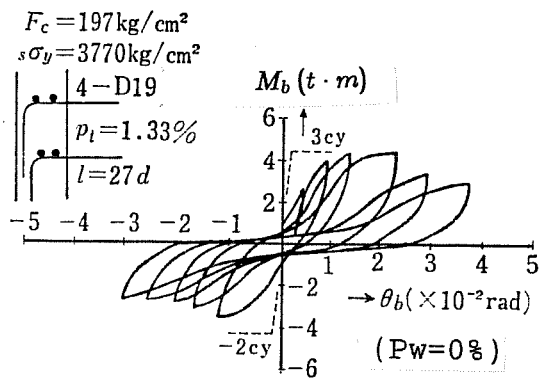

With transverse beams

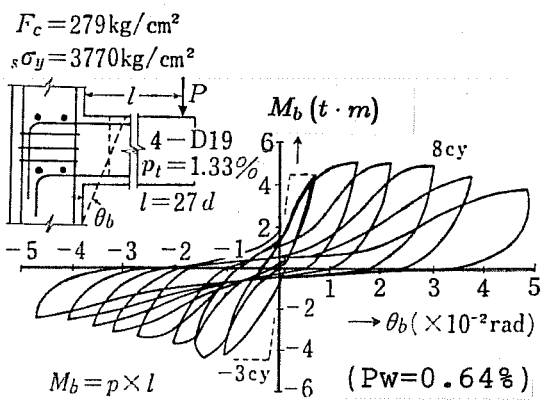

With transverse beams

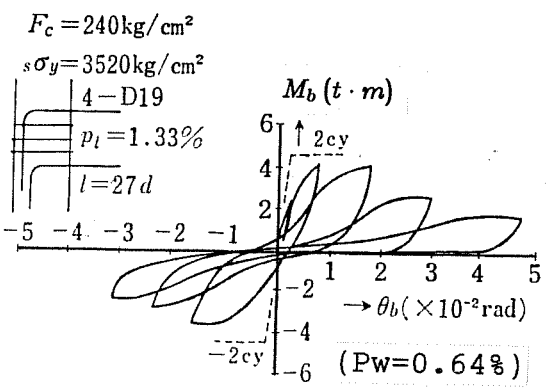

Without transverse beams

(Pw: joint reinforcement ratio)

(a) Type-H Specimens

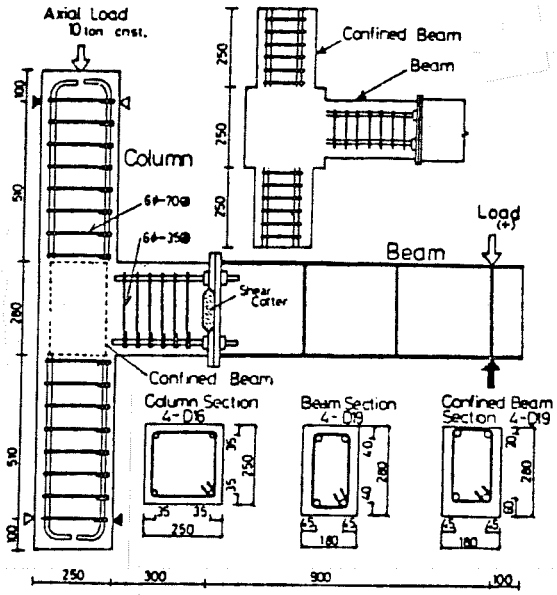

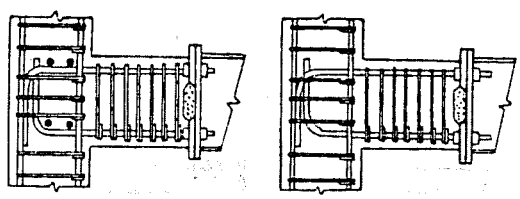

Specimen POC Specimen PO

POC: with transverse beams
PO: without transverse beams

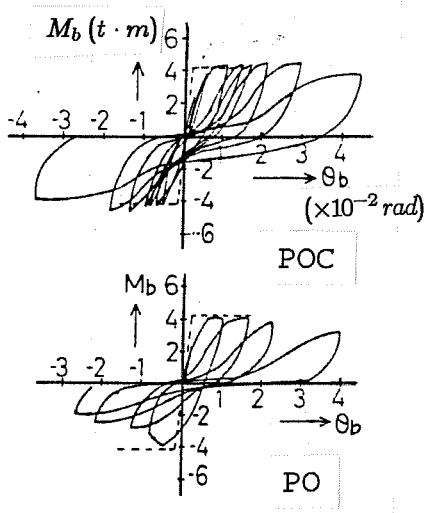

(b) Type-P Specimens

Fig. 4.7 Test of exterior joints with transverse beams

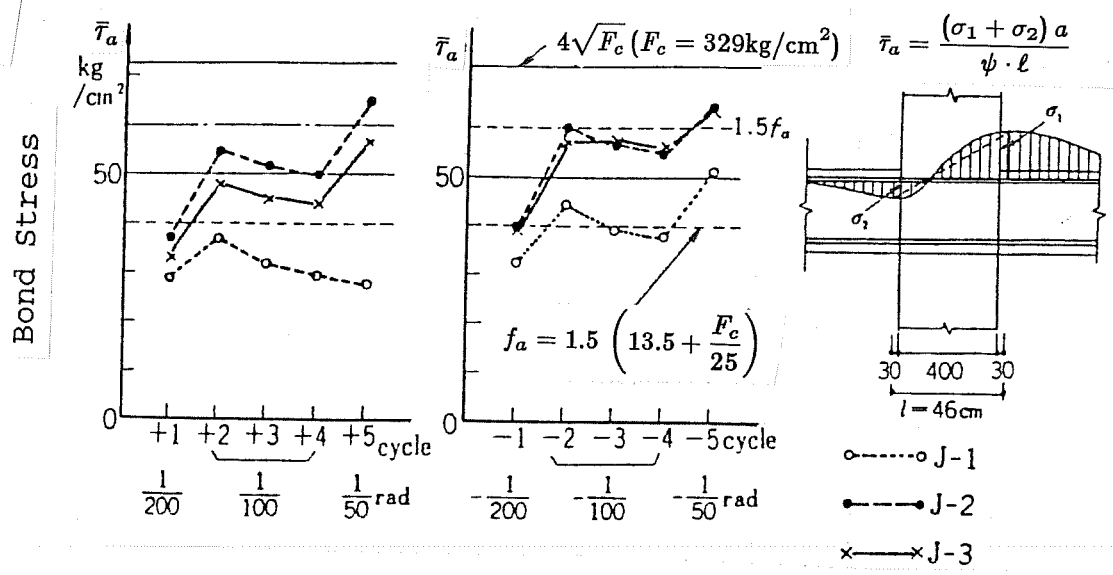

(f_a: allowable bond stress in *AIJ Standard*)

(a) Interior joint

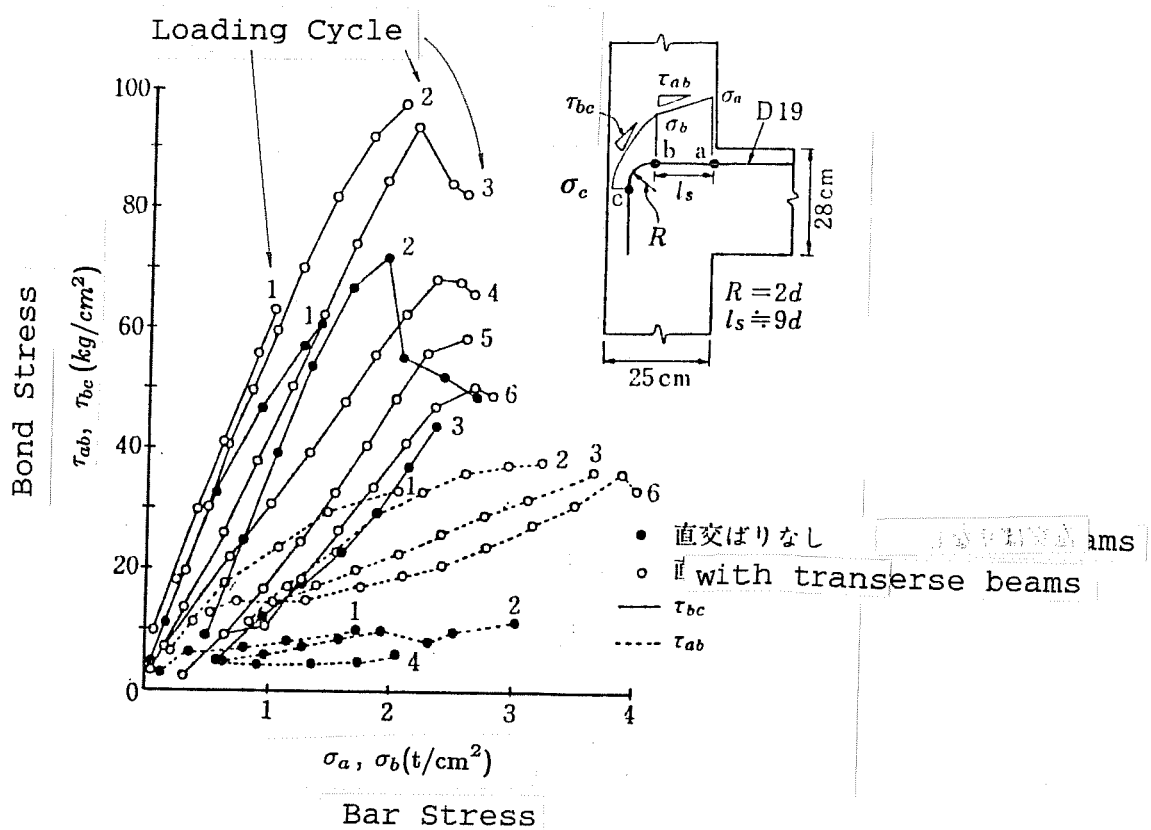

(b) Exterior joint

Fig. 4.8 Bond stress along beam bar within joint

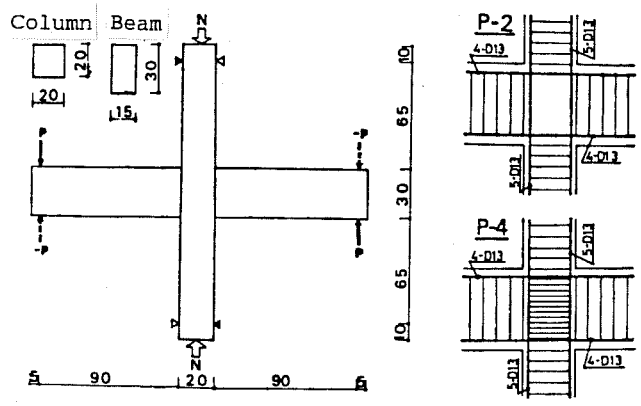

Specimens P-2 and P-4

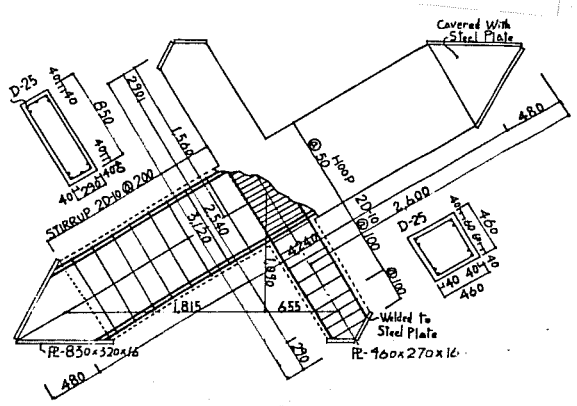

Specimens KX-2 and KX-3

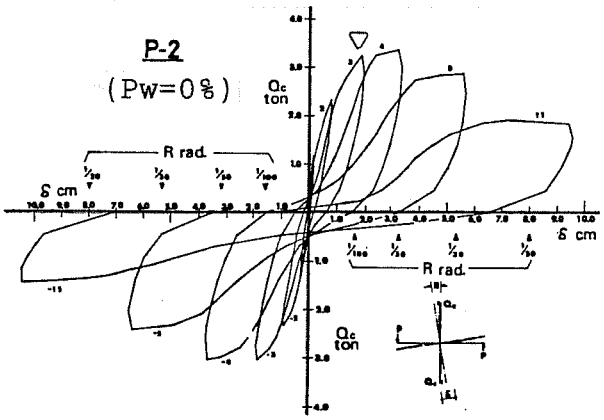

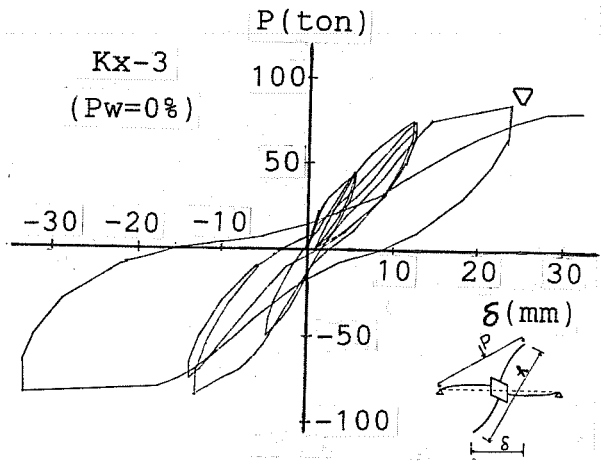

(Pw:joint reinforcement ratio, ▽:drift angle of 1/100rad)

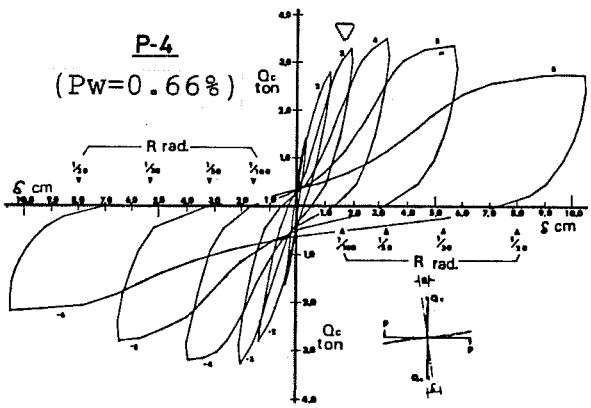

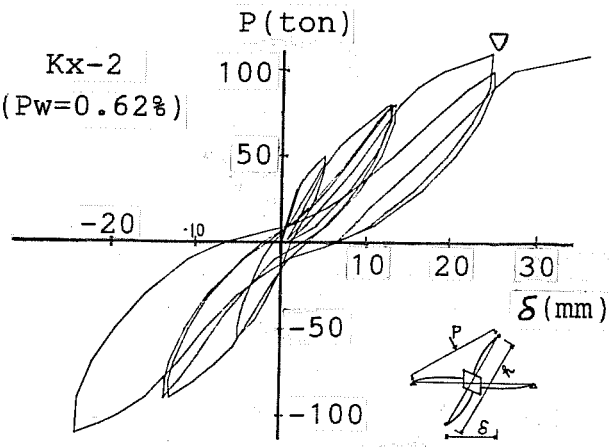

Load-deflection Relations

Fig. 4.9 Interior joints with/without lateral reinforcement

joints lateral reinforcement, while Specimens P-4 and KX-2 were reinforced with two-leg hoops having yield strength of 2500 kgf/cm^2 (P-4) to 4100 kgf/cm^2 (KX-2). Concrete strength was low and ranged from 140 to 160 kgf/cm^2. All specimens failed in joint shear. Specimen P-2 without joint reinforcement lost joint concrete at the final stage and showed considerable deterioration in the resistance. The joint lateral reinforcement in Specimen P-4 appeared effective in delaying deterioration rather than increasing the strength. On the other hand, Specimen KX-2 with joint reinforcement showed 30% higher strength than Specimen KX- 3 without joint reinforcement.

The other series of interior joint tests are shown in Fig. 4.10.[49] The specimens in this series modeled beam-column joints in high-rise buildings and had a transverse beam on one side of the joint. The specimens were detailed with different beam tensile reinforcement and joint lateral reinforcement.

The joint lateral reinforcement was fabricated with D10 bars having yield strength of 3760 to 3880 kgf/cm^2. Concrete strength ranged from 425 to 462 kgf/cm^2 and was approximately twice that in low-rise construction. All specimens failed in beam flexure and showed stable behavior in story shear-drift relations. Yielding of the lateral reinforcement was noted in the joint but the joint did not fail in shear. The measured joint shear stress exceeded the calculation using Kamimura's equation (Eq. 3), as shown in the table in Fig. 4.10.

The joint shear strengths measured in interior joint tests are plotted against the joint reinforcement index in Fig. 4.11.[42] The joint shear strength appears to increase with the joint reinforcement index. The AIJ equation (Eq. 2) covers most of the test results by changing the concrete term from 0.2 F_c to 0.4 F_c (F_c = concrete strength).

4.3.2 High Strength Reinforcement. High strength deformed bars for prestressing tendons, shown in Fig. 4.12, are sometimes used as lateral reinforcement in reinforced concrete members.[50] The bars, strengthened by ultrasonic-tempering, have nominal (0.2%-strain-offset) yield strength of 130 kgf/mm^2 and are approximately four times stronger than normal reinforcing bars. Hoops and spirals are fabricated with the high strength bars by cold bending and are used as shear reinforcement in RC members conforming to the specific design standard.[50]

Several seismic tests of RC members and frames with high strength shear reinforcement were conducted to develop high-rise construction systems. Figure 4.13 shows the test of beam-column joints reinforced with high strength hoops.[51,52] The D7.4 two-leg hoops were spaced at 70 mm in the interior joint and at 60 mm in the exterior joints. The joint reinforcement ratio was low, 0.2% in both cases. The yield strength of the joint hoops was 13,700 to 14,100 kgf/cm^2. Concrete strength was 379 to 408 kgf/cm^2. The interior specimen showed ductile behavior in the story shear-drift response. The joint shear distortion increased with loading cycles and contributed 35% of the story drift at the final stage. The maximum joint

Pt : tensile reinforcement ratio
Pw : lateral reinforcement ratio

因子 \ 試験体		NO.1	NO.2	NO.3	NO.4
Column	section	40×40cm			
	Pg	2.15% (12-D19)			
	Pt	0.78% (4-D19)			
	Pw	0.79% (4-D10@90)			
Beam	section	27.5×37.5cm			
	Pt	1.58% (2-D19+4-D16)	1.81% (2-D19+5-D16)	2.06% (2-D19+6-D16)	1.81% (2-D19+5-D16)
	Pw	1.03% (4-D10@100)		1.21% (4-D10@85)	1.03% (4-D10@100)
Joint	τD	88kg/cm²	100kg/cm²	113kg/cm²	100kg/cm²
	Pw	0.45% (2-D10@85.5)	0.77% (2-D10@42.5)	1.55% (4-D10@42.5)	1.55% (4-D10@42.5)
	hoop shape	フック付	フック付	フック付	溶接格子

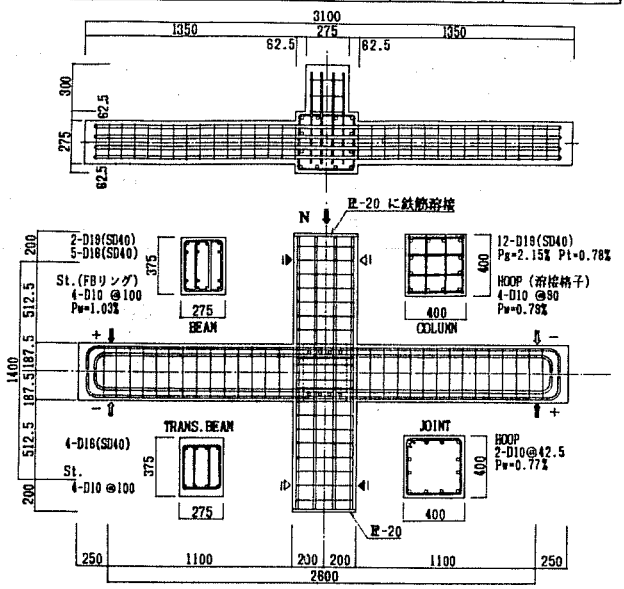

Specimen Details

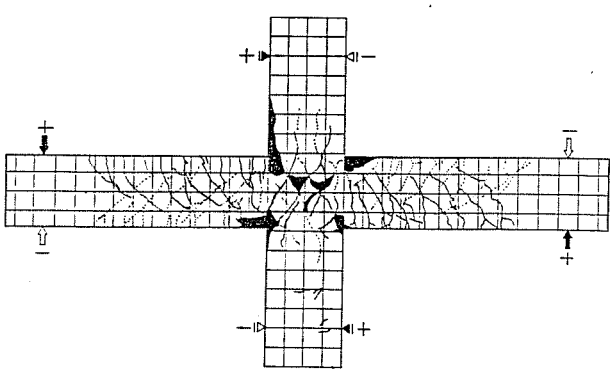

Final Crack Pattern (NO.2)

Joint Shear Stress

(kg/cm²)

	NO.1	NO.2	NO.3	NO.4
Test pτmax	106	120	141	123
Calculation pτu	104	110	124	125
pτmax / pτu	1.02	1.09	1.14	0.98

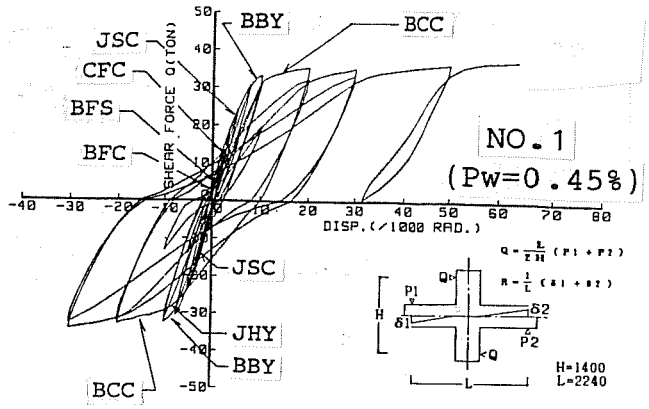

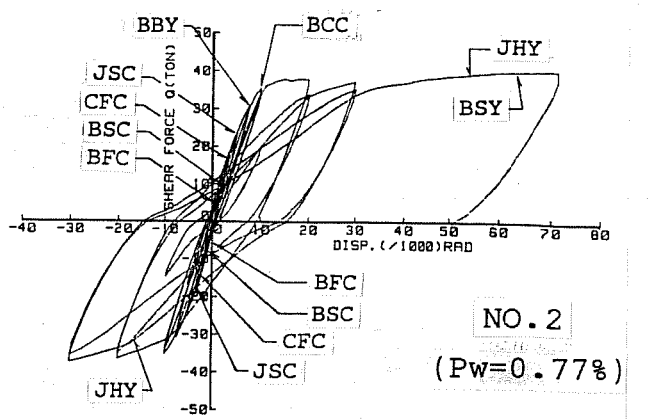

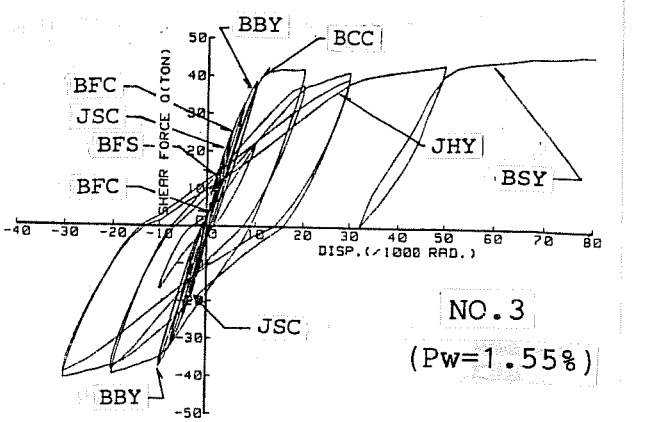

BFC : Beam Flexural Crack
BFS : Beam Flexural-Shear Crack
BSC : Beam Shear Crack
BCC : Beam Concrete Crushing
BBY : Beam Bar Yielding
BSY : Beam Stirrup Yielding
CFC : Column Flexural Crack
JSC : Joint Shear Crack
JHY : Joint Hoop Yielding

Story Shear-Drift Angle Relations

Fig. 4.10 Interior joints with various reinforcing details

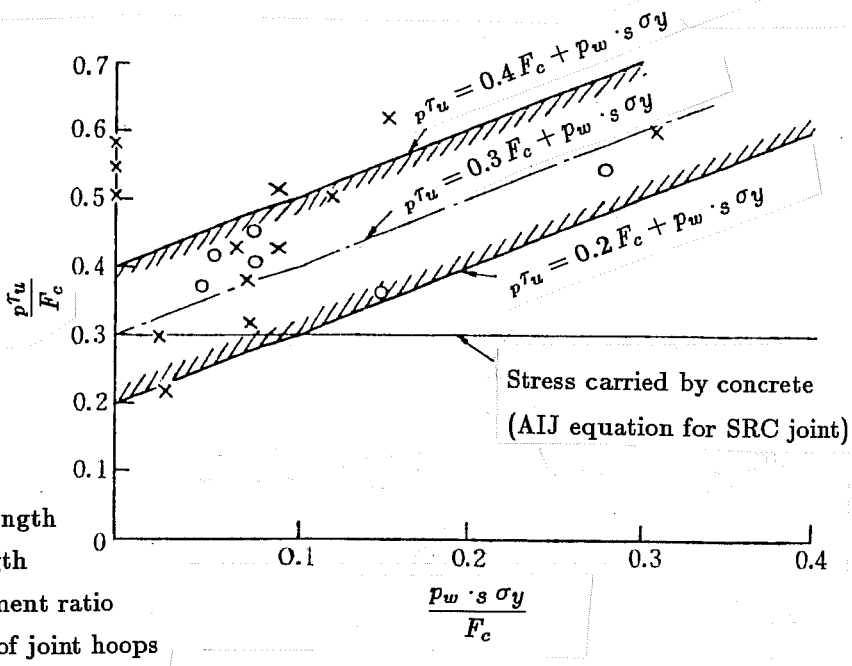

$_p\tau_u$: joint shear strength
F_c : concrete strength
p_w : joint reinforcement ratio
$_s\sigma_y$: yield strength of joint hoops

Fig. 4.11 Shear strength of interior joint

	D (mm)	D' (mm)	As (mm²)	N 本 図	W (kg/m)
SBPD 130 / 145 **	6.4	6.25	30	3 [a]	0.235
	7.4	7.25	40	3 [a]	0.315
	9.2	9.15	64	6 [b]	0.500
	11	11.10	90	6 [b]	0.710
	13	13.10	125	6 [b]	0.980

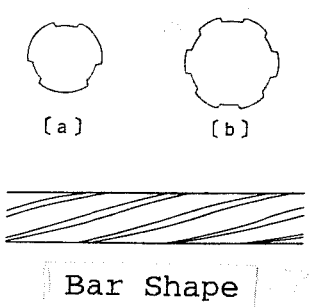

D : nominal diameter
D' : standard diameter
As : nominal sectional area
N : number of deformations
W : unit weight
** : nominal strength in kg/mm^2
(yield strength $\geq$ 130kg/mm^2
tensile strength $\geq$ 145kg/mm^2)

Fig. 4.12 High strength deformed bar

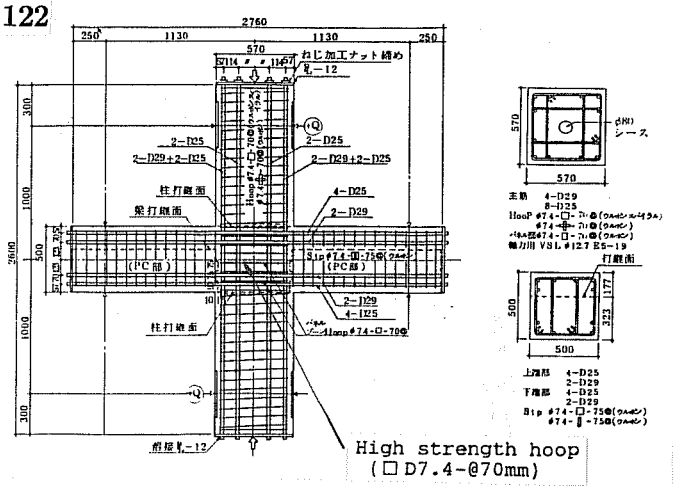

Interior Joint Specimen

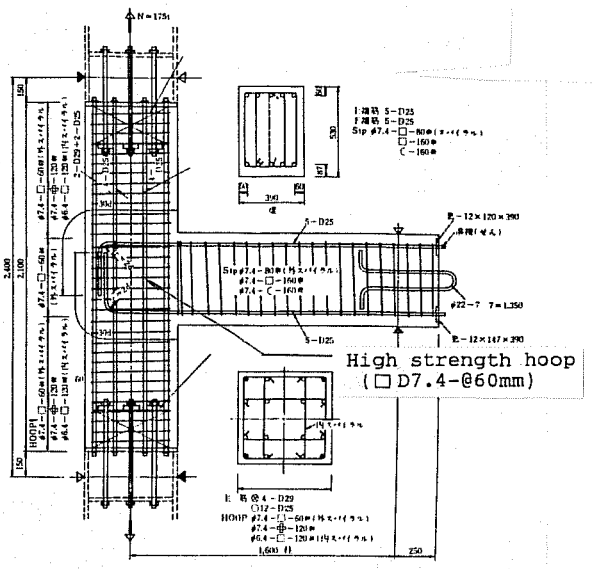

Exterior Joint Specimens
(Specimens BB-1 and BB-2)

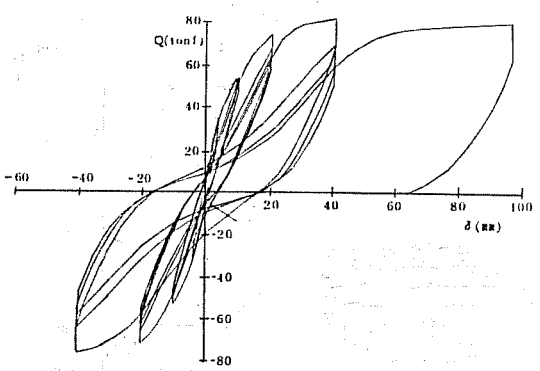

Story Shear-Drift Relation

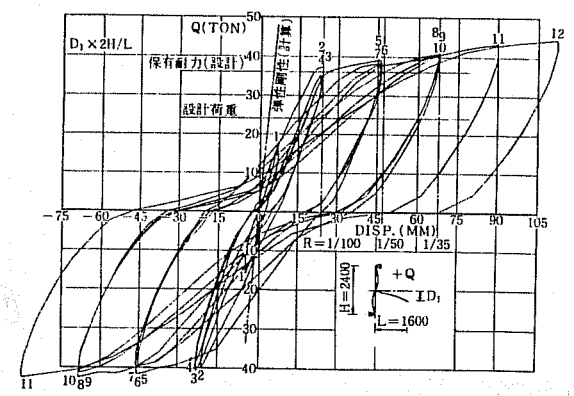

Load-Deflection Relation (BB-1)

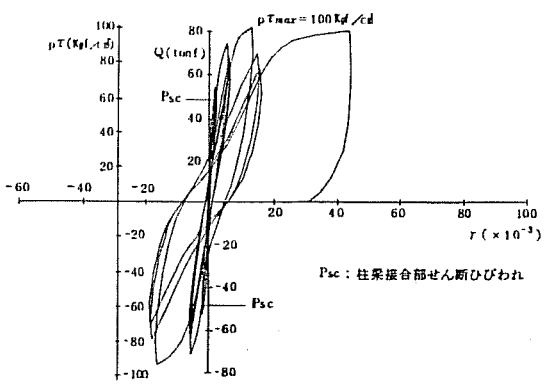

Story Shear-Joint Shear Distortion

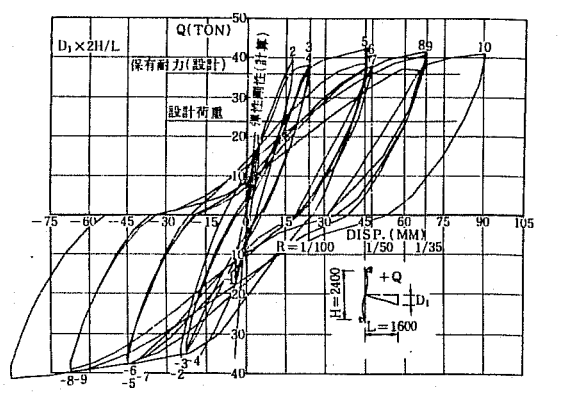

Load-Deflection Relation (BB-2)

Fig. 4.13 Test of joints with high strength reinforcement

shear stress was 100 kgf/cm^2 and a little lower than the calculated strength using Eq. 3. The two exterior joint specimens were tested under different axial loading conditions; i.e., axial tension for BB-1 and axial compression for BB-2. Both specimens failed in beam flexure and showed stable load-deflection relations. The axial tensile loading somewhat lowered the stiffness of Specimen BB-1, but no sign of joint distress was observed.

Figure 4.14 shows the test of an interior joint specimen in another series.[53] The specimen was a full-scale beam-column subassemblage having a transverse beam on one side of the joint. The joint was laterally reinforced with high strength D11 two-leg hoops spaced at 100 mm (lateral reinforcement ratio: $p_w = 0.2\%$). The yield strength of the hoops was 13,500 kgf/cm^2. The specimen modeled beam-column joints in high-rise buildings and was cast with high strength concrete (concrete strength: $F_c = 502$ kgf/cm^2). The story shear-drift angle relation showed deterioration in resistance because the specimen failed in joint shear after flexural yielding of beams. Although shell concrete spalled from the free side of the joint, the other side was confined by the transverse beam and underwent small shear distortion as shown in the figure. The joint hoops developed strains of more than 0.3% but did not reach the yield strain. The maximum joint shear stress was 118 kgf/cm^2 and exceeded the calculated value of 109 kgf/cm^2 (Eq. 3).

It should be noted that the joint of this specimen and Specimen No. 2 in Fig. 4.10 had the same value of $p_w \cdot f_{wy}$ (lateral reinforcement ratio times yield strength) and showed the same strengths. The smaller amount of high strength reinforcement appears to be as effective as the larger amount of normal strength reinforcement.

4.4 Bond Behavior of Longitudinal Reinforcement within Joint

4.4.1 Bond Behavior of Column Bars. Six interior joint specimens were tested to study the bond behavior of column longitudinal bars within the joint, as shown in Fig. 4.15.[54] Specimen J1 had standard details. Specimens J2 and J3 had a steel panel in the joint. Specimens J4 through J6 had a large joint resulting from deep or wide beams. All specimens showed inverse-S-shaped hysteresis in the load-deflection relations, because Specimens J1 and J3 failed in joint shear and the other specimens failed in bond along column bars within the joint. With bond failure (J2, J4, J5 and J6), larger strength deterioration was observed than with shear failure (J1 and J3). Although the column bars in Specimen J5 were greased to produce unbonded conditions, no great difference was observed in the behavior between Specimens J4 and J5 except that J5 showed a little lower strength than J4. The column moment capacity was calculated using a linear strain distribution along the section and the stress-strain relations shown in (i). The calculation took account of the bond stress along column bars as follows:

$$C_s \leq \tau_u \times \psi \times h_j - T \tag{11}$$

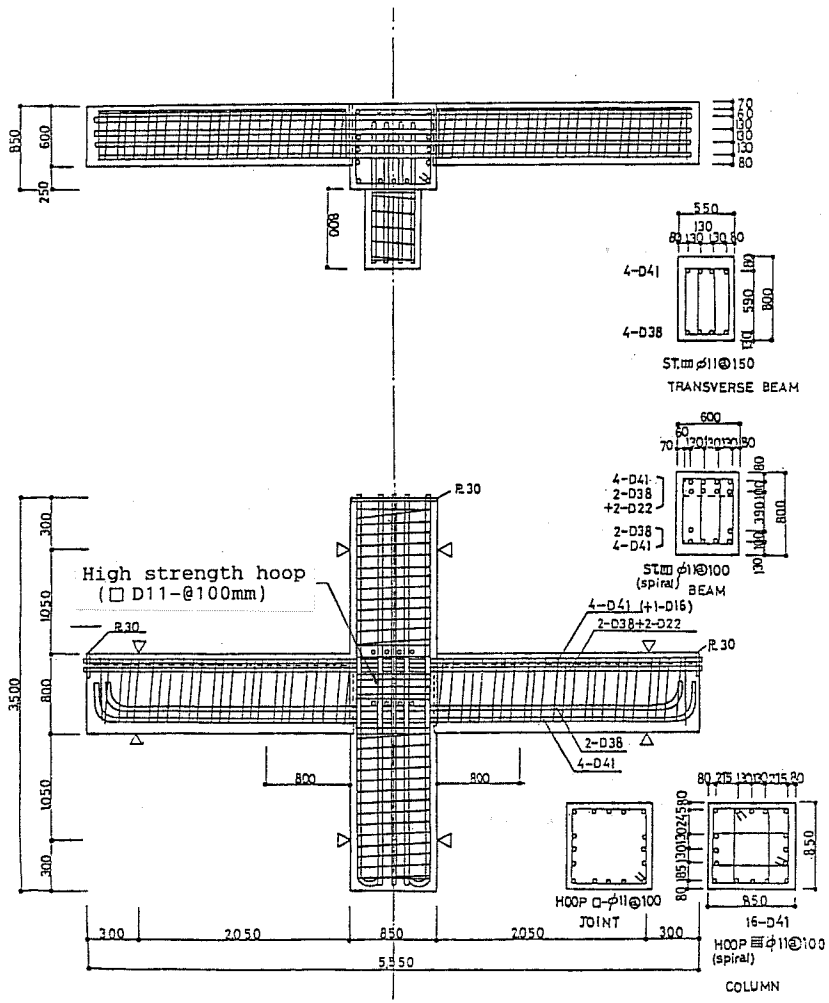

Specimen Details

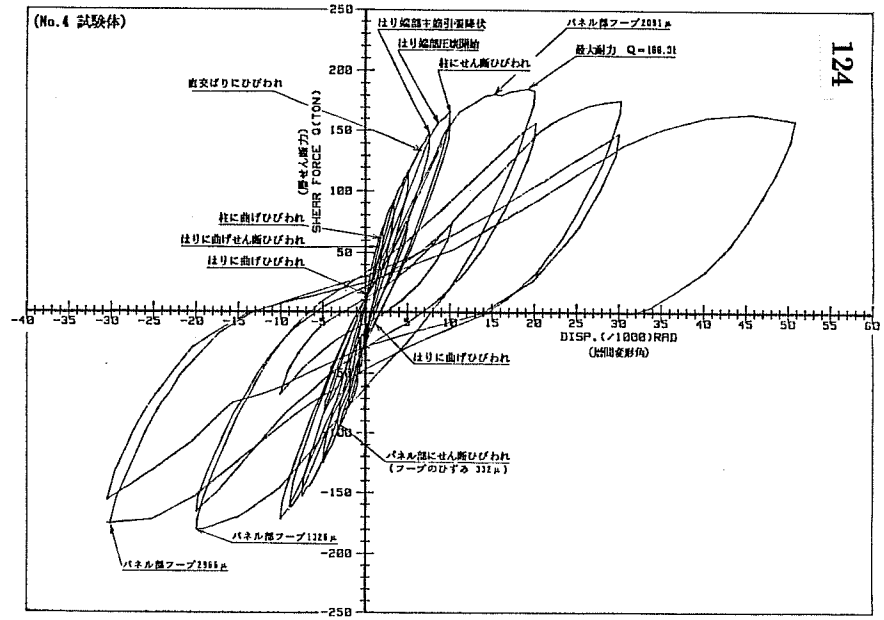

Story Shear-Drift Angle Relation

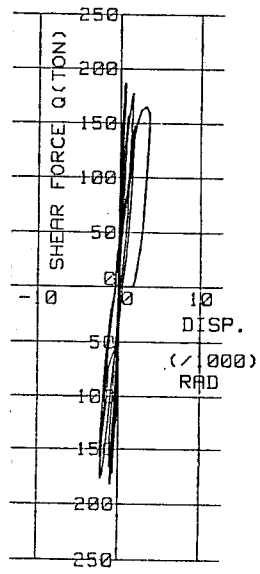

Joint Distortion

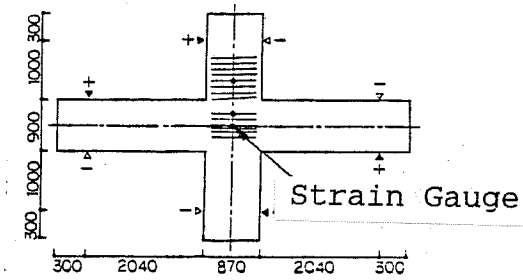

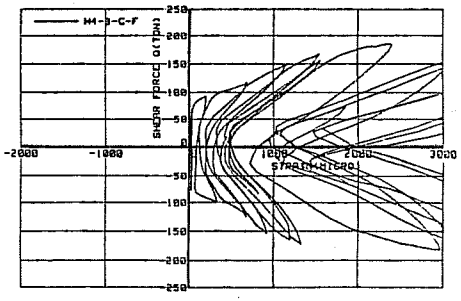

Joint Hoop Strain

Fig. 4.14 Test of interior joint with high strength reinforcement

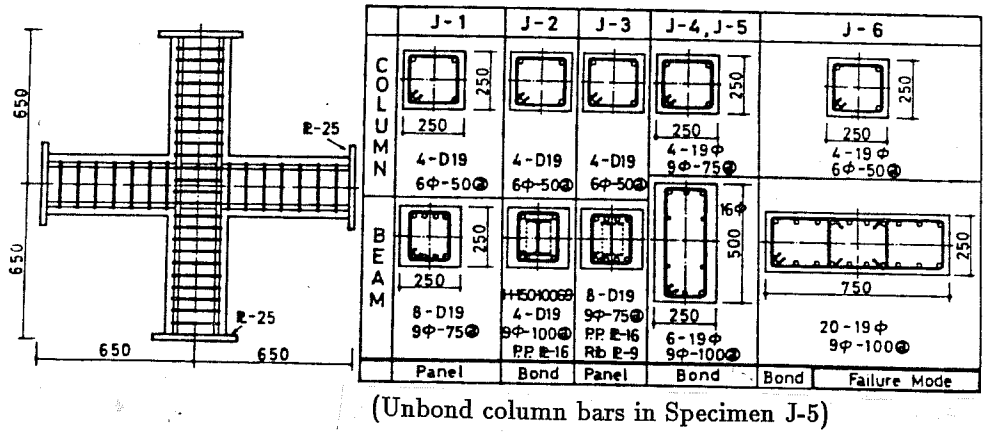

(Unbond column bars in Specimen J-5)

(a) Specimen details

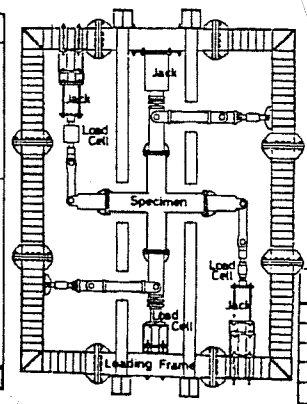

(b) Loading setup

(c) Materials concrete

Specimen	$_cσ_o$ (kg/cm²)	$_cε_o$ (%)
J-1	252	0.228
J-2	225	0.220
J-3	233	0.213
J-4	230	0.225
J-5	239	0.210
J-6	242	0.214

Steel

Steel	$_sσ_y$ (t/cm²)	$_sσ_u$ (t/cm²)	$_sε_u$ (%)
D19	3.351	5.168	24.1
19φ	3.099	4.601	28.8
16φ	2.935	4.333	31.0
9φ	3.362	4.591	31.3
6φ	2.964	4.250	29.7
H-150x100x6x9 Flange	3.006	4.485	24.1
H-150x100x6x9 Web	3.808	4.967	21.4
PL-16	2.739	4.278	28.0
PL-9	3.370	4.626	21.4

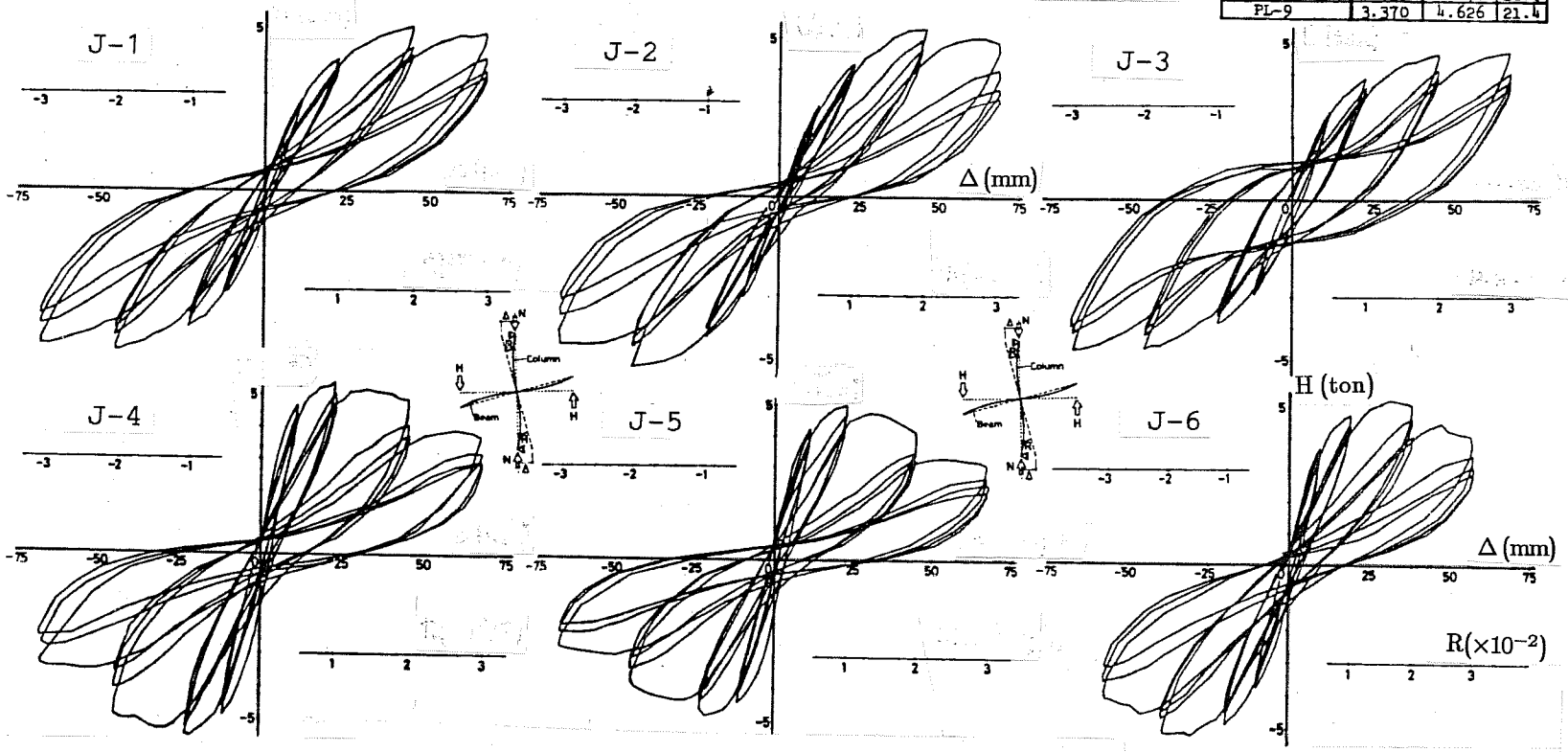

(d) Load-deflection relations

Fig. 4.15 Bond failure along column bars in interior joints

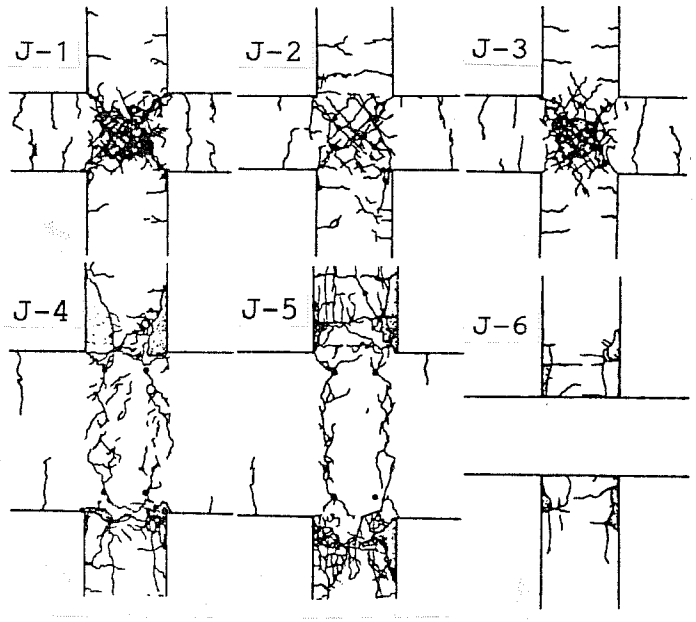

(e) Final crack patterns

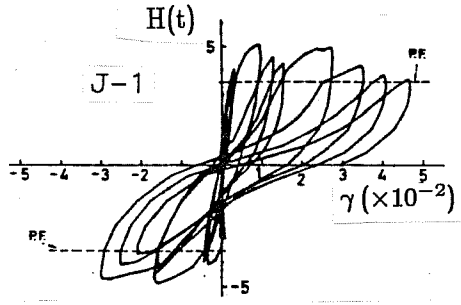

(f) Load-joint distortion

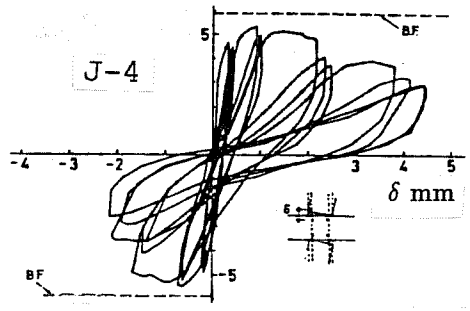

(g) Load-column bar slip

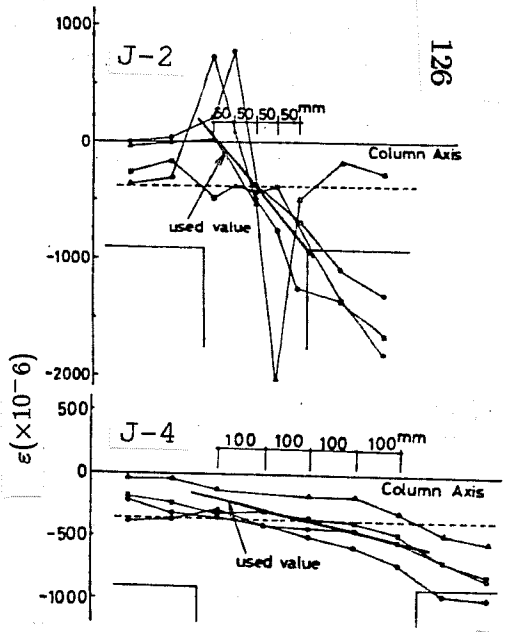

(h) Strains along column bars

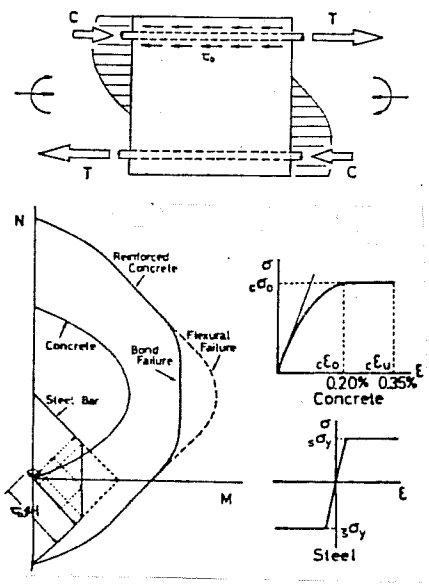

(i) Analytical model

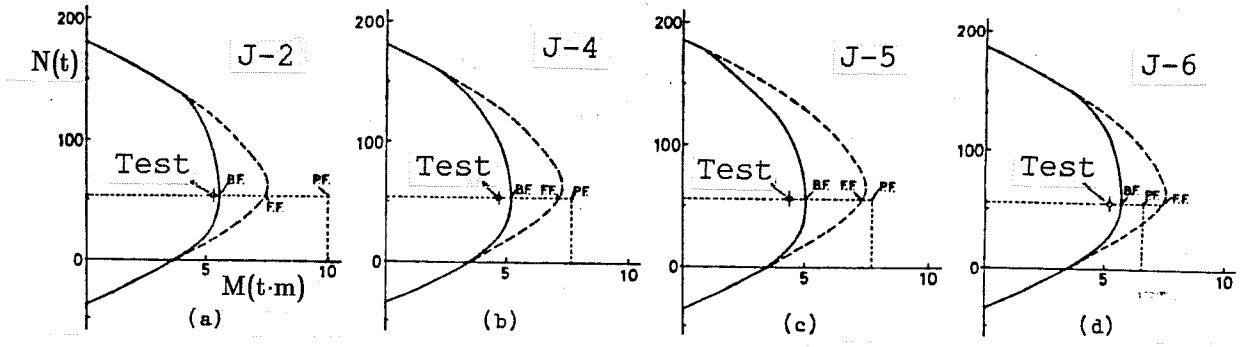

(j) Axial force-moment capacity relations

---- with perfect bond
—— with measured bond

(Fig. 4.15 Continued)

where

C_s = compressive force of a column bar at one end of the joint
T = tensile force of the bar at the other end of the joint
ψ = perimeter of the bar
h_j = joint depth (= beam depth)
τ_u = ultimate bond stress

The tensile force T was calculated from the same bending moment acting in the opposite direction. The compressive force C_s calculated from the strain distribution was reduced to the value of the right side of the above equation, if the average bond stress exceeded ultimate bond stress τ_u. The value of τ_u was determined from the strain measurements along column bars as shown in (h). The calculated moment capacities showed good agreement with the test results for the bond failure specimens as shown in (j).

4.4.2 Bond Behavior of Beam Bars. Several series of interior joint specimens were tested to study the bond behavior of beam longitudinal bars within the joint.

Figure 4.16 shows the tests of two full-scale interior joint specimens.[55] Specimen No. 1 had 60 cm deep beams with four D41 bars in tension and Specimen No. 2 had 55 cm deep beams with three D41 and two D32 bars in tension. The two specimens were designed to have the same beam moment capacity. For D41 beam bars, the column depth to bar diameter ratio was 19.5 and the bond index was 95 kgf/cm^2 (See Eq. 8). As shown in (b), the beam bars developed tensile strains at one end of the joint and compressive strains at the other end. Although the average measured bond stress exceeded the bond index value, no sign of bond failure was observed for the specimens. The load-deflection relations were stable as shown in (c). It should be noted that the joint of Specimen No. 1 with deeper beams had fewer shear cracks than Specimen No. 2, as shown in (d).

Figure 4.17 shows another series of interior joint tests.[10] As shown in (a), four full-scale specimens were reinforced with D51 longitudinal bars and D16 transverse bars and were cast with 300 kgf/cm^2 concrete. The beam bar development length within the joint was 13 times the bar diameter and the beam bar bond index was 158 kgf/cm^2. Specimen No. 1 with two D51 beam bars failed in beam flexure and showed a stable load-deflection relation. On the contrary, the other specimens with three D51 beam bars failed in joint shear and showed considerable deterioration in resistance. The joint of Specimens No. 2 through No. 4 underwent large shear distortions as shown in (c). Bar slip measurements are shown in (d). Large bar slip occurred in the joint and caused large rotations at beam ends. It should be noted that the pull-out deformations were generally smaller than the push-in deformations. This is probably because the flexural cracks penetrated into the joint and the concrete slid with pull-out of the bars. Strain distributions along beam bars are shown in (e). The compressive strains at the

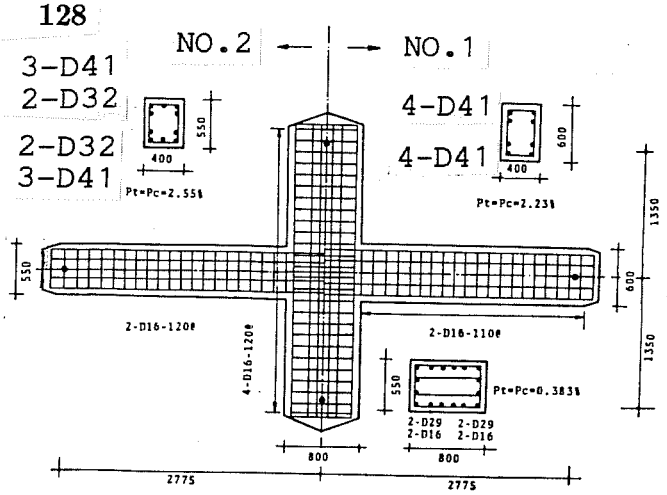

(a) Specimen Details

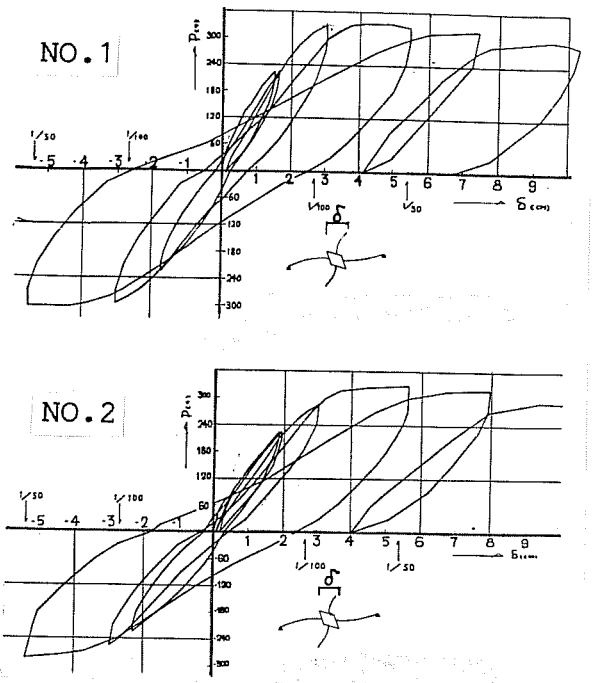

(c) Load-Deflection Relations

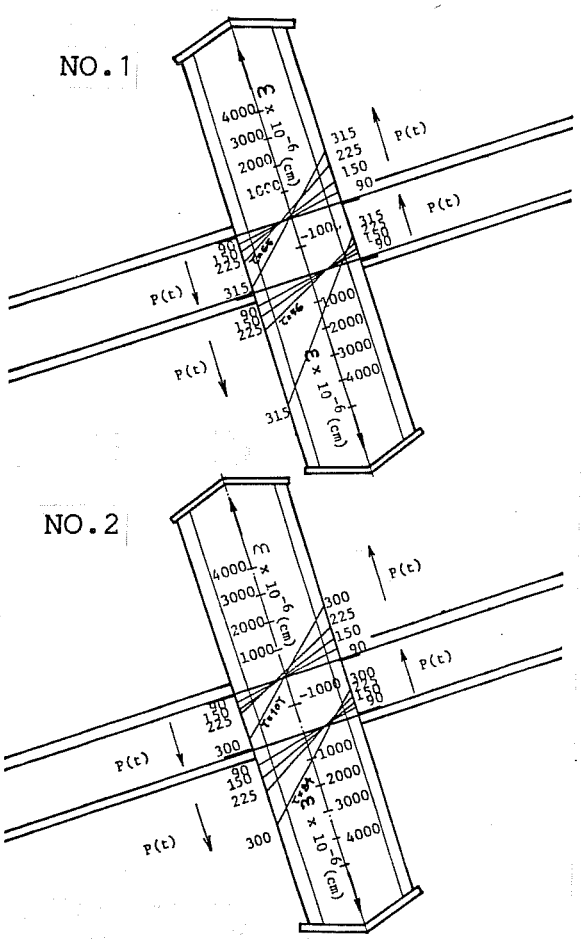

(b) Beam Bar Strains

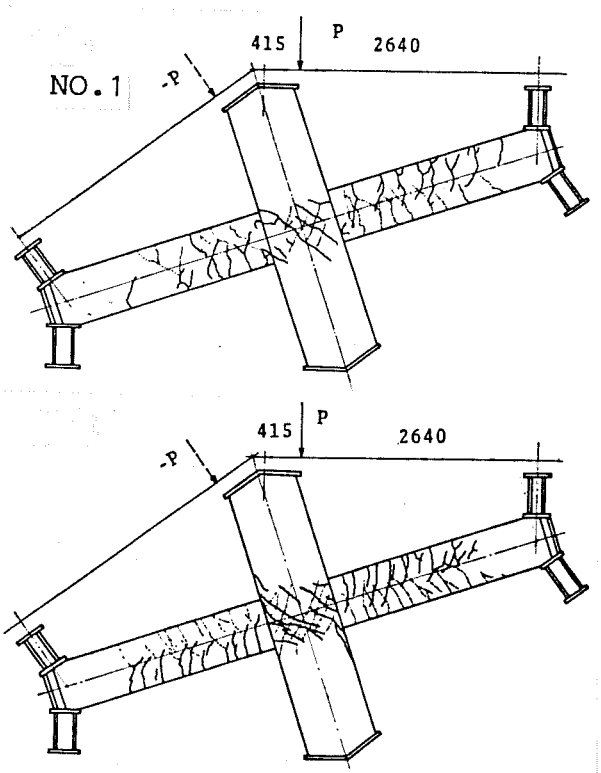

(d) Crack Patterns at Design Load

Fig. 4.16 Test of interior joints with D41 beam bars

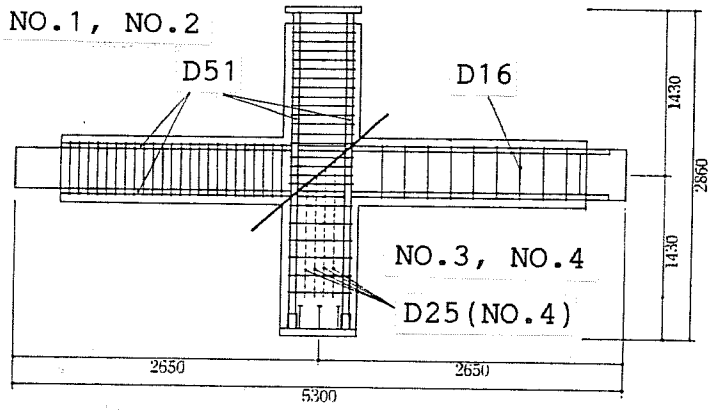

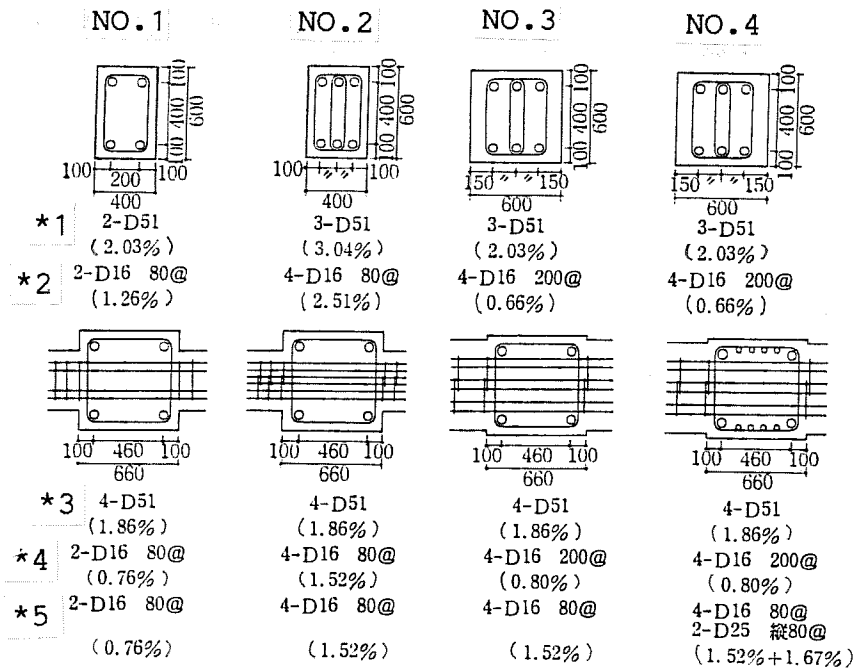

(a) Specimens

*1 : beam tensile bars
*2 : beam stirrups
*3 : column longitudinal bars
*4 : column hoops
*5 : joint hoops
( ) : reinforcement ratio

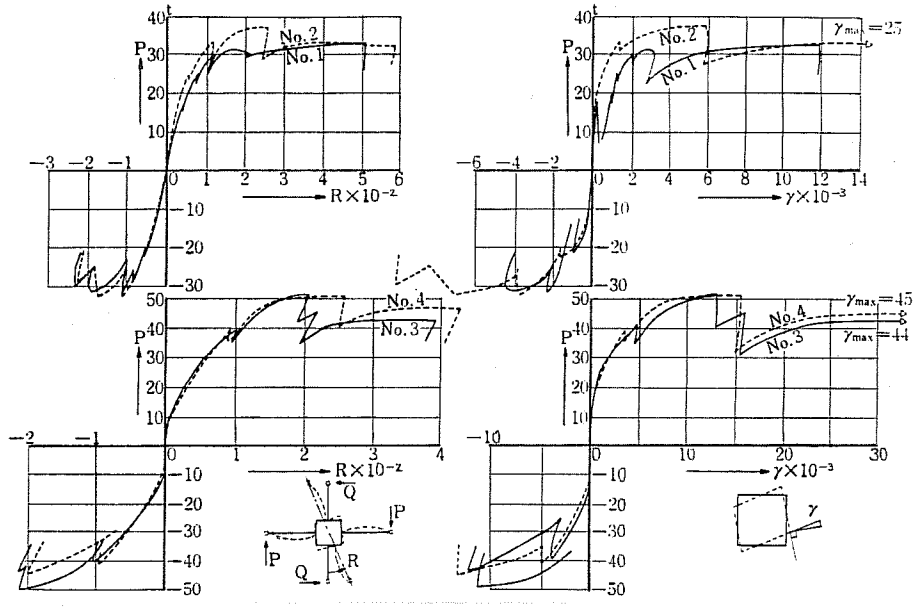

(b) Load-Drift Angle (c) Load-Joint Distortion

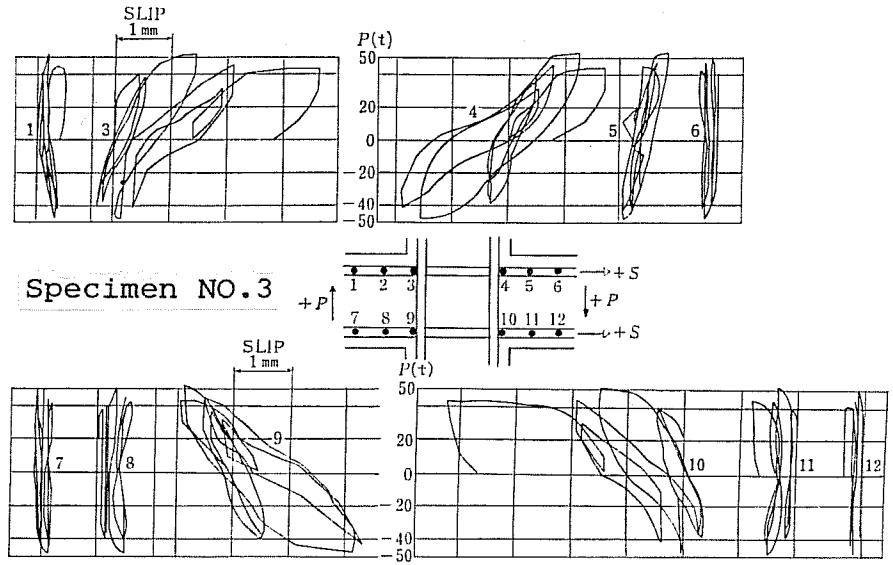

(d) Load-Beam Bar Slip

Fig. 4.17 Test of interior joints with D51 beam bars

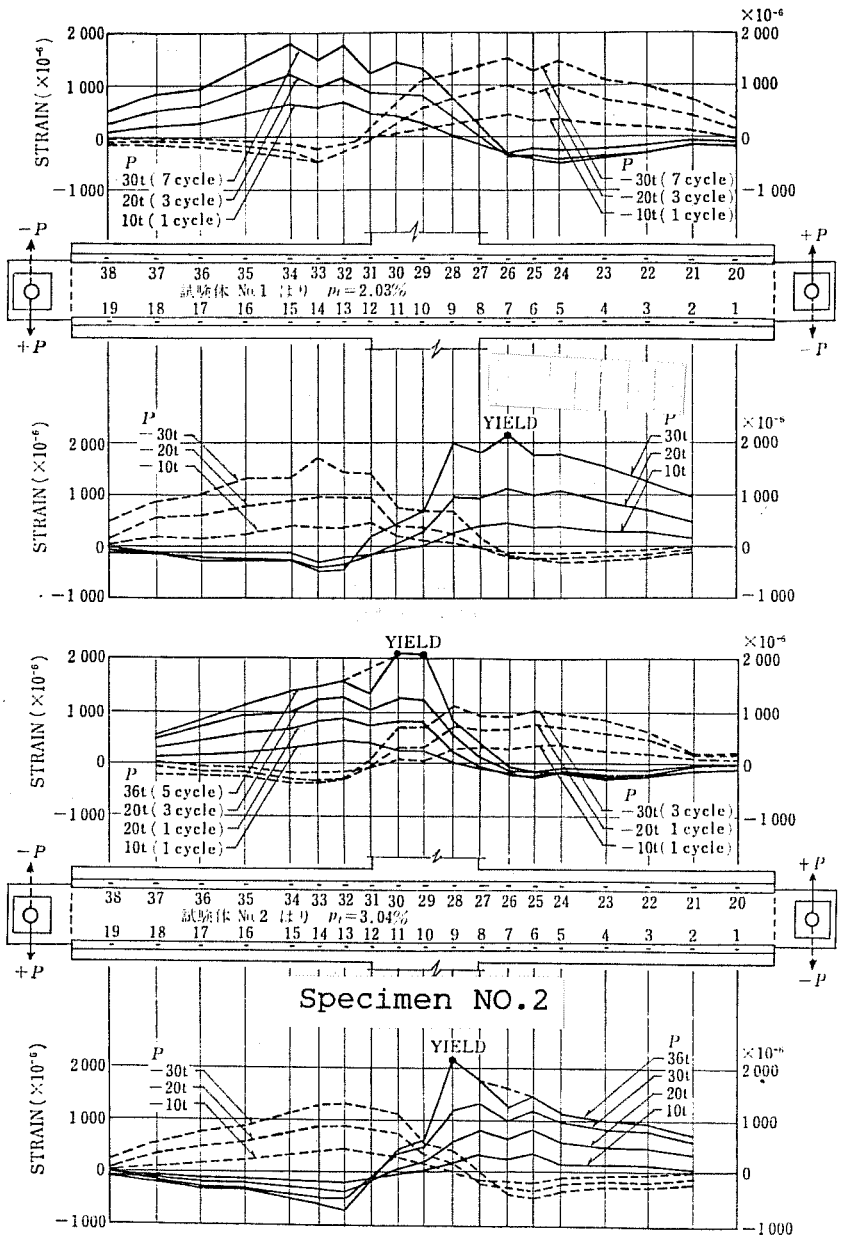

(e) Beam Bar Strains

(Fig. 4.17 Continued)

end of the joint decreased and were in tension as the load increased. According to the strain measurements, the average bond stress reached 70 kgf/cm^2.

Four interior joint specimens with various ratios of column depth to beam bar diameter are shown in Fig. 4.18.[40,56] Specimen 0 with a column depth of $37.5d_b$ (d_b = beam bar diameter) showed good spindle-shaped hysteresis without deterioration. As the column depth decreased from $37.5d_b$ to $19d_b$, the hysteresis loops became pinched. Particularly, Specimen E with the column depth of $14d_b$ failed in joint shear and showed large deterioration in the resistance as well as slip- type hysteresis.

4.5 Special Detailing

4.5.1 Ring Plate Reinforcement. Six interior and one exterior specimen were tested to study the behavior of a joint reinforced with steel ring plates, as shown in Fig. 4.19.[57] The specimens modeled beam-column joints in high-rise buildings where heavily reinforced rectangular beams frame into octagonal columns. The joint of the specimens was laterally reinforced with steel ring plates 9 mm thick except Specimen No. 1, which was provided with a spiral as joint lateral reinforcement. Specimens No. 5 and No. 6 had a larger joint volume as a result of an enlarged column capital, called a horizontal haunch. Specimen No. 7 modeled an exterior joint. Load-deflection relations are shown in (b). Specimen No. 1 with spiral reinforcement failed in beam flexure, but bond deterioration occurred along beam bars within the joint and caused the slip-type hysteresis. The other specimens with the ring plate reinforcement showed better hysteretic behavior than Specimen No. 1. However, the resistance of those specimens deteriorated at a large deflection because of shear failure in the joint (No. 4) or in the beams (No. 2, 3, 5 through 7). Note that the middle ring plate in No. 4 had half the depth of the others.

4.5.2 U-Shaped Bar Anchorage. The U-shaped bar anchorage is one of the methods for developing beam longitudinal bars within a joint. In this method, the top reinforcement is developed continuously into the bottom by bending in a U-shape so that the anchorage causes less congestion of the reinforcement in the joint than ordinary 90° hook anchorage.

Three full-scale specimens were tested to study the behavior of interior joints with U-shaped beam bar anchorages, as shown in Fig. 4.20.[58] The specimens modeled beam-column joints in high-rise buildings where precast concrete beams frame into columns with cast-in-place concrete in the joint. The beam bars were partially restrained by the precast concrete and subject to undesirable stresses by splices or gas pressure welding in the joint. Therefore U-shaped anchorages were used in the interior joints. As shown in (b), Specimens No. 1 and No. 2 had U-shaped anchorages with different embedment lengths and Specimen No. 3 had beam bars passing straight through the joint. All specimens developed flexural yielding

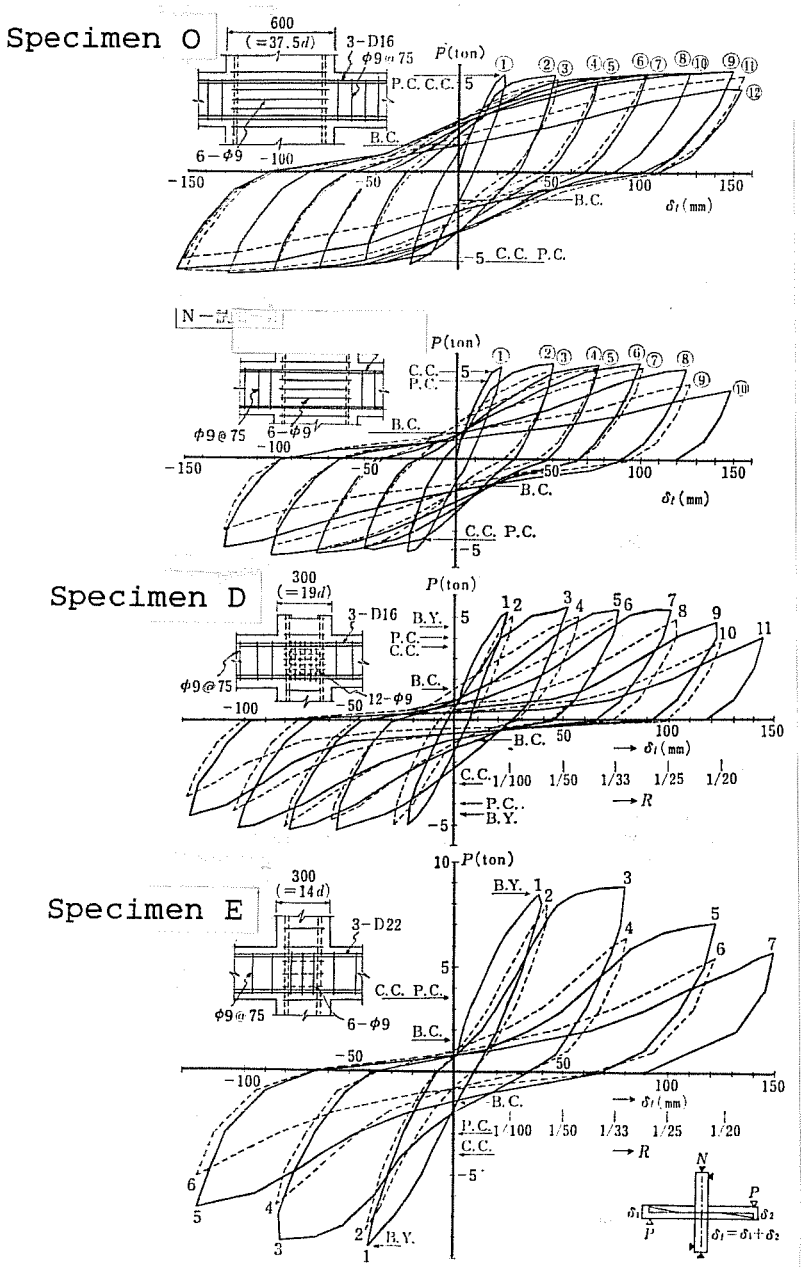

Fig. 4.18 Behavior of interior joints with various column depths

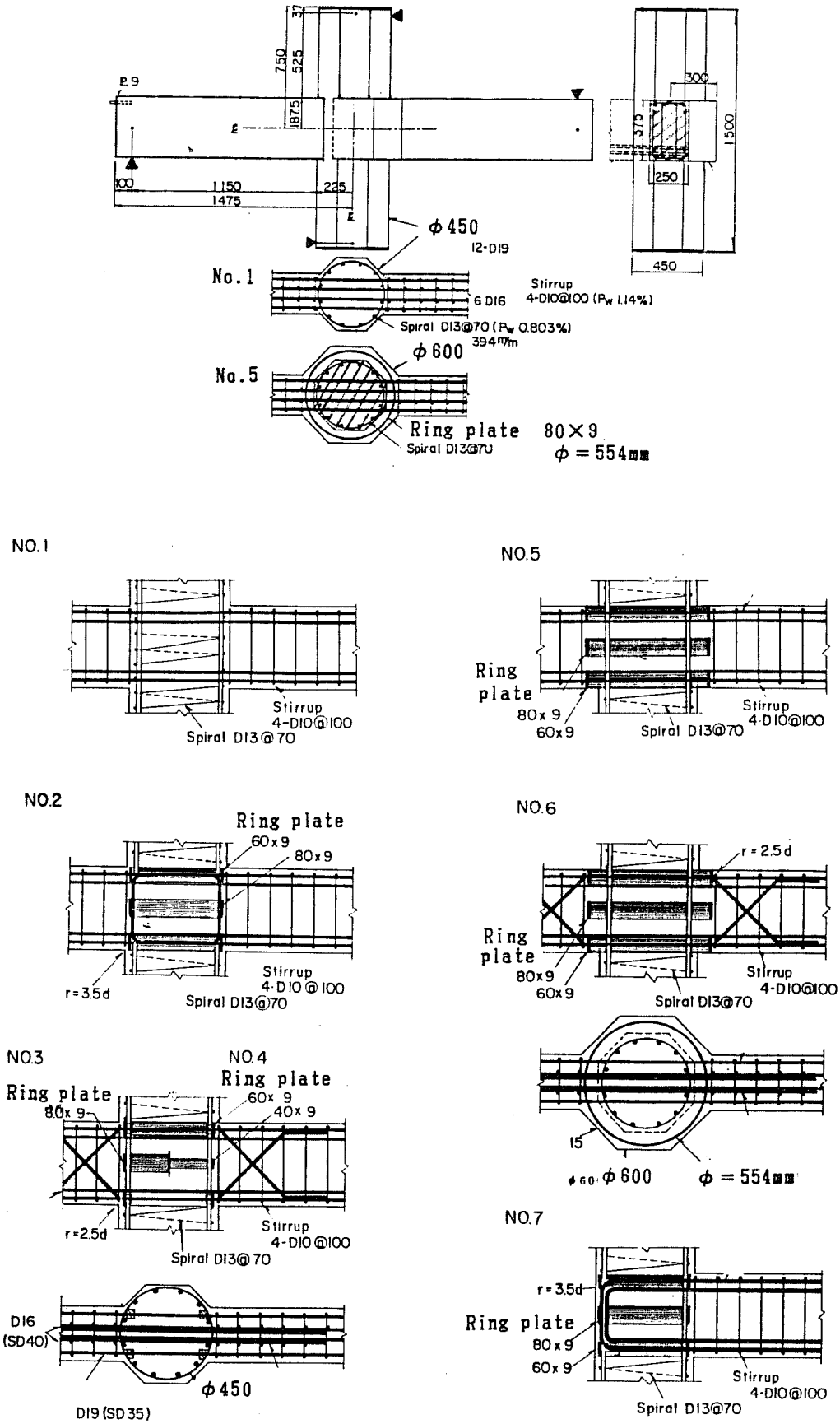

(a) Specimen details

Fig. 4.19 Test of interior joint reinforced with ring plates

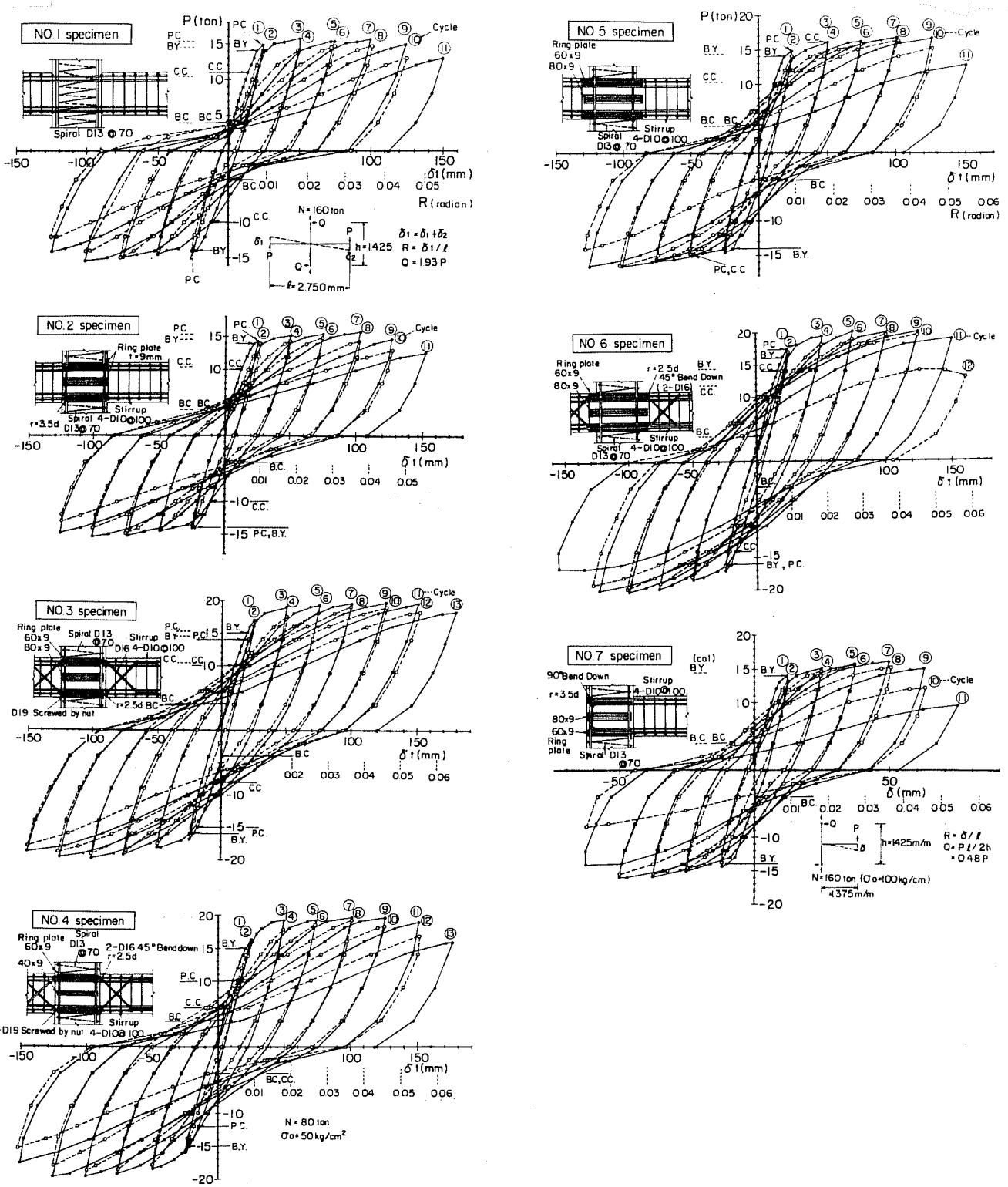

(b) Load-deflection relations

(Fig. 4.19 Continued)

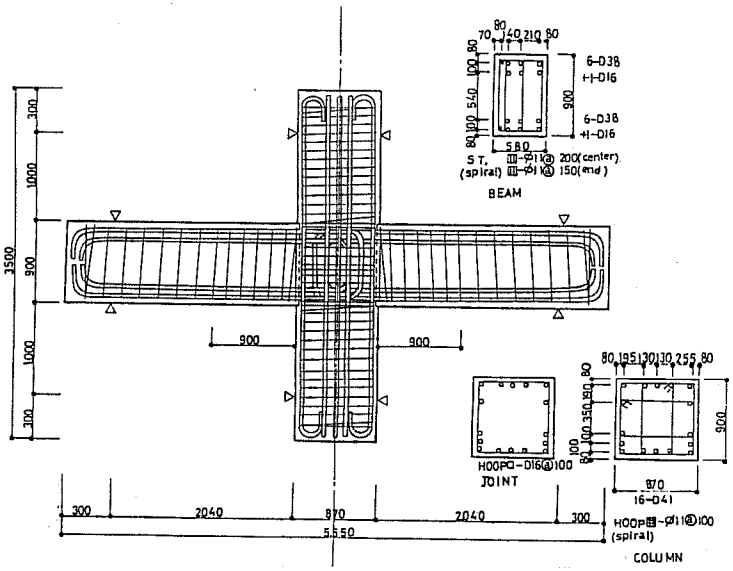

(a) Specimen details (No. 1)

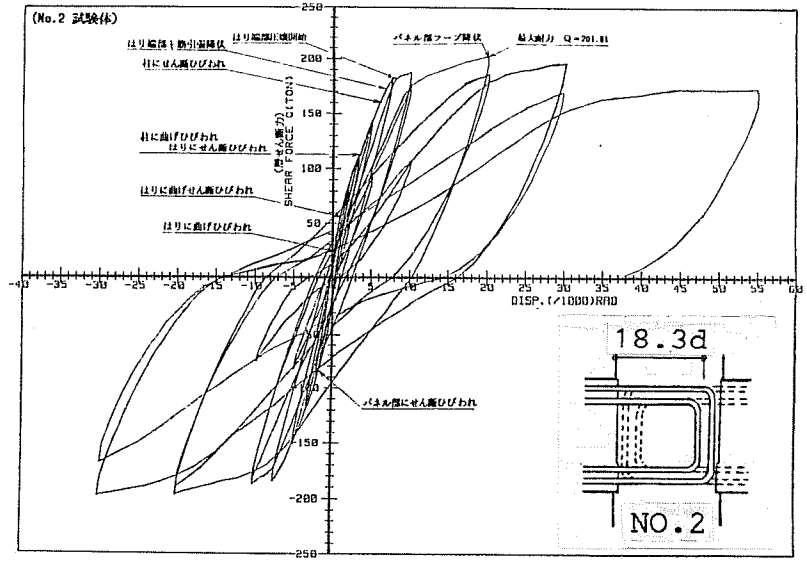

(d : beam bar diameter)

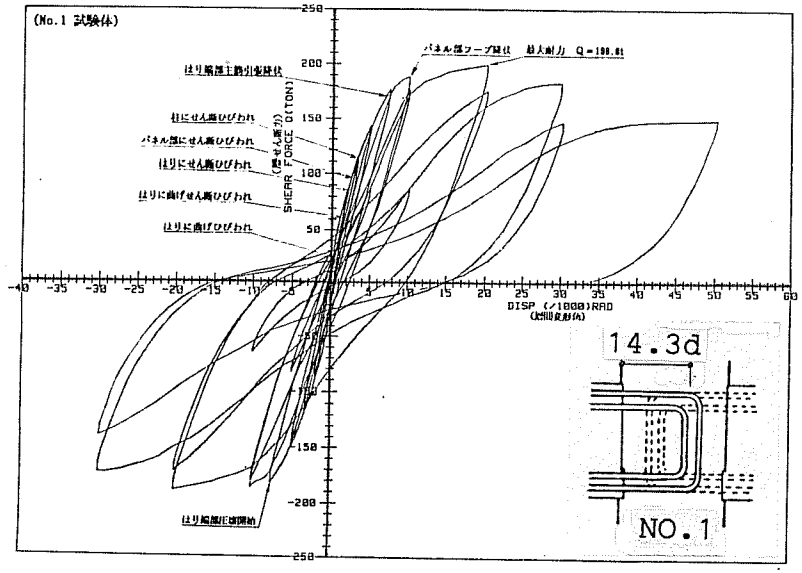

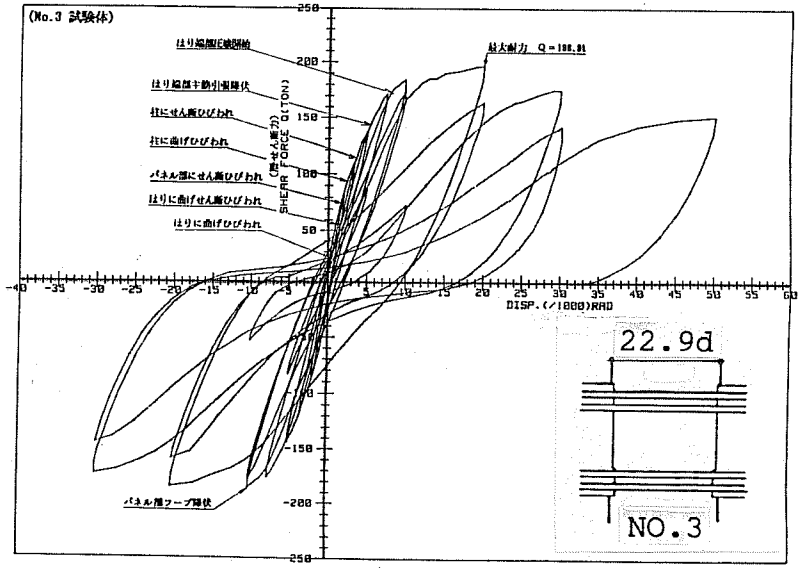

(b) Story shear-drift angle relations

Fig. 4.20 Test of interior joints with U-shaped bar anchorage

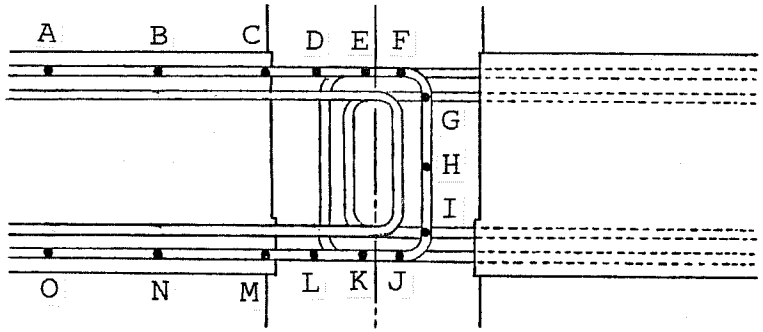

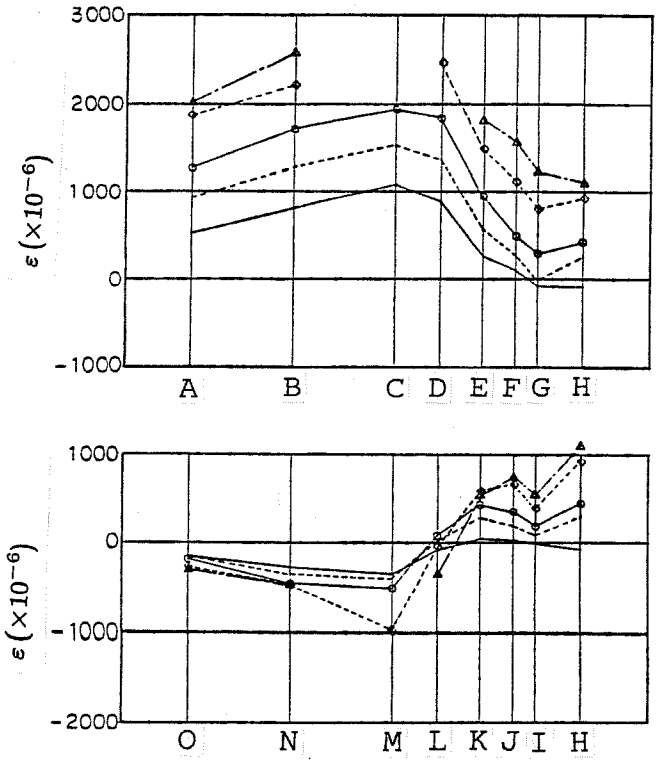

Specimen NO.1

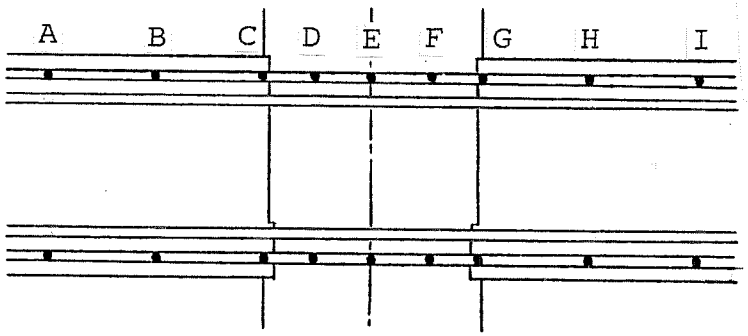

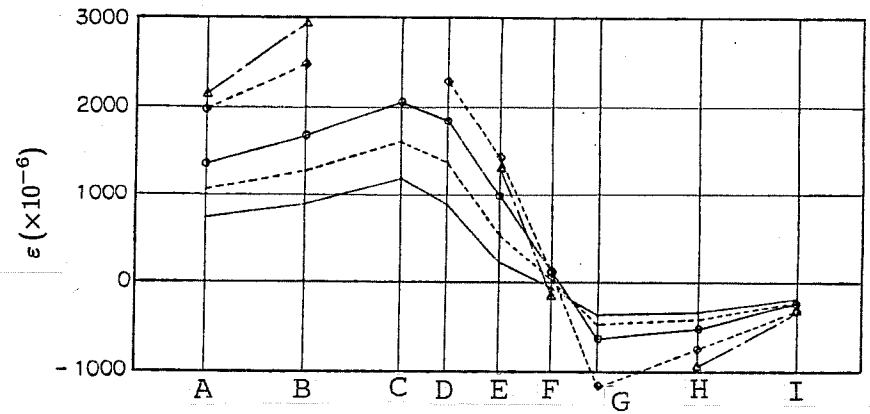

Specimen NO.3

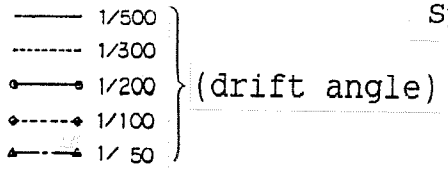

(c) Strain distributions along beam bars

(Fig. 4.20 Continued)

of the beams but failed in joint shear at the final stage. Specimen No. 2, having U-shaped anchorage with longer embedment, showed better hysteretic behavior and less deterioration in resistance than any other specimen. Specimen No. 1 with the U-shaped $14d_b$ embedment (d_b = bar diameter) and Specimen No. 3 with the straight development of $23d_b$ were just about equal in terms of story shear-drift angle relations. Beam bar strains are shown in (c). For Specimen No. 1, the tensile strains at the top decreased through the U-shaped anchorage and compression was measured in the bottom bars. The same behavior was observed for the strain distributions along the straight bar development of Specimen No. 3.

Another full-scale specimen was tested to study the behavior of an exterior joint with the U-shaped bar anchorage as shown in Fig. 4.21.[59] The specimen had a slab and transverse beams on both sides of the joint. The longitudinal beam was reinforced with double layers of tensile reinforcement terminating in the U-shaped anchorage. The specimen failed in beam flexure and showed ductile and stable behavior as shown in (b). The measured load exceeded calculated beam moment capacity and showed no deterioration even at 5% drift. The U-shaped anchorage worked efficiently, as seen in the strain distributions in (c). The compressive strains increased with the load and showed no sign of bond deterioration.

Figure 4.22 shows a series of exterior joint tests with U-shaped bar anchorages.[60] The beam and column dimensions shown in (a) were common to all specimens but the beam bar size varied from D22 to D35 as shown in (b). The beam bars terminated in the U-shaped anchorage and the ratio of straight embedment length to bar diameter changed from 7.9 to 16.5 with bar size. All specimens had transverse beams on both sides of the joint. One of the six specimens was cast with light-weight concrete and the others with normal-weight concrete of 210 kgf/cm^2 in design strength. All specimens failed in beam flexure and showed ductile behavior as shown in (c). However, the specimen cast with light-weight concrete showed large deterioration in resistance. It should be noted that there was no great difference in behavior between Specimen N22A with $16.5d_b$ embedment and N35A with $7.9d_b$ embedment.

4.5.3 Steel Anchor Plate. The steel anchor plate is a special anchorage for beam longitudinal bars terminating in a joint. The anchor plate is arc-welded to the end of the bar and resists pull-out of the bar. A series of exterior joint specimens were tested to study the behavior of the plate anchorage as shown in Fig. 4.23.[61] The specimens had one longitudinal beam and two short transverse beams. The beam bars in the longitudinal direction were anchored in the joint with 90° bent-down hooks for Specimen S16 and with the steel anchor plates for the other specimens. The anchor plate was welded to the end of the bar with an embedment length of 215 mm. The main variables are tabulated in (b). The anchor plates were 6 to 12 mm thick and 23 to 36 mm in diameter. As shown in (c), Specimen S6 with the bent-down bar anchorage showed lower strength and less ductility in negative loading (bottom bars in tension) than in positive loading, although the specimens with the plate anchorage showed

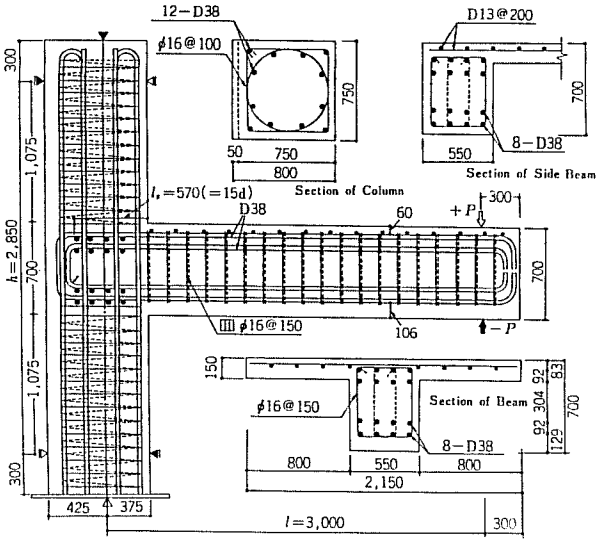

(a) Specimen Details

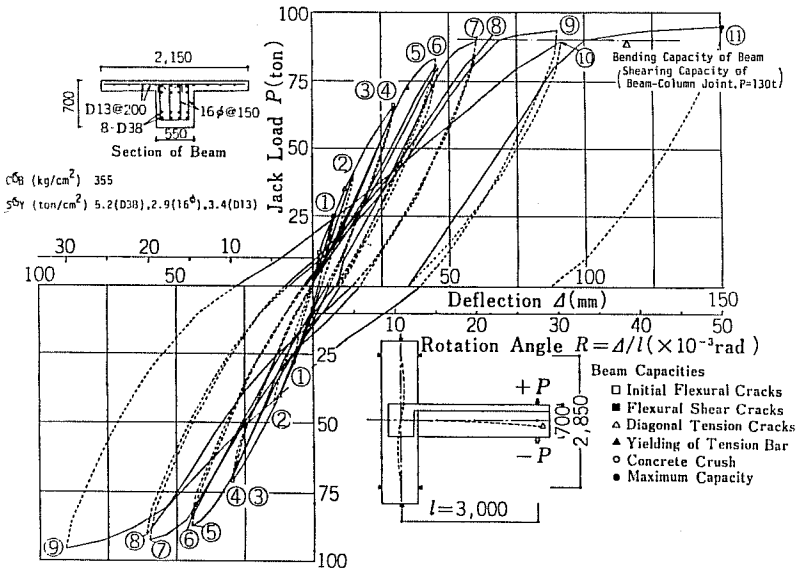

(b) Load-Deflection Relation

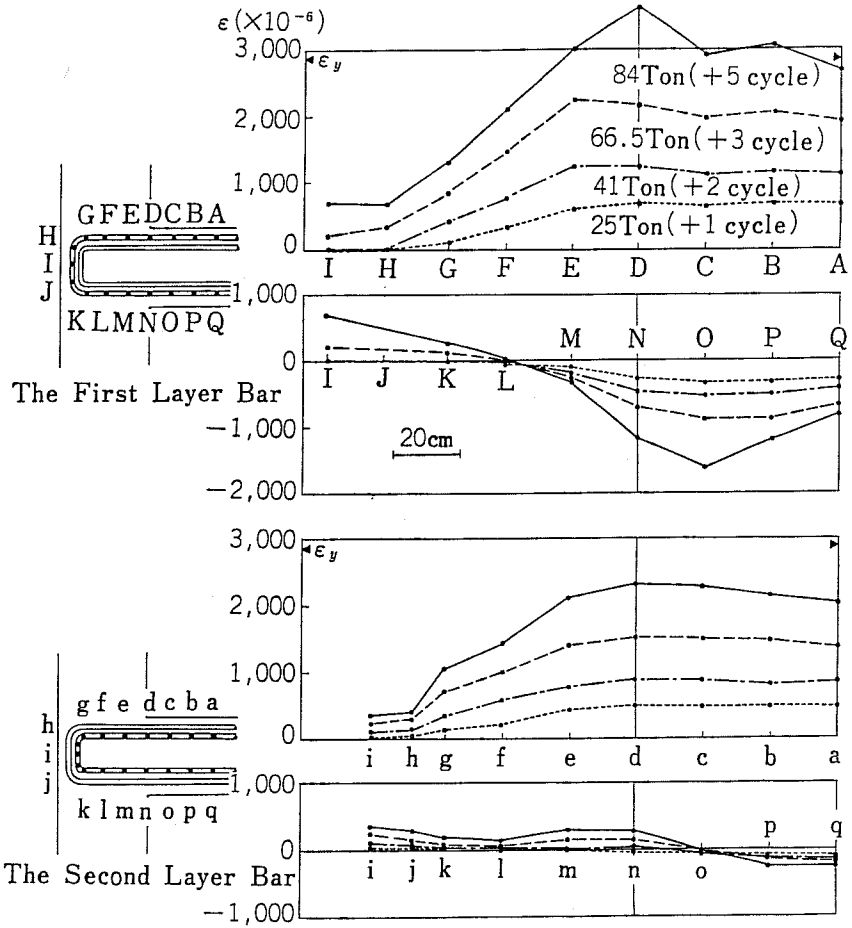

(c) Strain Distributions along Beam Bars

Fig. 4.21 Test of exterior joint with U-shaped bar anchorage

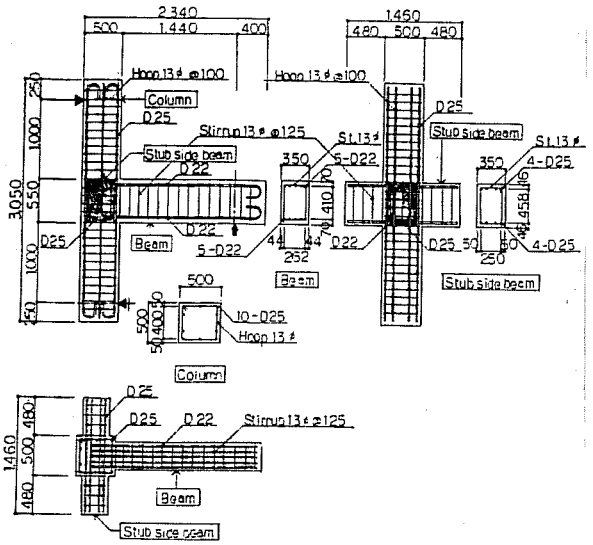

(a) Specimen Details (N22B)

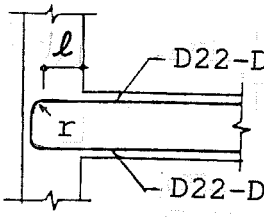

r=3d (D22,D25)

r=4d (D29,D35)

ℓ : straight embedment length

r : radius of bend

d : beam bar diameter

(b) U-shaped Bar Anchorage

(light-weight concrete specimen)

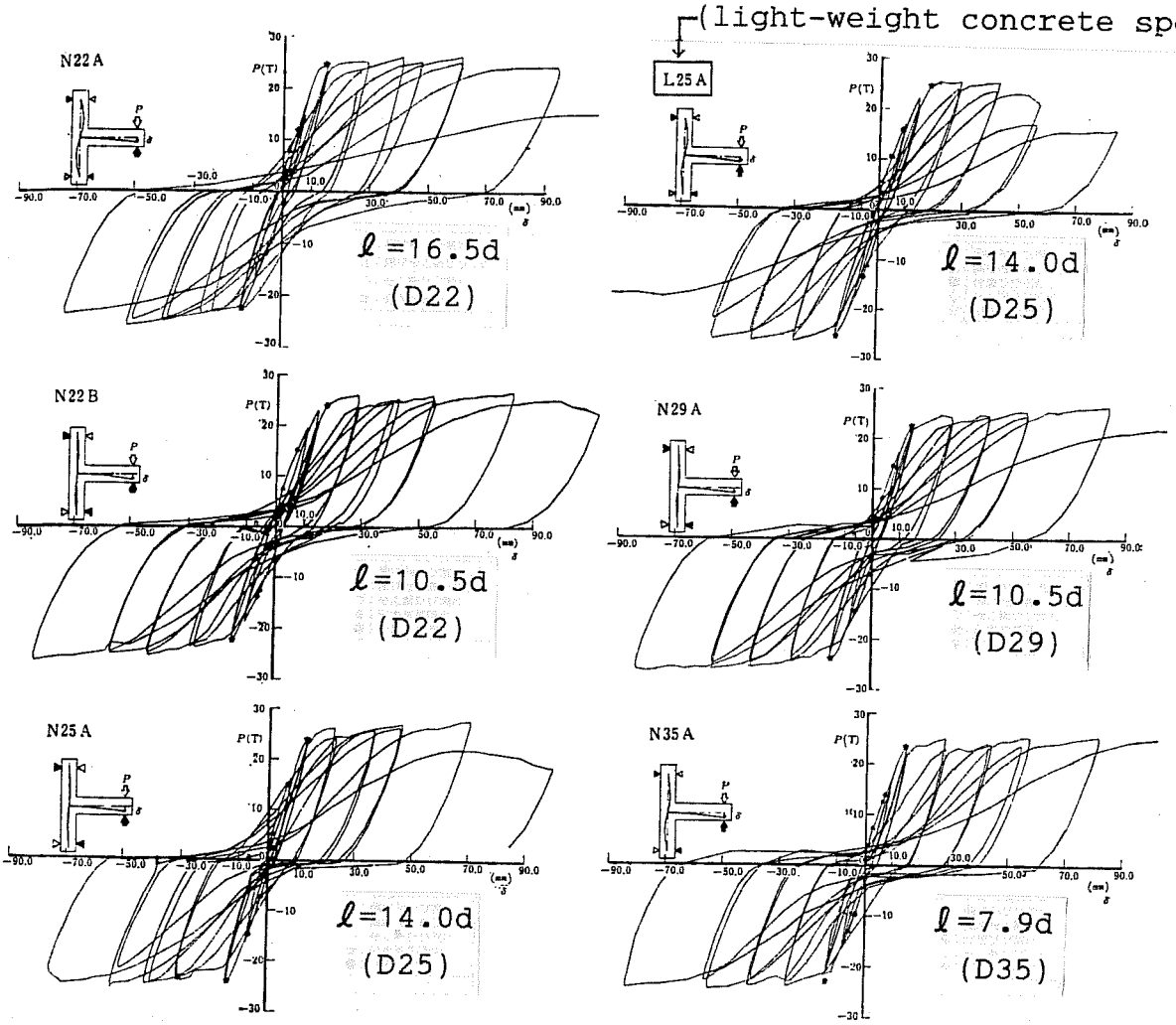

(c) Load-deflection relations

Fig. 4.22 Test of exterior joints with U-shaped bar anchorage

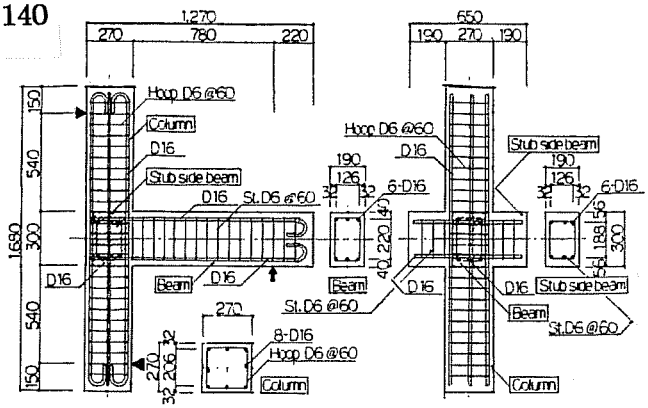

(a) Specimen Details (4P16)

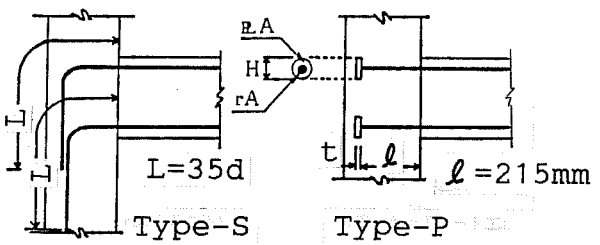

試験体名称	(1) d (mm)	(1) N	(1) Pt (%)	(2) n (ℓ/d)	(3) n_0 (rA/rA)	(3) H (mm)	(3) t (mm)
S16	D16	3	1.21	—			
4P16				13.4	4	36	12
2P16						28	9
2P19	D19	2	1.16	11.3	2	33	
2P13	D13	5	1.29	16.5		23	6

(1) Beam tensile bars

d : nominal bar diameter
N : number of bars
Pt : reinforcement ratio

(2) Straight embedment

n : ratio of ℓ to d
ℓ : embedment length

(3) Anchor plate

n_0 : ratio of ₨A to rA
₨A : area of anchor plate
rA : sectional area of bar
H : diameter of anchor plate
t : plate thickness

(b) Specimen Variations

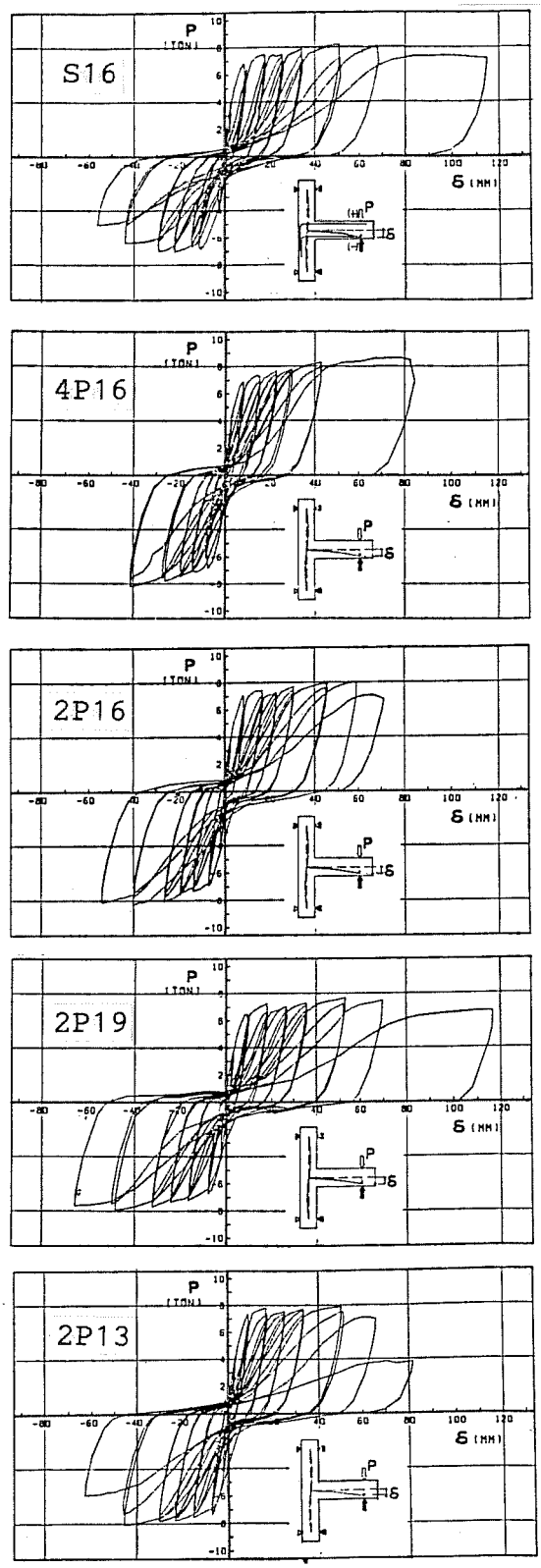

(c) Load-Deflection Relations

Fig. 4.23 Test of exterior joints with steel anchor plate

the same behavior in the two directions. The beam bars of Specimen 2P13 buckled at a large deflection and caused considerable deterioration in the resistance. The other specimens showed stable and ductile behavior in the load-deflection relations. Particularly, Specimen 4P16 with thick, large plates showed no deterioration in the resistance, even at 9% drift.

Figure 4.24 shows two interior joint test specimens with steel anchor plates welded to the beam bars.[56] The specimens showed slip-type hysteresis in the load-deflection relations because of bond deterioration along beam bars within the joint. The anchor plate was not effective in preventing pull-out of the bars from the joint because plastic strains resulted in elongation of the bars within the joint.

4.5.4 Various Details. Five interior joint specimens with various reinforcing details were tested as shown in Fig. 4.25.[40] Specimen A had standard details in which the joint was laterally reinforced with closely spaced hoops. Specimens B through E were reinforced horizontally with hoops and vertically with stirrups as in the beams. The stirrups of Specimen B were welded to the beam bars within the joint. The beam bars of Specimen C were partly strengthened by ultrasonic-tempering and were expected to remain elastic within the joint. Specimen D was provided with twice the amount of joint shear reinforcement as the others. Specimen E was detailed to fail in joint shear. The test results are shown in (b) through (d). Note that the beam end curvatures shown in (c) included bond slip deformations within the joint. Specimen A failed in beam flexure but showed slip-type hysteresis in the load-deflection relation because bond deterioration occurred along the beam bars within the joint as seen in (c). Specimen B showed ample spindle-shaped hysteresis indicating good bond behavior. Stirrups welded to the beam bars prevented bar slip but the joint concrete deteriorated progressively. Finally, the specimen failed in joint shear and the joint developed large shear strains as seen in (d). Specimen C showed better ductile and stable hysteresis than any other specimen. This is because the beam bars were tempered to remain elastic within the joint and developed no large plastic strains accelerating the bond deterioration. Specimen D showed the same slip-type hysteresis as Specimen A. The larger amount of shear reinforcement did not appear effective in preventing the bond slip. Specimen E failed in joint shear and exhibited large deterioration in the resistance.

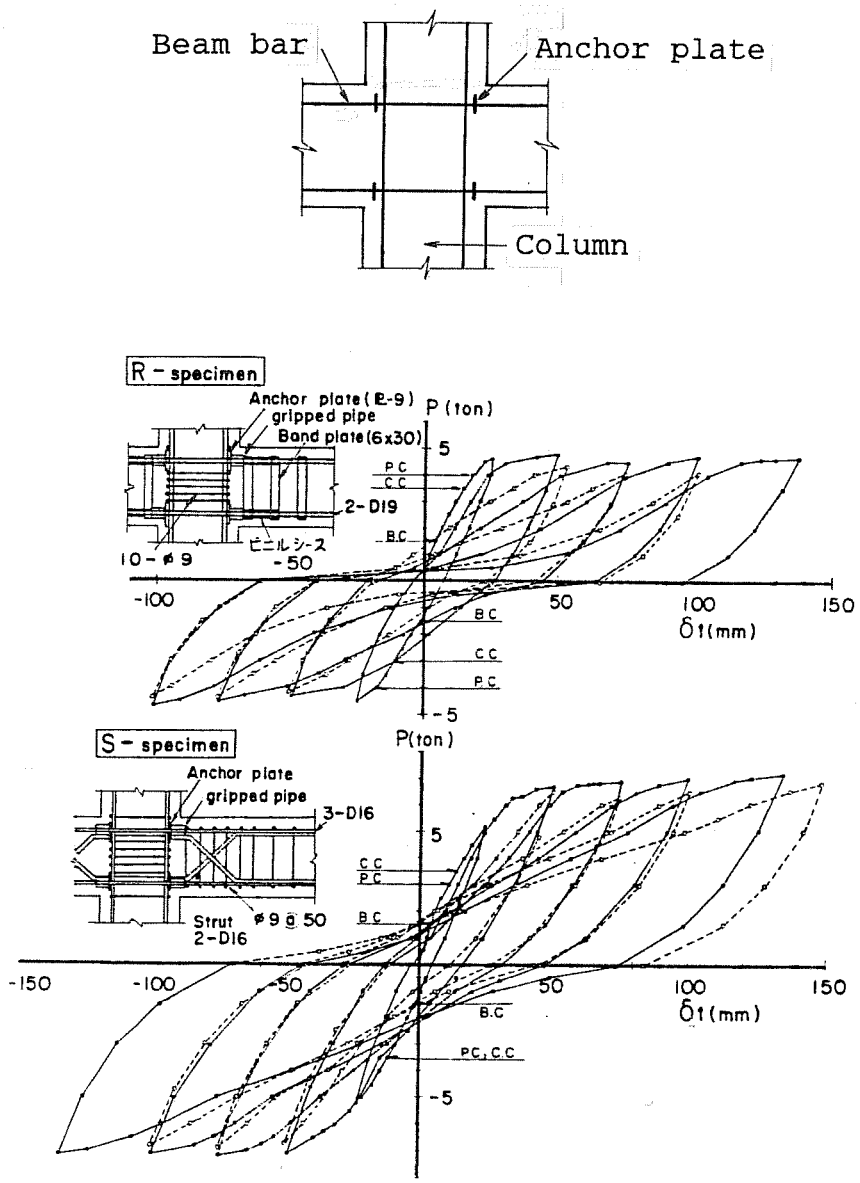

Fig. 4.24 Test of Interior joints with steel anchor plate

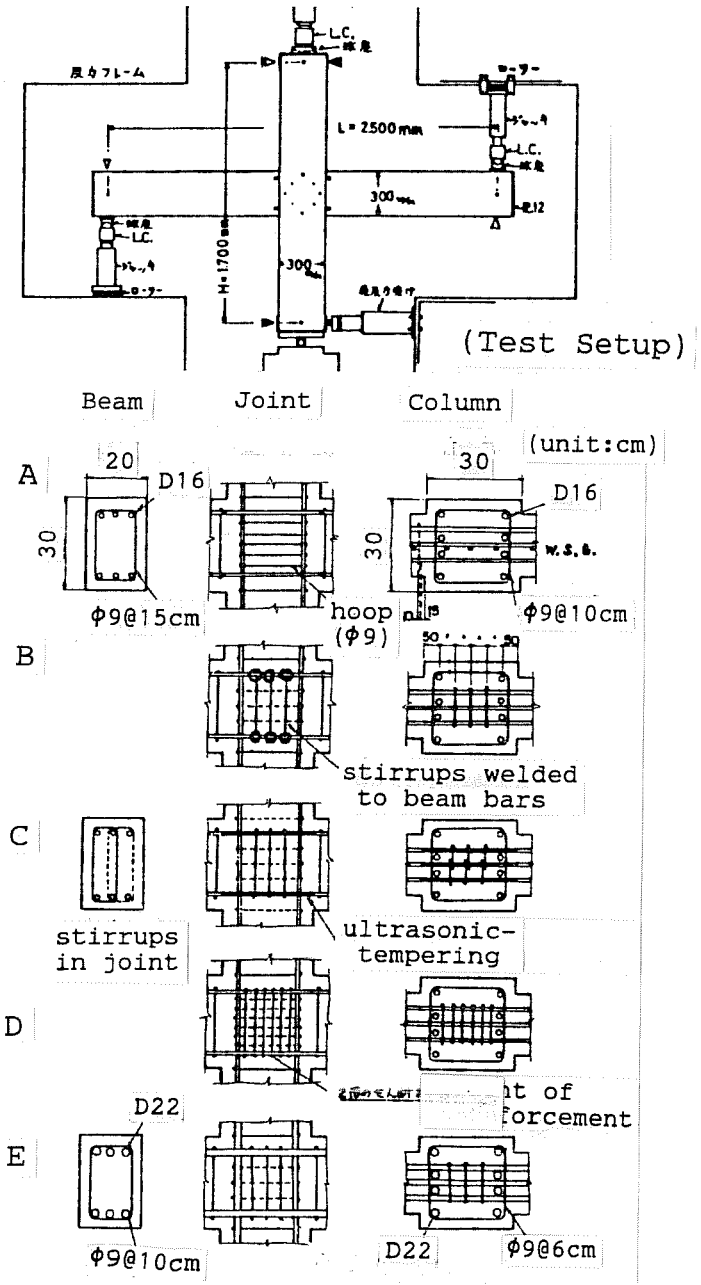

(a) Specimen details

Fig. 4.25 Test of interior joints with various reinforcing detailing

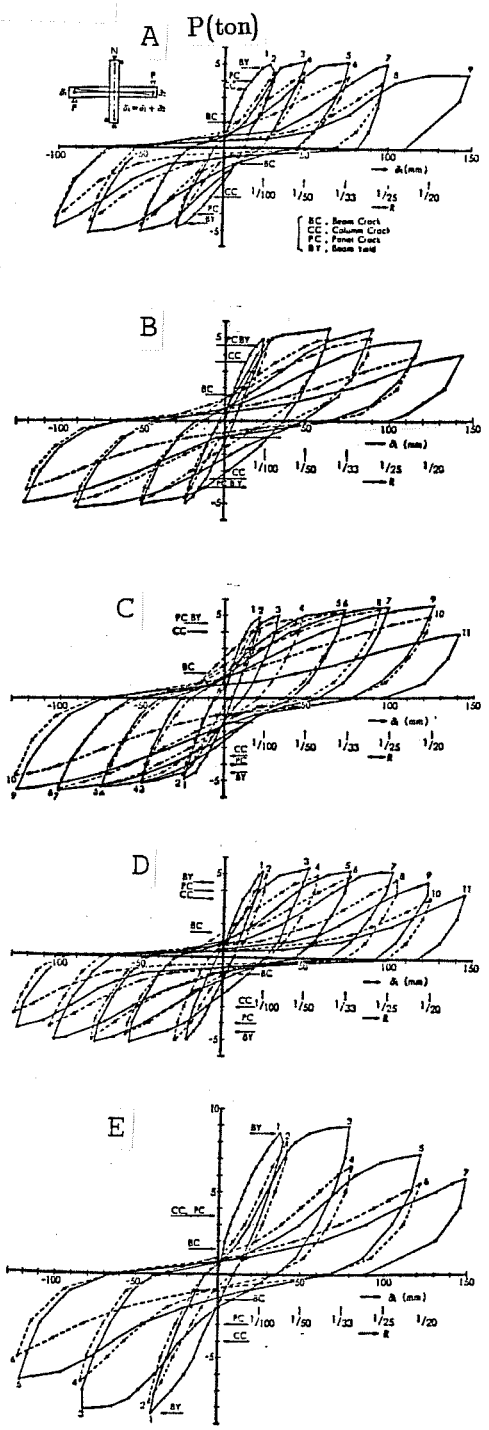

(b) Load vs beam tip deflection

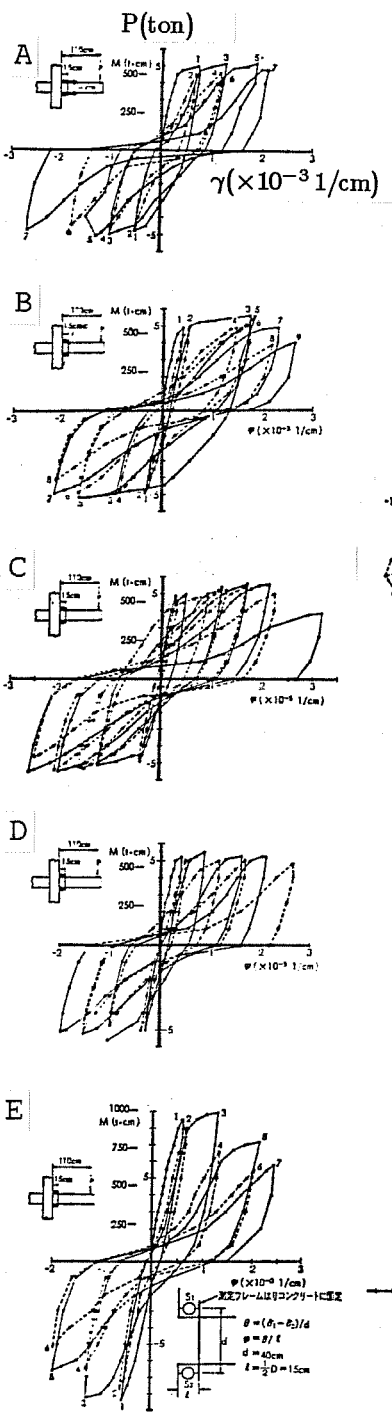

(c) Load vs beam end curvature

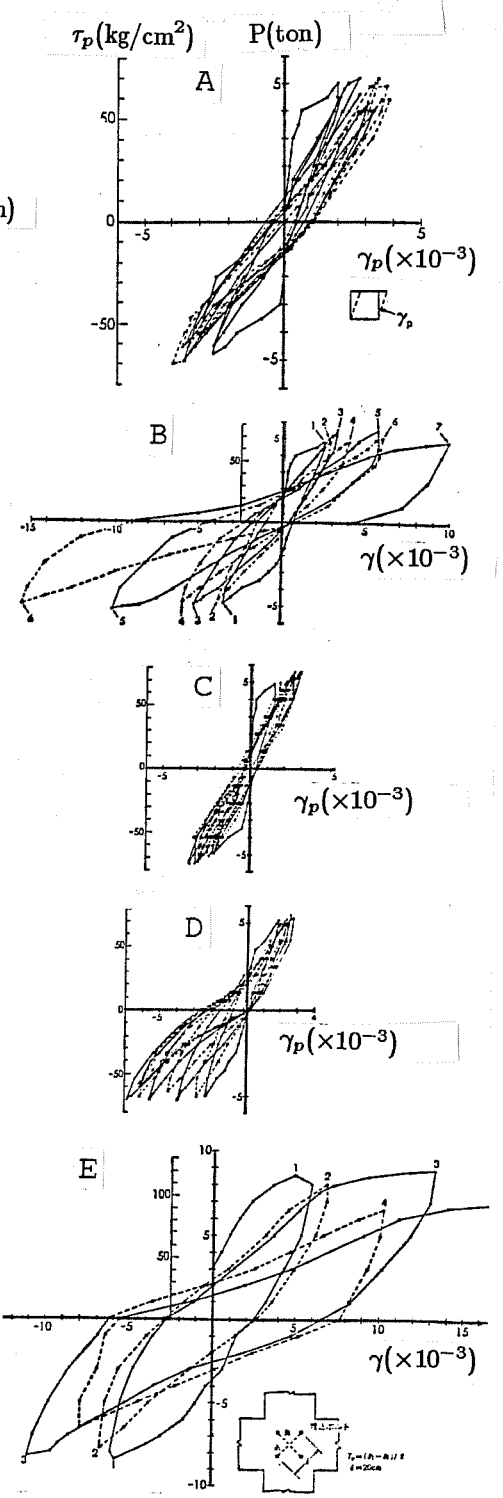

(d) Load vs joint shear strain

(Fig. 4.25 Continued)

5. SUMMARY

The results of the studies described previously are summarized as follows:

1. Design of RC beam-column joints for shear is based on empirical formulas derived from test results for interior joints which failed in shear. The formulas define the joint shear strength as the sum of concrete contribution and reinforcement contribution. The concrete contribution is much larger than the reinforcement contribution in the formulas.

2. Transverse beams on both sides of the joint certainly confine the joint and increase its strength and ductility. However, the effect of a transverse beam on one side only is not clearly understood.

3. The joint shear resisting mechanism is influenced by bond conditions along beam bars. The diagonal compressive strut appears to dominate the mechanism when bond becomes poor.

4. Joint lateral reinforcement is effective in strengthening the joint or at least in delaying deterioration of resistance. However, its effectiveness is affected by beam bar bond conditions and by transverse beams.

5. Joint shear failure may occur within a plane frame designed to fail in beam flexure if the frame undergoes large deflection reversals.

6. Joints loaded in two directions simultaneously show biaxial interaction of resistance, even when the resistance is controlled by beam moment capacities. Loading in one direction lowers the shear force in the other direction because of biaxial interaction so that the shear orbit does not reach the point corresponding to simultaneous yielding of beams in both directions.

7. Exterior joints with bent-down anchorage of beam bottom bars show lower strength and less ductility in negative bending than in positive bending.

8. The anchorage strength of bent-down beam bars is increased with an increase in straight embedment, column axial forces and lateral reinforcement at the bend portion.

9. The slab contributes to the beam flexural strength particularly in negative bending. The reinforcement within the entire slab width should be regarded effective at large deflections.

10. Large size beam bars accelerate bond deterioration within the joint and cause slip-type hysteresis.

11. The column depth is generally designed to be larger than 20 times the beam bar diameter and to develop a bond stress less than $4\sqrt{F_c}$ (F_c = concrete strength).

12. Further studies are needed on the following items.

    a. Design of eccentric joints.

    b. Behavior of joints other than interior.

    c. Effect of bond deterioration on the overall behavior of structures.

    d. Allowable maximum story drift to ensure ductile behavior of structures without bond deterioration and joint shear distress.

REFERENCES

1. AIJ "Report on Damages in 1968 Tokachioki Earthquake," December 1968.
2. AIJ "Materials for Ultimate Design of Reinforced Concrete (No. 28 Beam-Column Joint)," *Journal of AIJ*, Vol. 97, No. 1190, March 1982.
3. AIJ "Standard for Structural Calculation of Reinforced Concrete Structures," 1982.
4. AIJ "Standard for Structural Calculation of Steel Reinforced Concrete Structures," 1975
5. AIJ "Ultimate Lateral Strength and Deformability in Aseismic Design of Buildings," 1981.
6. JSC "Design Code for Reinforced Concrete Buildings with D51 Reinforcing Bars" (Draft), September 1977.
7. Kamimura, T., "Ultimate Shear Strength of Reinforced Concrete Beam-Column Joints," *Transactions of AIJ*, Extra, October 1975.
8. Endo, T., et al., "Strength and Stiffness of Reinforced Concrete Beam-Column Joints," *Transactions of AIJ*, Extra, September 1965.
9. Owada, Y., "Reinforced Concrete Beam-Column Joints," *Concrete Journal*, Vol. 13, No. 3, March 1975.
10. Sonobe, Y., et al., "Experimental Study on Beam-Column Joints with D51 Reinforcing Bars," Quarterly *Column*, No. 69, July 1978.
11. Aoyama, H., "Outline of Earthquake Provisions in the Recently Revised Japanese Building Code" (in English), *Bulletin of the New Zealand National Society for Earthquake Engineering*, Vol. 14, No. 2, June 1981.
12. Takeda, T., et al., "Advanced Design of Multi-story Reinforced Concrete Building" (in English), *Proceedings*, 12th Congress IABSE, Vancouver, September 1984.
13. Sugano, S., et al., "Aseismic Design Method for High-Rise Reinforced Concrete Buildings," *Takenaka Technical Research Report No. 36*, November 1986.
14. Otani, S., "SAKE– A Computer Program for Inelastic Analysis of R/C Frames to Earthquake" (in English), *SRS No. 413*, University of Illinois, November 1974.
15. Takeda, T., et al., "Reinforced Concrete Response to Simulated Earthquake" (in English), *Journal of the Structural Division, ASCE*, Vol. 96, ST 12, December 1970.
16. Takizawa, H., "Analysis of the Behavior of Reinforced Concrete Structures during Strong Earthquakes," *Concrete Journal*, Vol. 11, No. 2, February 1973.

17. Aoyama, H., "Overview of Japanese Building Codes and Design Examples" (in English), *1st U.S.-N.Z.-Japan Seminar on Design of Reinforced Concrete Beam-Column Joints*, Monterey, July-August 1984.

18. Noguchi, H., "Nonlinear Finite Element Analysis of Reinforced Concrete Beam-Column Joints" (in English), *1st U.S.-N.Z.-Japan Seminar*, Monterey, July-August 1984.

19. Morita, S. and Fujii, S., "Interactive Decay of Bent-Bar Anchorage and Joint-Shear Capacity at Exterior Beam- Column Joints under Reversed Cyclic Loadings" (in English), *1st U.S.-N.Z.-Japan Seminar*, Monterey, July-August 1984.

20. Otani, S., Kobayashi, Y. and Aoyama, H., "Reinforced Concrete Interior Beam-column Joints under Simulated Earthquake Loading" (in English), *1st U.S.-N.Z.-Japan Seminar*, Monterey, July-August 1984.

21. Shibata, T. and Joh, O., "Behavior of R/C Interior Beam-Column Joints with Various Details under Cyclic Lateral Loads" (in English), *1st U.S.-N.Z.-Japan Seminar*, Monterey, July-August 1984.

22. Wakabayashi, M. and Minami, K., "Review of Studies on the Shear Resistance of Composite Steel and Reinforced Concrete Beam-to-Column Connections in Japan" (in English), *1st U.S.-N.Z.-Japan Seminar*, Monterey, July-August 1984.

23. Aoyama, H., Kitayama, K. and Otani, S., "Design of Reinforced Concrete Beam-Column-Slab Specimens in Accordance with Japanese Practices" (in English), *2nd U.S.-N.Z.-Japan Seminar*, Tokyo, May 1985.

24. Kanada, K., Fujii, S. and Morita, S., "Effects of Joint Shear Reinforcement on Behaviors of Exterior Beam-Column Joints under Reversed Cyclic Loadings" (in English), *2nd U.S.-N.Z.-Japan Seminar*, Tokyo, May 1985.

25. Minami, K. and Nishimura,Y., "Anchorage Strength of Bent Bar in Exterior Joints" (in English), *2nd U.S.-N.Z.- Japan Seminar*, Tokyo, May 1985.

26. Ogura, K., "Some Problems in Placing Reinforcing Bars at Beam-Column Joints in Japan," (in English), *2nd U.S.- N.Z.-Japan Seminar*, Tokyo, May 1985.

27. Otani, S., Kitayama, K. and Aoyama, H., "Beam Bar Bond Stress and Behavior of Reinforced Concrete Interior Beam-Column Connections" (in English), *2nd U.S.-N.Z.-Japan Seminar*, Tokyo, May 1985.

28. Shibata, T. and Joh, O., "Behavior of Three-Dimensional R/C Beam-Column Subassemblages with Slab" (in English), *2nd U.S.-N.Z.-Japan Seminar*, Tokyo, May 1985.

29. Wakabayashi, M., "Behavior of Diagonally Reinforced Concrete Beam-to-Column Connections" (in English), *2nd U.S.-N.Z.-Japan Seminar*, Tokyo, May 1985.

30. Fujii, S. and Morita, S., "Behavior of Exterior Reinforced Concrete Beam-Column-Slab Subassemblages under Bi-Directional Loading" (in English), *3rd U.S.-N.Z.-Japan Seminar*, Christchurch, August 1987.

31. Kitayama, K., Otani, S. and Aoyama, H., "Behavior of Reinforced Concrete Beam-Column Connections with Slabs" (in English), *3rd U.S.-N.Z.-Japan Seminar*, Christchurch, August 1987.

32. Kitayama, K., Otani, S. and Aoyama, H., "Earthquake Resistant Design Criteria for Reinforced Concrete Interior Beam-Column Joints" (in English), *3rd U.S.-N.Z.-Japan Seminar*, Christchurch, August 1987.

33. Noguchi, H. and Kurusu, K., "The Effects of Beam Bar Bond and Joint Shear on the Behavior of Reinforced Concrete Interior Beam-Column Joints" (in English), *3rd U.S.-N.Z.- Japan Seminar*, Christchurch, August 1987.

34. Noguchi, H. and Watanabe, K., "Application of FEM to the Analysis of Shear Resistance Mechanism of RC Beam-Column Joints under Reversed Cyclic Loading" (in English), *3rd U.S.-N.Z.-Japan Seminar*, Christchurch, August 1987.

35. Shibata, T. and Joh, O., "Improvement on Seismic Behavior of Reinforced Concrete Interior Beam-Column Joints" (in English), *3rd U.S.-N.Z.-Japan Seminar*, Christchurch, August 1987.

36. Shibata, T. and Joh, O., "Influence of Transverse Reinforcement in Joint Panels and Beam Ends on the Behavior of R/C Beam-Column Subassemblages" (in English), *3rd U.S.- N.Z.-Japan Seminar*, Christchurch, August 1987.

37. New Zealand Standard, "Code of Practice for the Design of Concrete Structures (NZS3101)" (in English), Standards Association of New Zealand, 1982.

38. ACI, "Building Code Requirements for Reinforced Concrete (ACI 318-83)" (in English), 1983.

39. Kamimura, T. and Hamada, D., et al., "Experimental Study on Reinforced Concrete Beam-Column Joints (Parts 1-3)," *Transactions of AIJ*, Extra, September 1978 and 1979.

40. Tada, T., Takeda, T. and Takemoto, Y., "Experimental Study on the Reinforcing Method of RC Beam-Column Joints," *Proceedings* of AIJ Kanto District Symp., July 1976.

41. Wakabayashi, M., et al., "Design of Composite Structures," Shoukokusha, 1982.

42. Ogura, K. and Sekine, M., "Recent Trend in Studies on Reinforced Concrete Beam-Column Joints," *Concrete Journal*, Vol. 19, No. 9, September 1981.

43. Owada, Y., "Study on Reinforced Concrete Beam-Column Joints," *Proceedings* of AIJ Kanto District Symp., June 1966.

44. Owada, Y., "Experimental Study on Effect of Transverse Beams on Reinforced Concrete Beam-Column Joints," *Transactions of AIJ*, Extra, October 1976 and 1977, *Proceedings* of AIJ Kanto District Symp., July 1977.

45. Bessho, S., et al., "Experimental Study on Beam-Column Joints in Reinforced Concrete High-Rise Buildings," *Transactions of AIJ*, Extra, September 1979.

46. Ogura, K. and Sekine, M., "Experimental Study on Reinforced Concrete Beam-Column (⊢-shaped) Joints," *Transactions of AIJ*, Extra, September 1979.

47. Owada, Y., "Study on Reinforced Concrete Beam-Column Joints Subjected to Lateral Force," *Transactions of AIJ*, Extra, October 1973.

48. Aoyama, H., et al., "Experimental Study on Reinforced Concrete Beam-Column Joints," *Proceedings* of AIJ Kanto District Symp., 1970.

49. Sugano, S., et al., "Experimental Study on Columns and Frames of High-Rise Reinforced Concrete Buildings," *Transactions of AIJ*, Extra, August 1986.

50. Neturen Co. Ltd., "Design Standard for High Strength Lateral Reinforcement in Reinforced Concrete Beams and Columns," May 1983.

51. Mogami, T., et al., "Structural Tests for Developing High-Rise Reinforced Concrete Layered Construction System," Taisei Technical Research Report, No. 16, December 1983.

52. Yamada, T., et al., "Test of Structural Members and Frames in Tall buildings Utilizing the RC Layered Construction System," Taisei Technical Research Report, No. 18, March 1986.

53. Shinjuku Nishitoyama Project, "Report on Full-Scale Test of Reinforced Concrete Beam-Column Joints," January 1986.

54. Wakabayashi, M., et al., "Experimental Study on Force Transfer Mechanism and Strength of Reinforced Concrete Beam-Column Joints," *Transactions of AIJ*, Extra, October 1977, Bulletin of the Disaster Prevention Research Institute, Kyoto University, Vol. 21, No. B-1, April 1978.

55. Nakata, S., et al., "Experimental Study on PRC Beam-Column Joints (Part-1)," *Transactions of AIJ*, Extra, October 1973.

56. Tada, T. and Takeda, T., "Experimental Study on the Reinforcing Method of RC Beam-Column Joints," *Transactions of AIJ*, Extra, September 1980.

57. Tada, T. and Takeda, T., "Experimental Study on the Reinforcing Method of RC Beam-Column Joints," *Transactions of AIJ*, Extra, October 1982.

58. Nagashima, T., et al., "Experimental Study on Beam-Column Joints in High-Rise Reinforced Concrete Buildings," *Transactions of AIJ*, Extra, August 1986.

59. Bessho, S., et al., "Full Size Test of an External Beam-Column Joint of a Tall Reinforced Concrete Building using the Continuous U Anchorage Method for Two Layer Beams Bars," Kajima Technical Research Report, No. 25, June 1977.

60. Yamaguchi, Y., et al., "A Study on Reinforced Concrete Beam-Column Joints with U-Shaped Beam Reinforcement," Takenaka Technical Research Report, No. 16, October 1976.

61. Yamaguchi, Y., et al., "A Study on Anchorage of Beam Reinforcement in Beam-Column Joints," Takenaka Technical Research Report, No. 20, October 1978.

Blank page 152

APPENDIX A

APPENDIX A

Design Example of RC Interior Joint

1. Dimensions (cm)

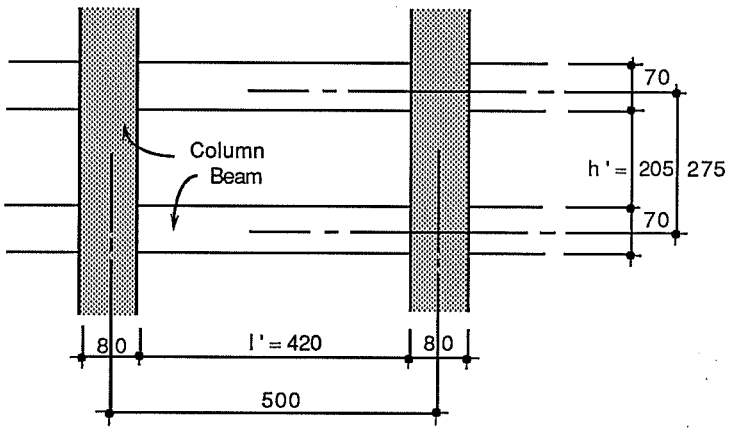

BEAM SECTION

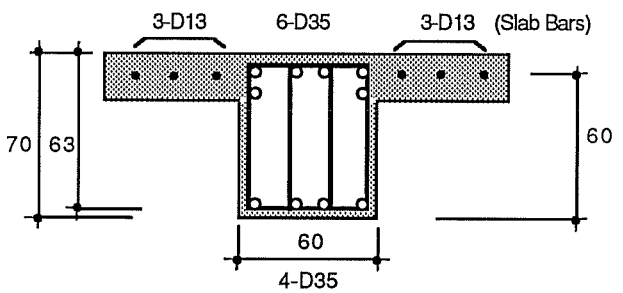

COLUMN SECTION

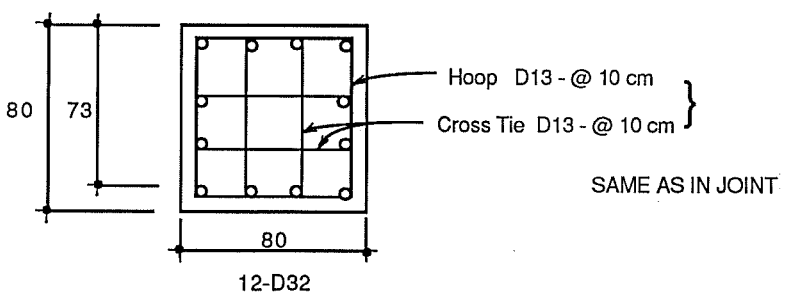

2. Materials

i) Concrete Strength $F_c = 270$ kgf/cm^2

allowable shear stress $f_S = \min \{F_c/20 \ , \ 1.5 \times (F_c/100 + 5)\}$

$$\left.\begin{aligned} \frac{F_c}{20} &= \frac{270}{20} = 13.5 \\ 1.5 \times \left(\frac{F_c}{100} + 5\right) &= 1.5 \times \left(\frac{270}{100} + 5\right) = 11.6 \end{aligned}\right\} \therefore f_S = 11.6 \,\text{kgf/cm}^2$$

ii) Reinforcement SD40 (nominal yield strength = 4000 kgf/cm^2)

$f_y = 1.1 \times 4000 = 4400$ kgf/cm^2 for longitudinal reinforcement
$f_{wy} = 3000$ kgf/cm^2 for lateral reinforcement

iii) The overstrength factor of 1.1 for longitudinal reinforcement and the design strength of 3000 kgf/cm^2 for lateral reinforcement are specified by the *Building Standard Law* and the *Enforcement Order*.

3. Beam Moment Capacity (Ref. 5)

$$uM_b = 0.9 \, A_S \, f_y \, \mathrm{d} \ \text{(kgf·cm)}$$

where

A_S	=	sectional area of tensile reinforcement (cm^2)
f_y	=	yield strength of reinforcement (kgf/cm^2)
d	=	effective depth (cm)

i) Positive Moment Capacity

$$\begin{aligned} A_s^+ &= 4 \times 9.57 = 38.3 \text{ cm}^2 \text{ (4-D35)} \\ \mathrm{d}^+ &= 63 \text{ cm} \quad \mathrm{fy} = 4400 \text{ kgf/cm}^2 \\ uM_b{}^+ &= 0.9 \times 38.3 \times 4400 \times 63 = 95.6 \times 10^5 \text{ kgf·cm} \end{aligned}$$

ii) Negative Moment Capacity

$$\begin{aligned} A_s^- &= 6 \times 9.57 + 6 \times 1.27 = 65.0 \text{ cm}^2 \text{ (6-D35 + 6-D13)} \\ \mathrm{d}^- &= 60 \text{ cm} \quad \mathrm{fy} = 4400 \text{ kgf/cm}^2 \\ uM_b{}^- &= 0.9 \times 65.0 \times 4400 \times 60 = 154.4 \times 10^5 \text{ kgf·cm} \end{aligned}$$

4. Column Moment Capacity (Ref. 5)

$$uM_c = 0.8A_S f_{yh} + 0.5 P_u h \left(1 - \frac{P_u}{bhF_c}\right) (\text{kgf} \cdot \text{cm})$$

where

A_S	=	sectional area of a set of tensile reinforcement (cm^2)
f_y	=	yield strength of reinforcement (kgf/cm^2)
b	=	column width (cm)
h	=	column depth (cm)
P_u	=	design axial force (kgf)
F_c	=	concrete strength (kgf/cm^2)

Top and Bottom Columns

$$P_u = 200\,\text{ton} = 2 \times 10^5\,\text{kgf (assumed)}$$

$$b = h = 80\,\text{cm} \quad F_c = 270\,\text{kgf/cm}^2 \quad f_y = 4400\,\text{kgf/cm}^2$$

$$A_S = 4 \times 7.94 = 31.8\,\text{cm}^2\ (4 - D32)$$

$$1^{st}\text{term} = 0.8 \times 31.8 \times 4400 \times 80 = 89.5 \times 10^5$$

$$2^{nd}\text{term} = 0.5 \times 2 \times 10^5 \times 80 \times \left(1 - \frac{2 \times 10^5}{80 \times 80 \times 270}\right) = 70.7 \times 10^5$$

$$\therefore uM_c = (89.5 + 70.7) \times 10^5 = 160.2 \times 10^5\ \text{kgf} \cdot \text{cm}$$

5. Joint Shear Stress

i) Effective Volume of Joint

$$eV_c = b_j \times j_b \times j_c\ (\text{cm}^3)$$

where

b_j	=	$(b_b + b_c)/2$ (b_b = beam width, b_c = column width)
j_b	=	$\frac{7}{8}d_b$ (d_b = beam effective depth)
j_c	=	$\frac{7}{8}d_c$ (d_c = column effective depth)

$$b_j = \frac{60 + 80}{2} = 70\ \text{cm}$$

$$j_b = \frac{7}{8}d_b = \frac{7}{8}\left(\frac{d_b{}^+ + d_b{}^-}{2}\right) = \frac{7}{8}\left(\frac{63 + 60}{2}\right) = 53.8\ \text{cm}$$

$$j_c = \frac{7}{8}d_c = \frac{7}{8} \times 73 = 63.9\ \text{cm}$$

$$\therefore eV_c = 70 \times 53.8 \times 63.9 = 2.41 \times 10^5\ \text{cm}^3$$

ii) Design Shear Stress

$$\tau_d = \min\left\{ \frac{\Sigma uM_b}{(1+\xi)eV_c} \quad , \quad \frac{\Sigma uM_c}{(1+\eta)eV_c} \right\} \text{ (kgf/cm}^2\text{)}$$

where

uM_b = beam moment capacity (kgf·cm)
uM_c = column moment capacity (kgf·cm)
eV_c = effective volume of joint (cm^3)
ξ = h_b/h' (h_b = beam depth, h' = clear story height)
η = h_c/ℓ' (h_c = column depth, ℓ' = clear span length)

$$\xi = \frac{70}{205} = 0.34 \qquad \eta = \frac{80}{420} = 0.19$$

$$\left.\begin{aligned} \frac{\Sigma uM_b}{(1+\xi)eV_c} &= \frac{(95.6+154.4)\times 10^5}{(1+0.34)\times 2.41\times 10^5} = 77.4 \\ \frac{\Sigma uM_c}{(1+\eta)eV_c} &= \frac{2\times 160.2\times 10^5}{(1+0.19)\times 2.41\times 10^5} = 111.7 \end{aligned}\right\} \therefore \tau_d = 77.4\,\text{kgf/cm}^2$$

iii) Joint Reinforcement Ratio

$$p_w = \frac{A_w}{b_c \cdot S}$$

where

A_w = sectional area of a set of joint stirrups (cm^2)
b_c = column width (cm)
s = spacing of joint stirrups (cm)

$$D13 - @10\,\text{cm} \Rightarrow A_w = 4\times 1.27 = 5.1\,\text{cm}^2 \quad s = 10\,\text{cm} \quad b_c = 80\,\text{cm}$$

$$\therefore p_w = \frac{5.1}{80\times 10} = 0.0064$$

iv) Joint Shear Strength (See Eqs. 2 and 3 in Chapter 2.)
<case 1> AIJ (SRC) Equation

$$\tau_p = 2\psi f_s + p_w\, f_{wy} \text{ (kgf/cm}^2\text{)}$$

where

ψ = confinement coefficient of joint
f_s = allowable shear stress of concrete (kgf/cm^2)
p_w = joint reinforcement ratio
f_{wy} = yield strength of joint stirrups (kgf/cm^2)

$$\psi = 3\ f_s = 11.6\ \text{kgf/cm}^2 \quad p_w = 0.0064 \quad f_{wy} = 3000\ \text{kgf/cm}^2$$
$$\tau_p = 2 \times 3 \times 11.6 + 0.0064 \times 3000 = 88.8\ \text{kgf/cm}^2 > \tau_d \qquad \text{OK}$$

<case 2> Kamimura's Equation

$$\tau_p = 95.1 + \frac{1}{2}\, p_w\, f_{wy} \ \ (\text{kgf/cm}^2)$$

$$p_w = 0.0064 \qquad f_{wy} = 3000\ \text{kgf/cm}^2$$
$$\tau_p = 95.1 + \frac{1}{2} \times 0.0064 \times 3000 = 104.7\ \text{kgf/cm}^2 > \tau_d \qquad OK$$

6. Column Depth

$$h_{min} = \frac{f_y\, d_b}{4\, u_a} \qquad u_a = 4\sqrt{F_c}$$

where

f_y = yield strength of beam bars (kgf/cm^2)
d_b = beam bar diameter (cm)
F_c = concrete strength (kgf/cm^2)

$$F_c = 270\ \text{kgf/cm}^2 \qquad fy = 4400\ \text{kgf/cm}^2 \qquad d_b = 3.5\ \text{cm}\ (D35)$$
$$u_a = 4\sqrt{270} = 65.7\ \text{kgf/cm}^2 \qquad h_c = 80\ \text{cm}$$
$$h_{min} = \frac{4400 \times 3.5}{4 \times 65.7} = 58.6\ \text{cm} < 80\ \text{cm} \qquad OK$$
$$\frac{h_c}{d_b} = \frac{80}{3.5} = 22.9 > 20 \qquad OK$$

APPENDIX B

APPENDIX B

Concrete and Reinforcement Commonly Used in Japan

1. Design Strength of Concrete in Common Use

kgf/cm^2	180	210	240	270
psi	2570	3000	3430	3860
MPa	18	21	24	26

High strength concrete of 360 to 420 kgf/cm^2 (5000 to 6000 psi) is used in high-rise 25 to 30 story buildings. However, the AIJ Standard for RC Structures covers concrete of 360 kgf/cm^2 or lower.

2. Nominal Yield Strength of Rebars in Common Use

Type	Grade	kgf/cm^2	ksi	MPa
Plain Bar	SR24	2400	34	235
	SR30	3000	43	294
Deformed Bar	SD30	3000	43	294
	SD35	3500	50	343
	SD40	4000	57	392

Deformed, rather than plain, bars are generally used.

Typical deformed bars are :

SD30: small size reinforcement (D10 and D13)
SD35: beam and column longitudinal bars in low- to medium-rise buildings
SD40: large size bars in medium- to high- rise buildings

3. Nominal Sectional Area of Rebars

i) Plain bars

Diameter (mm)	$\phi 4$	$\phi 5$	$\phi 6$	$\phi 7$	$\phi 8$	$\phi 9$	$\phi 12$	$\phi 13$	$\phi 16$	$\phi 19$	$\phi 22$	$\phi 25$	$\phi 28$	$\phi 32$
Area (cm^2)	0.13	0.20	0.28	0.38	0.50	0.64	1.13	1.33	2.01	2.84	3.80	4.91	6.16	8.04

(ϕ = mark for plain reinforcement)

ii) Deformed bars

Diameter (mm)												
D6	D8	D10	D13	D16	D19	D22	D25	D29	D32	D35	D38	D41
Area (mm^2)												
0.32	0.50	0.71	1.27	1.99	2.87	3.87	5.07	6.42	7.94	9.57	11.4	13.4

D = mark for deformed reinforcement)

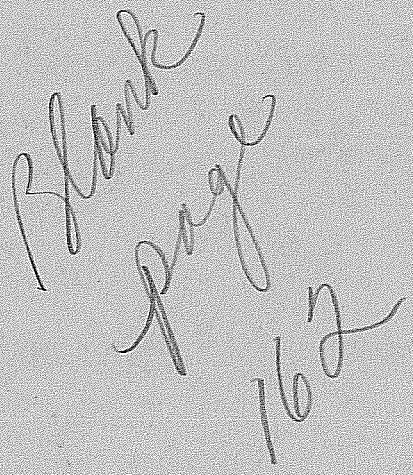
Blank
Page
162

APPENDIX C

APPENDIX C

Participants

U. S. A.

James O. Jirsa	University of Texas
Jack P. Moehle	University of California
James L. Stratta	Structural Engineer
James K. Wight	University of Michigan
Loring A. Wyllie, Jr.	H. J. Degenkolb Associates
Catherine E. French	University of Minnesota

New Zealand

Robert Park	University of Canterbury
Thomas Paulay	University of Canterbury
D. L. Hutchison	Ministry of Works and Development
Les Megget	University of Auckland
Arthur O'Leary	Morrison, Cooper and Partners
Richard Fenwick	University of Auckland
Garry McKay	Ministry of Works and Development
Patrick Cheung	University of Canterbury

Japan

Hiroyuki Aoyama	University of Tokyo
Osamu Joh	Hokkaido University
Koichi Minami	Osaka Institute of Technology
Shiro Morita	Kyoto University
Hiroshi Noguchi	Chiba University
Koichiro Ogura	Meiji University
Shunsuke Otani	University of Tokyo
Takuji Shibata	Hokkaido University
Minoru Wakabayashi	General Building Research Corporation
Kazuhiro Kitayama	University of Tokyo
Kiroshi Muguruma	Kyoto University

People's Republic of China

Chen Yong Chun	China Academy of Building Research